R/V *Mirai* Cruise Report
MR25-02

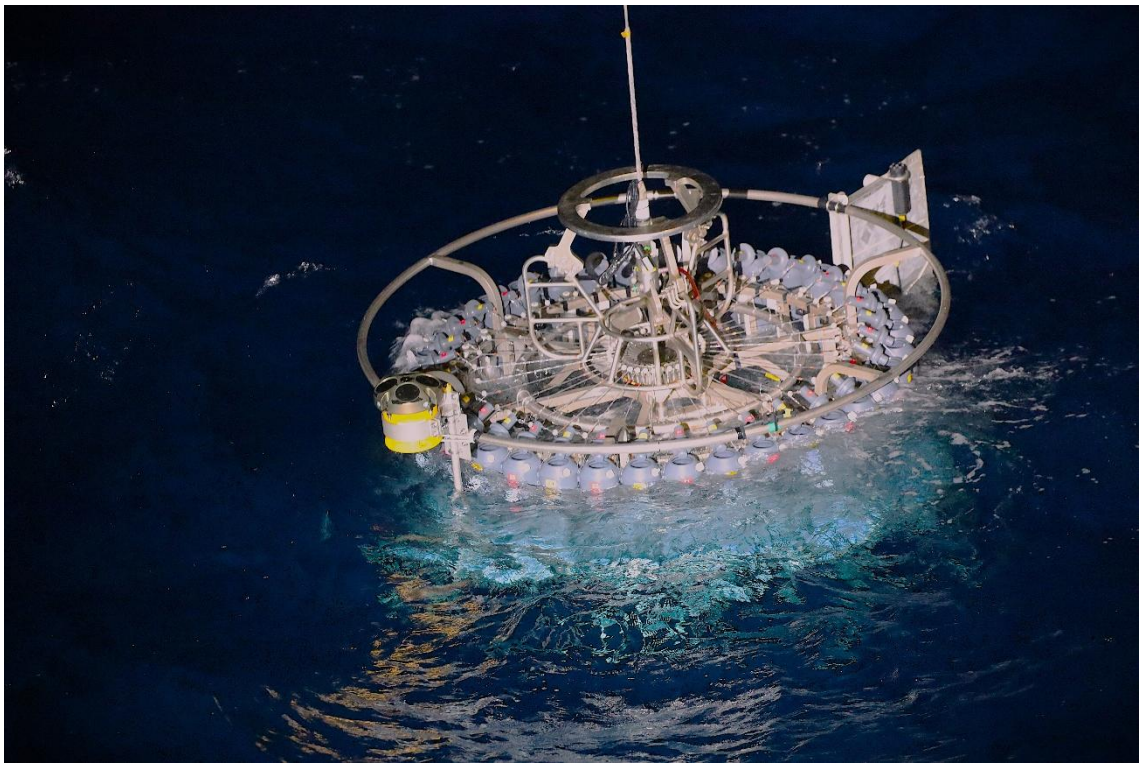

GO-SHIP Observation
– P04W –
Western Tropics in the North Pacific
3 Apr. 2025 — 12 May. 2025
Japan Agency for Marine-Earth Science and Technology (JAMSTEC)

Update History

26th June 2025

The first edition has been released.

23rd January 2026

Sections 3.13, 4.1.2, 4.4, 4.7, 4.8, 4.9, 4.12 and 4.24 have been updated.

6th February 2026

Corrected formatting errors in figures and tables and fixed incorrect figure and table numbering throughout the text.

Contents

1. Cruise Information

Cruise ID	MR25-02
Name of vessel	R/V *Mirai*
Title of cruise	GO-SHIP Observation P04W
	– quantitative observational experiment in the North Pacific –
Chief Scientist	Shinya Kouketsu,
	Global Ocean Observation Research Center,
	Research Institute for Global Change (RIGC),
	Japan Agency for Marine-Earth Science and Technology (JAMSTEC)
Cruise period	3rd April 2025 – 12th May 2025
Ports of departure / call / arrival	
	Shimizu, Japan
	No port calls
	Shimizu, Japan
Research area	Tropics in the western North Pacific

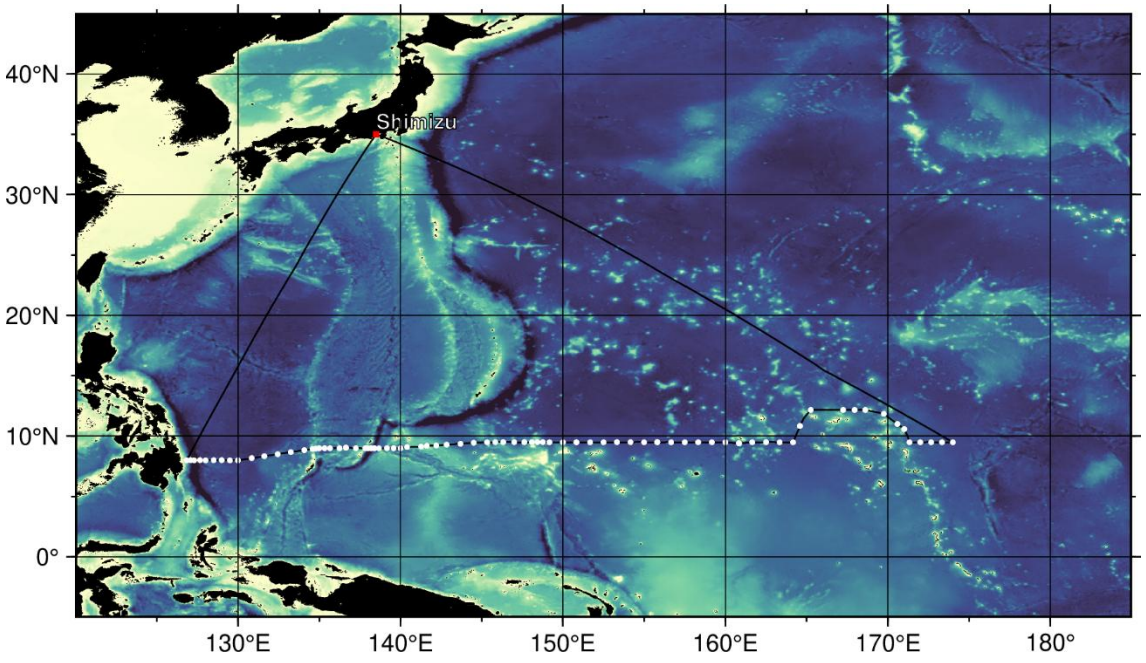

Fig. 1.1 Thin black line shows the cruise track. The whit3e dots show the CTD stations.

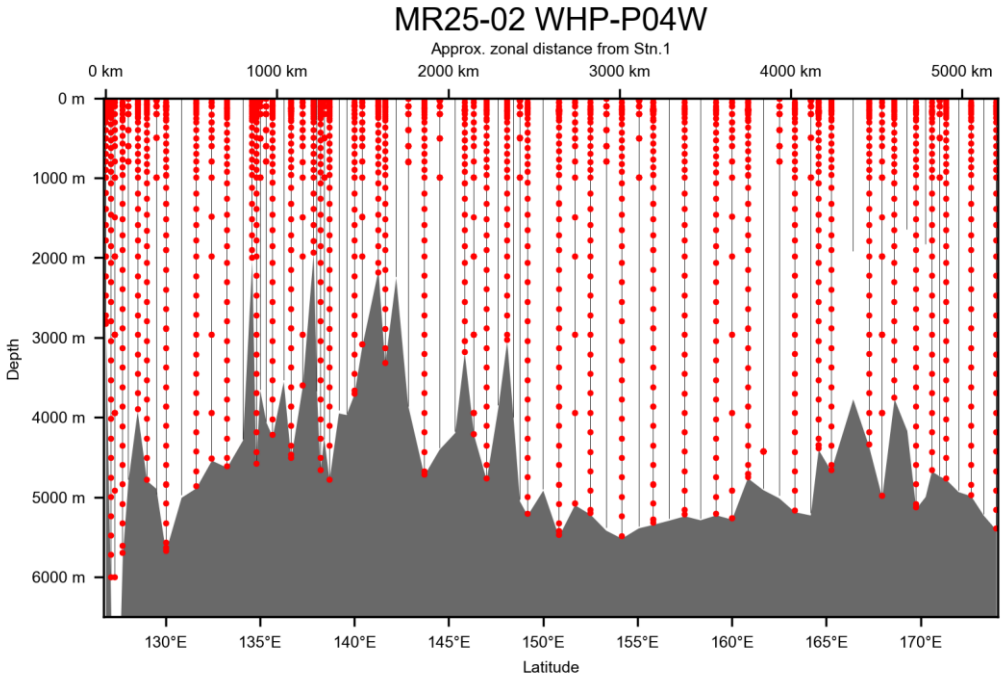

Fig. 1.2. Cross sections showing data sampling positions. Black line shows CTD trace and red dots show Niskin sampling. Gray is ocean bottom bathymetry.

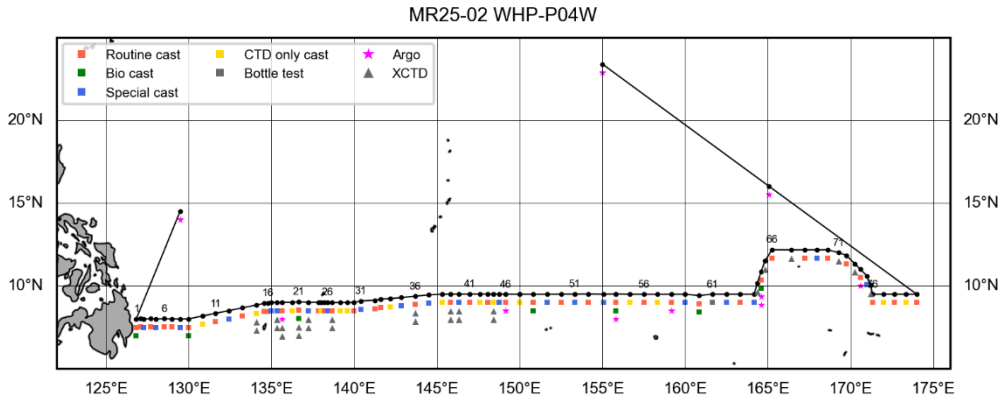

Fig. 1.3. Sampling stations and sampling/deployment performed therein.

Narrative (S. Kouketsu)

As part of our contribution to GO-SHIP (https://www.go-ship.org), the international framework for high-precision shipboard observations, we at the Japan Agency for Marine-Earth Science and Technology (JAMSTEC) have conducted large-scale basin-wide oceanographic section observations. In recent years, we have actively carried out observations in the North Pacific. In 2021, we surveyed the P01 line, followed by the P14N line in 2023. This expedition was aimed at completing the western section of the P04 line (P04W).

The P04W line passes through multiple countries' waters, requiring extensive coordination with stakeholders from various nations, as well as dedicated efforts from JAMSTEC's administrative staff. Recent international circumstances posed challenges, particularly regarding the import procedures for research equipment brought aboard by foreign scientists. For instance, the import tax exemption process for U.S. BGC float deployments (GO-BGC) proved cumbersome, ultimately leading to the cancellation of the float acceptance. This experience reinforced the importance of allowing sufficient time for expedition preparations.

In this expedition, we also welcomed trainees through the Partnership for Observation of the Global Ocean (POGO) to promote understanding of oceanographic observations. We are grateful to U.S. researchers Dr. Macdonald and Dr. Carter for their support in facilitating the application process, which enabled us to host PhD student Ms. Lucero from Argentina.

Our voyage commenced on April 2, 2025, with loading operations in Shimizu, followed by departure on April 3. Given the long journey to the westernmost observation point off the Philippines, we had ample time for onboard preparations. Once we reached the first station, we continued CTD observations eastward. This section was influenced by strong trade winds and the North Equatorial Current, slightly slowing the vessel's progress. However, we were fortunate with favorable weather, allowing the survey to proceed smoothly. Minor incidents, such as a large marine organism (perhaps a shark?) colliding with the bottom contact switch tether, requiring a replacement, added a touch of excitement to an otherwise monotonous expedition.

Ultimately, we completed observations up to Station 80 (9°29.25'N, 17°59.98'E), and returned to Shimizu on May 12, 2025. Given that this line traverses the northern part of the tropical North Pacific and is one of the longer GO-SHIP lines, the planned U.S. survey of the eastern section (P04E) was a source of encouragement for our work. We sincerely appreciate Dr. Macdonald's coordination efforts. Additionally, the implementation of observations in the Philippine Exclusive Economic Zone was made possible thanks to the assistance of Dr. Caroline and Dr. Charissa, for which we are grateful.

Thanks to the dedicated efforts of the captain, crew, and marine technician, the researchers were able to conduct their observations successfully. We deeply appreciate their hard work.

2. Science Party

Table 2.1 List of participants for MR25-02

Name	Responsibility	Affiliation
Shinya Kouketsu	Water sampling	RIGC
Yuichiro Kumamoto	DO/Cs/Ra/14C/13C/CFCs/Nutrients	RIGC
Hiroshi Uchida	Salinity/Density/XCTD	RIGC
Kosei Sasaoka	Chl-a/CDOM	RIGC
Masahito Shigemitsu	PH/FDOM/DOC	RIGC
Ryohei Yamaguchi	CTD/LADCP/turbulence/Water sampling/density/SUM file	RIGC
Mio Akamatsu	Water sampling	RIGC
Taichi Yokokawa	CH4/N2O/Bacteria/DNA/Water sampling	SUGAR
Akiko Makabe	CH4/N2O/Bacteria/DNA/Water sampling	SUGAR
Chisato Yoshikawa	CH4/N2O/Bacteria/DNA/Water sampling	SUGAR
Eiji Tasumi	CH4/N2O/Bacteria/DNA/Water sampling	SUGAR
Qiuyu Yang	Radio isotopes	MALT
Earle Delon	PH/Urea	UGI
Tzu-Hao Wang	Radio isotopes	DTU
Shinsuke Toyoda	CTD/LADCP/turbulence	JAMSTEC
Fumine Okada	Meteorology/Geophysics/ADCP/XCTD	NME
Satomi Ogawa	Meteorology/Geophysics/ADCP/XCTD	NME
Haruna Yamanaka	Meteorology/Geophysics/ADCP/XCTD	NME
Yasuhiro Arii	pH	MWJ
Katsunori Sagishima	DO/TSG/Chl-a	MWJ
Aine Yoda	CTD/Argo	MWJ
Nobuhiro Fujii	CTD/Argo	MWJ
Ko Arihara	CTD/Argo	MWJ
Tun Htet Aung	CTD/Argo	MWJ
Mikio Kitada	CTD/Argo	MWJ
Masahiro Orui	DO/TSG/Chl-a	MWJ
Nagisa Fujiki	DIC/TA/pCO2	MWJ
Misato Kuwahara	DO/TSG/Chl-a	MWJ
Yuko Miyoshi	Nutrients	MWJ
Shiori Ariga	Nutrients	MWJ
Kengo Fujita	Nutrients	MWJ
Tomoki Nakamura	DIC/TA	MWJ
Noriyuki Kisen	CFCs	MWJ
Yuta Oda	DIC/TA	MWJ
Yuto Ohishi	CFCs	MWJ
Yumi Takabayashi	CFCs	MWJ
Johana Ermelinda Lucero	Water sampling	JAMSTEC
Tatsuki Ueyama	Water sampling	JAMSTEC
Chisato Ito	Water sampling	JAMSTEC
Miyano Nishida	Water sampling	JAMSTEC
Akio Kato	Water sampling	JAMSTEC
Junsei Kugimoto	Water sampling	JAMSTEC
Yukino Hambara	DOC/CDOM/FDOM	JAMSTEC
Daichi Koshiishi	DOC/CDOM/FDOM	JAMSTEC

RIGC: Research Institute for Global Change, JAMSTEC; SUGAR: Super-cutting-edge Grand and Advanced Research Program, JAMSTEC; UGI: University of Galway Ireland; DTU: Denmark Technical University; MALT: Micro Analysis Laboratory Tandem accelerator, University of Tokyo; NME: Nippon Marine Enterprises; MWJ: Marine Works Japan

3. Underway Measurements

3.1 Navigation

(1) Personnel

Shinya Kouketsu	JAMSTEC: Principal investigator
Fumine Okada	Nippon Marine Enterprises, Ltd. (NME)
Satomi Ogawa	NME
Haruna Yamanaka	NME
Masanori Murakami	MIRAI crew

(2) System description

Ship's position and velocity were provided by Navigation System on R/V MIRAI. This system integrates GNSS position, Doppler sonar log speed, Gyro compass heading and other basic data for navigation. This system also distributed ship's standard time synchronized to GPS time server via Network Time Protocol. These data were logged on the network server as "SOJ" data every 5 seconds. Sensors for navigation data are listed below;

GNSS system:
R/V MIRAI has 2 GNSS systems, all GNSS positions were offset to radar-mast position, datum point.
Anytime changeable manually switched as to GNSS receiving state.
a) StarPack-D (version 11.07.04), Differential GNSS system.
Antenna: Located on compass deck, starboard.
b) StarPack-D (version 11.07.04), Differential GNSS system.
Antenna: Located on compass deck, portside.

Doppler sonar log:
FURUNO DS-30, which use three acoustic beams for current measurement under the hull.

Gyro compass:
TOKYO KEIKI TG-8000, Sperry type mechanical gyro compass.

GPS time server:
SEIKO TS-2550 Time Server, synchronizing to GPS satellites every 1 second.

(3) Data period (Times in UTC)

00:00 3 Apr. 2025 – 00:00 12 May. 2025

(4) Remarks (Times in UTC)

i) The following period, sea surface temperature and salinity were available.
08:10 03 Apr. 2025 - 04:00 11 May. 2025

ii) The following time, sea surface temperature and salinity were invalid.
03:17 16 Apr. 2025

iii) The following period, data acquisition of sea depth was suspended due to system maintenance.
20:04 20 Apr. 2025 - 20:22 20 Apr. 2025

iv) The following period, sea surface salinity was invalid.
00:15 29 Apr. 2025 - 00:19 29 Apr. 2025

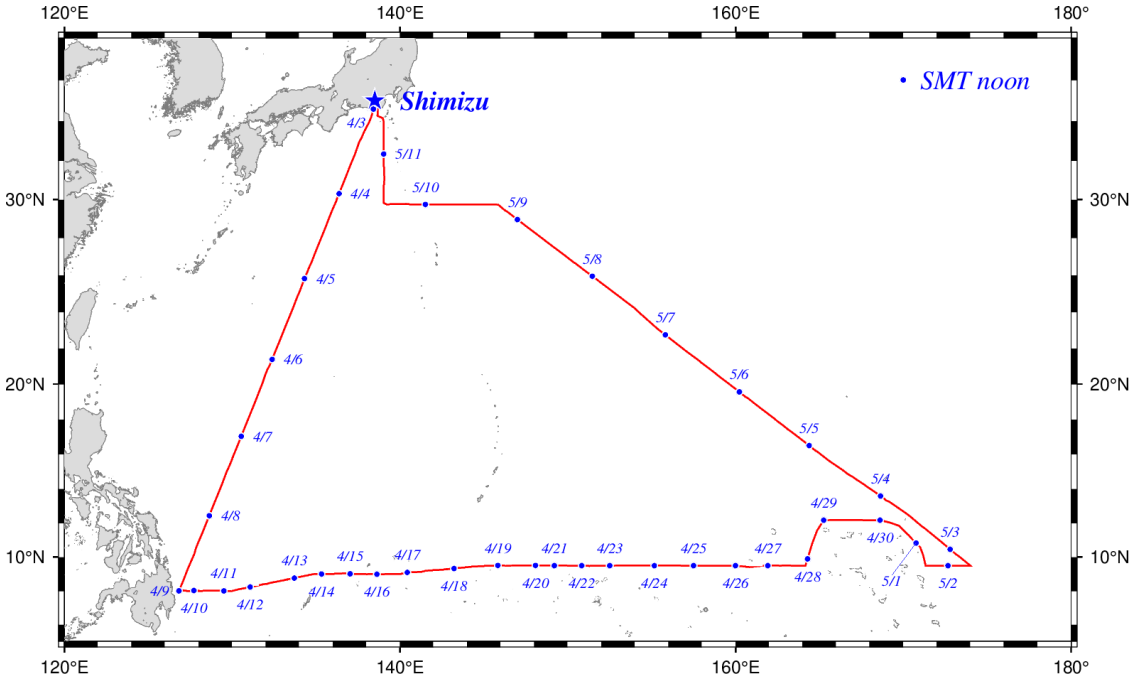

Fig. 3.1 Cruise track of MR25-02

3.2 Swath Bathymetry

May 10, 2025

(1) Personnel

Hiroshi Uchida	JAMSTEC: Principal investigator
Shinya Kouketsu	JAMSTEC
Fumine Okada	Nippon Marine Enterprises, Ltd（NME）
Satomi Ogawa	NME
Haruna Yamanaka	NME
Masanori Murakami	MIRAI crew

(2) Introduction

R/V MIRAI is equipped with a Multi narrow Beam Echo Sounding system (MBES), SEABEAM 3012 (L3 Communications, ELAC Nautik). The objective of MBES is collecting continuous bathymetric data along ship's track to contribute to geological and geophysical investigations and global datasets.

(3) Data Acquisition

The "SEABEAM 3012" on R/V MIRAI was used for bathymetry mapping during this cruise.

To get accurate sound velocity of water column for ray-path correction of acoustic multibeam, we used Surface Sound Velocimeter (MicoSV, Applied Microsystems Ltd.) data to get the sea surface sound velocity (at 6.62m), and the deeper depth sound velocity profiles were calculated by temperature and salinity profiles from CTD, XCTD and Argo float data by the equation in Del Grosso (1974) during this cruise.

Table 3.2-1 shows system configuration and performance of SEABEAM 3012.

Table 3.2-1 SEABEAM 3012 system configuration and performance

Frequency:	12 kHz
Transmit beam width:	2.0 degree
Transmit power:	4 kW
Transmit pulse length:	2 to 20 msec.
Receive beam width:	1.6 degree
Depth range:	50 to 11,000 m
Number of beams:	301 beams
Beam spacing:	Equi-angle
Swath width:	60 to 150 degrees
Depth accuracy:	< 1 % of water depth (average across the swath)

(4) Data processing

i) Sound velocity correction

The bathymetry data were corrected with sound velocity profiles calculated from the nearest CTD or XCTD data in the distance. The equation of sound velocity proposed by Del Grosso (1974) was used for calculating sound velocity. The data corrections were carried out using the HIPS software version 11.3 (Teledyne CARIS, Canada).

ii) Editing and Gridding

Editing for the bathymetry data was carried out using the HIPS software. Firstly, the bathymetry data during ship's turning was basically deleted, and the spike noise of each swath data was removed. Then the bathymetry data were checked by "Regular Grid Surface (resolution: 100 m averaged grid)".

Finally, all accepted data were exported as XYZ ASCII data (longitude [degree], latitude [degree], depth [m]), and converted to 150 m grid data using "nearneighbor" utility of GMT (Generic Mapping Tool) software. Parameters used to make grid data are listed in Table 3.2-2.

Table 3.2-2 Parameters for gridding on "nearneighbor" in GMT

Gridding mesh size:	150 m
Search radius size:	150 m
Number of sectors around grid point:	32
Minimum number of sectors with data required for averaging:	2

(5) Uncertainty of water depths directly beneath the vessel

The water depths extracted from the gridded MBES data were compared with water depths calculated from pressure and density data obtained from CTD observations using the hydrostatic relation with the height of the CTD above the sea floor at the maximum pressure measured by an acoustic altimeter (Uchida and Sueyoshi 2018). The median ± standard error of the difference between water depths estimated by the two methods was 3.8±1.4 m (about 0.1% of the water depths). The lengths of wire (maximum wire length plus 14 m for correction of the height of the CTD above the sea floor and offset at sea surface) were also compared with the calculated water depths, and the median ± standard error of the difference between the two was 3.9±0.4 m.

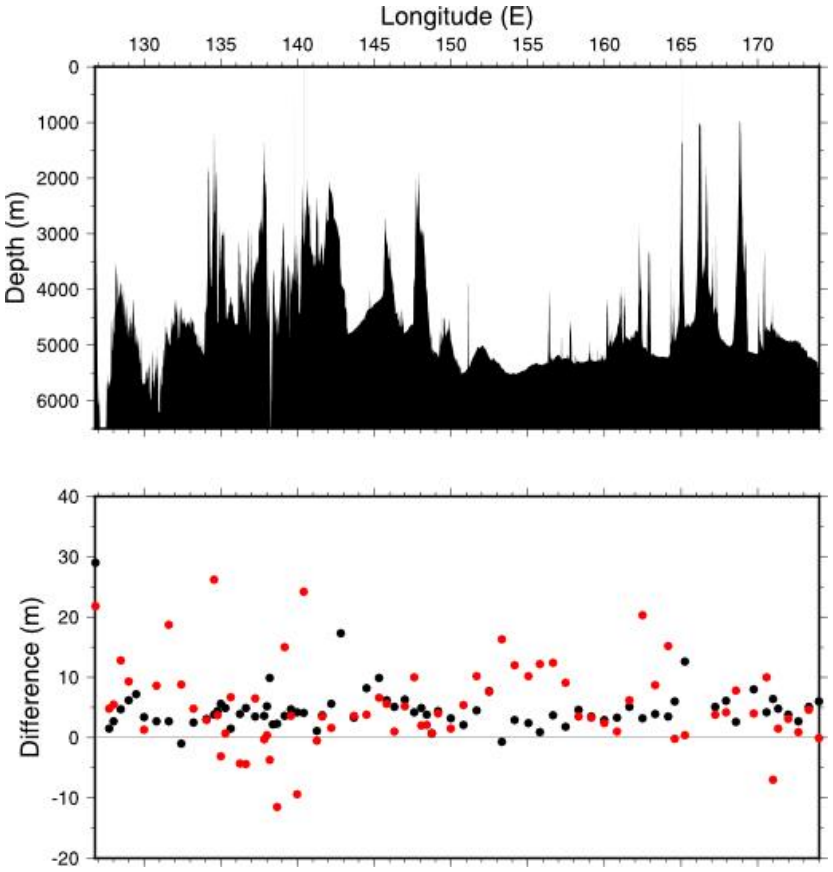

Figure 3.2-1 Bathymetry along P04W line (upper panel) and difference between the bathymetry data and the calculated water depths (red dots) directly beneath the vessel at the time when the CTD is closest to the seafloor (lower panel). Difference between water depths estimated from the length of wire and the calculated water depths are also shown (black dots).

(6) References

Del Grosso, V. A. (1974): New equation for the speed of sound in natural water (with comparison to other equations). The Journal of Acoustical Society of America, 56, 1084-1091.

Uchida, H. and S. Sueyoshi (2018): Bathymetry. Guideline of Ocean Observations, G703EN:001-009, The Oceanographic Society of Japan. (Available on-line at https://kaiyo-gakkai.jp/jos/en/guide/download)

(7) Data archives

These data obtained in this cruise will be submitted to the Data Management Group of JAMSTEC and will be opened to the public via “Data Research System for Whole Cruise Information in JAMSTEC (DARWIN)” in JAMSTEC web site.

https://www.godac.jamstec.go.jp/darwin/en/index.html

3.3 Surface Meteorological Observation

(1) Personnel

Shinya Kouketsu	JAMSTEC: Principal investigator
Masaki Katsumata	JAMSTEC (not on board)
Fumine Okada	Nippon Marine Enterprises, Ltd.（NME）
Satomi Ogawa	NME
Haruna Yamanaka	NME
Masanori Murakami	MIRAI crew

(2) Objectives

Surface meteorological parameters are observed as a basic dataset of the meteorology. These parameters provide the temporal variation of the meteorological condition surrounding the ship.

(3) Methods

Surface meteorological parameters were observed throughout MR25-02 cruise. During this cruise, we used two systems for the observation.

MIRAI Surface Meteorological observation (SMet) system

Instruments of SMet system are listed in Table 3.3-1 and measured parameters are listed in Table 3.3-2. Data were collected and processed by KOAC-7800 weather data processor made by Koshin-Denki, Japan. The data set consists of 6 seconds averaged data.

Shipboard Oceanographic and Atmospheric Radiation (SOAR) measurement system

SOAR system designed by BNL (Brookhaven National Laboratory, USA) consists of major five parts.

i) Analog meteorological data sampling with CR1000 logger manufactured by Campbell Scientific, Inc., Canada – wind, pressure, and rainfall (by a capacitive rain gauge (CRG)) measurement.

ii) Digital meteorological data sampling from individual sensors －air temperature, relative humidity and rainfall (by optical rain gauge (ORG)) measurement.

iii) Radiation data sampling with CR1000X logger manufactured by Campbell Scientific, Inc., Radiometers designed by Hukseflux Thermal Sensors B.V., Netherlands. – short and long wave downward radiation measurement.

iv) Photosynthetically Available Radiation (PAR) and Ultraviolet Irradiance (UV) sensor manufactured by Biospherical Instruments Inc., USA. – PAR and UV measurement.

v) Scientific Computer System (SCS) developed by NOAA (National Oceanic and Atmospheric Administration, USA) – centralized data acquisition and logging of all data sets.
SCS recorded wind, pressure, rainfall, air temperature, relative humidity, radiation, and PAR data. SCS composed event data (JamMet) from these data and ship's navigation data every 6 seconds. Instruments and their locations are listed in Table 3.3-3 and measured parameters are listed in Table 3.3-4.
For the quality control as post processing, we checked the following sensors, before and after the cruise.

vi) Young rain gauge (SMet and SOAR)
Inspect of the linearity of output value from the rain gauge sensor to change input value by adding fixed quantity of test water.

vii) Barometer (SMet and SOAR)
Comparison with the portable barometer value, PTB330, VAISALA

viii) Thermometer (air temperature and relative humidity) (SMet and SOAR)
Comparison with the portable thermometer value, HMP75, VAISALA

(4) Preliminary results

Fig. 3.3-1 shows the time series of the following parameters.

Wind (SMet)

Air temperature (SOAR)

Relative humidity (SOAR)

Precipitation (SOAR CRG)

Short/long wave radiation (SOAR)

Pressure (SMet)

Sea surface temperature (SMet)

Significant wave height (SMet)

(5) Data archive

These data obtained in this cruise will be submitted to the Data Management Group of JAMSTEC, and will be opened to the public via “Data Research System for Whole Cruise Information in JAMSTEC (DARWIN)” in JAMSTEC web site.

https://www.godac.jamstec.go.jp/darwin/en

(6) Remarks (Times in UTC)

i) The following period, SST (Sea Surface Temperature) data of SMet was available.
07:27 03 Apr. 2025 - 04:05 11 May. 2025

ii) The following period, SMet significant wave height and period data were invalid.
03:55 04 Apr. 2025 - 05:55 04 Apr. 2025

iii) The following time, increasing of SMet optical rain gauge data were doubtful due to birds perching on the compass deck.
19:53 25 Apr. 2025

iv) The following time, increasing of SMet capacitive rain gauge data were invalid due to transmitting for MF/HF radio.
05:34 14 Apr. 2025
05:32 21 Apr. 2025
04:18 27 Apr. 2025

v) The following period, T/RH data, barometer data, rain gauge data, wind data and radiation data were invalid due to system trouble.
02:41:59 09 Apr. 2025 - 02:42:41 09 Apr. 2025

vi) The following time, increasing of SOAR optical rain gauge data were doubtful due to birds perching on the foremast.
09:40:41 25 Apr. 2025 - 17:28:12 25 Apr. 2025

Table 3.3-1 Instruments and installation locations of MIRAI Surface Meteorological observation system

Sensors	Type	Manufacturer	Location (altitude from surface)
Anemometer	KS-5900	Koshin Denki, Japan	Foremast (25 m)
T/RH	HMP155	VAISALA, Finland	Compass deck (21 m)
with aspirated radiation shield	43408 Gill	R.M. Young, U.S.A.	starboard and port side
Thermometer: SST	RFN2-0	Koshin Denki, Japan	4th deck (-1 m, inlet -5 m) Bow thruster room
Barometer	Model-370	Setra System, U.S.A.	Captain deck (13 m) Weather observation room
Capacitive rain gauge	50202	R. M. Young, U.S.A.	Compass deck (19 m)
Optical rain gauge	ORG-815DS	Optical Scientific Inc., U.S.A.	Compass deck (19 m)
Radiometer (short wave)	MS-802	Eko Seiki, Japan	Radar mast (28 m)
Radiometer (long wave)	MS-202	Eko Seiki, Japan	Radar mast (28 m)
Wave height meter	WM-2	Tsurumi-seiki, Japan	Bow (10 m) Stern (8 m)

Table 3.3-2 Parameters of MIRAI Surface Meteorological observation system

Parameter	Units	Remarks
1 Latitude	degree	
2 Longitude	degree	
3 Ship's speed	knot	MIRAI log
4 Ship's heading	degree	MIRAI gyro
5 Relative wind speed	m/s	6sec./10min. averaged
6 Relative wind direction	degree	6sec./10min. averaged
7 True wind speed	m/s	6sec./10min. averaged
8 True wind direction	degree	6sec./10min. averaged
9 Barometric pressure	hPa	adjusted to sea surface level 6sec. averaged
10 Air temperature (starboard)	degC	6sec. averaged
11 Air temperature (port)	degC	6sec. averaged
12 Dewpoint temperature (starboard)	degC	6sec. averaged
13 Dewpoint temperature (port)	degC	6sec. averaged
14 Relative humidity (starboard)	%	6sec. averaged
15 Relative humidity (port)	%	6sec. averaged
16 Sea surface temperature	degC	6sec. averaged

17 Precipitation intensity (optical rain gauge)	mm/hr	hourly accumulation
18 Precipitation (capacitive rain gauge))	mm/hr	hourly accumulation
19 Downwelling shortwave radiation	W/m^2	6sec. averaged
20 Downwelling infra-red radiation	W/m^2	6sec. averaged
21 Significant wave height (bow)	m	hourly
22 Significant wave height (stern)	m	hourly
23 Significant wave period (bow)	second	hourly
24 Significant wave period (stern)	second	hourly

Table 3.3-3 Instruments and installation locations of SOAR system

Sensors (Meteorological)	Type	Manufacturer	Location*
Anemometer	05106	R.M. Young, USA	Foremast (25 m)
Barometer with pressure port	PTB210	VAISALA, Finland	Foremast (23 m)
	61002 Gill	R.M. Young, USA	
Rain gauge	50202	R.M. Young, USA	Foremast (24 m)
T/RH with aspirated radiation shield	HMP155	VAISALA, Finland	Foremast (23 m)
	43408 Gill	R.M. Young, USA	
Optical rain gauge	ORG-815DR	Optical Scientific Inc., U.S.A.	Foremast (24 m)

Sensors (Radiation)	Type	Manufacturer	Location*
Radiometer (short wave)	SR20	Hukseflux Thermal Sensors B.V., Netherlands	Foremast (25 m)
Radiometer (long wave)	IR20	Hukseflux Thermal Sensors B.V., Netherlands	Foremast (25 m)

Sensor (PAR&UV)	Type	Manufacturer	Location*
PAR&UV sensor	PUV-510	Biospherical Instruments Inc., USA	Navigation deck (18m)

*Location : Altitude from surface

Table 3.3-4 Parameters of SOAR system (JamMet)

Parameter	Units	Remarks
1 Latitude	degree	
2 Longitude	degree	
3 SOG	knot	
4 COG	degree	
5 Relative wind speed	m/s	
6 Relative wind direction	degree	

7 Barometric pressure	hPa	
8 Air temperature	degC	
9 Relative humidity	%	
10 Precipitation intensity (optical rain gauge)	mm/hr	
11 Precipitation (capacitive rain gauge)	mm/hr	reset at 50 mm
12 Down welling shortwave radiation	W/m^2	
13 Down welling infrared radiation	W/m^2	
14 Defuse irradiance	W/m^2	
15 PAR	$microE/cm^2/sec$	
16 UV 305 nm	$microW/cm^2/nm$	
17 UV 320 nm	$microW/cm^2/nm$	
18 UV 340 nm	$microW/cm^2/nm$	
19 UV 380 nm	$microW/cm^2/nm$	

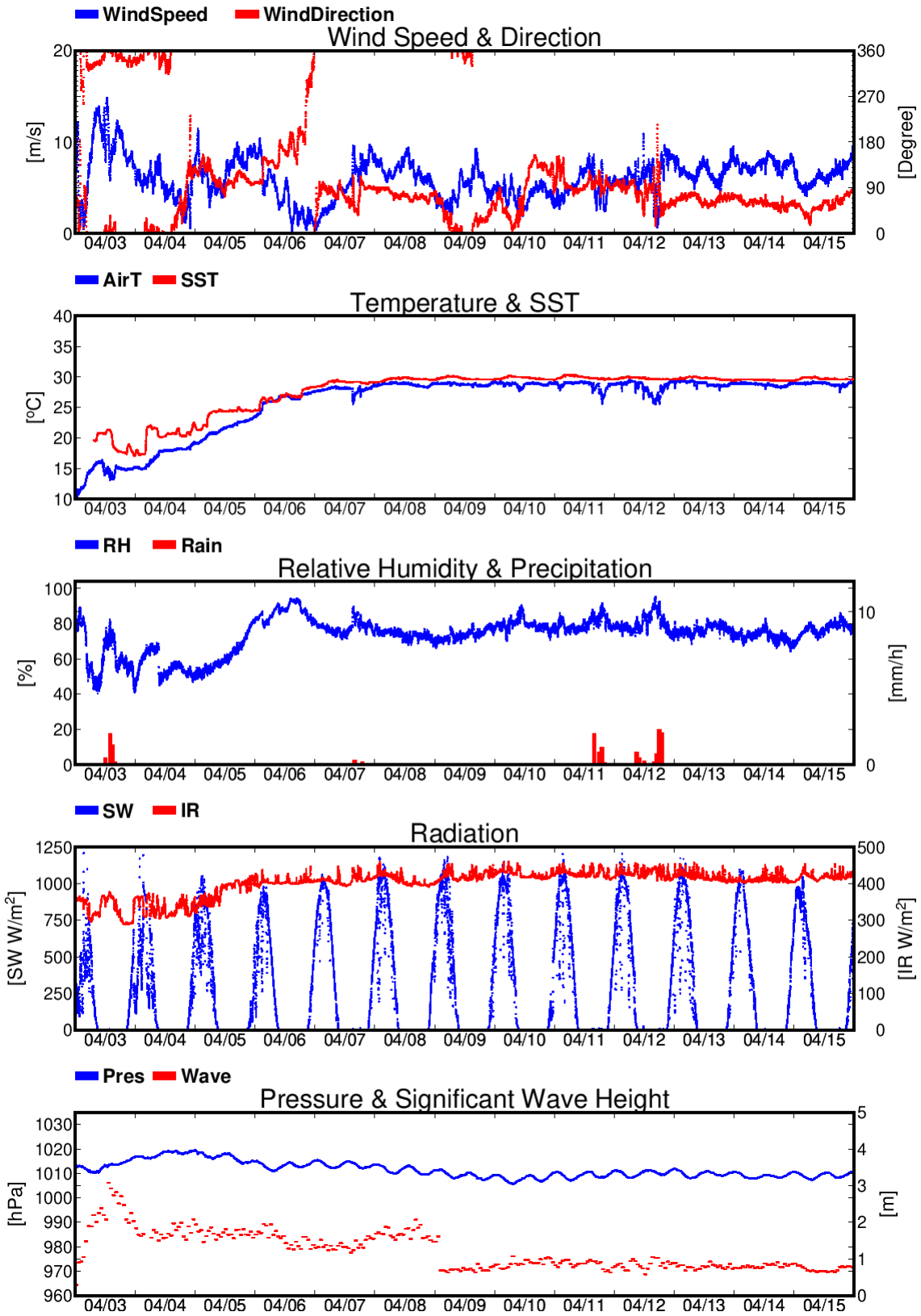

Fig. 3.3-1 Time series of surface meteorological parameters during this cruise

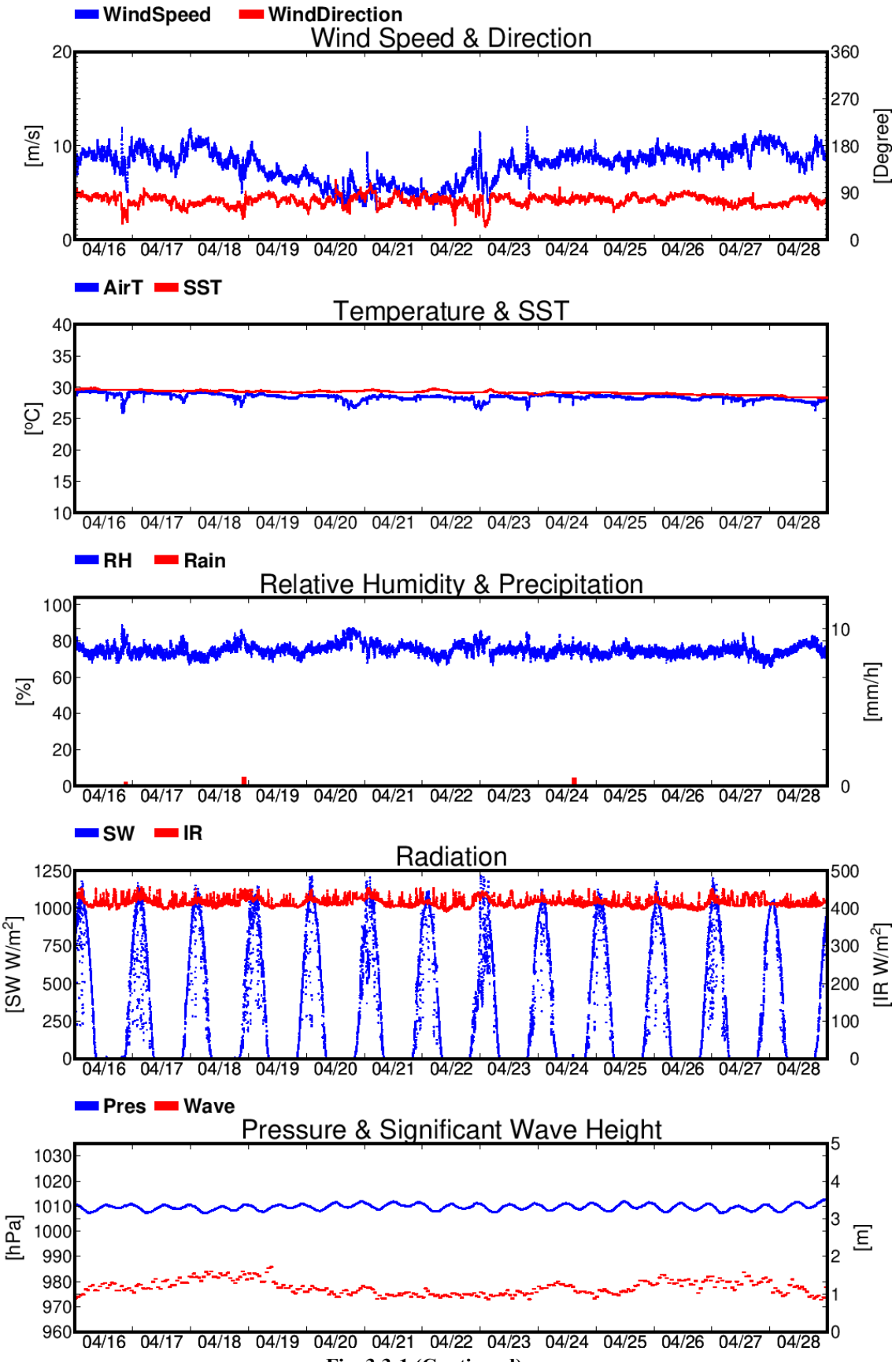

Fig. 3.3-1 (Continued)

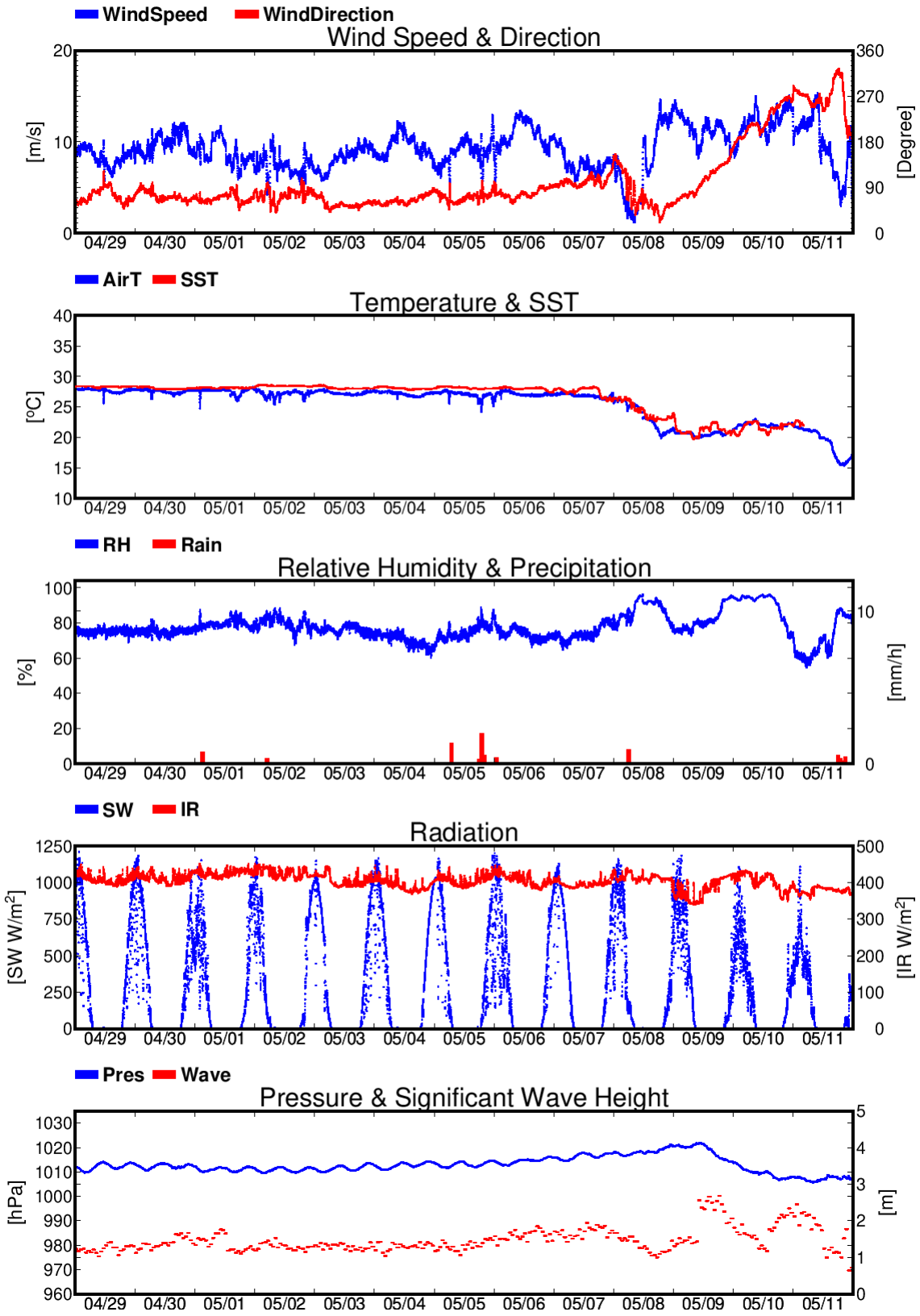

Fig. 3.3-1 (Continued)

3.4 Thermo-Salinograph and Related Properties

May 11, 2025

(1) Personnel

Hiroshi UCHIDA (JAMSTEC RIGC)
Katsunori SAGISHIMA (MWJ)
Masahiro ORUI (MWJ)
Misato KUWAHARA (MWJ)

(2) Objective

The objective of this measurements is to collect sea surface salinity, temperature, dissolved oxygen, fluorescence, and turbidity data continuously along the cruise track.

(3) Instruments and method

The Continuous Sea Surface Water Monitoring System (Marine Works Japan Co, Ltd., Yokosuka, Kanagawa, Japan) automatically measures salinity, temperature, dissolved oxygen, fluorescence, turbidity, total dissolved gas pressure in surface seawater at a sampling interval of 1 minute. This system is installed in the sea surface monitoring laboratory and bottom of the ship (only thermometer) and connected to shipboard LAN system. Measured data along with time and position of the ship were displayed on a monitor and stored in a personal computer. Seawater was continuously pumped up to the laboratory from about 5 m water depth and flowed into the system through a vinyl-chloride pipe or a tube. One thermometer is located just before the seawater pump at bottom of the ship. Flow rate in the system was manually adjusted about 1.0 L/min.

The total dissolved gas pressure sensor has malfunctioned, and a replacement is currently being prepared. Therefore, no data is available for this cruise.

Instruments used in this cruise are as follows:

Temperature (bottom of the ship), SBE 38, Sea-Bird Scientific, Inc., Bellevue, Washington, USA

Serial no. 3857820-0540

Temperature and conductivity, SBE 45, Sea-Bird Scientific, Inc.

Serial no. 4557820-0319

Dissolved oxygen, RINKO II, JFE Advantech, Co., Ltd., Osaka, Japan

Serial no. 0077

Chlorophyll fluorometer, C3, Turner Designs, Inc., Sunnwale, California, USA

Serial no. 2300707 (fluorescence and turbidity)

Data acquisition software, SeaMoni, Marine Works Japan, Co., Ltd.

Version 1.2.0.0

(4) Pre-cruise calibration

Pre-cruise sensor calibrations for the SBE 38, and SBE 45 were performed by the manufacturer.

Pre-cruise sensor calibration for C3 was performed by Marine Works Japan, Co., Ltd. The C3 chlorophyll fluorometer was calibrated with 100 ppb uranine solution, then the Secondary Solid Standard (SSS) was calibrated using the calibrated chlorophyll fluorometer.

Pre-cruise sensor calibration for RINKO was performed at JAMSTEC. The oxygen sensor was immersed in fresh water in a 1-L semi-closed glass vessel, which was immersed in a temperature-controlled water bath. Temperature of the water bath was set to 1, 10, 20 and 29ºC. Temperature of the fresh water in the vessel was measured by a thermistor of the portable dissolved oxygen sensor (expanded uncertainty of smaller than 0.01ºC, ARO-PR, JFE Advantech, Co., Ltd.). At each temperature, the fresh water in the vessel was bubbled with standard gases (4, 10, 17, and 25% oxygen consisted of the oxygen-nitrogen mixture, whose relative expanded uncertainty is 1%, Japan

Fine Products, Tochigi, Japan). Nitrogen standard gas (0% oxygen) (G1) and air (21% oxygen) were also used. Absolute pressure of the vessel's headspace was measured by a reference quartz crystal barometer (expanded uncertainty of 0.01% of reading, RPM4 BA100Ks, Fluke Co., Phoenix Arizona, USA) and ranged from about 1040 to 1070 hPa. The data were averaged over 5 minutes at each calibration point (a matrix of 24 points). As a reference, oxygen concentration of the fresh water in the calibration vessel was calculated from the oxygen concentration of the gases, temperature, and absolute pressure at the water depth (about 6 cm) of the sensor's sensing foil as follows:

$$O_2\ (\mu mol/L) = \{1000 \times c(T) \times (A_p - pH_2O)\} / \{0.20946 \times 22.3916 \times (1013.25 - pH_2O)\}$$

where c(T) is the oxygen solubility, A_p is absolute pressure (in hPa), and pH_2O is the water vapor pressure (in hPa). The RINKO was calibrated by the modified Stern-Volmer equation slightly modified from a method by Uchida et al. (2010):

$$O_2\ (\mu mol/L) = [(V_0 / V)^E - 1] / K_{sv}$$

where V is raw phase difference, V_0 is raw phase difference in the absence of oxygen, K_{sv} is Stern-Volmer constant. The coefficient E corrects nonlinearity of the Stern-Volmer equation. The V_0 and the K_{sv} are assumed to be functions of temperature as follows.

$$K_{sv} = C_0 + C_1 \times T + C_2 \times T^2$$

$$V_0 = 1 + C_3 \times T$$

$$V = C_4 + C_5 \times (N/10000)$$

where T is temperature (°C) and N is raw output.

(5) Data collection

Data from the Continuous Sea Surface Water Monitoring System were obtained at 1-minute intervals. Periods of measurement, maintenance and problems are listed in Table 3.4-1. Seawater samples for salinity, dissolved oxygen and chlorophyll-a analysis were taken from the Continuous Sea Surface Water Monitoring System once in a day to calibrate the sensors in situ. Details of these analysis are described in elsewhere of the cruise report.

Table 3.4-1. Events of the Continuous Sea Surface Water Monitoring System operation.

System Date [UTC]	System Time [UTC]	Events	Note
2025/04/03	08:10	Start data logging	
2025/04/29	00:16	Filter maintenance	Filter exchanged
2025/05/11	04:00	End data logging	

(6) Post-cruise calibration

Data from the Continuous Sea Surface Water Monitoring System were processed as follows. Spikes in the temperature and salinity data were removed using a median filter with a window of 3 scans (3 minutes) when difference between the original data and the median filtered data was larger than 0.1ºC for temperature and 0.5 for salinity. Data gaps were linearly interpolated when the gap was ≤ 13 minutes. Fluorometer and turbidity data were low-pass filtered using a median filter with a window of 3 scans (3 minutes) to remove spikes. Raw data from the RINKO oxygen sensor and fluorometer data were low-pass filtered using a Hamming filter with a window of 15 scans (15 minutes). The remaining erroneous data were manually removed.

Salinity (S [PSU]), dissolved oxygen (O [µmol/kg]), and fluorescence (Fl [RFU]) data were corrected using the water sampled data. Corrected salinity (S_{cor}), dissolved oxygen (O_{cor}), and estimated chlorophyll-*a* (Chl-a) were calculated from following equations

$$S_{cor}\ [PSU] = c_0 + c_1\ S + c_2\ t$$

$$O_{cor}\ [\mu mol/kg] = c_0 + c_1\ O + c_2\ T + c_3\ t + c_4\ T^2$$

$$Chl\text{-}a\ [\mu g/L] = c_0\ Fl$$

where S is practical salinity, t is days from a reference time (2025/04/03 08:10 [UTC]), T is temperature in ºC. The best fit sets of calibration coefficients (c_0~c_4) were determined by a least square technique to minimize the deviation from the water sampled data. The calibration coefficients were listed below.

Salinity

c_0 = 3.155314253988527e-02

c_1 = 0.9991532653438406

c_2 = 5.195997959897390e-04

Oxygen

c_0 = 8.328484655758693e-02

c_1 = 0.8615344986571447

c_2 = 2.322913026995527

c_3 = -0.3794013248662927

c_4 = -5.620119966290445e-02

Chlorophyll-a

c_0 = 0.1827865492286181

Comparisons between the Continuous Sea Surface Water Monitoring System data and water sampled data are shown in Figs. 3.4.1, 3.4.2 and 3.4.3.

(7) Reference

Uchida, H., G. C. Johnson, and K. E. McTaggart (2010): CTD oxygen sensor calibration procedures, The GO-SHIP Repeat Hydrography Manual: A collection of expert reports and guidelines, IOCCP Rep., No. 14, ICPO Pub. Ser. No. 134.

(8) Data archive

These data obtained in this cruise will be submitted to the Data Management Group (DMG) of JAMSTEC, and will open to the public via “Data Research System for Whole Cruise Information in JAMSTEC (DARWIN)” in JAMSTEC web site.

https://www.godac.jamstec.go.jp/darwin/en/index.html

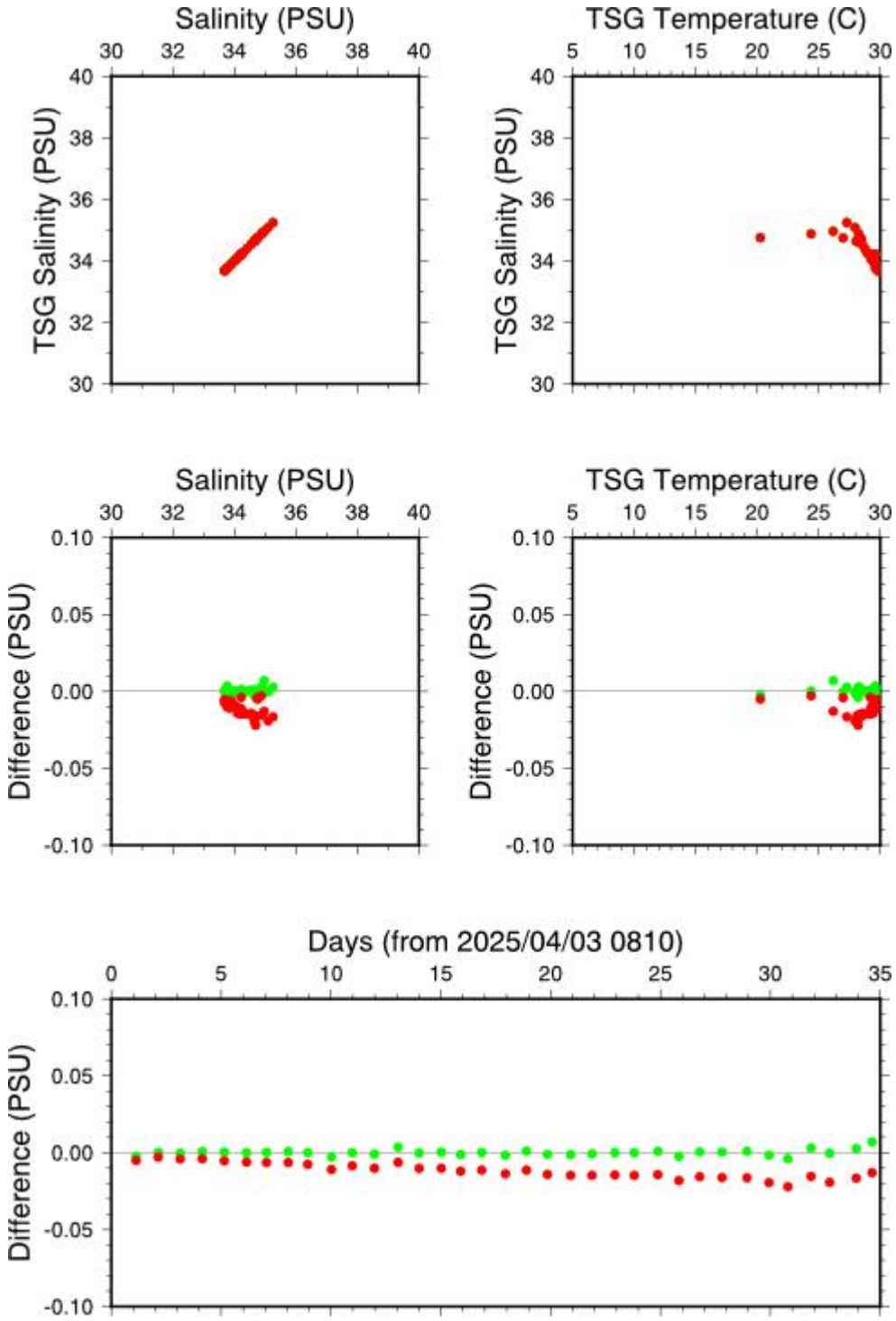

Fig. 3.4-1. Comparison between TSG salinity (red: before correction, green: after correction) and sampled salinity.

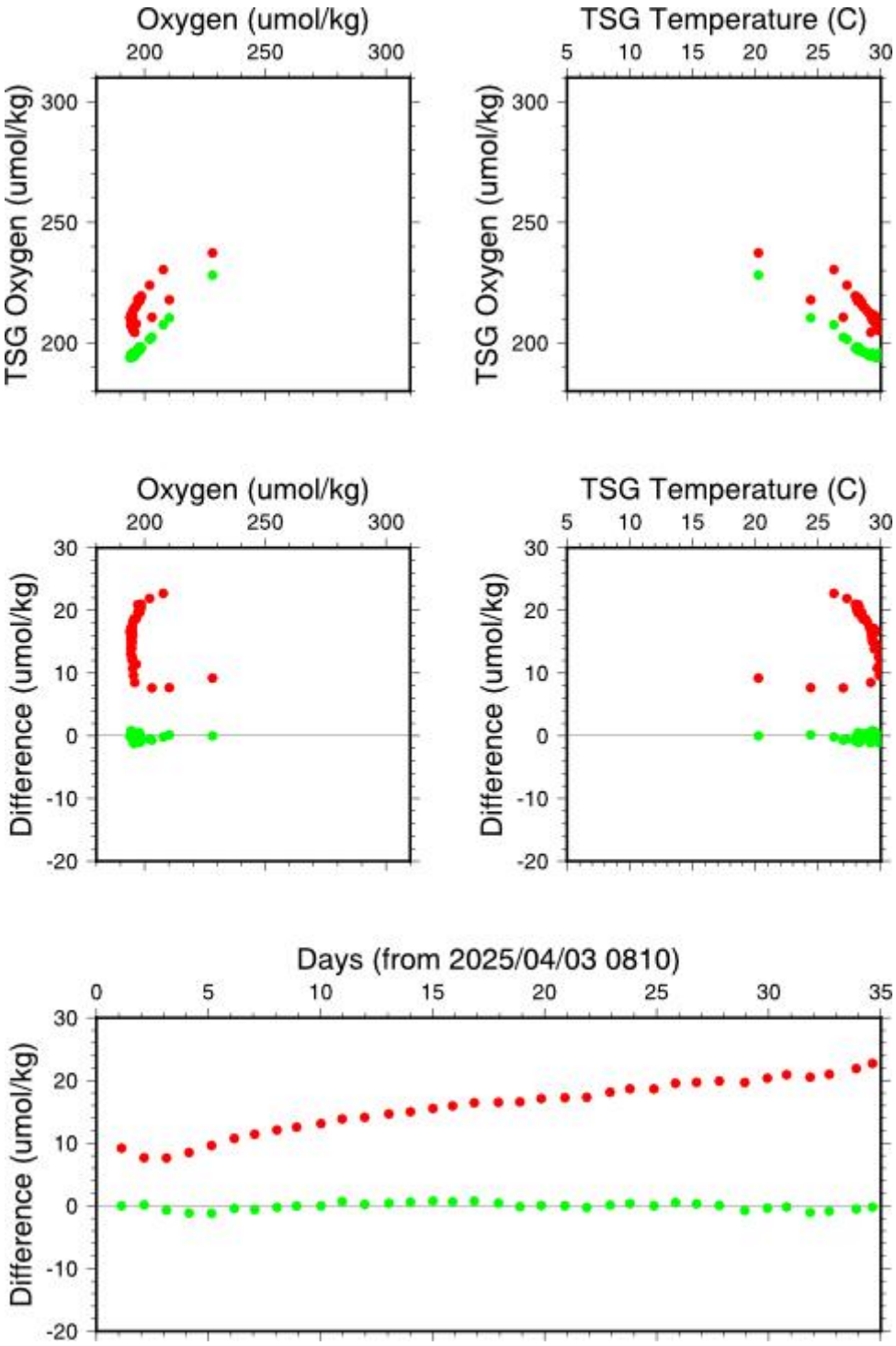

Fig. 3.4-2. Same as Fig. 3.4-1, but for dissolved oxygen.

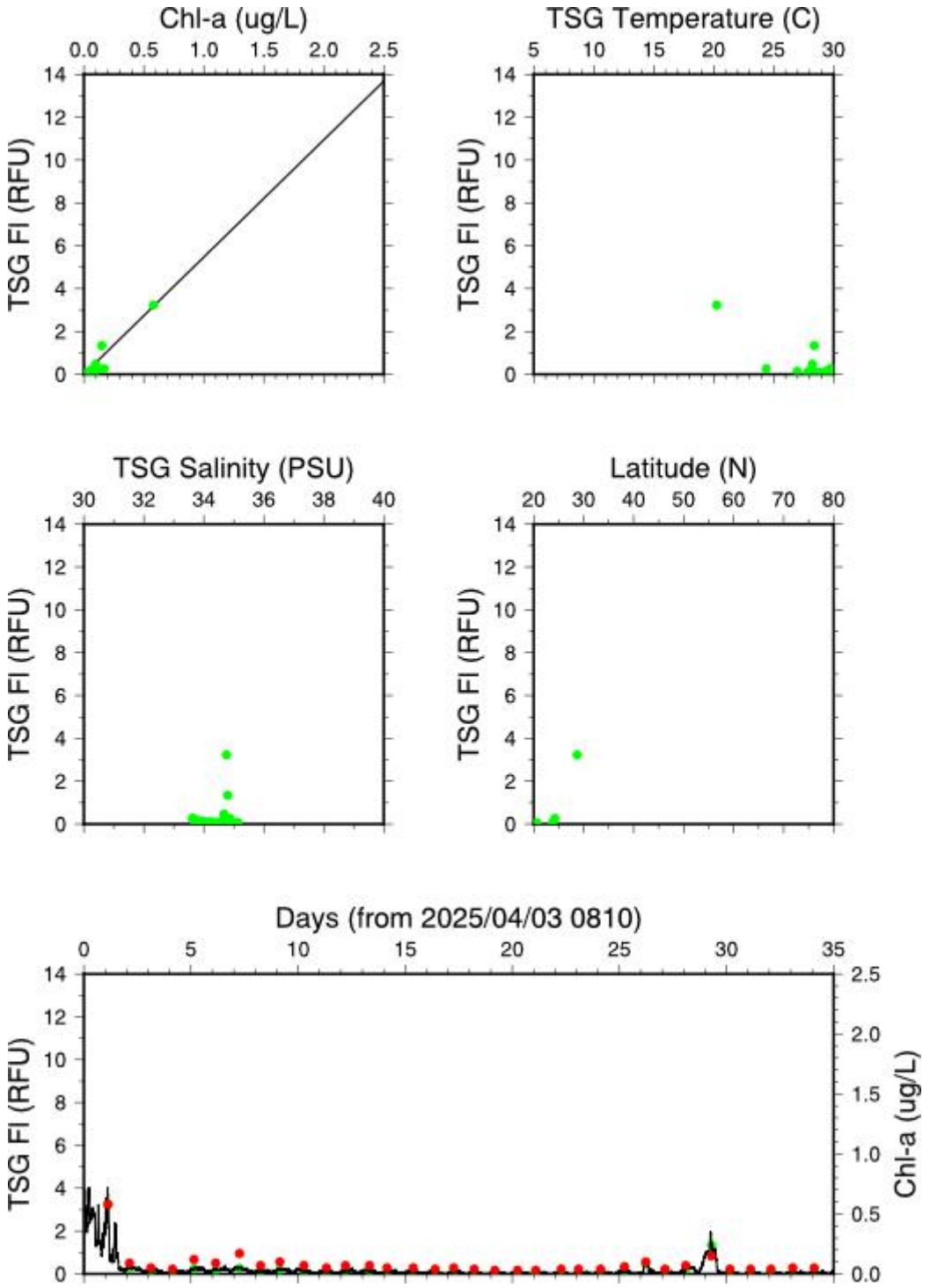

Fig. 3.4-3. Comparison between TSG fluorescence and sampled chlorophyll-a. For the lowest panel, green dots are TSG fluorescence, and red dots and line are sampled chlorophyll-a and estimated chlorophyll-a from TSG fluorescence, respectively.

3.5. Shipboard ADCP

(1) Personnel

Shinya Kouketsu	JAMSTEC: Principal investigator
Fumine Okada	Nippon Marine Enterprises, Ltd. (NME)
Satomi Ogawa	NME
Haruna Yamanaka	NME
Masanori Murakami	MIRAI crew

(2) Objectives

To obtain continuous measurement data of the current profile along the ship's track.

(3) Instruments and methods

Upper ocean current measurements were made in this cruise, using the hull-mounted Acoustic Doppler Current Profiler (ADCP) system. For most of its operation, the instrument was configured for water-tracking mode. Bottom-tracking mode, interleaved bottom-ping with water-ping, was made to get the calibration data for evaluating transducer misalignment angle in the shallow water. The system consists of following components;

i) R/V MIRAI has installed the Ocean Surveyor for vessel-mount ADCP (frequency 76.8 kHz; Teledyne RD Instruments, USA). It has a phased-array transducer with single ceramic assembly and creates 4 acoustic beams electronically. We mounted the transducer head rotated to a ship-relative angle of 45 degrees azimuth from the keel.

ii) For heading source, we use ship's gyro compass (Tokyo Keiki, Japan), continuously providing heading to the ADCP system directory. Additionally, we have Inertial Navigation System (Phins, IXBLUE SAS, France) which provide high-precision heading, attitude information, pitch and roll. They are stored in ".N2R" data files with time stamps.

iii) Differential GNSS system (StarPack-D, Fugro, Netherlands) providing precise ship's position

iv) We used VmDas software version 1.50 (TRDI) for data acquisition.

v) To synchronize time stamp of ping with Computer time, the clock of the logging computer is adjusted to GPS time server continuously by the application software.

vi) Fresh water is charged in the sea chest to prevent bio fouling at transducer face.

vii) The sound speed at the transducer does affect the vertical bin mapping and vertical velocity measurement, and that is calculated from temperature, salinity (constant value; 35.0 PSU) and depth (6.5 m; transducer depth) by equation in Medwin (1975).

Data was configured for "8 m" layer intervals starting about 19 m below sea surface, and recorded every ping as raw ensemble data (.ENR). Additionally, 15 seconds averaged data were recorded as short-term average (.STA). 300 seconds averaged data were long-term average (.LTA), respectively.

(4) Parameters

Major parameters for the measurement, Direct Command, are shown in Table 3.5-1.

Table 3.5-1. Major parameters

Environmental Sensor Commands

EA = 04500	Heading Alignment (1/100 deg)
ED = 00065	Transducer Depth (0 - 65535 dm)
EF = +001	Pitch/Roll Divisor/Multiplier (pos/neg) [1/99 - 99]
EH = 00000	Heading (1/100 deg)
ES = 35	Salinity (0-40 pp thousand)
EX = 00000	Coordinate Transform (Xform: Type; Tilts; 3Bm; Map)
EZ = 10200010	Sensor Source (C; D; H; P; R; S; T; U)

C (1): Sound velocity calculates using ED, ES, ET (temp.)
D (0): Manual ED
H (2): External synchro
P (0), R (0): Manual EP, ER (0 degree)
S (0): Manual ES
T (1): Internal transducer sensor
U (0): Manual EU

EV = 0 Heading Bias (1/100 deg)

Water-Track Commands

WA = 255	False Target Threshold (Max) (0-255 count)
WC = 120	Low Correlation Threshold (0-255)
WD = 111 100 000	Data Out (V; C; A; PG; St; Vsum; Vsum^2; #G; P0)
WE = 1000	Error Velocity Threshold (0-5000 mm/s)
WF = 0800	Blank After Transmit (cm)
WN = 100	Number of depth cells (1-128)
WP = 00001	Pings per Ensemble (0-16384)
WS = 800	Depth Cell Size (cm)
WV = 0390	Mode 1 Ambiguity Velocity (cm/s radial)

(5) Preliminary results

Horizontal velocity along the ship's track is presented in Fig.3.5-1, and longitude cross section of current profiles along P04W line is shown in Fig.3.5-2.

(6) Data archives

These data obtained in this cruise will be submitted to the Data Management Group of JAMSTEC and will be opened to the public via "Data Research System for Whole Cruise Information in JAMSTEC (DARWIN)" in JAMSTEC web site.

https://www.godac.jamstec.go.jp/darwin/en

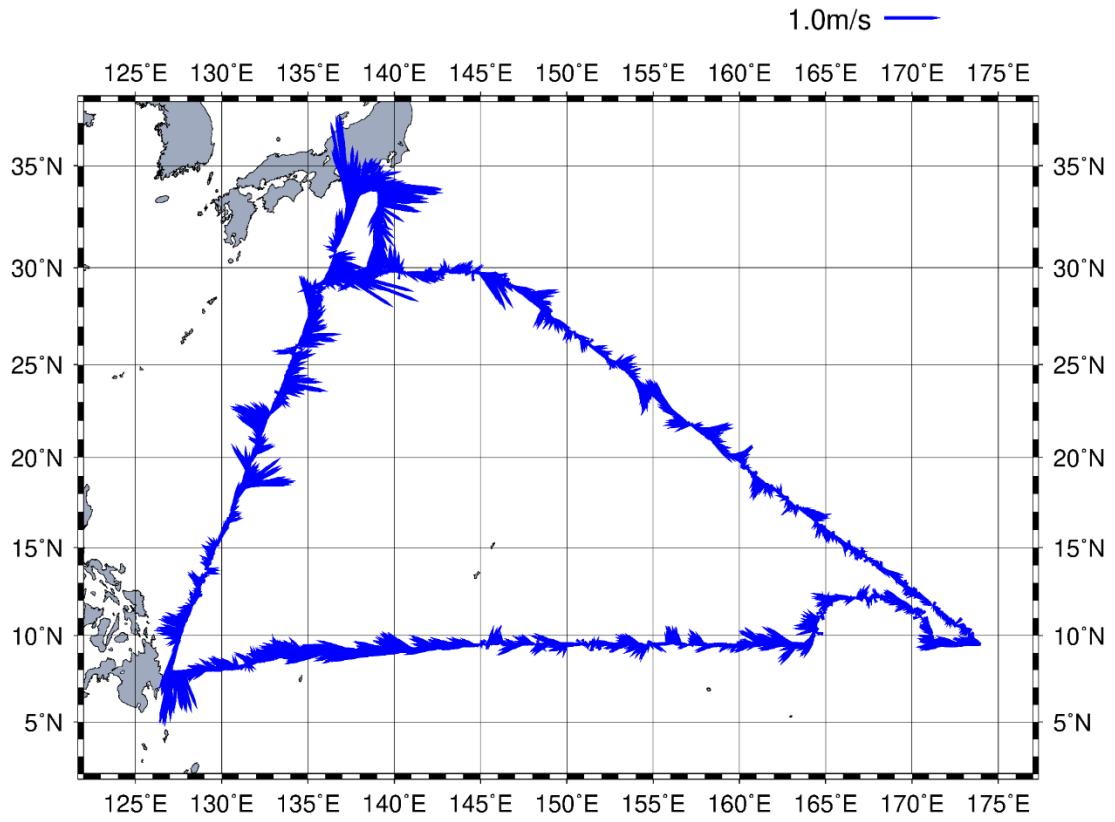

Fig. 3.5-1 Horizontal Velocity along the ship's track.
(15 min. Average / Layer: 39-55 m)

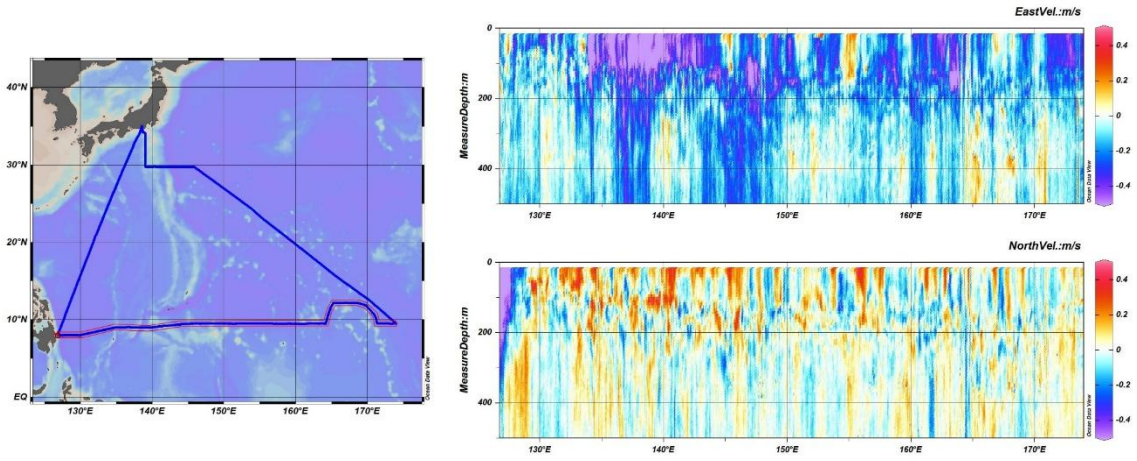

Fig. 3.5-2 Longitude cross section of current profiles along P04W line.

3.6 Ceilometer observation

(1) Personnel

Shinya Kouketsu	JAMSTEC: Principal investigator
Masaki KATSUMATA	JAMSTEC (not on board)
Fumine Okada	Nippon Marine Enterprises, Ltd.（NME）
Satomi Ogawa	NME
Haruna Yamanaka	NME
Masanori Murakami	MIRAI crew

(2) Objectives

The information of cloud base height and the liquid water amount around cloud base is important to understand a process on formation of the cloud. As one of the methods to measure them, the ceilometer observation was carried out.

(3) Parameters

1. Cloud base height [m].
2. Backscatter profile, sensitivity and range normalized at 10 m resolution.
3. Estimated cloud amount [octas] and height [m]; Sky Condition Algorithm.

(4) Methods

Cloud base height and backscatter profile were observed by ceilometer (CL51, VAISALA, Finland). The measurement configurations are shown in Table 3.6-1. On the archive dataset, cloud base height and backscatter profile are recorded with the resolution of 10 m.

Table 3.6-1 The measurement configurations

Property	Description
Laser source	Indium Gallium Arsenide (InGaAs) Diode
Transmitting center wavelength	910±10 nm at 25 degC
Transmitting average power	19.5 mW
Repetition rate	6.5 kHz
Detector	Silicon avalanche photodiode (APD)
Responsibility at 905 nm	65 A/W
Cloud detection range	0 ~ 13 km
Measurement range	0 ~ 15 km
Resolution	10 m in full range
Sampling rate	36 sec.
Sky Condition	Cloudiness in octas (0 ~ 9) 0 Sky Clear 1 Few 3 Scattered 5-7 Broken 8 Overcast 9 Vertical Visibility

(5) Preliminary results

Fig.3.6-1 shows the time series of 1st, 2nd and 3rd cloud base height during the cruise.

(6) Data archives

These data obtained in this cruise will be submitted to the Data Management Group of JAMSTEC and will be opened to the public via "Data Research System for Whole Cruise Information in JAMSTEC (DARWIN)" in JAMSTEC web site.

https://www.godac.jamstec.go.jp/darwin/en

(7) Remarks (Times in UTC)

i) The following time, the window was cleaned.
05:06, 07 Apr. 2025
07:28, 21 Apr. 2025
00:12, 29 Apr. 2025
05:40, 06 May. 2025

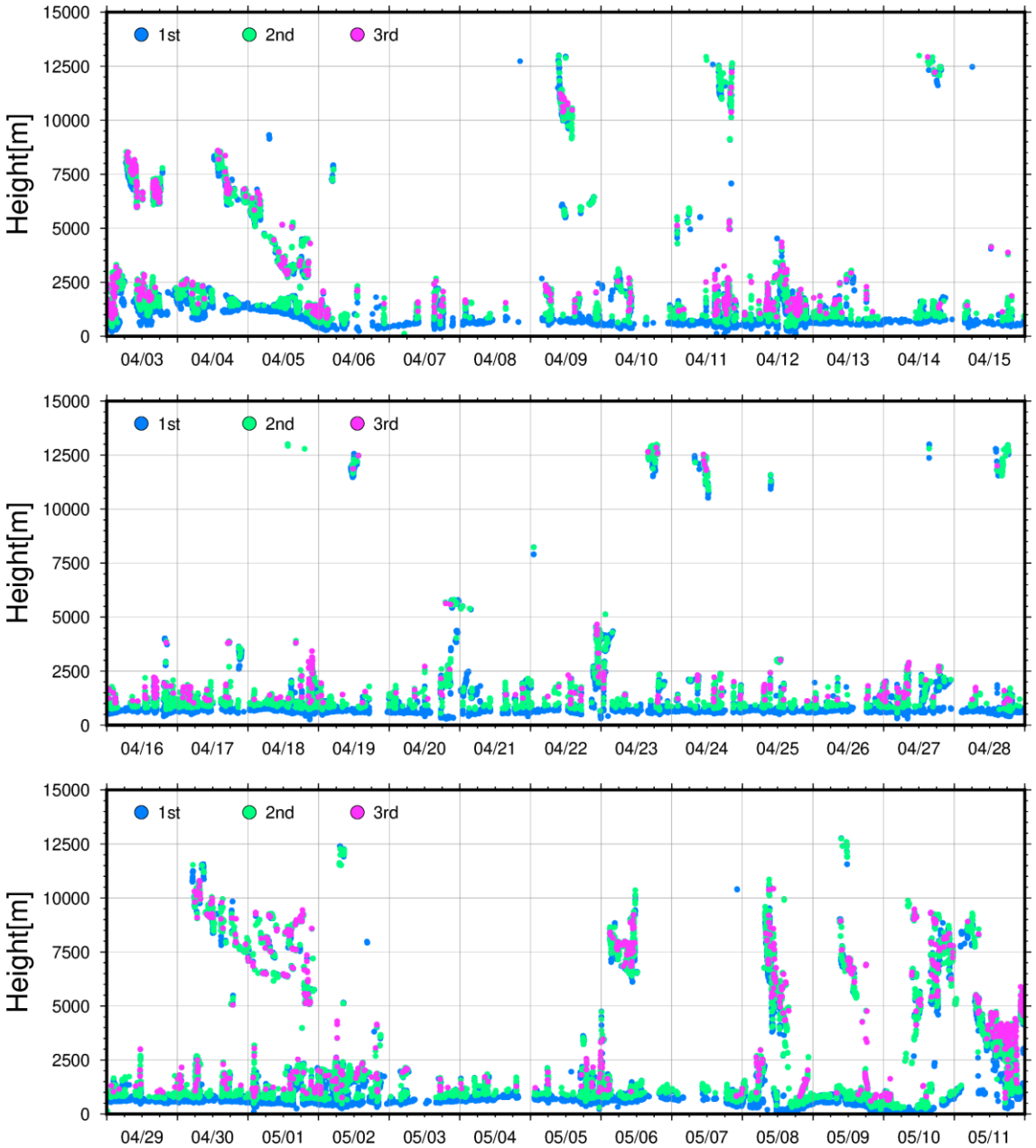

Fig. 3.6-1 1st, 2nd and 3rd cloud base height during this cruise.

3.7 C-band weather radar

(1) Personnel

Masaki KATSUMATA	(JAMSTEC)	Principal Investigator (not on board)
Fumine OKADA	(NME)	Operation Leader
Satomi OGAWA	(NME)	
Haruna YAMANAKA	(NME)	
Masanori MURAKAMI	(Mirai Crew)	

(2) Objective

Weather radar observations in this cruise aim to investigate the structure and evolution of precipitating systems over the tropical ocean.

(3) Radar specifications

The C-band weather radar on board the R/V Mirai is used. The basic specifications of the radar are as follows:

Frequency:	5370 MHz (C-band)
Polarimetry:	Horizontal and vertical (simultaneously transmitted and received)
Transmitter:	Solid-state transmitter
Pulse Configuration:	Using pulse-compression
Output Power:	6 kW (H) + 6 kW (V)
Antenna Diameter:	4 meters
Beam Width:	1.0 degrees
Inertial Navigation Unit:	PHINS (IXBLUE SAS France)

(4) Available radar variables

Radar variables, which are converted from the power and phase of the backscattered signal at vertically- and horizontally-polarized channels, are as follows:

Radar reflectivity:	Z
Doppler velocity:	Vr
Spectrum width of Doppler velocity:	SW
Differential reflectivity:	ZDR
Differential propagation phase:	ΦDP
Specific differential phase:	KDP
Co-polar correlation coefficients:	ρHV

(5) Operational methodology

The antenna is controlled to point the commanded ground-relative direction, by controlling the azimuth and elevation to cancel the ship attitude (roll, pitch, and yaw) detected by the navigation unit. The Doppler velocity is also corrected by subtracting the ship movement in the beam direction.

For maintenance, internal signals of the radar are checked and calibrated at the beginning and the end of the cruise. Meanwhile, the peak output power and the radar's pulse width are checked daily.

During the cruise, the radar is operated as shown in Table 3.7-1. The volume scan (every 6 minutes) was followed by (1) surveillance PPI at every 30 minutes, (2) RHI scans with (1) was absent. Exceptionally for a specific period (see (5)), the RHI scans and the vertical pointing scans were performed alternatively. A dual PRF mode is used for volume scans, while the single PRF mode is used for other scans (surveillance PPI, RHI and vertical pointing scans).

(6) Data

The C-band weather radar observations were conducted continuously during the cruise, except nearby the main islands of Japan.

The observation periods were

from: 2000UTC on 03 April 2025

to: 0400UTC on 11 May 2025.

Note that the vertical pointing scans were performed (alternatively with RHI scans)

from: 0518UTC on 04 May 2025

to: 1746UTC on 05 May 2025.

Analyses of the obtained data, as well as the quality controls, will be performed after the cruise.

(7) Data archive

The obtained data will be submitted to the Data Management Group of JAMSTEC, and will be opened to the public via "Data Research System for Whole Cruise Information in JAMSTEC (DARWIN)" in JAMSTEC web site https://www.godac.jamstec.go.jp/darwin/en .

Table 3.7-1: Scan modes of C-band weather radar

	Surveillance PPI Scan	Volume Scan						RHI Scan	Vertical Point Scan
Repeated Cycle (min.)	30	6						6	(none)
								12(*)	12(*)
Times in One Cycle	1	1						3	3
PRF(s) (Hz)	400	dual PRF (ray alternative)						1250	2000
		667	833	938	1250	1333	2000		
Azimuth (deg)	Full Circle							Option	Full Circle
Bin Spacing (m)	150								
Max. Range (km)	300	150		100		60		100	60
Elevation Angle(s) (deg.)	0.5	0.5		1.0, 1.8, 2.6, 3.4, 4.2, 5.1, 6.2, 7.6, 9.7, 12.2, 15.2		18.7, 23.0, 27.9, 33.5, 40.0		-0.2~ 60.0	90

(* Only for a specific period: See text for further details.)

3.8 Mie / Raman Lidar Observation

(1) Personnel

Masaki KATSUMATA	JAMSTEC
Kyoko TANIGUCHI	JAMSTEC
Fumine OKADA	NME
Satomi OGAWA	NME
Haruna YAMANAKA	NME

(2) Objective

The objective of this observation is to capture the vertical distribution of clouds, aerosols, and water vapor in high spatio-temporal resolution.

(3) Parameters

355nm Mie scattering signal

532nm Mie scattering signal

1064nm Mie scattering signal

387nm Raman nitrogen scattering signal (nighttime only)

408nm Raman water vapor scattering signal (nighttime only)

607nm Raman nitrogen scattering signal (nighttime only)

660nm Raman water vapor scattering signal (nighttime only)

(4) Instruments and methods

The Mirai Lidar system transmits a 10-Hz pulse laser in three wavelengths: 1064nm, 532nm, 355nm. For cloud and aerosol observation, the system detects Mie scattering at these wavelengths. The separate detections of polarization components at 532 nm and 355 nm obtain additional characteristics of the targets. The system also detects Raman water vapor signals at 660 nm and 408nm, Raman nitrogen signals at 607 nm and 387nm at nighttime. Based on the signal ratio of Raman water vapor to Raman nitrogen, the system offers water vapor mixing ratio profiles.

(5) Observation period

3 April 2025 to 11 May 2025 UTC

(6) Preliminary Results

The lidar system observed the lower atmosphere throughout the cruise. All data will be reviewed after the cruise to maintain data quality.

(7) Data Archive

The obtained data will be submitted to the Data Management Group of JAMSTEC, and will be opened to the public via “Data Research System for Whole Cruise Information in JAMSTEC (DARWIN)” in JAMSTEC web site.

https://www.godac.jamstec.go.jp/darwin/en/index.html

3.9 GPS Radiosonde

(1) Personnel

Masaki KATSUMATA	(JAMSTEC)	Principal Investigator (not on board)
Kyoko TANIGUCHI	(JAMSTEC)	(not on board)
Fumine OKADA	(NME)	Operation Leader
Satomi OGAWA	(NME)	
Haruna YAMANAKA	(NME)	
Masanori MURAKAMI	(Mirai Crew)	

(2) Objectives

To obtain atmospheric profile of temperature, humidity, and wind speed/direction, and their temporal variations

(3) Methods

Atmospheric sounding by radiosonde by using system by Vaisala Oyj was carried out. The GPS radiosonde sensor RS-41SGP was utilized. The on-board system to calibrate, to launch, to log the data and to process the data is MW41, which consists of processor (Vaisala, SPS-311), processing and recording software (MW41, ver.2.19.0), GPS antenna (GA20), UHF antenna (RB21), ground check kit for RS41 (RI41), pressure sensor for ground check (Vaisala PTB-330), and balloon launcher (ASAP). The sensor was launched with balloon (Totex TA-200). In case the relative wind to the ship is not appropriate for the launch using ASAP, handy launch was selected.

The radiosondes were launched approximately every 12 hours from Apr. 12 to May 06. In addition, a test launch was made at 00UTC on Apr. 5. In total, 50 launches were carried out as listed in Table 3.9-1.

(4) Preliminary Results

The data will be analyzed after the cruise. The all obtained profiles are plotted on emagram as in the Appendix A.

(5) Data archive

Data were sent to the world meteorological community via Global Telecommunication System (GTS) through the Japan Meteorological Agency, immediately after each observation. The ASCII data, corrected by MW41 software is available for every launch during ascent. Raw data, in the Vaisala original binary format, is also available for every launch during ascent and descent. These datasets will be submitted to the Data Management Group (DMG) of JAMSTEC, and will be opened to the public via “Data Research System for Whole Cruise Information in JAMSTEC (DARWIN)” in JAMSTEC web site https://www.godac.jamstec.go.jp/darwin/en .

(6) Acknowledgment

The operations of handy launch were kindly supported by the onboard scientists.

Table 3.9-1: Radiosonde launch log, with the surface conditions and the reached maximum height.

ID	Nominal Time YYYYMMDDhh	Launched Location		Surface Values					Max Height	Clouds	
		Lat.	Lon.	P	T	RH	WD	WS			
		deg.N	deg.E	hPa	deg.C	%	deg.	m/s	m	Amount	Types
RS001	2025040500	26.516	134.645	1017.0	19.3	50	136	6.1	11885.24	7	Cu、Cs
RS002	2025041200	8.173	130.834	1008.7	29.0	80	110	6.9	27785.96	3	Cu、As、Cs
RS003	2025041212	8.394	131.893	1008.8	28.0	84	47	6.3	27191.22	10	Ns
RS004	2025041300	8.668	133.245	1009.6	29.3	74	64	9.3	26764.01	4	Cu、As
RS005	2025041312	8.938	134.577	1008.3	29.1	73	55	8.0	25445.56	3	Cu
RS006	2025041400	9.000	135.091	1008.4	28.9	74	69	10.0	24847.64	5	Cu、As
RS007	2025041412	9.002	136.174	1007.0	28.6	77	48	8.3	20761.09	4	Cu、As
RS008	2025041500	9.034	136.642	1008.6	28.9	69	68	8.0	27487.39	8	As、Cu
RS009	2025041512	9.006	137.828	1007.7	29.0	77	50	5.6	27619.24	5	Sc、Cu
RS010	2025041600	8.993	138.387	1008.6	29.3	77	93	9.7	27604.32	6	Sc、Cu、As
RS011	2025041612	8.994	139.165	1008.1	29.2	76	67	9.8	23423.75	3	Cu、As
RS012	2025041700	9.039	140.212	1008.6	28.8	70	63	10.9	27168.56	6	Sc、Cu、As
RS013	2025041712	9.189	141.528	1007.6	29.0	76	87	10.6	25578.95	1	unknown
RS014	2025041800	9.284	142.837	1008.4	29.2	72	79	10.9	25342.14	4	Cu、As
RS015	2025041812	9.422	144.110	1007.4	28.9	76	76	9.3	26231.09	3	Cu
RS016	2025041900	9.481	145.486	1008.4	28.9	76	72	8.4	25742.55	7	Sc、As、Cu
RS017	2025041912	9.493	146.619	1008.1	28.6	76	78	8.1	24543.12	1	Sc
RS018	2025042000	9.502	147.797	1008.4	28.6	75	57	7.7	26819.04	4	Sc、Cu
RS019	2025042012	9.497	148.755	1009.2	28.6	77	72	5.4	27150.18	0	
RS020	2025042100	9.493	149.172	1009.6	28.1	75	88	4.6	26287.69	8	As、Sc、Ns
RS021	2025042112	9.491	149.993	1009.6	28.5	75	70	7.2	26939.98	1	Cu
RS022	2025042200	9.493	150.586	1009.0	28.7	74	84	8.0	26303.22	6	Sc、Cu、Ns
RS023	2025042212	9.487	151.120	1008.7	28.3	74	65	5.5	26432.08	0	-
RS024	2025042300	9.494	152.502	1008.8	27.5	80	57	8.4	26365.27	8	Sc、Cu
RS025	2025042312	9.503	153.600	1008.5	28.6	75	77	8.7	27460.42	1	Sc、Cu
RS026	2025042400	9.491	155.059	1008.7	28.9	75	78	8.8	25431.74	6	Sc、Cu、As
RS027	2025042412	9.503	155.807	1009.0	28.6	75	73	11.0	27402.68	unknown	unknown
RS028	2025042500	9.487	156.950	1008.7	28.7	75	73	10.5	25426.02	4	Cu、As、Sc
RS029	2025042512	9.483	158.323	1009.9	28.6	81	66	8.6	26490.01	5	unknown
RS030	2025042600	9.483	159.534	1008.8	28.7	73	78	9.7	27017.98	6	Sc、Cu
RS031	2025042612	9.408	160.831	1009.1	28.5	74	81	8.9	26552.89	5	unknown
RS032	2025042700	9.491	161.651	1008.7	28.5	80	78	9.8	26830.38	8	Sc、Cu
RS033	2025042712	9.497	163.087	1007.9	28.0	74	65	11.5	25719.80	3	Sc、Cu
RS034	2025042800	9.488	164.165	1008.3	28.4	73	66	10.6	26441.92	3	As、Cs
RS035	2025042812	10.834	164.583	1009.5	27.9	77	81	9.5	26320.90	2	unknown
RS036	2025042900	12.168	165.250	1010.3	28.0	75	70	9.7	26714.31	6	Sc、Cu、As
RS037	2025042912	12.178	166.986	1012.0	26.3	77	113	6.1	24867.10	5	Sc、As
RS038	2025043000	12.168	168.064	1011.4	27.9	74	71	10.0	26526.87	5	Sc、Cu、As
RS039	2025043012	11.845	169.711	1011.4	27.5	76	58	10.1	26161.19	1	As
RS040	2025050100	11.003	170.585	1010.3	27.8	78	79	8.5	25311.99	9	Cs、Cu、As
RS041	2025050112	9.730	171.272	1009.6	27.9	81	76	10.0	26530.25	3	unknown
RS042	2025050200	9.494	172.205	1009.5	28.2	77	72	8.5	26702.20	3	Sc、As、Ac
RS043	2025050212	9.487	173.333	1009.5	27.3	81	79	7.6	25077.39	4	Cu、St、Sc
RS044	2025050300	10.061	173.291	1009.5	27.5	79	94	7.4	22196.45	3	Sc、As
RS045	2025050312	11.700	171.261	1010.6	27.1	79	61	7.2	24875.66	5	Cu、Sc、As
RS046	2025050400	13.252	169.145	1011.1	27.6	72	60	7.6	27374.21	3	Sc、Cu
RS047	2025050412	14.734	166.916	1011.9	27.1	76	58	10.8	24734.84	6	Cu
RS048	2025050500	16.145	164.879	1011.9	27.4	69	89	7.6	26055.72	1	Sc、As
RS049	2025050512	17.664	162.827	1012.2	27.1	75	74	9.9	24257.73	6	Cu、Sc、As
RS050	2025050600	19.203	160.729	1012.3	26.1	84	86	14.2	26429.35	7	Ns、Sc

Appendices

A. Atmospheric profiles by the radiosonde observations

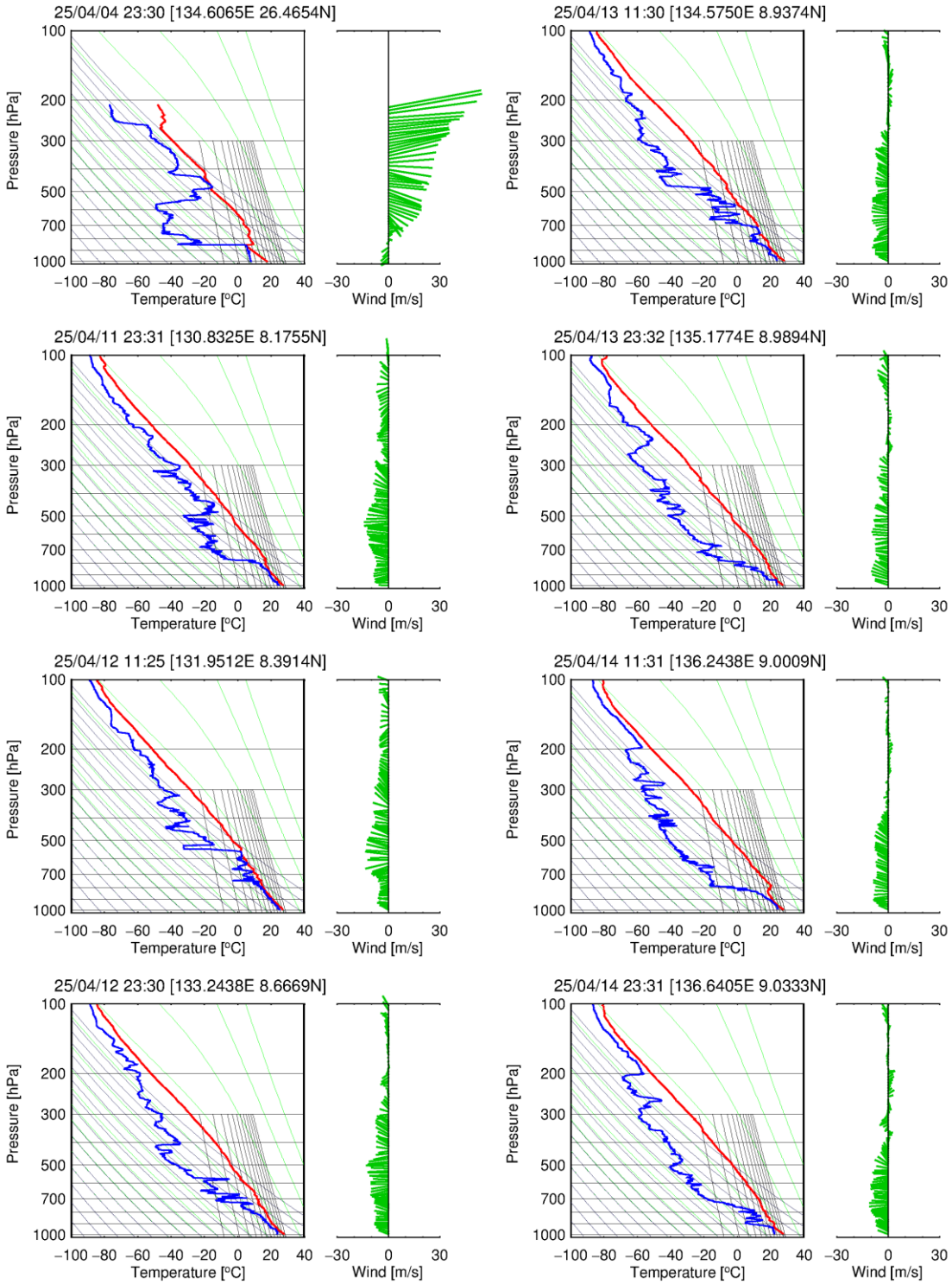

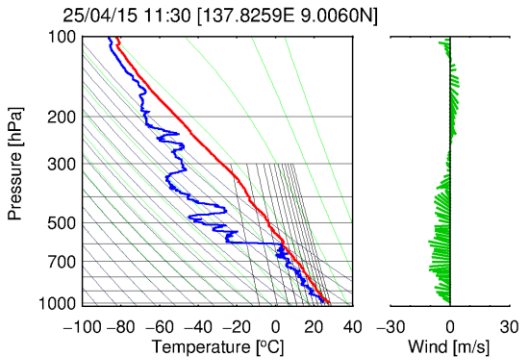
25/04/15 11:30 [137.8259E 9.0060N]
Pressure [hPa]
100
200
300
500
700
1000
−100 −80 −60 −40 −20 0 20 40
Temperature [°C]
−30 0 30
Wind [m/s]

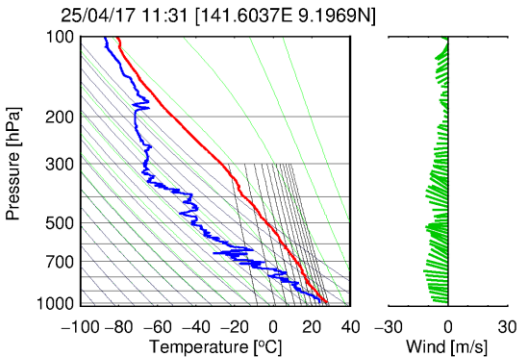
25/04/17 11:31 [141.6037E 9.1969N]
Pressure [hPa]
100
200
300
500
700
1000
−100 −80 −60 −40 −20 0 20 40
Temperature [°C]
−30 0 30
Wind [m/s]

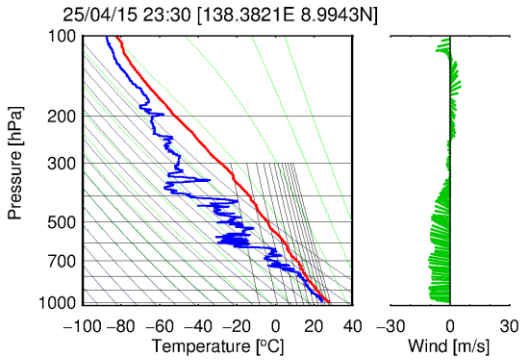
25/04/15 23:30 [138.3821E 8.9943N]
Pressure [hPa]
100
200
300
500
700
1000
−100 −80 −60 −40 −20 0 20 40
Temperature [°C]
−30 0 30
Wind [m/s]

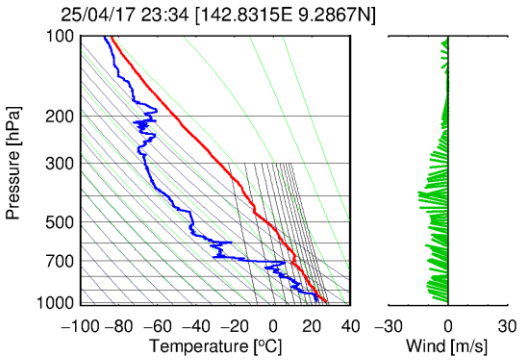
25/04/17 23:34 [142.8315E 9.2867N]
Pressure [hPa]
100
200
300
500
700
1000
−100 −80 −60 −40 −20 0 20 40
Temperature [°C]
−30 0 30
Wind [m/s]

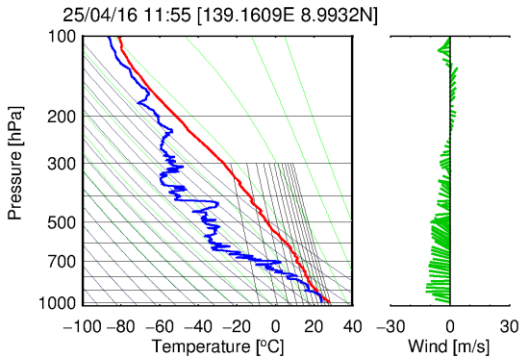
25/04/16 11:55 [139.1609E 8.9932N]
Pressure [hPa]
100
200
300
500
700
1000
−100 −80 −60 −40 −20 0 20 40
Temperature [°C]
−30 0 30
Wind [m/s]

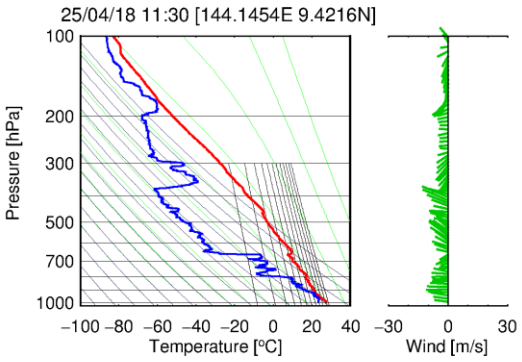
25/04/18 11:30 [144.1454E 9.4216N]
Pressure [hPa]
100
200
300
500
700
1000
−100 −80 −60 −40 −20 0 20 40
Temperature [°C]
−30 0 30
Wind [m/s]

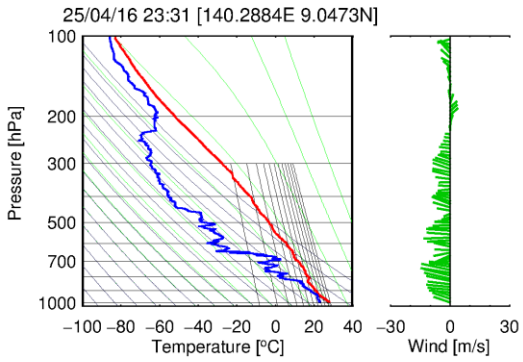
25/04/16 23:31 [140.2884E 9.0473N]
Pressure [hPa]
100
200
300
500
700
1000
−100 −80 −60 −40 −20 0 20 40
Temperature [°C]
−30 0 30
Wind [m/s]

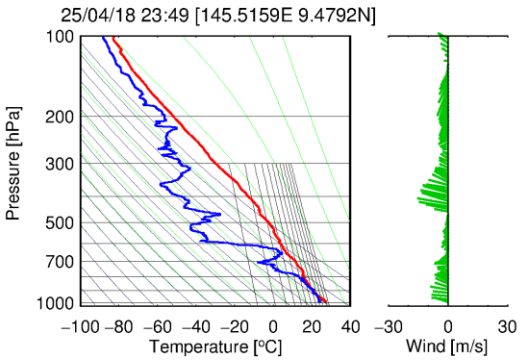
25/04/18 23:49 [145.5159E 9.4792N]
Pressure [hPa]
100
200
300
500
700
1000
−100 −80 −60 −40 −20 0 20 40
Temperature [°C]
−30 0 30
Wind [m/s]

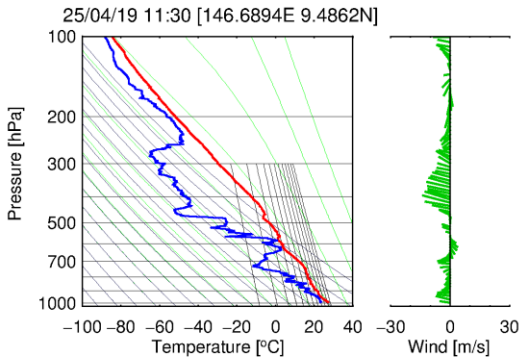
25/04/19 11:30 [146.6894E 9.4862N]
Pressure [hPa]
Temperature [°C]
Wind [m/s]

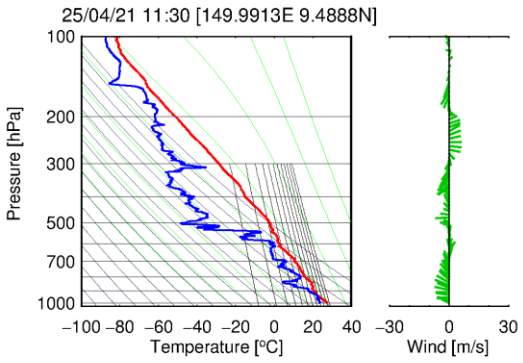
25/04/21 11:30 [149.9913E 9.4888N]
Pressure [hPa]
Temperature [°C]
Wind [m/s]

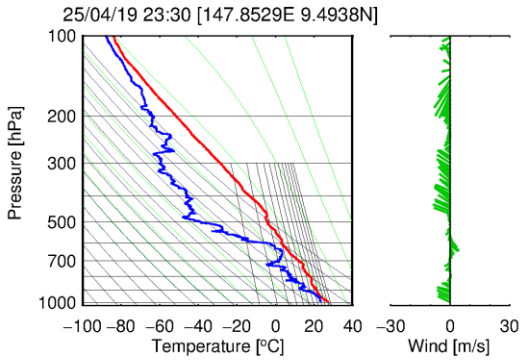
25/04/19 23:30 [147.8529E 9.4938N]
Pressure [hPa]
Temperature [°C]
Wind [m/s]

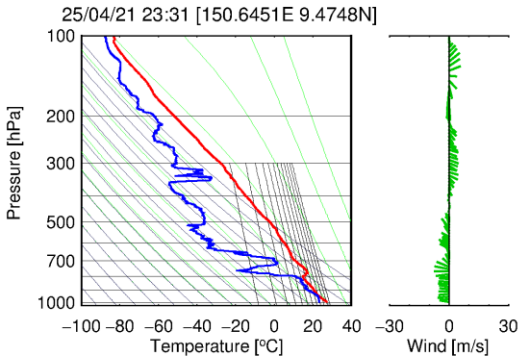
25/04/21 23:31 [150.6451E 9.4748N]
Pressure [hPa]
Temperature [°C]
Wind [m/s]

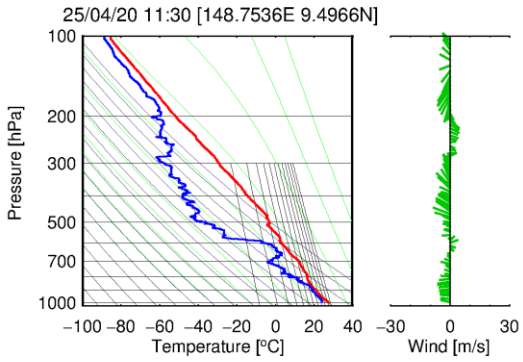
25/04/20 11:30 [148.7536E 9.4966N]
Pressure [hPa]
Temperature [°C]
Wind [m/s]

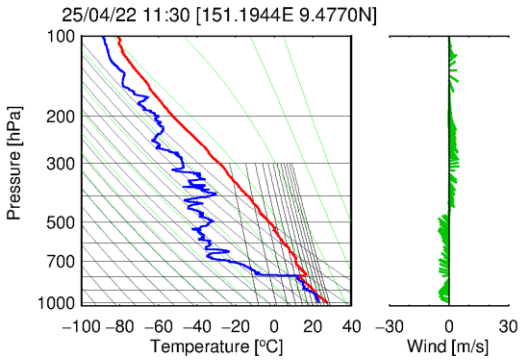
25/04/22 11:30 [151.1944E 9.4770N]
Pressure [hPa]
Temperature [°C]
Wind [m/s]

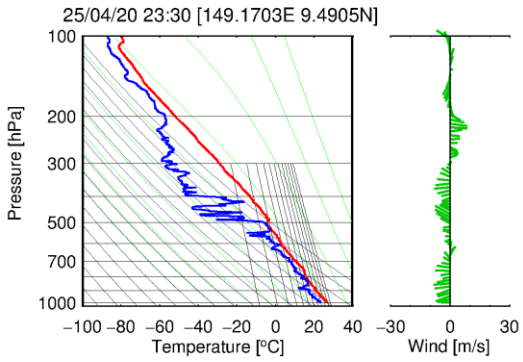
25/04/20 23:30 [149.1703E 9.4905N]
Pressure [hPa]
Temperature [°C]
Wind [m/s]

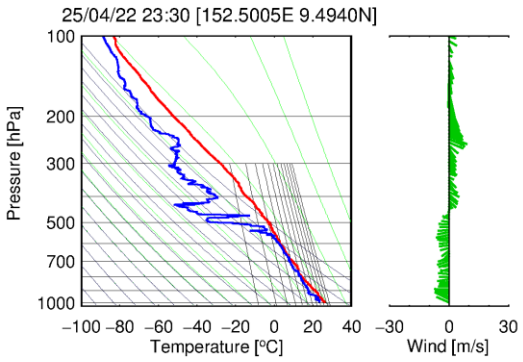
25/04/22 23:30 [152.5005E 9.4940N]
Pressure [hPa]
Temperature [°C]
Wind [m/s]

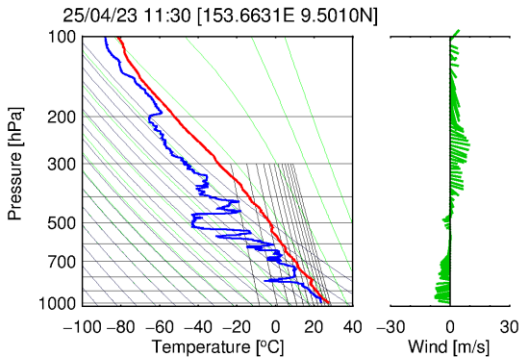
25/04/23 11:30 [153.6631E 9.5010N]
Pressure [hPa]
Temperature [°C]
Wind [m/s]

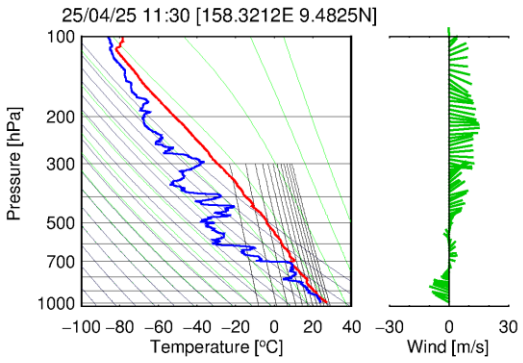
25/04/25 11:30 [158.3212E 9.4825N]
Pressure [hPa]
Temperature [°C]
Wind [m/s]

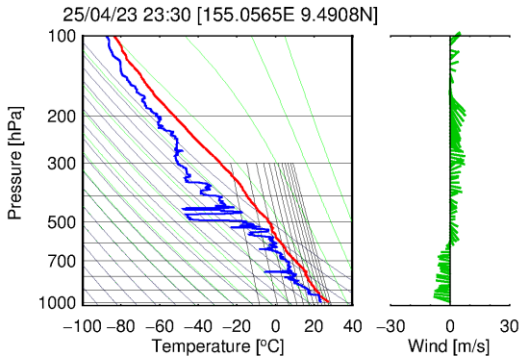
25/04/23 23:30 [155.0565E 9.4908N]
Pressure [hPa]
Temperature [°C]
Wind [m/s]

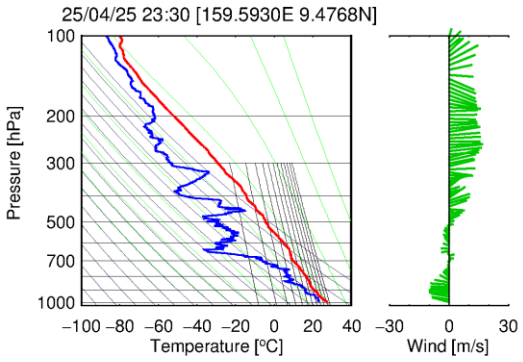
25/04/25 23:30 [159.5930E 9.4768N]
Pressure [hPa]
Temperature [°C]
Wind [m/s]

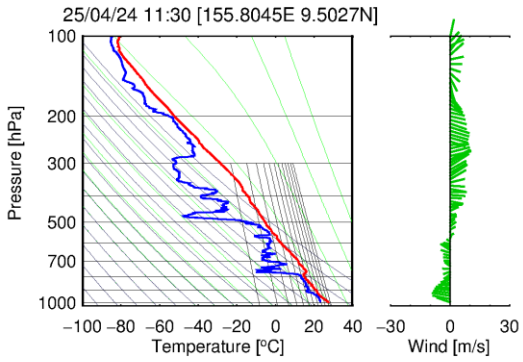
25/04/24 11:30 [155.8045E 9.5027N]
Pressure [hPa]
Temperature [°C]
Wind [m/s]

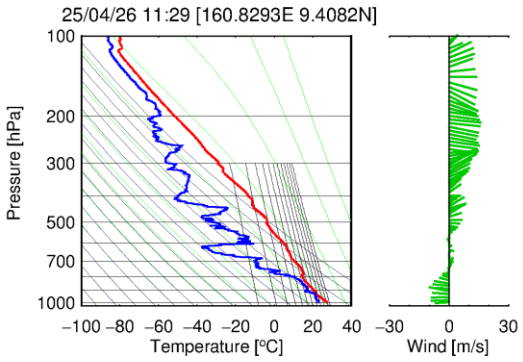
25/04/26 11:29 [160.8293E 9.4082N]
Pressure [hPa]
Temperature [°C]
Wind [m/s]

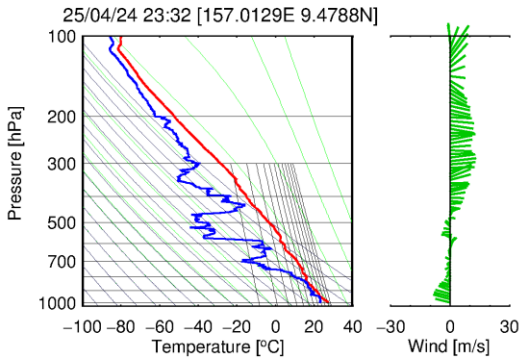
25/04/24 23:32 [157.0129E 9.4788N]
Pressure [hPa]
Temperature [°C]
Wind [m/s]

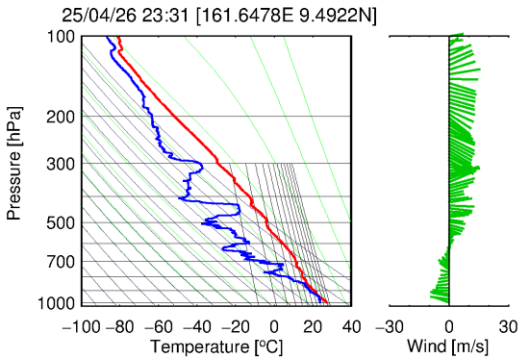
25/04/26 23:31 [161.6478E 9.4922N]
Pressure [hPa]
Temperature [°C]
Wind [m/s]

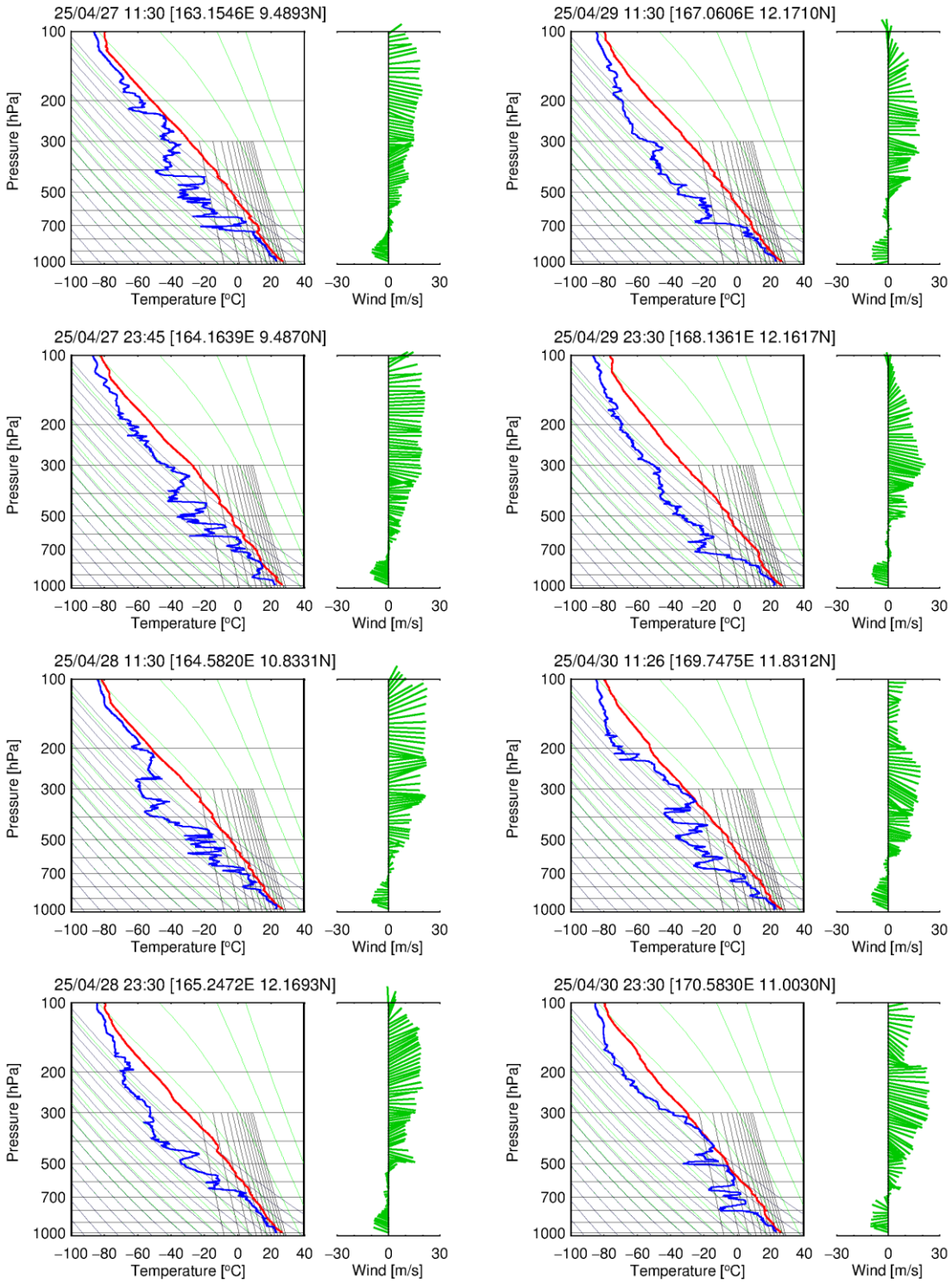
25/04/27 11:30 [163.1546E 9.4893N]
25/04/29 11:30 [167.0606E 12.1710N]
25/04/27 23:45 [164.1639E 9.4870N]
25/04/29 23:30 [168.1361E 12.1617N]
25/04/28 11:30 [164.5820E 10.8331N]
25/04/30 11:26 [169.7475E 11.8312N]
25/04/28 23:30 [165.2472E 12.1693N]
25/04/30 23:30 [170.5830E 11.0030N]
Pressure [hPa]
100
200
300
500
700
1000
−100 −80 −60 −40 −20 0 20 40
Temperature [°C]
−30 0 30
Wind [m/s]

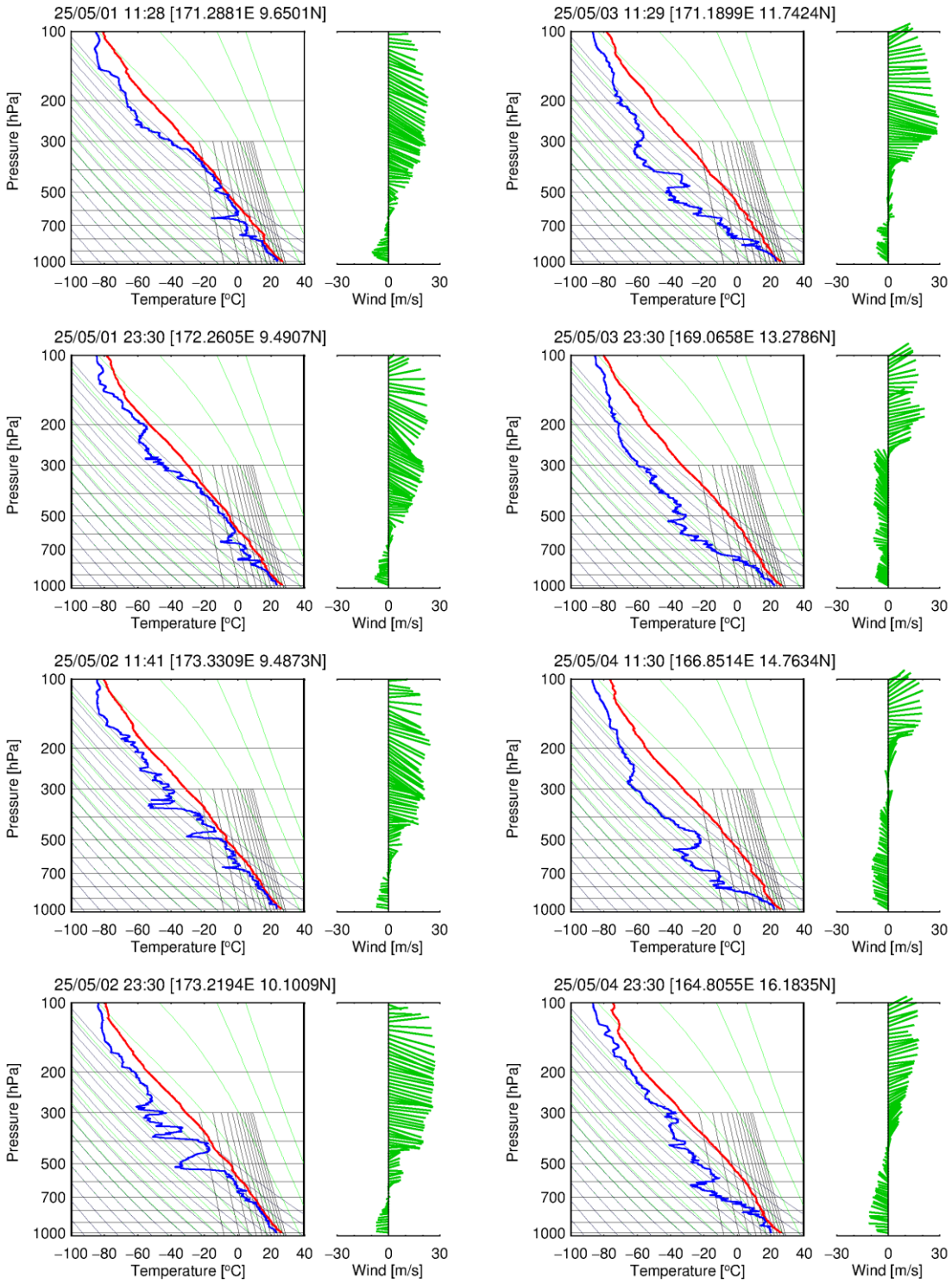
25/05/01 11:28 [171.2881E 9.6501N]
25/05/03 11:29 [171.1899E 11.7424N]
25/05/01 23:30 [172.2605E 9.4907N]
25/05/03 23:30 [169.0658E 13.2786N]
25/05/02 11:41 [173.3309E 9.4873N]
25/05/04 11:30 [166.8514E 14.7634N]
25/05/02 23:30 [173.2194E 10.1009N]
25/05/04 23:30 [164.8055E 16.1835N]
Pressure [hPa]
100
200
300
500
700
1000
−100 −80 −60 −40 −20 0 20 40
Temperature [°C]
−30 0 30
Wind [m/s]

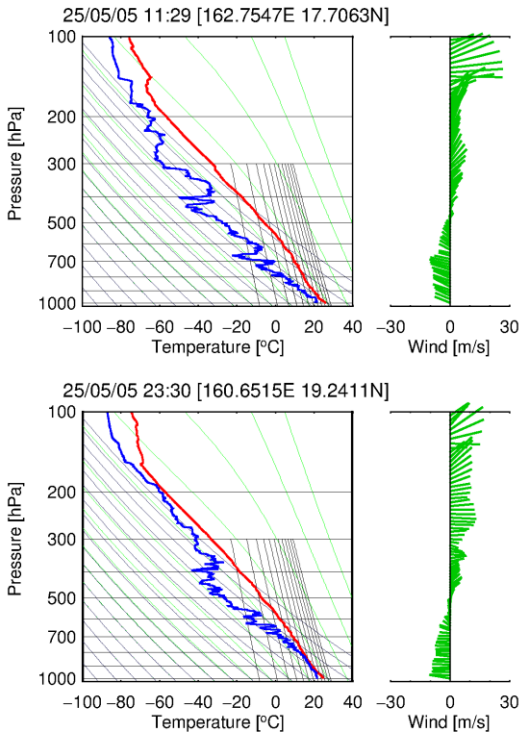
25/05/05 11:29 [162.7547E 17.7063N]
Pressure [hPa]
100
200
300
500
700
1000
−100 −80 −60 −40 −20 0 20 40
Temperature [ºC]
−30 0 30
Wind [m/s]
25/05/05 23:30 [160.6515E 19.2411N]
Pressure [hPa]
100
200
300
500
700
1000
−100 −80 −60 −40 −20 0 20 40
Temperature [ºC]
−30 0 30
Wind [m/s]

3.10 Microwave Radiometer

(1) Personnel

Masaki KATSUMATA	(JAMSTEC)	(not on board)
Akira KUWANO-YOSHIDA	(Kyoto Univ.)	(not on board)
Masahiro MINOWA	(Furuno Electric Co., Ltd.)	(not on board)

(2) Objective

To retrieve the total column integrated water vapor, and the vertical profiles of water vapor and temperature, in the atmosphere

(3) Method

Two microwave radiometers (hereafter MWR; manufactured by Furuno Electric Co., Ltd.) are used. The MWRs received natural microwave within the angle of 20 deg. from zenith. One of the MWRs for the water vapor observes at the frequencies around 22 GHz, to retrieve the column integrated water vapor (or precipitable water), and the vertical profile of the water vapor. The other MWR measures at the frequencies around 55 GHz to retrieve vertical profile of the air temperature. The observation was made approximately every 20 seconds except when periodic auto-calibration was on-going (once in several minutes). The rain sensor is equipped to identify the period of rainfall.

In addition to the MWRs, the whole sky camera was installed beside the MWR. This is to monitor cloud cover, which also affects the microwave signals. The camera obtained the whole-sky image every 2 minutes.

All instruments were installed at the top of the roof of aft wheelhouse, as in Fig. 3.10-1. The data was continuously obtained all through the cruise period.

(4) Results

The data has been obtained all through the cruise. Further analyses for the water vapor (column-integrated amount and vertical profile), the air temperature (vertical profile), etc., will be carried out after the cruise.

(5) Data archive

The data will be submitted to the JAMSTEC Data Management Group (DMG).

(6) Acknowledgment

The observation was supported by the JSPS KAKENHI Grant 23H00519. Nippon Marine Enterprise Ltd. kindly supported the operation.

Fig. 3.10-1: Outlook of the instruments installed at the roof of the aft wheelhouse; the microwave radiometer for the air temperature (right), microwave radiometer for the water vapor (middle), and the whole-sky camera (left).

3.11 Aerosol optical characteristics measured by shipborne sky radiometer

(1) Personel

Kazuma Aoki University of Toyama; not onboard

Sky radiometer operation was supported by Nippon Marine Enterprises, Ltd.

(2) Objectives

Objective of this observation is to study distribution and optical characteristics of marine aerosols by using a ship-borne sky radiometer (POM-01 MK-III: PREDE Co. Ltd., Japan). Furthermore, collections of the data for calibration and validation to the remote sensing data were performed simultaneously.

(3) Instruments and methods

i) Sky radiometer measurement

The sky radiometer measures the direct solar irradiance and the solar aureole radiance distribution with seven interference filters (0.315, 0.4, 0.5, 0.675, 0.87, 0.94, and 1.02 μm). Analysis of these data was performed by SKYRAD.pack version 4.2 developed by Nakajima et al. 1996 and 2020.

ii) Parameters

Aerosol optical thickness at five wavelengths (400, 500, 675, 870 and 1020 nm)

Ångström exponent

Single scattering albedo at five wavelengths

Size distribution of volume (0.01 μm – 20 μm)

GPS provides the position with longitude and latitude and heading direction of the vessel, and azimuth and elevation angle of the sun. Horizon sensor provides rolling and pitching angles.

(4) Data archive

Aerosol optical data are to be archived at University of Toyama (K.Aoki, SKYNET/SKY: http://skyrad.sci.u-toyama.ac.jp/sobs/) after the quality check and will be submitted to JAMSTEC.

(5) References

Nakajima,T., G.Tonna, R.Rao, P.Boi, Y.Kaufman and B.Holben (1996) Use of sky brightness measurements from ground for remote sensing of particulate polydispersions, Appl. Opt., 35, 2672–2686, https://doi.org/10.1364/AO.35.002672.

Aoki. K., T.Takemura, K.Kawamoto, and T.Hayasaka (2013), Aerosol climatology over Japan site measured by ground-based sky radiometer, AIP Conf. Proc. 1531, 284-287 (2013); doi: 10.1063/1.4804762.

Nakajima,T., Campanelli,M., Che,H., Estellés,V., Irie,H., Kim,S.-W., Kim,J., Liu,D., Nishizawa,T., Pandithurai,G., Soni,V.K., Thana,B., Tugjsurn,N.-U., Aoki,K., Hashimoto,M., Higurashi,A., Kazadzis,S., Khatri,P., Kouremeti,N., Kudo,R., Marenco,F., Momoi,M., Ningombam,S. S., Ryder,C.L., and Uchiyama,A.(2020) An overview and issues of the sky radiometer technology and SKYNET, Atmos. Meas. Tech., 13, 4195–4218, 2020, https://doi.org/10.5194/amt-13-4195-2020.

3.12 Trace gas observations over the tropical north Pacific

(1) Personnel

Fumikazu TAKETANI	JAMSTEC - Principal Investigator-	not on board
Yugo KANAYA	JAMSTEC	- not on board
Hisahiro TAKASHIMA	Fukuoka Univ./JAMSTEC	- not on board

Operation for all instruments was supported by Nippon Marine Enterprises, Ltd

(2) Objectives

To investigate roles of trace gases (O_3, CO, and IO etc.) in the marine atmosphere in relation to climate change

(3) Methods

i) CO and O3 observations

Ambient air was continuously sampled on the compass deck and drawn through ~20-m-long Teflon tubes connected to a gas filter correlation CO analyzer (Model 48i-TLE, Thermo Fisher Scientific) and a UV photometric ozone analyzer (Model 205, 2B Tech), located in the Research Information Center. The data will be used for characterizing air mass origins.

ii) Aerosol extinction coefficient (AEC) and trace gases

Multi-Axis Differential Optical Absorption Spectroscopy (MAX-DOAS), a passive remote sensing technique measuring spectra of scattered visible and ultraviolet (UV) solar radiation, was used for atmospheric aerosol and gas profile measurements. MAXDOAS were installed at the deck above stabilizer of ship. Our MAX-DOAS instrument consists of two main parts: an outdoor telescope unit and an indoor spectrometer (Acton SP-2358 with Princeton Instruments PIXIS-400B), connected to each other by a 14-m bundle optical fiber cable. The line of sight was in the directions of the portside of the vessel and the scanned elevation angles were 2, 3, 5, 10, 20, 30, 90 degrees in the 30-min cycle. The roll motion of the ship was measured to autonomously compensate additional motion of the prism, employed for scanning the elevation angle. For the selected spectra recorded with elevation angles with good accuracy, DOAS spectral fitting was performed to quantify the slant column density (SCD) of NO_2 (and other gases) and O_4 (O_2-O_2, collision complex of oxygen) for each elevation angle. Then, the O_4 SCDs were converted to the aerosol optical depth (AOD) and the vertical profile of aerosol extinction coefficient (AEC) using an optimal estimation inversion method with a radiative transfer model. Using derived aerosol information, retrievals of the tropospheric vertical column/profile of NO_2, IO, and other gases were made.

(4) Data archive

These data obtained in this cruise will be submitted to the Data Management Group of JAMSTEC and will be opened to the public via “Data Research System for Whole Cruise Information in JAMSTEC (DARWIN)” in JAMSTEC web site.
<https://www.godac.jamstec.go.jp/darwin/en/index.html >

(5) Acknowledgments

We thank the crew of the R/V Mirai, Fumine OKADA, Tomomi OGAWA, and Haruna YAMANAKA staff of Nippon Marine Enterprises, Ltd., and Dr. Shinya KOUKETSU for their support with observations throughout the cruise.

3.13 Atmospheric and surface seawater pCO_2

January 23, 2026

(1) Personnel

Masahito Shigemitsu (JAMSTEC)

Akihiko Murata (JAMSTEC)

Yumiko Tange (JAMSTEC)

Nagisa Fujiki (MWJ)

Yuta Oda (MWJ)

Tomoki Nakamura (MWJ)

(2) Objectives

The concentration of CO_2 in the atmosphere is now anthropogenically increasing at a rate of about 5.1 PgC yr^{-1} owing to fossil fuel and net land-use change emissions (Friedlingstein et al., 2020). It is an urgent task to estimate as accurately as possible the absorption capacity of the ocean against the increased atmospheric CO_2, and to clarify the mechanism behind the CO_2 absorption, because the magnitude of projected global warming depends on the levels of CO_2 in the atmosphere, and because the ocean currently absorbs ~20% of the 11 Pg of carbon emitted into the atmosphere each year by human activities.

In this cruise, we measured pCO_2 (partial pressure of CO_2) in the atmosphere and surface seawater continuously along cruise tracks in the Pacific in order to quantify how much CO_2 is absorbed in the region. Although the main purpose of the measurement was to collect pCO_2 data, we also measured atmospheric and surface seawater pCH_4.

(3) Apparatus

Atmospheric and surface seawater pCO_2 and pCH_4 were measured with a system having the off-axis integrated-cavity output spectroscopy gas analyzer (Off-Axis ICOS; 911-0011, Los Gatos Research). Standard gases were measured every about 12 hours, and atmospheric air taken from the bow of the ship (approx.13 m above the sea level) were measured every about 3 hours. Seawater was taken from an intake placed at the approximately 4.5 m below the sea surface and introduced into the equilibrator at the flow rate of (4 - 5) L min^{-1} by a pump. The equilibrated air was circulated in a closed loop by a pump at flow rate of (0.6 - 0.7) L min^{-1} through two electric cooling units, a starling cooler, and the Off-Axis ICOS.

(4) Preliminary result

Distributions of atmospheric and surface seawater CO_2 were shown in Figure 3.13.1. Those of CH_4 were displayed in Figure 3.13.2.

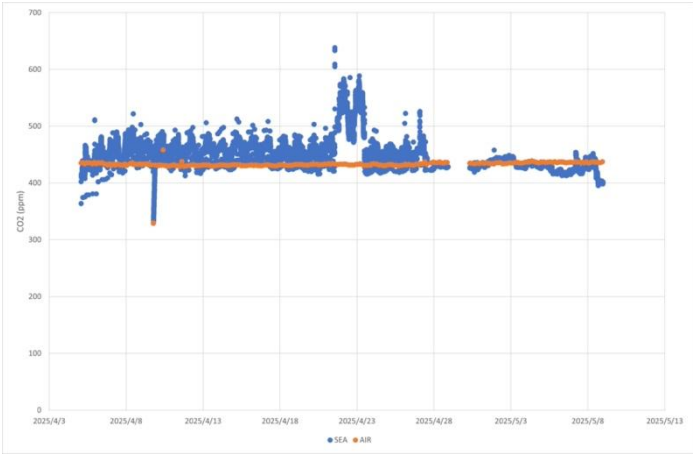

Fig. 3.13-1 Distributions of atmospheric (orange) and surface seawater CO_2 (blue) along the observation line as a function of time

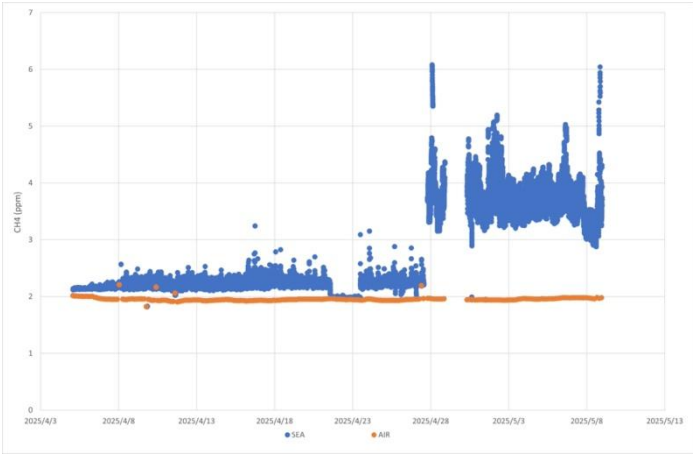

Fig. 3.13-2 Distributions of atmospheric (orange) and surface seawater CH_4 (blue) along the observation line as a function of time

The measurement results of the three standard gases were shown in the following tables. The precisions of pCO_2 and pCH_4 were low, which was probably due to the poor removal of water in the loop.

pCO_2	STD1	STD2	STD3
Average (ppm)	242.05	382.35	437.57
SD (ppm)	0.60	1.42	1.79
n	65	65	65

CH_4	STD1	STD2	STD3
Average (ppm)	1.648	1.928	2.132
SD (ppm)	0.001	0.002	0.002
n	65	65	65

3.14 Satellite image acquisition

(1) Personnel

Shinya Kouketsu	JAMSTEC: Principal investigator
Fumine Okada	Nippon Marine Enterprises, Ltd.（NME）
Satomi Ogawa	NME
Haruna Yamanaka	NME
Masanori Murakami	MIRAI crew

(2) Objectives

The objectives are to collect cloud data in a high spatial resolution mode from the Advance Very High-Resolution Radiometer (AVHRR) on the NOAA and MetOp polar orbiting satellites.

(3) Methods

We received the down link High Resolution Picture Transmission (HRPT) signal from satellites, which passed over the area around the R/V MIRAI. We processed the HRPT signal with the in-flight calibration and computed the brightness temperature. A cloud image map around the R/V MIRAI was made from the data for each pass of satellites. We received and processed polar orbiting satellites data throughout this cruise.

(4) Data archives

These data obtained in this cruise will be submitted to the Data Management Group of JAMSTEC and will be opened to the public via “Data Research System for Whole Cruise Information in JAMSTEC (DARWIN)” in JAMSTEC web site.

https://www.godac.jamstec.go.jp/darwin/en

3.15 Sea Surface Gravity

(1) Personnel

Shinya Kouketsu	JAMSTEC: Principal investigator
Fumine Okada	Nippon Marine Enterprises, Ltd（NME）
Satomi Ogawa	NME
Haruna Yamanaka	NME
Masanori Murakami	MIRAI crew

(2) Introduction

The local gravity is an important parameter in geophysics and geodesy. The gravity data were collected during this cruise.

(3) Parameters

Relative Gravity [CU: Counter Unit]

[mGal] = (coef1: 0.9946) * [CU]

(4) Data Acquisition

The relative gravity using LaCoste and Romberg air-sea gravity meter S-116 (Micro-g LaCoste, LLC) was measured during this cruise. To convert from the relative gravity to absolute one, we measured gravity using portable gravity meter (Scintrex gravity meter CG-5) at Shimizu port as the reference points.

(5) Preliminary Results

Absolute gravity table is shown in Table 3.15-1.

Table 3.15-1. Absolute gravity table of the MR25-02 cruise

No.	Date	UTC	Absolute Gravity Port	Sea Gravity	Ship Level	Gravity at Draft	S-116 Sensor *
	mm/dd		[mGal]	[cm]	[cm]	[mGal]	[mGal]
#1	04/03	22:46	Shimizu	979728.89	221	650	979729.84	11999.62
#2	05/12	23:55	Shimizu	979728.89	224	606	979729.75	11999.39

*:Gravity at Sensor = Absolute Gravity + Sea Level*0.3086/100 + (Draft-530)/100*0.2222

(6) Data archives

These data obtained in this cruise will be submitted to the Data Management Group of JAMSTEC and will be opened to the public via “Data Research System for Whole Cruise Information in JAMSTEC (DARWIN)” in JAMSTEC web site.

https://www.godac.jamstec.go.jp/darwin/en

(7) Remarks (Times in UTC)

i) The following period, sea depth data were invalid.

20:04 - 20:22, 20 Apr. 2025

3.16 Sea Surface Magnetic Field

(1) Personnel

Shinya Kouketsu	JAMSTEC: Principal investigator
Fumine Okada	Nippon Marine Enterprises, Ltd. (NME)
Satomi Ogawa	NME
Haruna Yamanaka	NME
Masanori Murakami	MIRAI crew

(2) Introduction

Measurement of magnetic force on the sea is required for the geophysical investigations of marine magnetic anomaly caused by magnetization in upper crustal structure. We measured geomagnetic field using a three-component magnetometer during this cruise.

(3) Principle of ship-board geomagnetic vector measurement

The relation between a magnetic-field vector observed on-board $\boldsymbol{H_{ob}}$ (in the ship's fixed coordinate system) and the geomagnetic field vector $\boldsymbol{F}$ (in the Earth's fixed coordinate system) is expressed as:

$$\boldsymbol{H_{ob} = A * R * P * Y * F + H_p} \quad \text{(a)}$$

where $\boldsymbol{R}$, $\boldsymbol{P}$ and $\boldsymbol{Y}$ are the matrices of rotation due to roll, pitch and heading of the ship, respectively. $\boldsymbol{A}$ is a 3 x 3 matrix which represents magnetic susceptibility of the ship, and $\boldsymbol{H_p}$ is a magnetic field vector produced by a permanent magnetic moment of the ship's body. Rearrangement of Eq. (a) makes

$$\boldsymbol{B * H_{ob} + H_{bp} = R * P * Y * F} \quad \text{(b)}$$

where $\boldsymbol{B} = \boldsymbol{A^{-1}}$, and $\boldsymbol{H_{bp}} = \boldsymbol{-B * H_p}$. The magnetic field $\boldsymbol{F}$ can be obtained by measuring $\boldsymbol{R}$, $\boldsymbol{P}$, $\boldsymbol{Y}$ and $\boldsymbol{H_{ob}}$, if $\boldsymbol{B}$ and $\boldsymbol{H_{bp}}$ are known. Twelve constants in $\boldsymbol{B}$ and $\boldsymbol{H_{bp}}$ can be determined by measuring variation of $\boldsymbol{H_{ob}}$ with $\boldsymbol{R}$, $\boldsymbol{P}$ and $\boldsymbol{Y}$ at a place where the geomagnetic field $\boldsymbol{F}$ is known.

(4) Instruments on R/V MIRAI

A shipboard three-component magnetometer system (Tierra Tecnica SFG2018) is equipped on-board R/V MIRAI. Three-axes flux-gate sensors with ring-cored coils are fixed on the fore mast. Outputs from the sensors are digitized by a 20-bit A/D converter (1 nT/LSB), and sampled at 8 times per second. Ship's heading, pitch, and roll are measured by the Inertial Navigation System (INS, PHINS). Ship's position and speed data are taken from LAN every second.

(5) Data archives

These data obtained in this cruise will be submitted to the Data Management Group of JAMSTEC and will be opened to the public via “Data Research System for Whole Cruise Information in JAMSTEC (DARWIN)” in JAMSTEC web site.

https://www.godac.jamstec.go.jp/darwin/en

(6) Remarks (Times in UTC)

i) The following periods, we made a “figure-eight” turn (a pair of clockwise and anti-clockwise rotation) for calibration of the ship’s magnetic effect.

11:38 - 12:03, 05 Apr. 2025 around 24-13N, 133-37E

06:47 - 07:09, 21 Apr. 2025 around 09-30N, 150-00E

22:41 - 23:06, 08 May. 2025 around 28-28N, 147-43E

ii) The following period, sea depth data were invalid.

20:04 - 20:22, 20 Apr. 2025

4. Hydrographic Measurements

4.1 $CTDO_2$

4.1.1 Routine measurements of $CTDO_2$

May 10, 2025

(1) Personnel

Hiroshi UCHIDA (JAMSTEC RIGC) (Principal investigator)
Ryohei YAMAGUCHI (JAMSTEC RIGC)
Aine YODA (MWJ) (Operation leader)
Tun Htet Aung (MWJ)
Nobuhiro FUJII (MWJ)
Ko ARIHARA (MWJ)
Shinsuke TOYODA (KANSO Technos)
Chiho SUKIGARA (JAMSTEC RIGC) (not onboard, for ECO backscatter sensor)

(2) Objective

The $CTDO_2$/water sampling measurements were conducted to obtain vertical profiles of seawater properties by sensors and water sampling.

(3) Instruments and method

Instruments used in this cruise are as follows:

Winch and cable

Traction winch system (3.0 ton) (Dynacon, Inc., Bryan, Texas, USA) (Fukasawa et al. 2004)

Armored cable (φ = 9.5 mm) (OCC Corporation, Minato-Mirai, Nishi-ku, Yokohama, Japan)

Compact underwater slip ring swivel (Hanayuu Co., Ltd., Shizuoka, Japan) (Uchida et al. 2018)

Frame

592 kg stainless steel frame for 36-position 12-L water sample bottles

Aluminum rectangular fin (54 × 90 cm) to resist frame's rotation

Water sampler and sampling bottle

36-position carousel water sampler, SBE 32 (Sea-Bird Scientific, Washington, USA)

Serial no. 3254451-0826

12-L sample bottle, model OTE 110 (OceanTest Equipment, Inc., Fort Lauderdale, Florida, USA)

(No TEFLON coating, with Viton O-rings)

Deck unit

SBE11plus (Sea-Bird Scientific, Washington, USA)

Serial no. 11P39850-0705

Underwater unit

Pressure sensor, SBE 9plus (Sea-Bird Scientific, Washington, USA)

Serial no. 09P54451-1027 (117457) (calibration date: December 6, 2024)

Deep ocean standard thermometer, SBE 35 (Sea-Bird Scientific, Washington, USA)

Serial no. 45 (calibration date: February 11, 2025)

Temperature sensor, SBE 3Plus (Sea-Bird Scientific, Washington, USA)

Primary, Serial no. 03P2730 (calibration date: January 18, 2024)

Secondary, Serial no. 03P4418 (calibration date: September 7, 2024)

Conductivity sensor, SBE 4C (Sea-Bird Scientific, Washington, USA)

Primary, Serial no. 041203 (calibration date: February 16, 2024)

Secondary, Serial no. 043036 (calibration date: November 27, 2024)

Dissolved oxygen sensor, Primary, RINKO III (JFE Advantech Co., Ltd., Hyogo, Japan)

Serial no. 0287, Sensing foil no. 163011BA (in situ calibrated on MR23-07 cruise)

Dissolved oxygen sensor, Secondary, SBE 43 (Sea-Bird Scientific, Washington, USA)

Serial no. 430949 (calibration date: December 16, 2023)

Transmissometer, C-Star, (WET Labs, Inc., Philomath, Oregon, USA)

Serial no. 2532DR (calibration date April 05, 2025, calibrated on this cruise)

Chlorophyll fluorometer (Seapoint Sensors Inc., New Hampshire, USA)

Serial no. 3700, Gain: 10X (0-15 ug/L) for stations 1-11

Serial no. 3701, Gain: 10X (0-15 ug/L) for stations 12-80

Ultraviolet fluorometer (Seapoint Sensors Inc., New Hampshire, USA)

Serial no. 6240, Gain setting: 30X (0-50 QSU) for stations 1-8

PAR sensor, PAR-Log ICSW (Sea-Bird Scientific, Washington, USA)

Serial no. 2201 (calibration date: December 16, 2021) for stations 1-6

Serial no. 2180 (calibration date: September 14, 2021) for stations 7-18

Backscatter sensor, ECO BB(RT)D (Sea-Bird Scientific, Washington, USA)

Serial no. BBRTD-9098 (range: 0-3 m^{-1}, output frequency: 1 Hz)

(calibration date: September 13, 2024)

Altimeter, PSA-916T (Teledyne Benthos, Inc.)

Serial no. 1100

Pump, SBE 5T (Sea-Bird Scientific, Washington, USA)

Primary, Serial no. 055816

Secondary, Serial no. 054598

Bottom contact switch (Sea-Bird Scientific, Washington, USA)

Other additional sensors

Upward and downward looking lowered acoustic Doppler current profilers (see section 4.4)

MicroRider (two FP07 micro temperature sensors) (see section 4.5)

Other additional digital sensors (see section 4.1.2)

Software

Data acquisition software, SEASAVE-Win32, version 7.26.7.121

Data processing software, SBEDataProcessing-Win32, version 7.26.7.129 and some original modules

(4) Pre-cruise calibration

(4.1) Pressure

Pre-cruise sensor calibration for linearization was performed at Sea-Bird Scientific. The time drift of the pressure sensor was adjusted by periodic recertification corrections by using electric dead-weight

testers (model E-DWT-H A70M, Fluke Co., Phoenix, Arizona, USA) and a barometer (model RPM4 BA100Ks, Fluke Co.):

Serial no. 181 (A70M) (for 10-70 MPa) (calibration date: January 6, 2023)

Serial no. 1453 (BA100Ks) (for 0 MPa) (calibration date: January 6, 2023)

These reference pressure sensors were calibrated by Ohte Giken, Inc. (Ibaraki, Japan) traceable to National Institute of Standards and Technology (NIST) pressure standards. The pre-cruise correction was performed at JAMSTEC (Kanagawa, Japan) by Marine Works Japan Ltd. (MWJ) (Kanagawa, Japan).

(4.2) Temperature sensors

Pre-cruise sensor calibrations of the SBE 3s were performed at Sea-Bird Scientific. Pre-cruise sensor calibration of the SBE 35s for linearization were also performed at Sea-Bird Scientific. The slow time drift of the SBE 35 was adjusted by periodic recertification corrections by measurements in thermodynamic fixed-point cells (water triple point [0.01 °C] and gallium melt point [29.7646b °C]) (Uchida et al., 2015). Since 2016, pre-cruise calibration was performed at JAMSTEC by using fixed-point cells traceable to National Institute of Standards and Technology (NIST) and National Metrology Institute of Japan (NMIJ) temperature standards (Fig. 4.1-1).

Triple Point of Water cell: serial no. 1094 (model 5901D-Q, Fluke Co.)

Melting Point of Gallium cell: serial no. Ga-43129 (model 5943, Fluke Co.)

Temperature dependency of the SBE 3 was corrected as follows.

Tcor = T + c0 P

where T is raw data, Tcor is corrected temperature, P is pressure in dbar, and c0 is the correction coefficient.

c0 = 2.11007877e-08 (for primary temperature sensor [serial no. 03P2730])

The correction coefficient for the secondary temperature sensor was not determined yet since the secondary sensor was new.

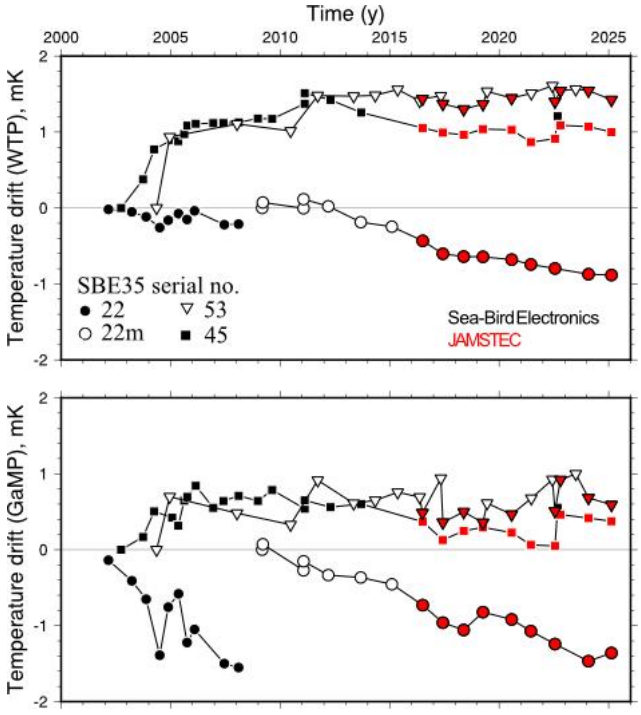

Fig. 4.1-1. Time drifts (temperature offsets relative to the first calibration) of four SBE 35s based on laboratory calibrations in fixed-point cells (water triple point: WTP, gallium melt point: GaMP).

(4.3) Conductivity sensors

Pre-cruise sensor calibrations were performed at Sea-Bird Scientific.

(4.4) Dissolved oxygen sensors

Pre-cruise sensor in-situ calibration of RINKO sensor was performed on the R/V Mirai MR23-07 cruise. Pre-cruise sensor calibration of SBE 43 was performed at Sea-Bird Scientific.

(4.5) Transmissometer

Light transmission (T_r in %) is calibrated as

$$T_r = (V–V_d) / (V_r–V_d) \times 100$$

where V is the measured signal (voltage), V_d is the dark offset for the instrument, and V_r is the signal for clear water. V_d can be obtained by blocking the light path. The calibration coefficients were estimated from the air and dark offset measurements conducted at the beginning of this cruise (April 5, 2025) and the calibration coefficients provided by the manufacturer (calibration date: August 8, 2023) according to the manufacturer's manual (Sea-Bird Scientific 2024).

(4.6) Ultraviolet fluorometer

Pre-cruise laboratory calibration of the ultraviolet fluorometer (FDOM sensor) was performed at JAMSTEC on August 20, 2023 by using deep sea water and ultrapure water.

$$\text{CTDUVFLUORcorr [in RU]} = c0 \times \{(\text{CTDUVFLUOR} – \text{Voffset})/(1.0 + \rho \times [T – Tr])\}$$

$$\rho = –0.0048, \text{Voffset} = 0.1505, c0 = 0.06464499$$

where CTDUVFLUOR is the raw sensor data (in volt), T is temperature (in °C) and Tr is reference temperature (20 °C). The c0 was determined from fdom measurement for the seawater by using a benchtop FDOM meter.

(4.7) Chlorophyll fluorometer, PAR, backscatter sensor, altimeter

Periodic recertification was not performed by the manufacturer for these sensors.

(5) Data Collection and processing

(5.1) Data collection

The CTD system was powered on at least 15 minutes in advance of data acquisition to stabilize the pressure sensor. The data was acquired at least two minutes before and after the CTD cast to collect atmospheric pressure data on the ship's deck.

The CTD package was lowered into the water from the starboard side and held 10 m beneath the surface to activate the pump. After the pump was activated, the package was lifted to the surface and lowered at a rate of 1.0 m/s to 200 m then the package was stopped to operate the heave compensator of the crane. The package was lowered again and at 1.0m/s and after passing the depths where vertical gradient of water properties was large, it was lowered at a rate of 1.2m/s to the bottom. For the up cast, the package was lifted at a rate of 1.2 m/s except for bottle firing stops. As a rule, the bottle was fired after waiting from the stop for more than 30 seconds and the package was stayed at least 5 seconds for measurement of the SBE 35 at each bottle firing stops. For depths where vertical gradient of water properties was expected to be large, the bottle was fired after waiting from the stop for 60 seconds to enhance changing the water between inside and outside of the bottle. At 200m from the surface, the package was stopped to stop the heave compensator of the crane.

The water sample bottles and the stainless-steel frame of the CTD package were wiped with acetone before a cast taken for CFCs.

(5.2) Data collection problems

There were shifts in PAR sensor (serial no. 2201) output voltage to zero at station 2 (from 4370 dbar to 199 dbar of up cast), station 3 (from 4670 dbar of down cast to 117dbar of up cast), station 4 (from 4641 dbar of down cast to 104 dbar of up cast), station 5 (from 4250 dbar of down cast to 192 dbar of up cast), station 6 (from 2915 dbar of down cast to 73 dbar of up cast). We tried cleaning the connectors and changing cables in between those casts, but the problem remained, so, PAR sensor was replaced with a spare one (serial no. 2180) after station 6. Again, from station 9 to station 18, PAR

sensor output voltage again shifted to zero, mostly from about 800 dbar to surface, and occasionally during the surface layer of down cast. We tried cleaning connectors and changing cables in between casts but the problem remained, so, PAR sensor was removed after station 18.

At station 5, there was a shift in ultraviolet fluorometer output from 4200 dbar of up cast to surface. The sensor output profile was irregular during stations 6 and 7. The output became zero at 4492 dbar during down cast at station 8. The sensor was removed after this cast.

At station 9 cast 2, there was a slight shift in chlorophyll fluorometer (serial no. 3700) data at about 4708 dbar during up cast. At station 10, it again shifted at about 714 dbar during down cast. The sensor connector was cleaned, and the cable resistance was checked but no problem was found. At station 10, there was a slight shift in data at about 1075 dbar and then the sensor output became zero from 4046 dbar during up cast. The fluorometer was changed to a spare one (serial no. 3701) after this cast. At station 54, the sensor shifted at 3601 dbar during down cast (see subsection 6.6 below).

At station 1, the bottom contact switch (BCS) alarm sounded about 10 dbar from surface. CTD was recovered and BCS and its cable were replaced with spare ones, and CTD was redeployed without problem. At station 49, 230 dbar during down cast, BCS alarm sounded. After multiple attempts of stopping and lowering again, the issue still remained so CTD package was recovered. Upon inspection, it was found that the Dyneema rope used to hang the weight of BCS was damaged about a length of 14 cm. It was speculated that something was pulling up the rope, causing the BCS alarm to sound. The rope was replaced and CTD was deployed again without problem.

At station 4, near the bottom, the operator confused the unit of decibar with meter on operational PC displays. The echo sounder depth showed about 5720 m, so CTD was stopped at 5710 dbar, mistaking that it was 5710 m, and fired the bottle intended to be fired at bottom minus 10 m depth. After realizing that CTD was not at bottom minus 10 m depth, CTD was lowered again to bottom minus 10 m depth and fired another the bottle, which was initially intended to be fired at 5640 dbar.

(5.3) Data Processing

The following are the data processing software (SBEDataProcessing-Win32) and original software data processing module sequence and specifications used in reduction of CTD data in this cruise.

(The process in order)

DATCNV converted the raw data to engineering unit data. DATCNV also extracts bottle information where scans were marked with the bottle confirm bit during acquisition. The scan duration to be included in bottle file was set to 4.4 seconds, and the offset was set to 0.0 seconds. The hysteresis correction for the SBE 43 data (voltage) was applied for both profile and bottle information data.

TCORP (original module, version 1.1) corrected the pressure sensitivity of the temperature (SBE3) sensor for both profile and bottle information data.

RINKOCOR (original module, 1.0) corrected the time-dependent, pressure-induced effect (hysteresis) of the RINKOIII profile data.

RINKOCORROS (original module) corrected the time-dependent, pressure-induced effect (hysteresis) of the RINKOIII bottle information data by using the hysteresis-corrected profile data.

BOTTLESUM created a summary of the bottle data. The data were averaged over 4.4 seconds.

ALIGNCTD converted the time-sequence of sensor outputs into the pressure sequence to ensure that all calculations were made using measurements from the same parcel of water. For a SBE 9plus CTD with the ducted temperature and conductivity sensors and a 3000-rpm pump, the typical net advance of the conductivity relative to the temperature is 0.073 seconds. So, the SBE 11plus deck unit was set to advance the primary and the secondary conductivity for 1.73 scans (1.75/24 = 0.073 seconds). Oxygen data are also systematically delayed with respect to depth mainly because of the long time constant of the oxygen sensor and of an additional delay from the transit time of water in the pumped plumbing line. This delay was compensated by 5 seconds advancing the SBE 43 oxygen sensor output (voltage) relative to the temperature data. Delay of the RINKOIII data was also compensated by 1 second advancing sensor output (voltage) relative to the temperature data. Delay of the transmissometer data was also compensated by 2 seconds advancing sensor output (voltage) relative

to the temperature data.

WILDEDIT marked extreme outliers in the data files. The first pass of WILDEDIT obtained the accurate estimate of the true standard deviation of the data. The data were read in blocks of 1000 scans. Data greater than 10 standard deviations were flagged. The second pass computed a standard deviation over the same 1000 scans excluding the flagged values. Values greater than 20 standard deviations were marked bad. This process was applied to pressure, depth, temperature, conductivity, and SBE 43 output.

CELLTM used a recursive filter to remove conductivity cell thermal mass effects from the measured conductivity. Typical values for SBE 9plus with TC duct and 3000 rpm pump which were 0.03 for thermal anomaly amplitude alpha and 7.0 for the time constant 1/beta were used.

FILTER performed a low-pass filter on pressure and depth with a time constant of 0.15 second. In order to produce zero phase lag (no time shift) the filter runs forward first then backward.

WFILTER performed as a median filter to remove spikes in transmissometer data, fluorometer data, and ultraviolet fluorometer data. A median value was determined by 49 scans of the window.

SECTIONU (original module, version 1.1) selected a time span of data based on scan number in order to reduce a file size. The minimum number was set to be the starting time when the CTD package was beneath the sea-surface after activation of the pump. The maximum number was set to be the end time when the depth of the package was 1 dbar below the surface. The minimum and maximum numbers were automatically calculated in the module.

LOOPEDIT marked scans where the CTD was moving less than the minimum velocity of 0.0 m/s (traveling backwards due to ship roll).

DESPIKE (original module, version 1.0) removed spikes of the data. A median and mean absolute deviation was calculated in 1-dbar pressure bins for both down and up cast, excluding the flagged values. Values greater than 4 mean absolute deviations from the median were marked bad for each bin. This process was performed twice for temperature, conductivity and RINKOIII output.

DERIVE was used to compute dissolved oxygen (SBE43), salinity, potential temperature, and sigma-theta.

BINAVG averaged the data into 1-decibar pressure bins and 1-sec time bins. The center value of the first bin was set equal to the bin size. The bin minimum and maximum values are the center values plus and minus half the bin size. Scans with pressures greater than the minimum and less than or equal to the maximum were averaged. Scans were interpolated so that a data recorded exist every dbar.

BOTTOMCUT (original module, version 0.1) deleted the deepest pressure bin when the averaged scan number of the deepest bin was smaller than the average scan number of the bin just above.

SPLIT was used to split data into down cast and up cast.

Remaining spikes in the CTD data were manually eliminated from the 1-dbar-averaged data. And the data gaps resulting from the elimination were linearly interpolated with a quality flag of 6. The detailed information above these irregularities is recorded in the remarks sheet which will be included data submission.

(6) Post-cruise calibration

(6.1) Pressure

The CTD pressure sensor offset (-0.13 dbar) in the period of the cruise was estimated from the pressure readings on the ship's deck at the pre- and post-cast by subtracting the atmospheric pressure deviation from a standard atmospheric pressure (1013.25 hPa) (Fig. 4.1-2). The post-cruise correction of the pressure data is not deemed necessary for the pressure sensor.

(6.2) Temperature

The CTD temperature sensors (SBE 3) were calibrated with the SBE 35 under the assumption that discrepancies between SBE 3 and SBE 35 data were due to pressure sensitivity, the viscous heating effect, and time drift of the SBE 3 (Uchida et al., 2015). The CTD temperature was calibrated as

Calibrated temperature = T – (c0 × P + c1 × t + c2)

where T is CTD temperature in °C, P is pressure in dbar, t is time in days from pre-cruise calibration date of the CTD temperature and c0, c1, and c2 are calibration coefficients. The coefficients for the primary temperature sensor were determined using the data for the depths deeper than 1950 dbar.

c0 = 4.40676590e-08, c1 = -4.04904e-08, c2 = -2.6527e-04 (for primary sensor)

c0 = -5.36360913e-08, c1 = -5.74690e-06, c2 = 1.7971e-03 (for secondary sensor)

The results of the post-cruise calibration for the CTD temperature are shown in Figs 4.1-3 and 4.1-4.

The secondary temperature data were calibrated to use for station 48 cast 2.

(6.3) Conductivity

The discrepancy between the CTD conductivity and the conductivity calculated from the bottle sampled salinity data with the CTD temperature and pressure data is considered to be a function of conductivity, pressure and time. The CTD conductivity was calibrated as

Calibrated conductivity = C – (c0 × C + c1 × P + c2 × C × P + c3 × C^2 + c4 × t + c5)

where C is CTD conductivity in S/m, P is pressure in dbar, t is time in days and c0 – c5 are calibration coefficients. The coefficients for the primary conductivity sensor were determined.

c0 = 1.8231847793e-03, c1 = 6.4317690457e-07, c2 = -1.9036490392e-07,

c3 = -2.2633135740e-04, c4 = 3.6317749325e-06, c5 = -3.5840418921e-03

(for primary conductivity sensor)

c0 = 9.0484552054e-04, c1 = 6.2537359748e-07, c2 = -1.9123705124e-07,

c3 = -6.2440509127e-05, c4 = 5.7868495663e-06, c5 = -2.2439692672e-03

(for secondary conductivity sensor)

The results of the post-cruise calibration for the CTD salinity are shown in Figs. 4.1-5 and 4.1-6.

The secondary conductivity data were calibrated to use for station 48 cast 2.

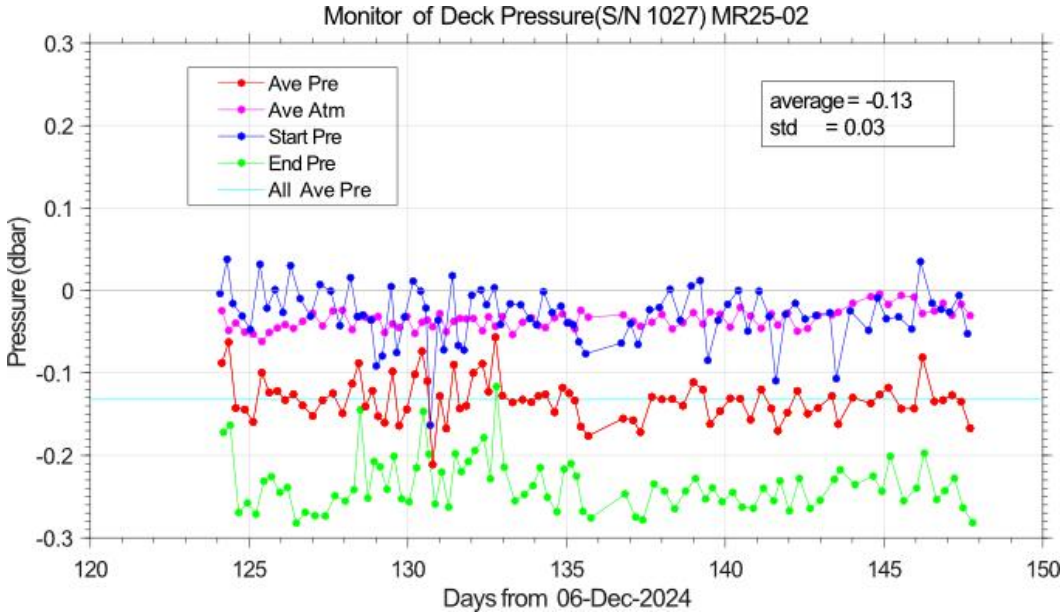

Fig. 4.1-2. Time series of the CTD deck pressure. Atmospheric pressure deviation (magenta dots) from a standard atmospheric pressure was subtracted from the CTD deck pressure. Blue and green dots indicate pre- and post-cast deck pressures, respectively. Red dots indicate averages of the pre- and the post-cast deck pressures.

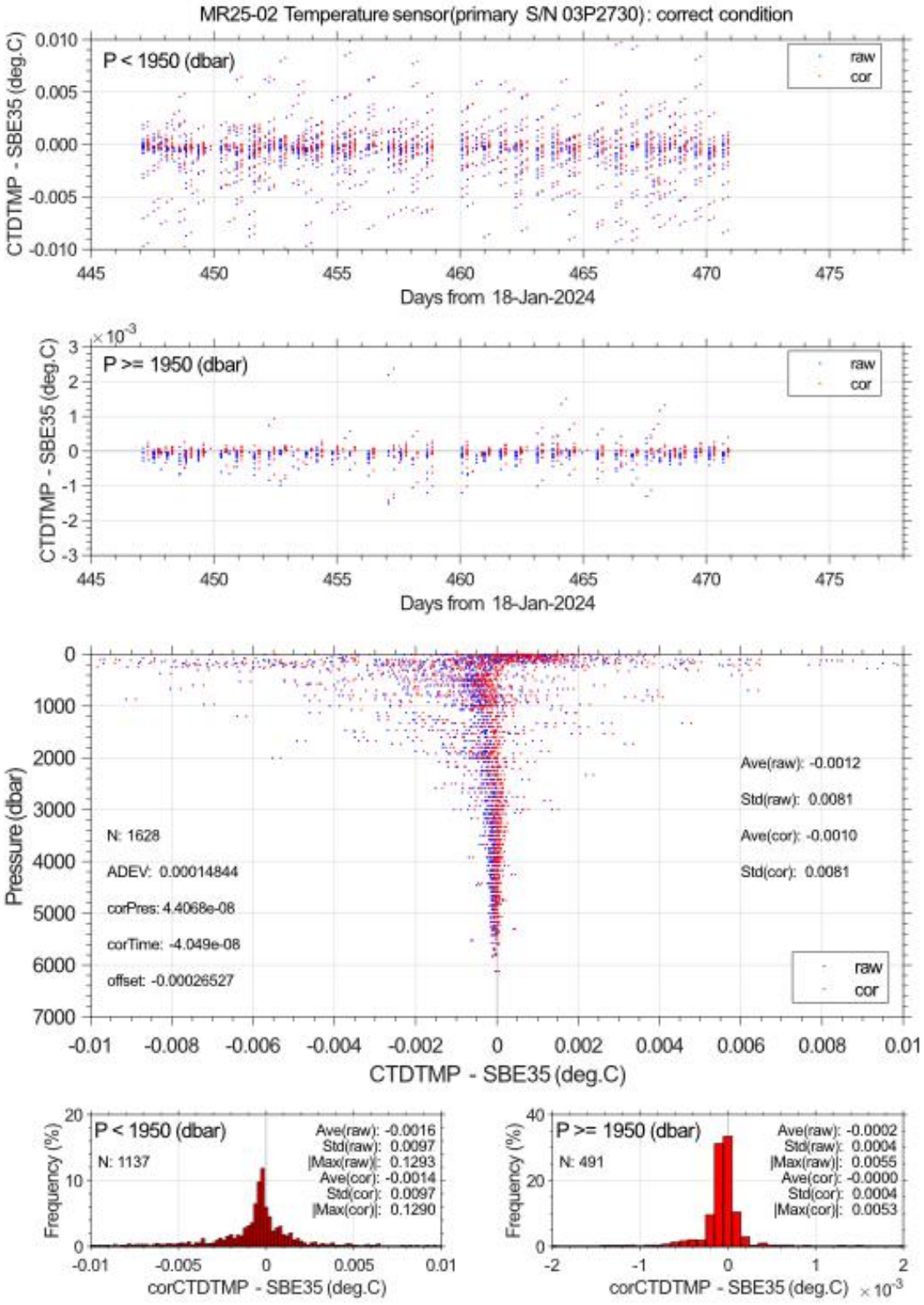

Fig. 4.1-3. Difference between the CTD temperature (primary) and the SBE 35. Blue and red dots indicate before and after the post-cruise calibration using the SBE 35 data, respectively.

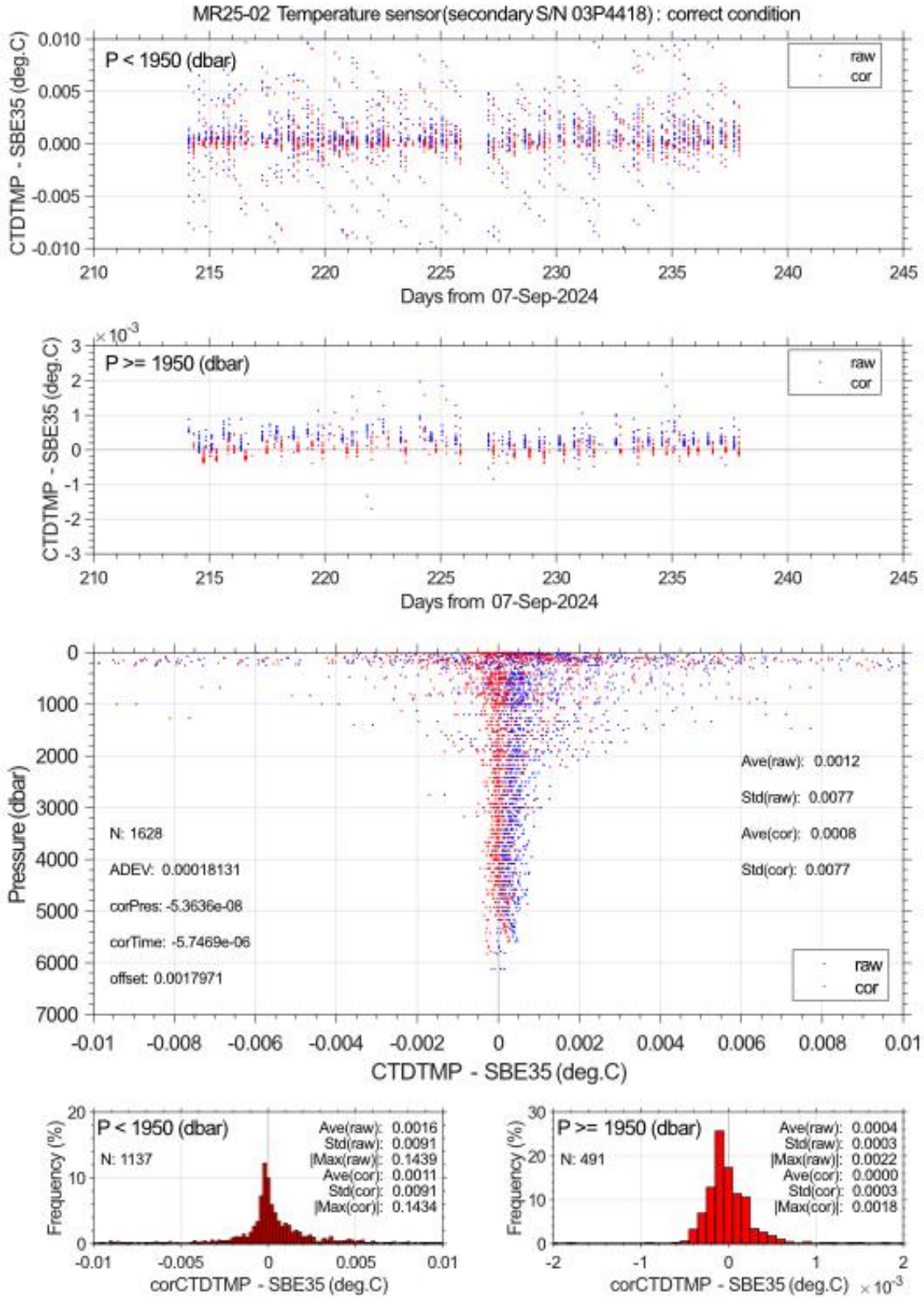

Fig. 4.1-4. Same as Fig. 4.1-3, but for secondary temperature sensor.

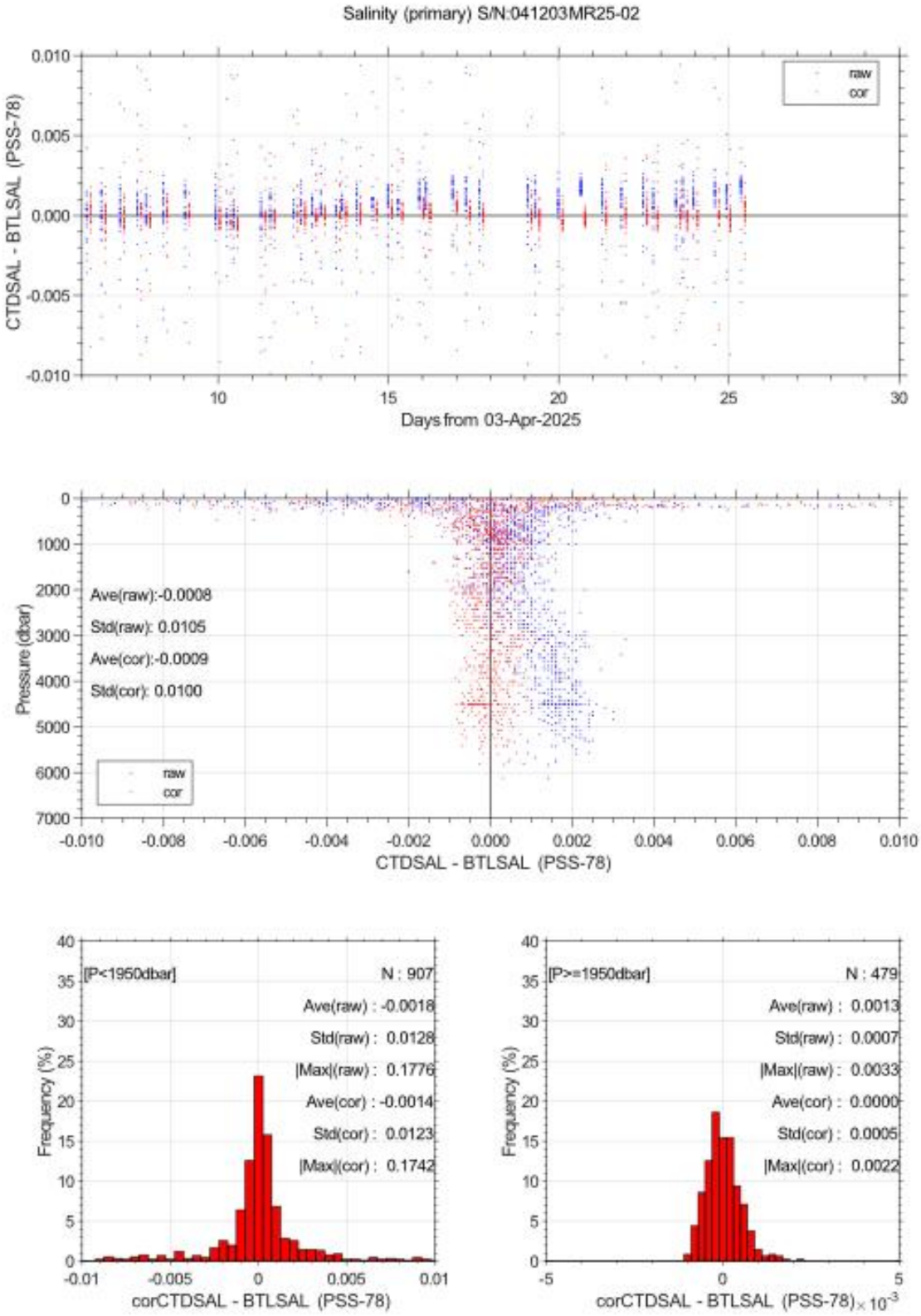

Fig. 4.1-5. Difference between the CTD salinity (primary) and the bottle salinity. Blue and red dots indicate before and after the post-cruise calibration, respectively.

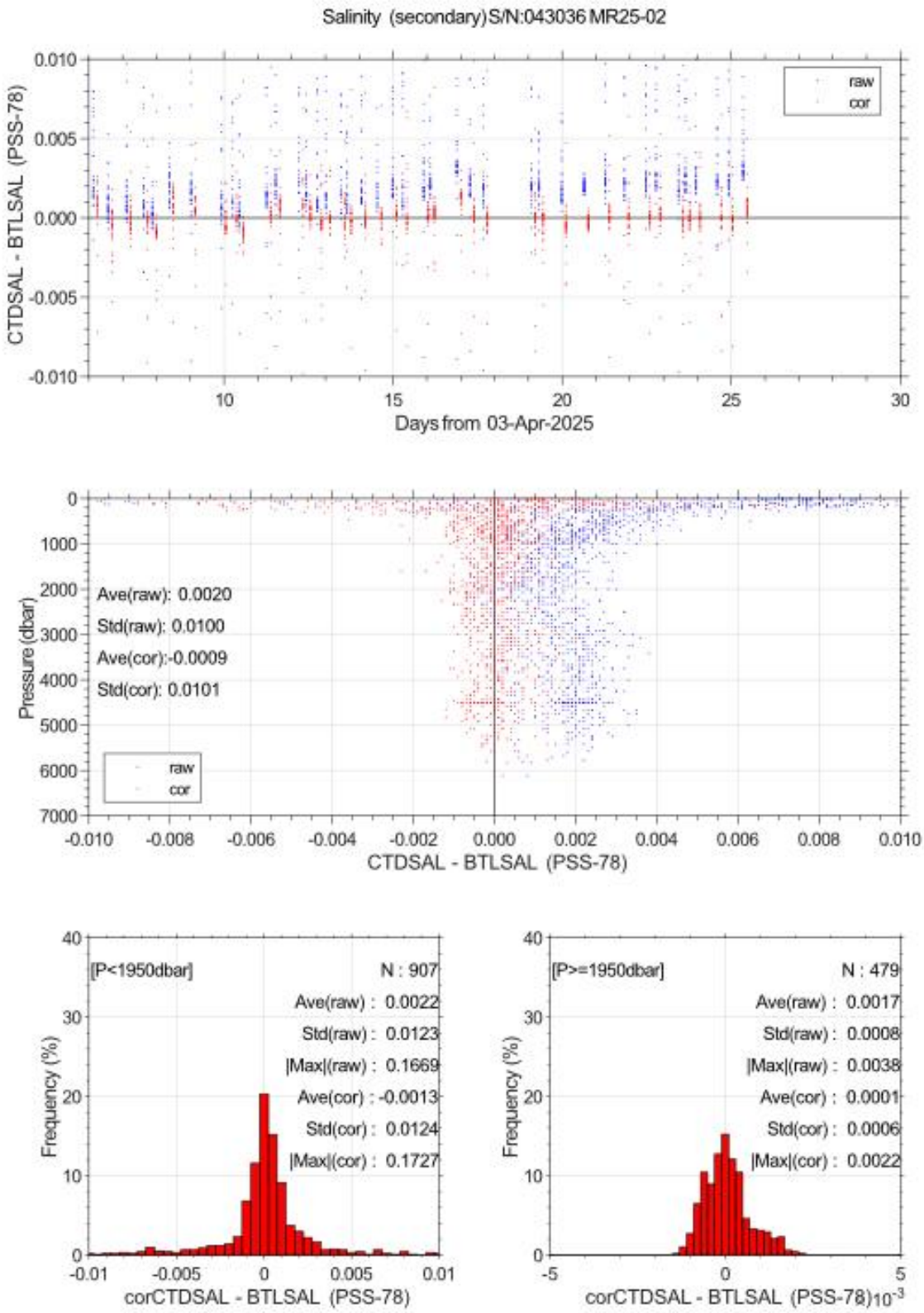

Fig. 4.1-6. Same as Fig. 4.1-5, but for the CTD salinity (secondary).

(6.4) Dissolved oxygen

Data from the RINKO can be corrected for the time-dependent, pressure-induced effect by means of the same method as that developed for the SBE 43 (Edwards et al., 2010). The calibration coefficients, H1 (amplitude of hysteresis correction), H2 (curvature function for hysteresis), and H3 (time constant for hysteresis) were determined to minimize the down cast and up cast data.

H1 = 0.004, H2 = 5000.0, H3 = 2000.0

Outputs from RINKO are the raw phase shift data. The RINKO can be calibrated by the modified Stern-Volmer equation slightly modified from a method by Uchida et al. (2010):

$$O_2\ (\mu mol/l) = [(V0 / V)^E - 1] / Ksv$$

where V is voltage, V0 is voltage in the absence of oxygen, Ksv is Stern-Volmer constant. The coefficient E corrects nonlinearity of the Stern-Volmer equation. The V0 and the Ksv are assumed to be functions of temperature as follows.

$$Ksv = c0 + c1 \times T + c2 \times T^2$$

$$V0 = 1 + d0 \times T$$

$$V = d1 + d2 \times Vb + d3 \times t + d4 \times t \times Vb + d5 \times t2 \times Vb$$

where T is CTD temperature (°C) and Vb is raw output (volts). V0 and V are normalized by the output in the absence of oxygen at 0°C, and t is working time (days) integrated from the fist CTD cast. The oxygen concentration is calculated using accurate temperature data from the CTD temperature sensor instead of temperature data from the RINKO. The pressure-compensated oxygen concentration O2c can be calculated as follows.

$$O2c = O2\ (1 + cp \times P / 1000)$$

where P is CTD pressure (dbar) and cp is the compensation coefficient. Since the sensing foil of the optode is permeable only to gas and not to water, the optode oxygen must be corrected for salinity. The salinity-compensated oxygen can be calculated by multiplying the factor of the effect of salt on the oxygen solubility (Garcia and Gordon, 1992).

c0 = 4.528709702978711e-03, c1 = 1.750470542262877e-04, c2 = 3.847419918700986e-06,

d0 = -1.159542363232624e-03, d1 = -1.090002323120869e-01, d2 = 3.237022115274463e-01,

d3 = 3.173832615146149e-04, d4 = 9.340368532624542e-05,

E = 1.2, cp = 0.027

The results of the post-cruise calibration for the RINKO oxygen are shown in Figs. 4.1-7.

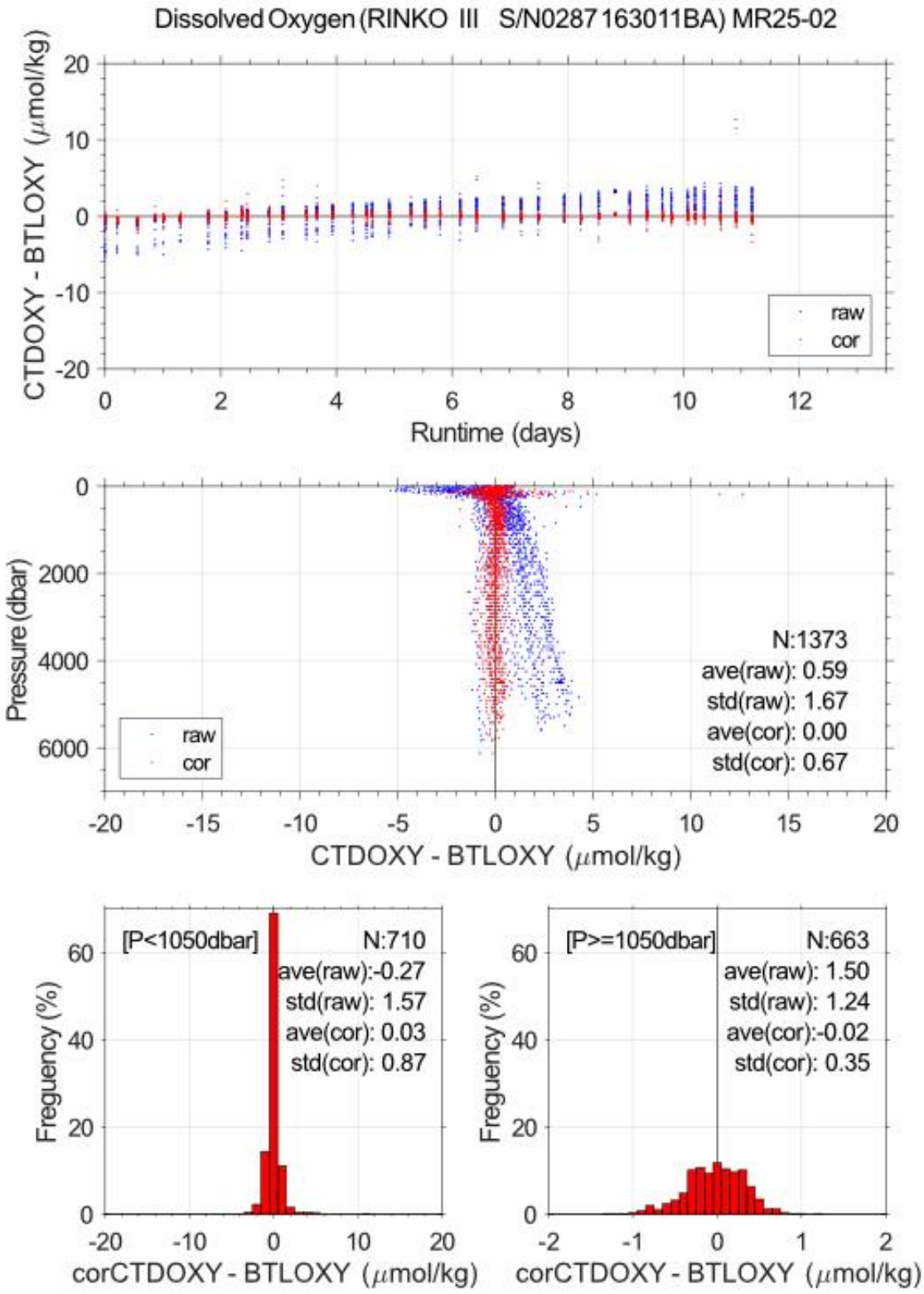

Fig. 4.1-7. Difference between the CTD oxygen and the bottle oxygen. Blue and red dots indicate before and after the post-cruise calibration, respectively.

(6.5) Transmissometer

Light transmission Tr (in %) and beam attenuation coefficient cp are calculated from the sensor output V (in volt) as follows:

$$Tr = (V–Vd) / (Vr–Vd) \times 100$$

$$cp = – (1 / 0.25) \ln(Tr / 100)$$

where Vd is the dark offset for the instrument, and Vr is the signal for clear water. Vd can be obtained by blocking the light path. Vd was measured on deck before each cast. Vr is estimated from the measured maximum signal in the deep ocean at each cast. The sensor output in the air (Vair) was also measured on deck before each cast to monitor the sensor drift. Since the transmissometer drifted in time (Fig. 4.1-8), Vr is expressed as

$$Vr = c0 + c1 \times t$$

where t is working time (in days) of the transmissometer integrated from the first CTD cast, and c0 and c1 are calibration coefficients. Maximum signal was extracted for each cast and appropriate data detected deep ocean maximum were selected to estimate Vr.

Vd = 0.0024, c0 = 4.712990093300466, c1 = 0.001279834519557

As shown in Fig. 4.1-8, the transmissometer showed a time drift of exceptionally positive trend.

(6.6) Chlorophyll fluorometer

In this cruise, we used split cable to analog voltage output from the fluorometer to both SBE9plus auxiliary port and analog input channel of the data logger (see section 4.1.2). It was found that there was a slight offset (+0.02 ug/L) in the fluorometer data when the fluorometer was connected to both SBE9plus and the data logger. So, the offset value was subtracted from the data from the fluorometers.

In addition to this, systematic difference between the two fluorometers was corrected. The systematic difference (0.018 ug/L) was estimated from the relationship between the fluorometers and the deep-ocean FDOM sensor (serial no. 0001, see section 4.1.2) for depths between 2000 dbar and 3500 dbar, and was added to the fluorometer data (serial no. 3700) to match with the other fluorometer (serial no. 3701).

At stations 54_1, 54_2, 55_1, 56_1, and 57_1, shifts of the fluorometer (serial no. 3701) data were observed, probably due to the failure of the data logger (see section 4.1.2). the offset values were also estimated from the relationship between the fluorometer and the deep-ocean FDOM sensor (serial no. 0001) for depths deeper than 2000 dbar. For station 54_1, the offset was +0.016 ug/L from surface to 3600 dbar of down cast and -0.013 ug/L from 3601 dbar of down cast to the end of the up cast. For stations 54_2, 55_1, and 56_1, the offset was +0.018 ug/L. For station 57_1, the offset was +0.007 ug/L. These additional offsets were subtracted from the corrected fluorometer data.

Post-cruise calibration of the fluorometer will be conducted after the cruise.

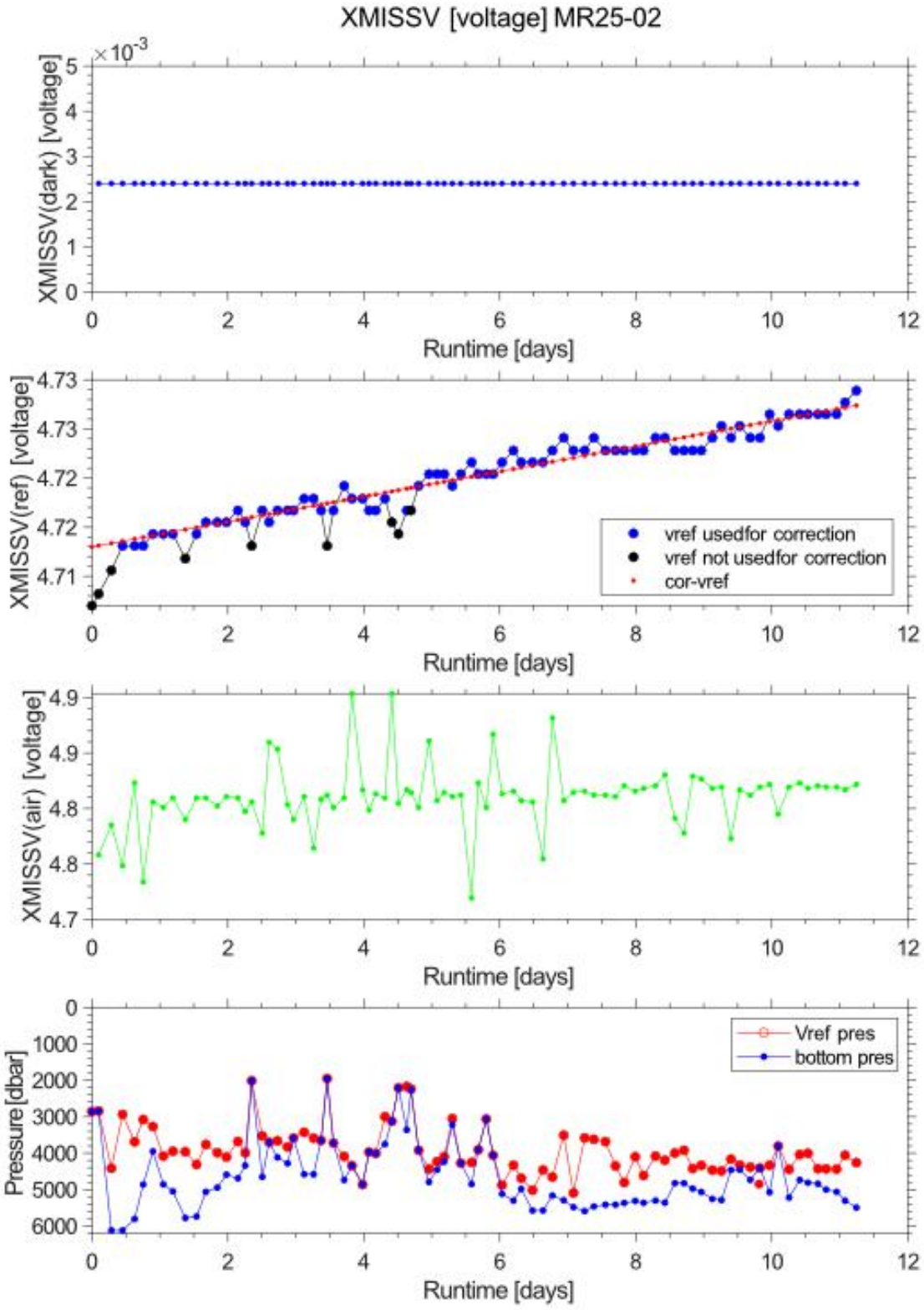

Fig. 4.1-8. Time series of V_d, the maximum value of the transmissometer output, V_{air}, and maximum pressure and pressure measured at the maximum value at each cast. Red dots in the second panel show the estimated V_r.

(6.7) Ultraviolet fluorometer and PAR

For the ultraviolet fluorometer and PAR sensor, data from the additional digital sensors (section 4.1.2) are used as the CTD data.

(7) References

Edwards, B., D. Murphy, C. Janzen and N. Larson (2010): Calibration, response, and hysteresis in deep-sea dissolved oxygen measurements, *J. Atmos. Oceanic Technol.*, 27, 920–931.

Fukasawa, M., T. Kawano and H. Uchida (2004): Blue Earth Global Expedition collects CTD data aboard Mirai, BEAGLE 2003 conducted using a Dynacon CTD traction winch and motion-compensated crane, *Sea Technology*, 45, 14–18.

García, H. E. and L. I. Gordon (1992): Oxygen solubility in seawater: Better fitting equations. *Limnol. Oceanogr.*, 37 (6), 1307–1312.

Sea-Bird Scientific (2024): Calculating calibration coefficients for C-Star Transmissometer. Application Note 91, rev. 3. (available on-line at https://www.seabird.com/)

Uchida, H., G. C. Johnson, and K. E. McTaggart (2010): CTD oxygen sensor calibration procedures, The GO-SHIP Repeat Hydrography Manual: A collection of expert reports and guidelines, IOCCP Rep., No. 14, ICPO Pub. Ser. No. 134.

Uchida, H., Y. Maeda and S. Kawamata (2018): Compact underwater slip ring swivel: Minimizing effect of CTD package rotation on data quality, Sea Technology, 11, 30–32.

Uchida, H., T. Nakano, J. Tamba, J. V. Widiatmo, K. Yamazawa, S. Ozawa and T. Kawano (2015): Deep ocean temperature measurement with an uncertainty of 0.7 mK, J. Atmos. Oceanic Technol., 32, 2199–2210.

(8) Data archive

These data obtained in this cruise will be submitted to the Data Management Group of JAMSTEC, and will be opened to the public via “Data Research System for Whole Cruise Information in JAMSTEC (DARWIN)” in JAMSTEC web site.

4.1.2 Additional digital sensors for CTD measurement

January 8, 2026

(1) Personnel

Hiroshi UCHIDA (JAMSTEC RIGC)

(2) Objective

To obtain vertical profiles of seawater properties by using a data logger and several digital sensors, including sensors currently under development, that cannot be connected to the CTD to acquire data.

(3) Instruments and method

Instruments used in this cruise are as follows:

Refractive index density sensor (Uchida et al. 2019)
Serial no. 1 (internal memory with the external battery [56 D size alkaline batteries])
Data logger (two 16 bit A/D channels and four serial [RS-232C] channels, JAMSTEC)
Serial no. 1 for stations 001-056
Serial no. 2 for stations 057-080
Analog channel
Chlorophyll fluorometer signal from SBE 9plus
Turbidity meter (Seapoint Sensors Inc., New Hampshire, USA)
Serial no. 14954, Gain setting: 100X (0-25 FTU)
Serial channel
Deep-ocean fluorometer/turbidity meter, ACLD70 (JFE Advantech Co., Ltd.)
Serial no. 0001
Fluorometer/backscatter/FDOM sensor, RBRtridente (RBR Ltd., Ottawa, Canada)
Serial no. 235555
PAR sensor, MPE-PAR-HP (Biospherical Instruments Inc., San Diego, CA, USA)
Serial no. 3313
Velocimeter, MiniSVS OEM (Valeport Ltd., Devon, United Kingdom)
Serial no. 24001 (sound path length: 5 cm)
Deep-ocean fluorometer/turbidity meter, ACLD70-USB (JFE Advantech Co., Ltd.)
Serial no. 0004, 0005 (internal battery and memory)
Deep-ocean FDOM sensor, AOMD-USB (JFE Advantech Co., Ltd.)
Serial no. 0001, 0002 (internal battery and memory)

The refractive index density sensor was powered from an external battery synchronized with the power supply of the CTD and recorded data in its internal memory at a rate of 32 Hz. No data was obtained for station 001_1, due to the operation error. Also, no data was obtained for stations 016_1 to 033_1, due to the internal memory error of the spectroscopic unit.

The data logger and its connected sensors were powered from the CTD 9plus and the data logger recorded data from the connected sensors in its internal memory at a rate of 12 Hz. No data was obtained for stations 054_1 to 056_1, due to a malfunction of the data logger.

The deep-ocean fluorometer/turbidity meter (ACLD70-USB) is an improved version of that connected to the data logger (ACLD70). And the deep-ocean FDOM sensor (AOMD-USB) is a prototype of the FDOM sensor. These sensors were attached to the CTD frame with the detection surface facing downward. The data were recorded in its internal memory at a rate of 1 Hz. These sensors were tested at stations from 001_1 to 005_1, from 006_1 to 009_2, and 011_1 to 014_1. For station 005_1, down cast data from one deep-ocean FDOM sensor (serial no. 0001) was only available due to battery failure. For stations from 001_1 to 004_1, serial no. 0004 of ACLD70 and serial no. 0002 of AOMD were used side by side to investigate the effects of interference between the ACLD70 and AOMD. As a result, the AOMD data were largely affected by the ACLD70 signal. For stations from 001_1 to 004_1, the turbidity data of the ACLD70s (serial no. 0004 and 0005) were biased due to the effect of reflection on the CTD frame. For stations from 006_1 to 009_2, the ACLD70s (serial no. 0004 and 0005) were used side by side to investigate the effects of interference between the ACLD70s. As a result, the chlorophyll data were

slightly affected by each other. For stations from 011_1 to 014_1, the AOMDs (serial no. 0001 and 0002) were used side by side to investigate the effects of interference between the AOMDs. As a result, the FDOM data were slightly affected by each other. After these tests, one AOMD (serial no. 0001) was used at all stations, and one ACLD70 (serial no. 0004) was used at stations from 075_1 to 080_1. As a result, FDOM data from the AOMD (serial no. 0001) were available at all stations, except for station 010_1.

(4) Data Processing

Data processing for the refractive index density sensor is not yet finished.

For the ACLD70-USB and AOMD-USB sensors, the data recorded at 1 second intervals were merged with the CTD pressure data averaged at 1 second intervals. Spikes in the data were manually removed. And the data were linearly interpolated at 1 dbar intervals for both down-cast and up-cast.

For the datalogger, the data obtained at a rate of 12 Hz were merged with the CTD pressure and conductivity data linearly interpolated at a rate of 12 Hz by using the raw data at a rate of 24 Hz. Then the data from the datalogger were merged with the CTD pressure data by estimating the time of submersion at the sea surface from the CTD conductivity data and the sound velocity data, and matching each time of the data accordingly.

The data where the CTD was moving less than the minimum velocity of 0.0 m/s (traveling backwards due to ship roll) were replaced with missing value and were resampled into 1-dbar pressure bins by determining a median value for the 1-dbar bin, to remove spikes in the data, for both down-cast and up-cast. Remaining spikes in the data were manually removed.

Pressure dependencies of the old deep-ocean fluorometer/turbidity meter (ACLD70) were estimated by comparing with the new deep-ocean fluorometer/turbidity meter (ACLD70-USB, serial no. 0004). The fluorometer and turbidity data were corrected as

$$\text{Corrected\_data} = c0 \times \text{Raw\_data} + c1 \times P + c2 \times P^2 + c3$$

where P is pressure in dbar and c0 – c3 are correction coefficients. The coefficients were determined as follows.

(for fluorometer)
c0 = 1.004183762459386, c1 = -1.959172840657376e-06, c2 = 4.297684885024123e-10,
c3 = 3.030775599784215e-03
(for turbidity meter)
c0 = 1.167549141007097, c1 = -1.887032493365992e-06, c2 = 3.224940505303277e-10,
c3 = 0.007

The coefficient c3 for turbidity meter was arbitrary adjusted so that its minimum value would be near zero in the deep ocean.

Regarding the old deep-ocean fluorometer/turbidity meter data, outliers in the surface layer affected by solar radiation were removed.

Data of the datalogger shown below were deemed bad data and replaced with missing value.

Station 042, cast 1, up cast, ALCD70, fluorometer: from 529 to 0 dbar
Station 042, cast 1, up cast, ALCD70, turbidity: from 540 to 0 dbar
Station 057, cast 1, down cast, RBRtridente, all data: from 859 dbar to bottom
Station 057, cast 1, up cast, all data: from bottom to 0 dbar
Station 064, cast 1, up cast, all data: from 3166 to 0 dbar
Station 077, cast 1, up cast, all data: from 2763 to 0 dbar

For the RBRtridente, no FDOM data was available due to a malfunction of the FDOM channel.

(5) Post-cruise calibration

Data from the velocimeter was largely drifted in time. Therefore, the sound velocity data were used only for estimation of the time of submersion at the sea surface.

There was a hysteresis in the fluorometer data from the RBRtridente, and there was a shift in the backscatter data from the RBRtridente. Since fluorometer data from ACLD70 and backscatter data from the ECO BB(RT)D on the CTD system are available, the data from the RBRtridente were not used.

The SBS PAR sensor on the CTD system malfunctioned during the cruise, so PAR data from the MPE-PAR was adopted without conducting post-cruise calibration, instead of the SBS PAR data.

The Seapoint CDOM sensor on the CTD system malfunctioned during the cruise, so FDOM data from the AOMD was adopted with conducting post-cruise calibration as mentioned below, instead of the Seapoint CDOM data.

Although the backscatter data from the ECO BB(RT)D on the CTD system is available, turbidity data from the ACLD70 was also adopted without conducting post-cruise calibration, because spatial distribution in the deep ocean was different between the two sensors.

Although the fluorometer data from the Seapoint Fluorometer on the CTD system is available, fluorometer data from the ACLD70 was adopted. However, if the ACLD70 fluorometer data was unavailable, the Seapoint fluorometer data was used instead. Therefore, post-cruise calibration was performed on both the ACLD70 fluorometer data and the Seapoint fluorometer data, as mentioned below.

(5.1) FDOM

Pre-cruise laboratory calibration of the FDOM sensor (AOMD) was performed at JAMSTEC by using deep sea water and ultrapure water.

$$\text{Corrected\_raw\_data} = (\text{raw\_data} - \text{raw\_zero}) / (1 + \rho \times [T - Tr]) - \text{bias\_anomaly}$$

$$\text{Raw\_zero} = 807.8,\ \rho = -0.0032$$

where raw_data is the raw sensor data, T is temperature (in °C) and Tr is reference temperature (20 °C) (Shigemitsu et al. 2019). Bias_anomaly is correction term for time-dependent bias revealed through comparison with the fluorometer data (ACLD70). The bias was estimated for each group of stations defined based on the period during which sensors were not removed from the CTD frame for battery replacement or data extraction. For each group (group of stations: [1, 2, 3, 4, 5], [6, 7, 8, 9], [11, 12, 13, 14], [15, 16, 17, 18, 19, 20], [21, 22, 23, 24, 25], [26, 27, 28, 29, 30, 31], [32, 33, 34, 35, 36], [37, 38, 39, 40, 41], [42, 43, 44, 45, 46], [47, 48], [49, 50], [51], [52, 53], [54], [55], [56, 57], [58, 59], [60, 61, 62], [63, 64], [65], [66], [68, 69, 70], [72], [74], [75], [76, 77], [78], [79], [80]), the relationship between the ACLD70 fluorometer data and the AOMD data was approximated by a linear equation between 2000 and 4000 dbar, and the FDOM (corrected_raw_data) value when the fluorometer value (pre-cruise calibrated value in µg/L) was 0.11 was averaged. The anomaly of this averaged FDOM value from the overall period average was taken as the bias (bias_anomaly). For the two groups ([54] and [55]) lacking the ACLD70 data, the average of the bias anomaly values of the immediately preceding and following groups ([52, 53], [56, 57]) was used.

The bias-corrected sensor data was calibrated with the water sampled data.

$$\text{CTDCDOM [in RU]} = c0 + c1 \times \text{Corrected\_raw\_data}$$

$$c0 = -4.647129e{-}3,\ c1 = 3.382694e{-}5$$

The results of the post-cruise calibration are shown in Figs. 4.1-9 and 4.1-10.

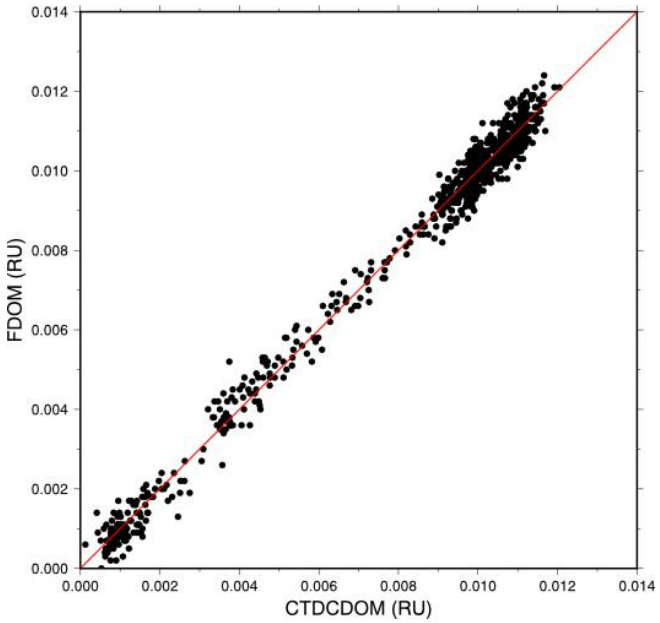

Fig. 4.1-9. Comparison of FDOM data between the calibrated sensor data (CTDCDOM) and the water sampled data (FDOM).

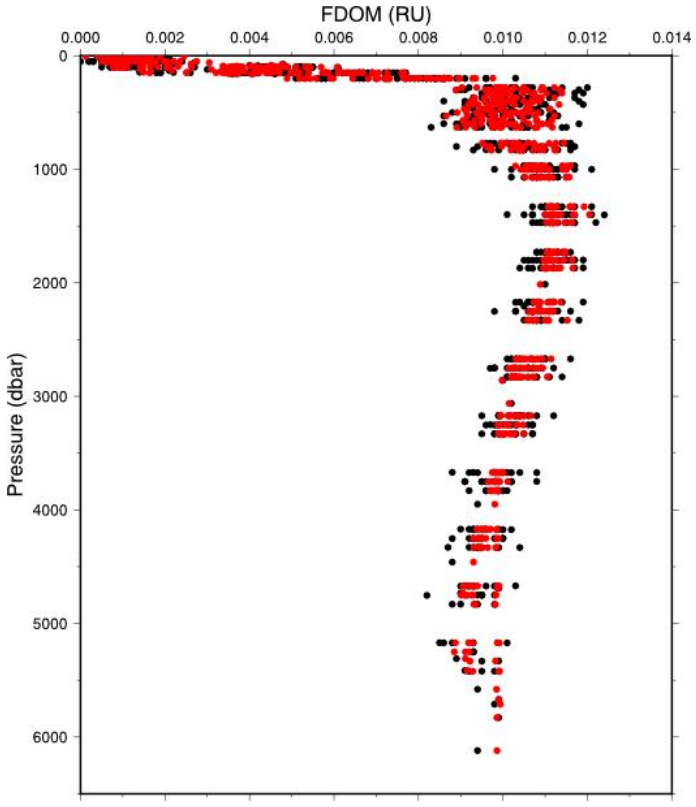

Fig. 4.1-10. Vertical distribution of FDOM for the water sampled data (black dots) and the calibrated sensor data (red dots).

(5.2) Chlorophyll a

To combine the ACLD70 fluorometer data and the Seapoint fluorometer data for use together, the scale of the Seapoint fluorometer data was adjusted to match the scale of the ACLD70 fluorometer data as follows.

Adjusted_Seapoint_fluorometer_data = 0.954648 × Seapoint_fluorometer_data

The chlorophyll fluorometer data show positive biases in the deep ocean because of the interference by FDOM (Xing et al., 2017). Therefore, the effect of the interference by FDOM was corrected by using the FDOM data for pressure larger than 1000 dbar as follows:

$CTDFLUOR_{fdom\_corr} = CTDFLUOR - c_0 \times CTDCDOM$

$c_0 = 10.88169$ (for ACLD70 fluorometer)

$c_0 = 6.798897$ (for Seapoint fluorometer)

where CTDCDOM is the FDOM (AOMD) data (in Raman Unit), and c_0 is the correction coefficients. Since no FDOM data was available for station 10, FDOM profile at station 10 was estimated from the average of the FDOM profiles at station 9 cast 2 and station 11 cast 1 for the fluorometer calibrations.

The chlorophyll fluorometer data thus corrected was calibrated in situ by using the bottle sampled chlorophyll-a data. The calibration equation is as follows:

$CTDFLUORcorr = c_0 \times CTDFLUOR_{fdom\_corr} + c_1 \times CTDFLUOR_{fdom\_corr}^2$

$c_0 = 0.8947265$, $c_1 = -0.4796690$ (for ACLD70 fluorometer)

$c_0 = 0.6827887$, $c_1 = -0.2388883$ (for Seapoint fluorometer)

where c_0 and c_1 are the calibration coefficients.

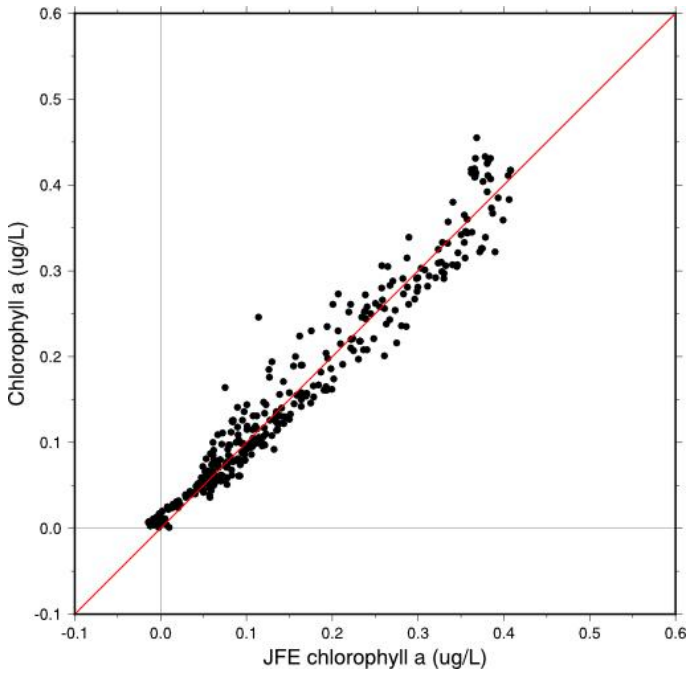

Fig. 4.1-11. Comparison of chlorophyll-a data between the calibrated sensor data (CTDFLUORcorr) by ACLD70 and the water sampled data.

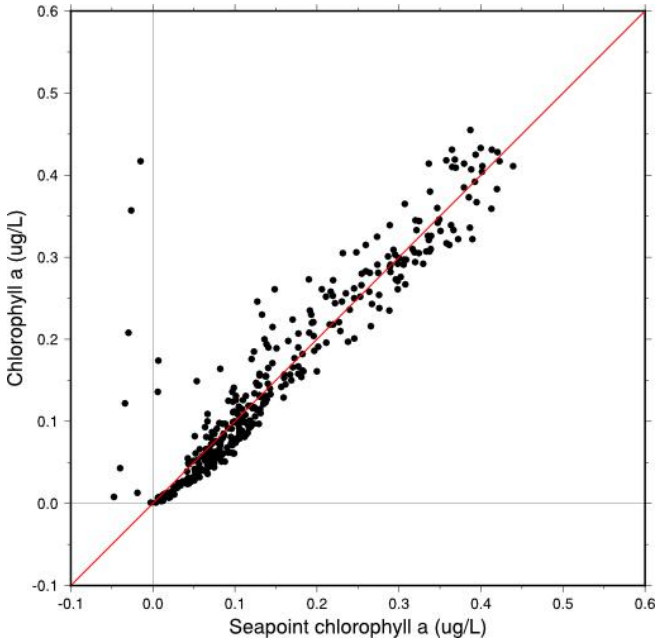

Fig. 4.1-12. Comparison of chlorophyll-a data between the calibrated sensor data (CTDFLUORcorr) by Seapoint fluorometer and the water sampled data.

(6) Reference

Shigemitsu, M., H. Uchida, T. Yokokawa, K. Arulananthan, and A. Murata (2020): Determining the distribution of fluorescent organic matter in the Indian Ocean using in situ fluorometry. Front. Microbiol., 11, doi:10.3389/fmicb.2020.589262.

Uchida, H., Y. Kayukawa, and Y. Maeda (2019): Ultra high-resolution seawater density sensor based on a refractive index measurement using the spectroscopic interference method. Sci. Rep., 9:15482, doi:10.1038/s41598-019-52020-z.

Xing, X., H. Claustre, E. Boss, C. Roesler, E. Organelli, A. Poteau, M. Barbieux, and F. D'Ortenzio (2017): Correction of profiles of in-situ chlorophyll fluorometry for the contribution of fluorescence originating from non-algal matter. Limnol., Oceanogr.: Methods, 15, 80-93, doi:10.1002/lom3.10144.

(7) Data archive

These data obtained in this cruise will be submitted to the Data Management Group of JAMSTEC, and will be opened to the public via "Data Research System for Whole Cruise Information in JAMSTEC (DARWIN)" in JAMSTEC web site.

4.2 Salinity

May 8, 2025

(1) Personnel

Hiroshi UCHIDA JAMSTEC RIGC

(2) Objective

The objective of this study is to collect bottle sampled salinity data to calibrate the CTD and thermo-salinograph salinity data.

(3) Instruments and method

Salinity measurement was conducted basically based on the method by Kawano (2010) with modification of the time drift correction method (Uchida et al., 2020). Materials used in this cruise are as follows:

Standard Seawater: IAPSO Standard Seawater, Ocean Scientific International Ltd., Hampshire, UK, Batch P167

Salinometer: Autosal model 8400B; Guildline Instruments, Ltd., Ontario, Canada

Serial no. 62556 (stations 001-054)

Serial no. 72874 (stations 056-080)

A peristaltic-type sample intake pump: Ocean Scientific International Ltd.

Thermometers: PRT model 1502A, Fluke Co., Everett, Washington, USA

Serial no. B81550 (for monitoring the bath temperature) (for serial no. 62556)

Serial no. B78466 (for monitoring the bath temperature) (for serial no. 72874)

Serial no. B81549 (for monitoring the room temperature)

Stabilized power supply: model PCR1000LE, Kikusui Electronics Co., Japan, Serial no. XH004198

Data acquisition software: Vs8400B, Virtual Systems Co., Japan, Version 1.05T, Rev.02

Sample bottles: 250 mL brown borosilicate glass bottles with screw caps (PTFE liners)

100 mL borosilicate glass bottles with screw caps (PTFE liners) (for testing)

Secondary Standard Seawater: Multiparametric Standard Seawater, KANSO TECHNOS Co., Ltd., Lot PRE20

Ultra-pure water: Milli-Q water, Millipore, Billerica, Massachusetts, USA

Sub-standard seawater: Surface seawater collected in the cruise MR23-05 Leg 1 by filtering with a 0.20 μm pore capsule cartridge filter, ADVANTEC, Toyo Roshi Kaisha Ltd., Japan

Detergent: 2% neutral detergent, SCAT 20X-N, Dai-ichi Kogyo Seiyaku Co., Ltd., Japan

The bath temperature of the salinometer was set to 24 °C. The salinometer was standardized previously by using the IAPSO Standard Seawater (SSW). The standardization dial was set to 610 for serial no. 62556 and 480 for serial no. 72874, and never changed during the cruise. The mean ± SD of the STANDBY, ZERO, ambient room temperature, and bath temperature are listed in Table 4.2-1.

The double conductivity ratios measured by the salinometer were used to calculate Practical Salinity using the algorithm for Practical Salinity Scale 1978 (IOC et al., 2010). A constant temperature of 24 °C was used in the calculation instead of using the measured bath temperature.

The measurement cell of the salinometer was rinsed with ultra-pure water and 2% neutral detergent after each day of measurement, and the electrode in the cell was soaked in the neutral detergent until the next day of measurement.

Ultra-pure water and the IAPSO SSW were measured at the beginning and the end of each day of measurement (for samples of 1 to 3 stations). Sub-standard seawater was measured every about 20 samples to monitor stability of the salinometer during each day of measurement.

The results of the ultra-pure water and the IAPSO SSW measurement (Fig 4.2-1) suggest that the

salinometer drifted in time by changing the span of the slope. Therefore, correction factors of the salinometer were estimated from the mean Practical Salinity value of the SSW measurements and the certified Practical Salinity value for each day (Uchida et al., 2020). The measured Practical Salinities for the water samples were corrected by using the correction factors. For serial no. of day of 19 (April 27, 2025), slight linear time drift of the salinometer was estimated from the IAPSO SSW and sub-standard seawater measurements and corrected for the samples of the day. The standard deviation of the IAPSO SSW measurements was 0.0002 in Practical Salinity after the time drift correction. The mean ± SD of the ultra-pure water measurements was 0.0002±0.0001.

Table 4.2-1. The mean ± SD of the STANDBY, ZERO, ambient room temperature, and bath temperature for the salinometers.

Serial no.	STANDBY	ZERO	Bath temperature	Room temperature
62556	5133.8±0.5	0.00000±0.00000	24.0183±0.0010 °C	22.1±0.7 °C
72874	5956.1±0.9	−0.00001±0.00001	24.0363±0.0009 °C	22.4±0.7 °C

(4) Results

A total of 93 pairs of replicate samples was collected and the SD of the replicate samples was 0.00027 in Practical Salinity.

At station 061, all Niskin bottles were closed at 4500 dbar and samples for salinity and dissolved oxygen measurements were collected from each bottle. The mean ± SD of the 36 salinity measurements was 34.6943±0.00033.

A total of 5 bottles (serial no. 003, 033, 042, 043, 045) of MSSW PRE20 was measured and the mean ± SD was 34.2769±0.0002 in Practical Salinity.

The sample bottles currently in use have been discontinued and are no longer available. Therefore, we are considering using 100 ml bottles (DURAN GL32 Laboratory Square Bottle with screw cap [PTFE liner]) as a replacement sample bottle. Six bottles were used to evaluate stability of long-term storage, and two bottles were used to evaluate repeatability. For the stability test, seawater was collected from niskin #16 at station 001_1. Salinity of the niskin #16 was 34.6574 (April 10), and three test bottles were measured on April 21 (34.6581±0.00015), and on May 3 (34.6579±0.00006). For the repeatability test, two test bottles were used to collect seawater from niskin #16 at 27 stations. The mean ± SD of difference between the normal bottle and the test bottle was −0.0001±0.0005 in Practical Salinity, and the SD of the replicate test samples was 0.0002 in Practical Salinity.

(5) References

IOC, SCOR and IAPSO (2010): The international thermodynamic equation of seawater – 2010: Calculation and use of thermodynamic properties. Intergovernmental Oceanographic Commission, Manuals and Guides No. 56, UNESCO (English), 196 pp.

Kawano, T. (2010): Salinity. The GO-SHIP Repeat Hydrography Manual: A collection of Expert Reports and Guidelines, IOCCP Report No. 14, ICPO Publication Series No. 134, Version 1.

Uchida, H., T. Kawano, T. Nakano, M. Wakita, T. Tanaka and S. Tanihara (2020): An updated batch-to-batch correction for IAPSO standard seawater. J. Atmos. Oceanic Technol., 37, 1507-1520, doi:10.1175/JTECH-D-19-0184.1.

(6) Data archive

These data obtained will be submitted to JAMSTEC Data Management Group (DMG).

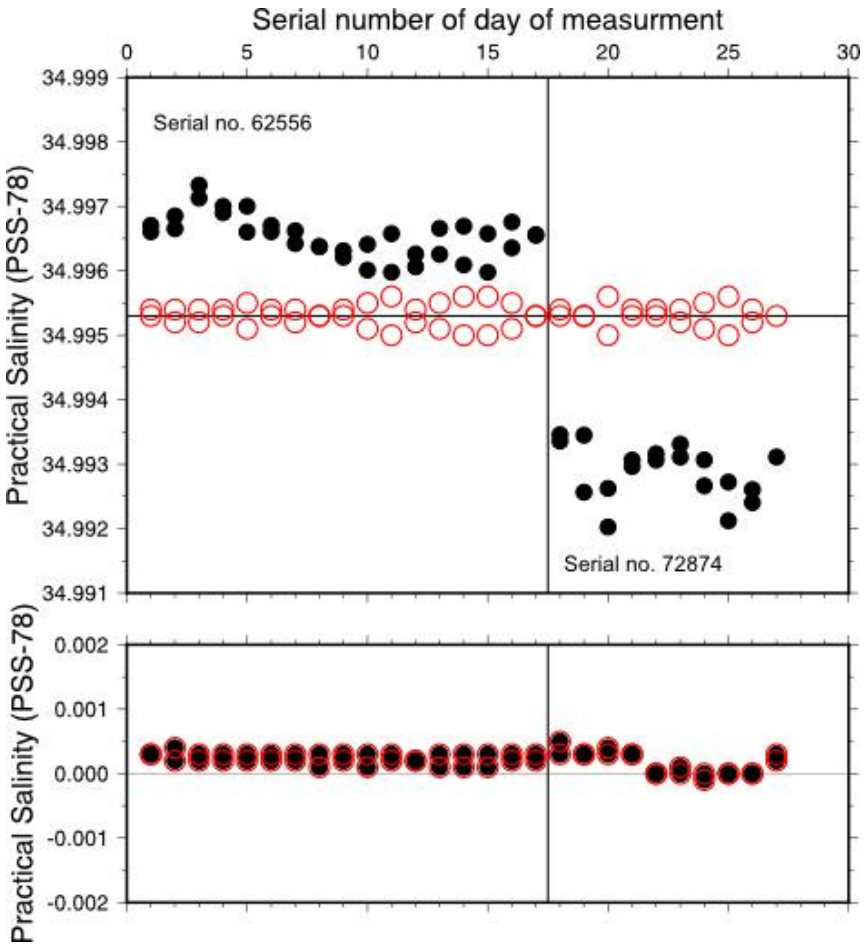

Figure 4.2-1. Time-series of the measured Practical Salinities for the ultra-pure water (lower panel) and the IAPSO SSW (upper panel) (black circles). The time-drift corrected Practical Salinities were also shown (red circles).

4.3 Seawater density

May 4, 2025

(1) Personnel

Hiroshi UCHIDA JAMSTEC RIGC

(2) Objective

The objective of this study is to collect Absolute Salinity (also called "density salinity") data and to evaluate the algorithm to estimate Absolute Salinity anomaly provided along with TEOS-10 (the International Thermodynamic Equation of Seawater 2010) (IOC et al. 2010).

(3) Instruments and method

Seawater density for water samples was measured with a vibrating-tube density meter (DMA 5000M [serial no. 80570578], Anton-Paar GmbH, Graz, Austria) with a sample changer (Xsample 122 [serial no. 8548492], Anton-Paar GmbH). The sample changer was used to load samples automatically from up to ninety-six 12-mL glass vials.

The water samples collected in 250 mL brown borosilicate glass bottles with translucent screw caps (PTFE packing) for Practical Salinity measurement were measured by taking the water sample into a 12-mL glass vial for each bottle just before Practical Salinity measurement. The glass vial was sealed with Parafilm M (Pechiney Plastic Packaging, Inc., Menasha, Wisconsin, USA) immediately after filling. Densities of the samples were measured at 20 °C by the density meter.

The density meter was initially calibrated previously by measuring air and pure water according to the instrument manual. However, measured density for the IAPSO Standard Seawater deviates from density of TEOS-10 calculated from Practical Salinity and composition of seawater, probably due to non-linearity of the density meter (Uchida et al. 2011). The non-linearity can be corrected by measuring a reference sample simultaneously as:

$$\rho_{corr} = \rho - (\rho_{ref} - \rho_{ref\_true}) + c\,(\rho - \rho_{ref\_true}),$$

where ρ_{corr} is the corrected density of the sample, ρ is measured density of the sample, ρ_{ref} is measured density of the reference, ρ_{ref_true} is true density of the reference, and c is non-linearity correction factor.

Time drift of the density meter was monitored by periodically measuring the density of ultra-pure water (Milli-Q water, Millipore, Billerica, Massachusetts, USA) produced on the R/V Mirai and pure water (Pure Water [water hardness 0], Ako Kasei Co. Ltd., Ako Hygo, Japan) made from seawater collected from a depth of 344 m off Muroto, Kochi, Japan, by filtering twice with a reverse osmosis membrane. In addition, Pure Water was deionized using ion exchange resin (Pure Maker, Sanei Corp., Arao, Kumamoto, Japan) conducted on 6 October 2019 and stored in a 2-L PET bottle at room temperature. The true density at 20 ºC of the Pure Water was estimated to be 998.2074 kg m^{-3} from the isotopic composition ($\delta D = -3.4$ ‰, $\delta^{18}O = -1.3$ ‰) and International Association for the Properties of Water and Steam (IAPWS)-95 standard.

Although the non-linearity factor is estimated to be 0.000341 for the density meter (serial no. 80570578), additional correction for time drift of the non-linearity factor of the density meter was carried out by periodically measuring the density of the IAPSO Standard Seawater (batch P167). True density at 20 °C for the batch P167 at April 2025 is estimated to be 1024.7650 kg/m^3 from Practical Salinity and composition changes of Standard Seawater using TEOS-10 (see Uchida et al. 2025a).

A total of 5 bottles of Multiparametric Standard Seawater (MSSW lot PRE20, KANSO TECHNOS Co., Ltd., Uchida et al. 2025b) was also measured and the mean ± SD was 1024.2208 ± 0.0009 kg/m^3.

(4) Results

Absolute Salinity (also called density salinity, "DNSSAL") can be back calculated from the measured density and temperature (20 °C) with TEOS-10. A total of 86 pairs of replicate samples was measured and the standard deviation of the replicate samples was 0.0016 g/kg. The measured Absolute Salinity anomalies (δS_A) are shown in Fig. 4.3-1. The measured δS_A were well agree with the δS_A estimated from Pawlowicz et al. (2011) which exploits the correlation between δS_A and nutrient concentrations and carbonate system parameters based on mathematical investigation using a

model relating composition, conductivity and density of arbitrary seawaters.

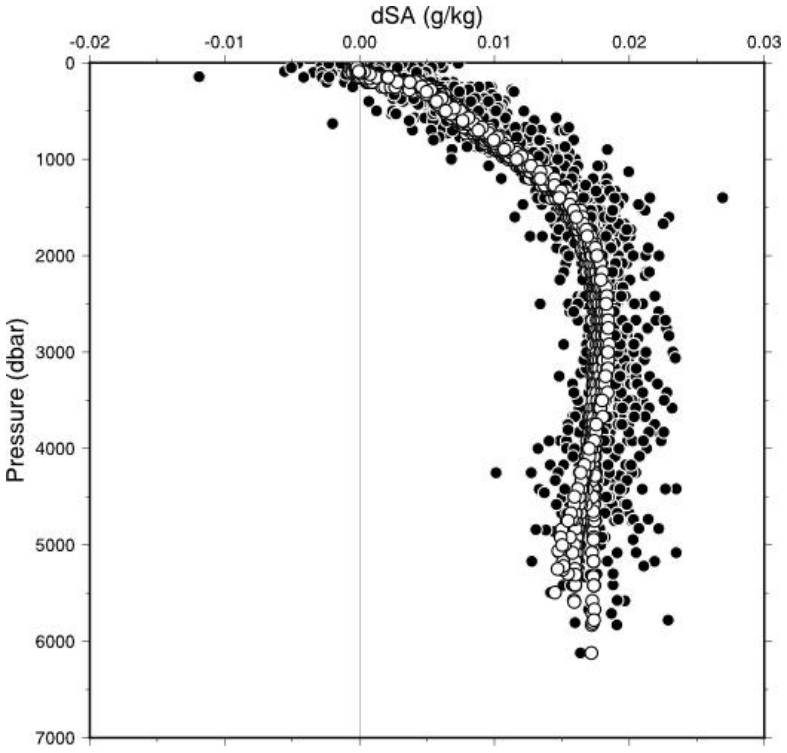

Figure 4.3-1. Vertical distribution of Absolute Salinity anomaly measured by the density meter (closed circles). Absolute Salinity anomaly estimated from nutrients and carbonate system parameters (Pawlowicz et al., 2011) are also shown (open circles).

(5) References

IOC, SCOR and IAPSO (2010): The international thermodynamic equation of seawater – 2010: Calculation and use of thermodynamic properties. Intergovernmental Oceanographic Commission, Manuals and Guides No. 56, UNESCO (English), 196 pp.

Pawlowicz, R., D.G. Wright and F. J. Millero (2011): The effects of biogeochemical processes on ocean conductivity/salinity/density relationships and the characterization of real seawater. Ocean Science, 7, 363-387.

Uchida, H., T. Kawano, M. Aoyama and A. Murata (2011): Absolute salinity measurements of standard seawaters for conductivity and nutrients. La mer, 49, 237-244.

Uchida, H., M. Wakita, A. Makabe, A. Murata and A. Petrovic (2025a): Changes of the Composition of International Association for the Physical Sciences of the Ocean Standard Seawater. In: Aoyama, M., Cheong, C., Murata, A. (eds) Chemical Reference Materials for Oceanography. Springer Oceanography. Springer, Singapore. https://doi.org/10.1007/978-981-96-2520-8_10

Uchida, H. et al. (2025b): Development of Multiparametric Standard Seawater (MSSW) for CO_2 Parameters, Dissolved Oxygen, and Density of Seawater. In: Aoyama, M., Cheong, C., Murata, A. (eds) Chemical Reference Materials for Oceanography. Springer Oceanography. Springer, Singapore. https://doi.org/10.1007/978-981-96-2520-8_12

(6) Data archive

These data obtained will be submitted to JAMSTEC Data Management Group (DMG).

4.4 Lowered Acoustic Doppler Current Profiler

December 16, 2025

(1) Personnel

Shinya Kouketsu	JAMSTEC (principal investigator)
Ryohei Yamaguchi	JAMSTEC
Shinsuke Toyoda	JAMSTEC

(2) Overview of the equipment

Two acoustic Doppler current profilers (ADCP) were integrated with the CTD/CWS package. The lowered ADCP (LADCP)s, Workhorse Monitor WHM300 (Teledyne RD Instruments, San Diego, California, USA), which has 4 facing transducers with 20-degree beam angles, rated to 6000 m, make direct current measurements at the depth of the CTD, thus providing a full profile of velocity. The LADCPs were powered during the CTD casts by a 48 volts battery pack. The LADCP unit was set for recording internally prior to each cast. After each cast the internally stored observed data were downloaded to the computer in the onboard laboratory. After the cruise, by combining the measured velocity of the sea water and ocean bottom relative to the instrument, shipboard navigation data, and pressure time series from the CTD, the absolute velocity profiles were obtained with the software implemented by A.Thunherr. The software is based on the method of Visbeck (2002) and available online at ftp://ftp.ldeo.columbia.edu/pub/LADCP;.

The instruments used in this cruise were as follows.

WHM300(S/N 24545; downward), WHM300(S/N 20754; upward)

(3) Data collection

In this cruise, data was collected with the following configuration.

WHM300: Bin size: 8.0 m, Number of bins: 12, Pings per ensemble: 1, Ping interval: 1.0 sec

At Station 13, the data from the up-looking instrument (S/N 24545) was lost some time after it started due to cable problems.

(4) Reference

Visbeck, M. (2002): Deep velocity profiling using Lowered Acoustic Doppler Current Profilers: Bottom track and inverse solutions. *J. Atmos. Oceanic Technol.*, **19**, 794-807.

4.5 Microstructure in Temperature

(1) Personnel

Shinya Kouketsu	JAMSTEC (Principal investigator)
Ryohei Yamaguchi	JAMSTEC
Shinsuke Toyoda	JAMSTEC

(2) Objective

The objective is to measure microstructure in temperature to evaluate vertical mixing.

(3) Instruments and method

Micro structure observations were carried out by micro-Rider 6000 (MR6000; Rockland Scientific International Inc.), which was mounted on the CTD frame and was powered from SBE 9plus. We installed two FP07 thermistors to observe the high-frequency changes in temperature. We had to replace probes, as some of the probes failed during the cruise. High-frequency pressure and acceleration profiles are also obtained by the internal sensors in MR6000. Low-frequency profiles of temperature and conductivity were recorded in the MR6000 with the input from the SBE-3 sensor and SBE-4 sensor on the CTD system. We downloaded the raw data from the MR6000 after each cast. We plan to examine methods for calibration and quality check of the data after the cruise.

(4) Measurements

Micro Temperature

We sometimes replaced FP07s due to measurement problems as below:

Sensor socket 1 (SN286):
St. 1-21: T1341
St. 22-26: T2120
St. 27-46: T2084
St. 47-80: T2187
Sensor socket 2 (SN190):
St. 1-46: T1320
St. 47-80: T1973

4.6 Oxygen

May 12, 2025

Yuichiro Kumamoto

Japan Agency for Marine-Earth Science and Technology

(1) Personnel

Yuichiro Kumamoto (Principal Investigator)

Japan Agency for Marine-Earth Science and Technology

Masahiro Orui, Katsunori Sagishima, and Misato Kuwahara

Marine Works Japan Co. Ltd

(2) Objectives

Dissolved oxygen is one of chemical tracers for the ocean circulation. Climate models predict a decline in dissolved oxygen concentration and a consequent expansion of oxygen minimum layer due to global warming, which results mainly from decreased interior advection and ongoing oxygen consumption by remineralization. In order to discuss the temporal change in oxygen concentration in the water column, we measured dissolved oxygen concentration from surface to bottom layer at all the water sampling stations in the North Pacific Ocean during this cruise.

(3) Reagents

Pickling Reagent I: Manganous chloride solution (3M) Lot: 1-24B01, B02, and B03

Pickling Reagent II: Sodium hydroxide (8M) / sodium iodide solution (4M) Lot: 2-24B01, B02, and B03

Sulfuric acid solution (5M) Lot: S-24B01, B02, and B03

Sodium thiosulfate (0.025M) Lot: T-24C and -24D

Potassium iodate (0.001667M): Lot TPJ1039, FUJIFILM Wako Pure Chemical Industries Ltd, Mass fraction: 99.98 ± 0.04 % (expanded uncertainty), lot of solution: K25A01-08

(4) Instruments

Detector: Automatic photometric titrator, DOT-15X manufactured by Kimoto Electronic Co. Ltd. Lot: DOT-09, -10

Burette: APB-620 and APB-510 manufactured by Kyoto Electronic Co. Ltd. / 10 cm^3 of titration piston Lot: DOT-09, MB-11/MY10-11; DOT-10, MB-12/MY10-12 or MB-02/MY10-02; KIO_3, MB-10/MY10-10

Dispenser: FORTUNA Optifix 1 cm^3 Lot: Pickling Reagent I, MO-54; Pickling Reagent II, MO-33

(5) Seawater sampling

Seawater samples were collected using niskin-type 12-liter water samplers attached to the CTD-system. The seawater was transferred to a volume-calibrated glass flask (ca. 100 cm^3) through a plastic tube. Three times volume of the flask of seawater was overflowed. Sample temperature was measured during the water sampling using a thermometer. Then two reagent solutions (Reagent I, II) of 1.0 cm^3 each were added immediately into the sample flask and the stopper was inserted carefully into the flask. The sample flask was then shaken to mix the contents and to disperse the precipitate finely throughout. After the precipitate has settled at least halfway down the flask, the flask was shaken again to disperse the precipitate. The sample flasks containing pickled samples were stored in an air-conditioned laboratory until they were measured.

(6) Sample measurement

At least two hours after the re-shaking, the pickled samples were measured on board. A magnetic stirrer bar and 1 cm^3 sulfuric acid solution were added into the sample flask and stirring began. Samples were titrated by sodium thiosulfate solution whose molarity was determined by potassium iodate solution. Temperature of sodium thiosulfate during titration was recorded by a thermometer. We measured dissolved oxygen concentration using two sets of the titration apparatus system, named DOT-09 and DOT-10. Molal concentration of dissolved oxygen ($\mu mol\ kg^{-1}$) was calculated by the sample temperature during the water sampling, salinity, flask volume, and concentration and titrated volume of

the sodium thiosulfate solution (titrant).

(7) Standardization

Concentration of the sodium thiosulfate titrant (0.025M) was determined by the potassium iodate standard solution. The potassium iodate was dried in an oven at 130°C. 1.78 g potassium iodate weighed out accurately was dissolved in deionized water and diluted to final volume of 5 dm^3 in a calibrated volumetric flask (0.001667M). Then the aliquot (about 400 ml) of the solution was stored in a brown glass bottle (500 ml). 10 cm^3 of the potassium iodate solution was added to a flask using a volume-calibrated dispenser. Then 90 cm^3 of deionized water, 1 cm^3 of sulfuric acid solution, and 1.0 cm^3 of pickling reagent solution II and I were added into the flask in order. Amount of titrated volume of sodium thiosulfate (usually 5 times measurements average) gave the molarity of the sodium thiosulfate titrant. Table 4.6.1 show results of the standardization during this cruise. The averaged coefficient of variation (C.V.) for the standardizations was 0.013 ± 0.005 % (standard deviation, n = 18).

(8) Blank determination

The oxygen in the pickling reagents I (1.0 cm^3) and II (1.0 cm^3) was assumed to be 7.6×10^{-8} mol (Murray *et al.*, 1968). The redox species apart from oxygen in the reagents (the pickling reagents I, II, and the sulfuric acid solution) also affect the titration, which is called the reagent blank. The reagent blank was determined as follows. 1 and 2 cm^3 of the standard potassium iodate solution were added to two flasks respectively. Then 100 cm^3 of deionized water, 1 cm^3 of sulfuric acid solution, and 1.0 cm^3 of pickling reagent II and I each were added into the two flasks in order. The reagent blank was determined by difference between the two times of the first (1 cm^3 of KIO_3) titrated volume of the sodium thiosulfate and the second (2 cm^3 of KIO_3) one. The three results of the blank determination were averaged (Table 4.6.1). The averaged coefficient of variation (C.V.) for the reagent blank determination against the titration volume of the potassium iodate standard (about 4 ml) or 250 μmol kg^{-1} of dissolved oxygen concentration was 0.018 ± 0.008 % (standard deviation, n = 18). The redox species in seawater sample itself are measured as “dissolved oxygen”, which is called as the seawater blank, unless they are corrected. Because we did not measure the seawater blank in this cruise, the dissolved oxygen concentration reported here includes the seawater blank concentration that is less than 1 μmol kg^{-1} in the open ocean except those in suboxic and anoxic waters (Kumamoto *et al.*, 2015).

(9) Instrumental error

The difference in the concentrations of sodium thiosulfate solution determined by the standardization and blank determination using DOT-09 and DOT-10 were less than 0.029% (Table 4.6.1). These instrumental errors were within the error (standard deviation) of the standardization and blank determination, 0.022 ± 0.010 % The T-test at 95% confidence level suggests that there is no reason to believe that the two concentrations are different. Thus, we concluded that there was no instrumental error in measurements using DOT-09 and DOT-10.

Table 4.6.1 Results of standardization (End Point, cm^3) and reagent blank determination (cm^3).

Date (UTC)	KIO_3 Lot	$Na_2S_2O_3$ Lot	DOT-09		DOT-10		Δ (%)*	Remarks
			E.P.	blank	E.P.	blank		
2025/Apr/06	K25A01	T-24C	3.938	-0.002	3.937	-0.004	-0.021	Stn.01
2025/Apr/09	K25A02	T-24C	3.937	-0.002	3.934	-0.005	-0.017	Stn.02-09
2025/Apr/12	K25A03	T-24C	3.940	0.001	3.934	-0.004	0.016	Stn.11-25
2025/Apr/16	K25A04	T-24C	3.940	-0.001	3.935	-0.004	0.029	Stn.27-39
2025/Apr/19	K25A05	T-24D	3.946	-0.004	3.948	-0.002	-0.009	Stn.41-48
2025/Apr/23	K25A06	T-24D	3.945	-0.002	3.944	-0.003	0.010	Stn.50-58
2025/Apr/26	K25A07	T-24D	3.949	0.000	3.947	-0.002	-0.003	Stn.60-80
2025/May/03	K25A08	T-24D	3.950	0.000	3.950	0.000	-0.021	Final standardization
2025/May/03	Reference 25-03	T-24D	3.950	0.001	3.952	0.001	-0.014	

*Difference between DOT-09 and DOT-10 (DOT-09 minus DOT-10) in sodium thiosulfate concentration determined by the standardization and blank determination.

(10) Replicate sample measurement

At all the water sampling stations, a pair of replicate samples was collected at one or two depths. The standard deviations from the difference of pairs of replicate measurements was estimated to be 0.09 μmol kg^{-1} (n = 68), which corresponds to 0.036% of the relative standard deviation against 250 μmol kg^{-1}, using the standard operating procedure 23 in Dickson *et al.* (2007). The standard deviations of the difference between the pair of replicate measurement for the samples whose oxygen concentration is lower and higher than 100 μmol kg^{-1} are 0.10 (n = 28) and 0.07 μmol kg^{-1} (n = 40), respectively (Fig. 4.6.1). The difference between the two standard deviations is not significant (F-test at 95% confidence level) and there is no reason to believe contamination of atmospheric O_2 during the water sampling for the lower concentration samples.

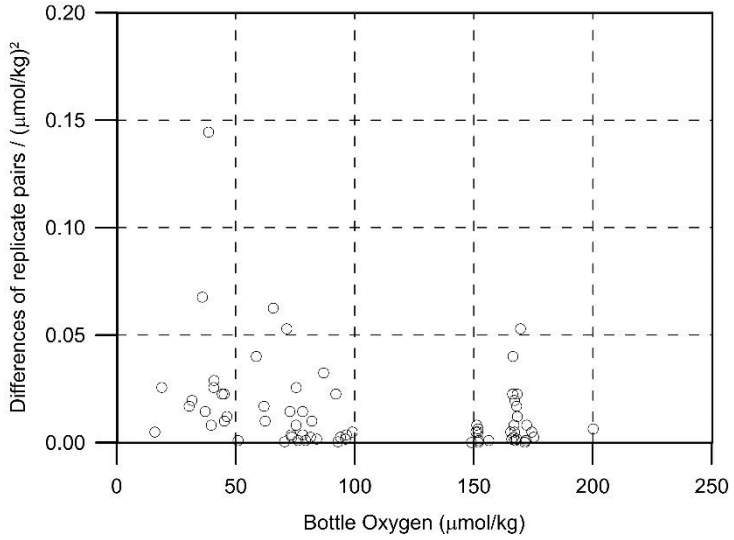

Figure 4.6.1 Oxygen difference between measurements of a replicate pair against oxygen concentration.

(11) Duplicate sample measurement

At station 61, we conducted a duplicate sample measurement to check whether the 36 niskin-type water samplers trip correctly. We took seawater sample from the 36 niskin-type water samplers all who collected seawater at 4500 dbar. The average and standard deviation from the duplicate measurement were estimated to 176.74 ± 0.08 μmol kg^{-1} (n = 36). The good agreement in the standard deviation between the duplicate (0.09 μmol kg^{-1}) and (0.08 μmol kg^{-1}) replicate measurements suggests that all the niskin-type water samplers trip correctly.

(12) Quality control flag assignment

Quality flag values for oxygen data from sample bottles were assigned according to the code defined in Table 4.9 of WHP Office Report WHPO 90-1 Rev.2 section 4.5.2 (Joyce *et al*., 1994). Measurement flags of 2 (good), 3 (questionable), 4 (bad), and 5 (missing) have been assigned (Table 4.6.3). For the choice between 2, 3, or 4, we basically followed a flagging procedure as listed below:

a. If there was a glaring problem or error in the measurement, the datum was flagged 4.

b. Bottle oxygen concentration at the sampling layer was plotted against sampling pressure and potential density. Any points not lying on a generally smooth trend were noted.

c. Difference between bottle oxygen concentration and oxygen sensor output was then plotted against sampling pressure. If the noted datum deviated from a group of plots, it was flagged 3 or 4.

d. If the bottle flag was 4 (did not trip correctly), a datum was flagged 4 (bad). In case of the bottle flag 3 (leaking) or 5 (unknown problem), a datum was flagged based on steps a, b, and c.

Table 4.6.3 Summary of assigned quality control flags.

Flag	Definition	Number*
2	Good	1378
3	Questionable	0
4	Bad	0
5	Not report (missing)	1
	Total	1379

*The replicate samples (n = 68) were not included.

(13) Uncertainty

We assume that the uncertainty of dissolved oxygen determination is derived from those of items listed in Table 4.6.4. Because we did not measure the seawater blank, the dissolved oxygen concentration reported here does include the seawater blank concentration (Section 8). Without the correction by the seawater blank, the combined uncertainty (k = 1) and the expanded combined uncertainty (k = 2) were calculated to be 0.05% and 0.10%, respectively. Note that this combined uncertainty does not include that derived from temporal change in temperature of sodium thiosulfate solution. However, that was negligible because the its variation was small (20.1-22.0ºC) When we subtract the seawater blank from the oxygen concentration, the uncertainty due to the seawater blank should be added. If it is assumed that the seawater blank concentration is 0.50 ± 0.50 μmol kg^{-1} and the distribution of the possible values is uniform or rectangular, its standard uncertainty is calculated to be 0.29 μmol kg^{-1} (= 0.50/√3). This value corresponds to the standard uncertainty of 0.116% relative to 250 μmol kg^{-1} of dissolved oxygen concentration. The combined standard uncertainty, which includes the uncertainty of the seawater blank concentration, is calculated to be 0.13% (the extended combined uncertainty is 0.26%). These combined uncertainties, however, are applicable only for the dissolved oxygen concentration corrected by the seawater blank concentration (0.50 μmol kg^{-1}). We did not apply this correction to the data obtained in this cruise.

(14) Problems

There was no serious problem during this cruise.

Table 4.6.4 Uncertainties of estimated items for the oxygen determination.

#	Estimated items	Relative uncertainty to 250 μmol kg^{-1} (%)	References
1	Sodium thiosulfate concentration	0.037	#2, 3, 4
2	Potassium iodate concentration	0.030	Kumamoto *et al.* (2015)
3	Titration of potassium iodate	0.013	Section 7
4	Reagent blank determination	0.018	Section 8
5	Titration of seawater sample	0.036	Section 10
6	Volume of sample flask	0.015	Kumamoto *et al.* (2015)
	Combined uncertainty (k=1)	0.05	#1, 5, 6
	Expanded combined uncertainty (k=2)	0.10	
7	Seawater blank	0.116	Kumamoto *et al.* (2015)
	Combined uncertainty (k=1)	0.13	#1, 5, 6, 7
	Expanded combined uncertainty (k=2)	0.26	

(15) Data archives

The data obtained in the cruises will be submitted to the Data Management Group of JAMSTEC and will be opened to the public via “Data Research System for Whole Cruise Information in JAMSTEC (DARWIN)” in the JAMSTEC web site.

References

Dickson, A. G., C.L. Sabine, and J.R. Christian (Eds.) (2007) Guide to best practices for ocean CO_2 measurements, PICES Special Publication 3, 191 pp.

Joyce, T., and C. Corry, eds., C. Corry, A. Dessier, A. Dickson, T. Joyce, M. Kenny, R. Key, D. Legler, R. Millard, R. Onken, P. Saunders, M. Stalcup (1994) Requirements for WOCE Hydrographic Programme Data Reporting, WHPO Pub. 90-1 Rev. 2, May 1994 Woods Hole, Mass., USA.

Kumamoto, Y., Y. Takatani, T. Miyao, H. Sato, and K. Matsumoto (2015) Dissolved oxygen, Guideline of Ocean Observations, vol. 3, chap. 1, G301JP:001−029 (in Japanese).

Murray, C.N., J.P. Riley, and T.R.S. Wilson (1968) The solubility of oxygen in Winkler reagents used for determination of dissolved oxygen, Deep-Sea Res., 15, 237-238.

4.7 Nutrients

November 17, 2025
Yuichiro Kumamoto
Japan Agency for Marine-Earth Science and Technology

Personnel

Yuichiro Kumamoto (Principal Investigator)
Japan Agency for Marine-Earth Science and Technology
Yuko Miyoshi, Shiori Ariga, and Kengo Fujita
Marine Works Japan Co. Ltd

(2) Objectives

In order to discuss the temporal change in nutrients (nitrate, nitrite, silicate, phosphate, and ammonia) in water column, we measured nutrients concentrations from surface to bottom layer at all the water sampling stations in the South Pacific Ocean during this cruise.

(3) Instruments and methods

The analytical platform was upgraded from QuAAtro 2-HR to QuAAtro 39 in March 2021. However, following this replacement, several issues were reported with the QuAAtro 39 system (see the cruise report of MR21-05C). In July 2022, to address these issues and improve analytical precision, the following modifications were made: (1) the pumps were replaced with a 14-tube pump (model number: TRA+B014-02, BL TEC K.K.), instead of the original 13-tube pump (model number: 166+B214-01, BL TEC K.K.); (2) the motor brackets were upgraded to a new type that is a stainless model (model number: Motor-Braket-01-Rev-1 and Motor-Braket-02-Rev-1, BL TEC K.K.); and (3) the light source units were secured to reduce vibration. The modified platform, referred to as the “QuAAtro 39-J” was used for this cruise.

The analytical methods for nitrate, nitrite, silicate, and phosphate used in this cruise align with those described in the GO-SHIP repeat hydrography nutrients manual (Hydes et al., 2010; Becker et al., 2019). The method for ammonium follows a vaporization membrane permeability approach (Kimura, 2000).

(3.1) Nitrate + nitrite and nitrite

Nitrate + nitrite and nitrite were analyzed using a methodology modified from Grasshoff (1976). The flow diagrams are shown in Fig. 4.7.1 for nitrate + nitrite and Fig. 4.7.2 for nitrite. In the nitrate + nitrite analysis, samples were mixed with the alkaline imidazole buffer and then pushed through a cadmium coil coated with metallic copper. This step facilitated the reduction of nitrate to nitrite in the sample, allowing for the determination of total nitrate + nitrite in seawater. For the nitrite analysis, the samples were mixed with reagents without undergoing the reduction step. In the flow system, the seawater sample – either with or without the reduction step - was mixed with an acidic sulfanilamide reagent through a mixing coil to produce a diazonium ion. The mixture was then combined with the N-1-naphthylethylenediamine dihydrochloride (NED), producing a red azo dye. This azo dye was subsequently directed to the spectrophotometric detection to monitor the signal at 545 nm. Therefore, for the nitrite analysis, sample bypassed the Cd coil, and nitrate concentrations were calculated by the difference between nitrate + nitrite and nitrite concentrations.

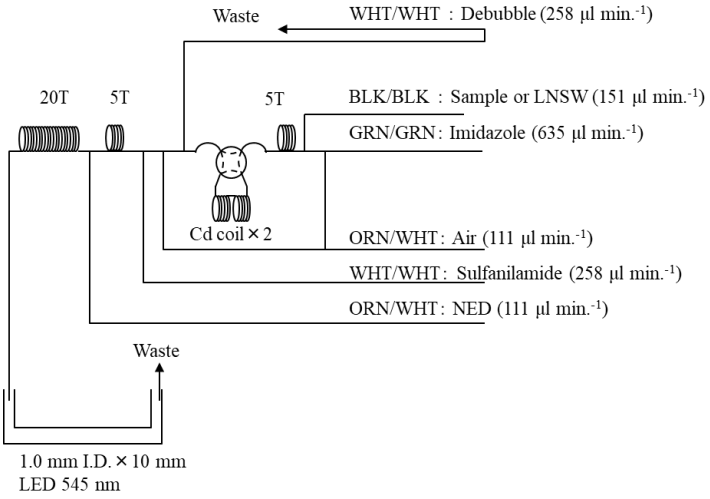

Figure 4.7.1 NO_3+NO_2 (1ch.) flow diagram.

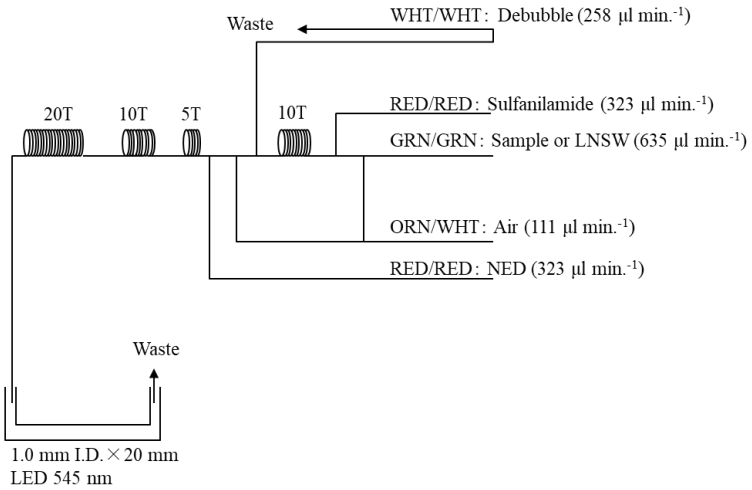

Figure 4.7.2 NO_2 (2ch.) flow diagram.

Reagents

a) 50 % Triton solution: 50 mL of Triton® X-100 (CAS No. 9002-93-1) was mixed with 50 mL of ethanol (99.5 %).

b) Imidazole (buffer), 0.06 M (0.4 % w/v): Dissolved 4 g of the imidazole (CAS No. 288-32-4) in 1000 mL ultra-pure water, and then added 2 mL of the hydrogen chloride (CAS No. 7647-01-0). After mixing, 1 mL of the 50 % triton solution was added.

c) Sulfanilamide, 0.06 M (1 % w/v) in 1.2 M HCl: Dissolved 10 g of 4-aminobenzenesulfonamide (CAS No. 63-74-1) in 900 mL of ultra-pure water, and then add 100 mL of the hydrogen chloride (CAS No. 7647-01-0). After mixing, 2 mL of the 50 % triton solution was added.

d) NED, 0.004 M (0.1 % w/v): Dissolved 1 g of N-(1-naphthalenyl)-1,2-ethanediamine dihydrochloride (CAS No. 1465-25-4) in 1000 mL of ultra-pure water and then added 10 mL of hydrogen chloride (CAS No. 7647-01-0). After mixing, 1 mL of the 50 % triton solution was added. This reagent was stored in a dark bottle.

(3.2) Silicate

The method for silicate is analogous to that described for phosphate (4.3) and is essentially based on

the method outlined by Grasshoff et al. (1999). The flow diagram is shown in Fig. 4.7.3. Silicomolybdic acid compound was first formed by mixing the silicate in the sample with the molybdic acid. This silicomolybdic acid was then reduced to silicomolybdous acid, known as "molybdenum blue," using L-ascorbic acid as the reductant. The signal was monitored at 630 nm.

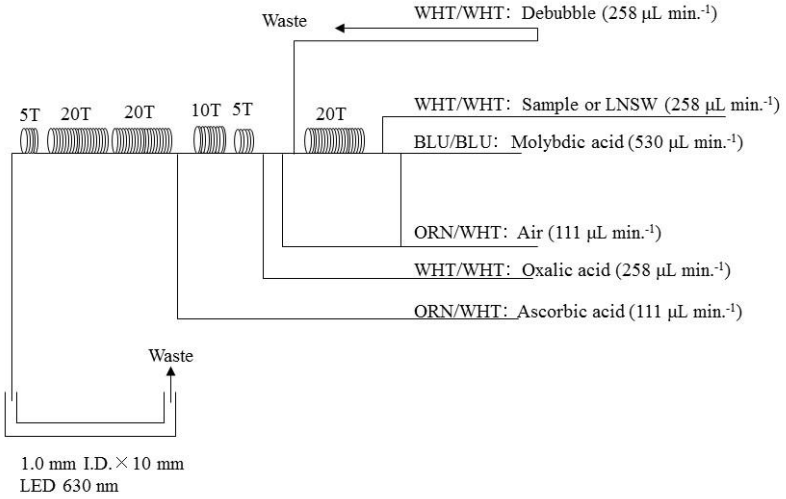

Figure 4.7.3 SiO_2 (3ch.) flow diagram.

Reagents

a) 15 % Sodium dodecyl sulfate solution: 75 g of sodium dodecyl sulfate (CAS No. 151-21-3) was mixed with 425 mL ultra-pure water.

b) Molybdic acid, 0.03 M (1 % w/v): Dissolved 7.5 g of sodium molybdate dihydrate (CAS No. 10102-40-6) in 980 mL ultra-pure water, and then added 12 mL of 4.5M sulfuric acid. After mixing, 20 mL of the 15 % sodium dodecyl sulfate solution was added. Note that the amount of sulfuric acid was reduced from the previous report (MR19-03C) since we have modified the method of Grasshoff et al. (1999).

c) Oxalic acid, 0.6 M (5 % w/v): Dissolved 50 g of oxalic acid (CAS No. 144-62-7) in 950 mL of ultra-pure water.

d) Ascorbic acid, 0.01 M (3 % w/v): Dissolved 2.5 g of L-ascorbic acid (CAS No. 50-81-7) in 100 mL of ultra-pure water. This reagent was freshly prepared every day.

(3.3) Phosphate

The methodology for the phosphate analysis is a modified procedure based on Murphy and Riley (1962). The flow diagram is shown in Fig. 4.7.4. Molybdic acid was added to the seawater sample to form the phosphomolybdic acid compound, which was then reduced to phosphomolybdous acid using L-ascorbic acid as the reductant. The signal was monitored at 880 nm.

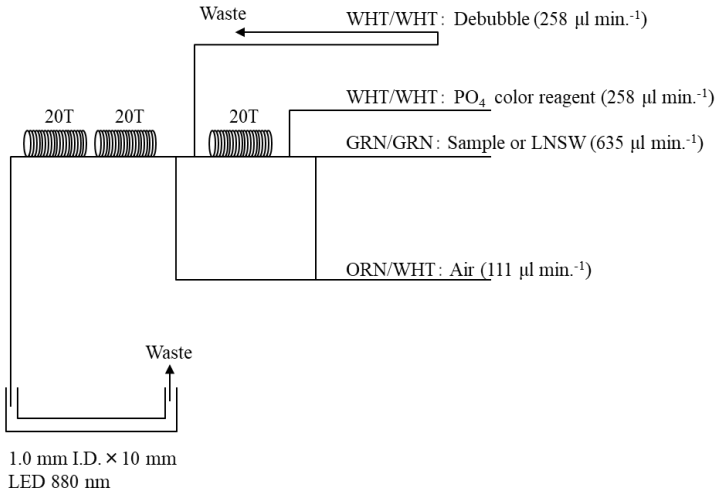

Figure 4.7.4 PO_4 (4ch.) flow diagram.

Reagents

a) 15 % Sodium dodecyl sulfate solution: 75 g of sodium dodecyl sulfate (CAS No. 151-21-3) was mixed with 425 mL of ultra-pure water.

b) Stock molybdate solution, 0.03 M (0.8 % w/v): Dissolved 8 g of sodium molybdate dihydrate (CAS No. 10102-40-6) and 0.17 g of antimony potassium tartrate trihydrate (CAS No. 28300-74-5) in 950 mL of ultra-pure water, and then added 50 mL of sulfuric acid (CAS No. 7664-93-9).

c) PO4 color reagent: Dissolved 1.2 g of L-ascorbic acid (CAS No. 50-81-7) in 150 mL of the stock molybdate solution. After mixing, 3 mL of the 15 % sodium dodecyl sulfate solution was added. This reagent was freshly prepared before every measurement.

(3.4) Ammonia

The ammonia in seawater was determined using the flow diagrams shown in Fig. 4.7.5. The sample was mixed with an alkaline solution containing EDTA, which converted ammonia into its gaseous state. The ammonia gas was then absorbed in a sulfuric acid though a 0.5 µm pore-size membrane filter (ADVANTEC PTFE) at the dialyzer attached to the analytical system. The ammonia absorbed in sulfuric acid was subsequently determined by coupling it with phenol and hypochlorite to form indophenols blue, with the signal monitored at 630 nm.

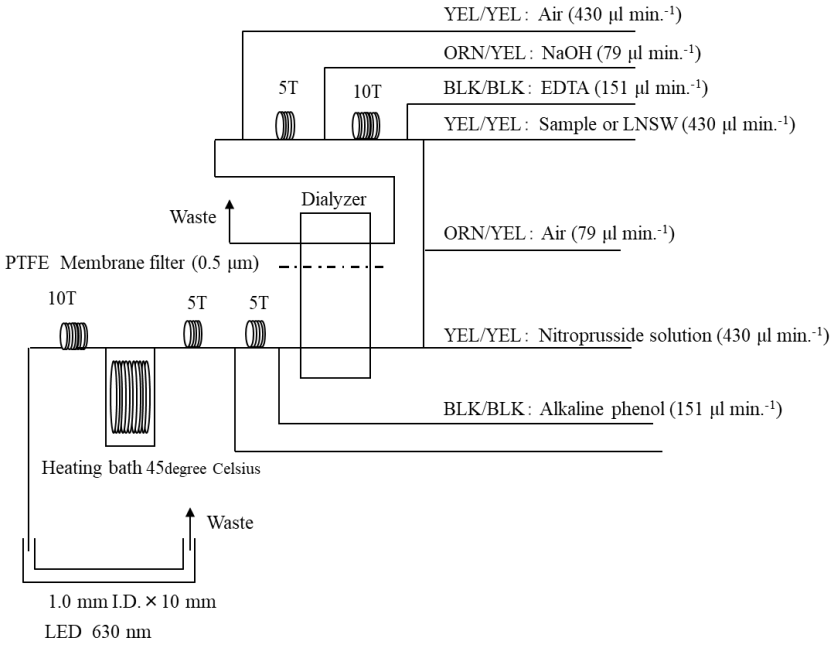

Figure 4.7.5 NH_4 (5ch.) flow diagram.

Reagents

a) 30 % Triton solution: 30 mL of the Triton® X-100 (CAS No. 9002-93-1) was mixed with 70 mL ultra-pure water.

b) EDTA: Dissolved 41 g of tetrasodium;2-[2-[bis(carboxylatomethyl)amino]ethyl-(carboxylatemethyl)amino]acetate;tetrahydrate (CAS No. 13235-36-4) and 2 g of boric acid (CAS No. 10043-35-3) in 200 mL of ultra-pure water. After mixing, 1 mL of the 30 % triton solution was added. This reagent is prepared every week.

c) NaOH liquid: Dissolved 1.5 g of sodium hydroxide (CAS No. 1310-73-2) and 16 g of tetrasodium;2-[2-[bis(carboxylatomethyl)amino]ethyl-(carboxylatemethyl)amino]acetate;tetrahydrate (CAS No. 13235-36-4) in 100 mL of ultra-pure water. This reagent was prepared every week. Note that we reduced the amount of sodium hydroxide from 5 g to 1.5 g because pH of C standard solutions has been lowered 1 pH unit due to the change of recipe of B standards solution (the details of those standard solutions, see (6.4)).

d) Stock nitroprusside: Dissolved 0.25 g of sodium nitroferricyanide dihydrate (CAS No. 13755-38-9) in 100 mL of ultra-pure water, and then added 0.2 mL of 1M sulfuric acid. Stored in a dark bottle and prepared every month.

e) Nitroprusside solution: Added 4 mL of the stock nitroprusside and 4 mL of 1M sulfuric acid in 500 mL of ultra-pure water. After mixing, 2 mL of the 30 % triton solution was added. This reagent was stored in a dark bottle and prepared every 2 or 3 days.

f) Alkaline phenol: Dissolved 10 g of phenol (CAS No. 108-95-2), 5 g of sodium hydroxide (CAS No. 1310-73-2) and 2 g of sodium citrate dihydrate (CAS No. 6132-04-3) in 200 mL of ultra-pure water. Stored in a dark bottle and prepared every week.

g) NaClO solution: Mixed 3 mL of sodium hypochlorite (CAS No. 7681-52-9) in 47 mL of ultra-pure water. Stored in a dark bottle and fleshly prepared before every measurement. This reagent needs to be 0.3 % available chlorine.

(3.5) Sampling procedures

Sampling for the nutrient samples was conducted after collecting samples for other gas parameters. Seawater samples were collected in two new 10 mL polyacrylate vial tubes without using the sample

drawing tube typically used for the oxygen samples. Each vial tube was rinsed three times before filling and sealed immediately without any head space. The vial tubes were then placed in a water bath at 21.0 degree Celsius for over 30 minutes before measurement. Then, the vial tube was loaded directly on a tray of an autosampler (AIM 4000, BL TEC K.K.) for analysis. The autosampler housing was purged with N_2 gas flow (5 L min^{-1}) that was provided by a nitrogen gas generator (model number: ITN2-04-1, IBS Inc.) to prevent contamination from the atmosphere. A humidifier was placed into the autosampler housing to keep appropriate humidity in it. The seawater samples were analyzed within 24 hours of collection.

(3.6) Data processing

Raw data from QuAAtro 39-J were processed as follows:

a) Checked if there were any baseline shifts.

b) Checked the shape of each peak and positions of peak values. If necessary, a change was made for the positions of peak values.

c) Conducted carry-over correction and baseline drift correction followed by sensitivity correction to apply to the peak height of each sample.

d) Conducted baseline correction and sensitivity correction using linear regression. Conducted baseline correction and sensitivity correction using linear regression.

e) Using the salinity (from CTD data* for bio samples, and determined data on the ship for routine samples) and the laboratory room temperature (20 degree Celsius), the density of each sample was calculated. The obtained density was used to calculate the final nutrient concentration with the unit of μmol kg-1.

f) Calibration curves to obtain the nutrient concentrations were assumed second-order equations.

* Raw CTD pre-calibrated data have been used.

(4) Certified Reference Material of nutrients in seawater

Certified reference materials (CRMs) produced by KANSO Co., Ltd. were used to ensure the comparability and traceability of nutrient measurements during this cruise. The KANSO CRMs cover inorganic nutrients (nitrate, nitrite, silicate, phosphate, and ammonia) in seawater and are produced using autoclaved natural seawater, following a quality control system based on ISO Guide 34 (JIS Q 0034). KANSO Co., Ltd. has been accredited as a CRM producer under the National Institute of Technology and Evaluation (ASNITE) System since 2011. (ASNITE 0052 R)

Certified values for the CRMs were calculated as the arithmetic means of measurements from 30 bottles per batch (measured in duplicates), performed by both KANSO Co., Ltd. and Japan Agency for Marine-Earth Science and Technology (JAMSTEC) using the colorimetric method (continuous flow analysis, CFA). The salinity of the calibration standards solution for each calibration curve was adjusted to match the CRM salinity within ± 0.5.

Each certified value of nitrate, nitrite, and phosphate in KANSO CRMs was calibrated using Japan Calibration Service System (JCSS) standard solutions for the respective ions. The JCSS standard solutions were in turn calibrated using JCSS secondary solutions, which was calibrated with primary solutions produced by the Chemicals Evaluation and Research Institute (CERI), Japan. CERI primary solutions were further calibrated with the National Metrology Institute of Japan (NMIJ) primary standards solution of nitrate, nitrite, and phosphate ions, respectively. The certified value of silicate of KANSO CRM was calibrated using a newly developed silicon standards solution ("exp31" produced by JAMSTEC and KANSO, and Lot. AA produced by KANSO), produced via an alkaline dissolution technique. The mass fraction of silicon in this solution was calibrated based on NMIJ CRM 3645-a Si standard solution through the technology consulting system of the National Institute of Advanced Industrial Science and Technology (AIST), providing traceability to the International System of Units (SI).

During this cruise, 23 sets of CRM lots CQ, CU, CW, CT, CN and 12 sets of CRM lot CX were used (Table 4.7.1), with serial numbers selected randomly. The CRM bottles were stored in the ship's "BIOCHEMICAL LABORATORY" at a maintained temperature of approximately 20.65 degree Celsius – 23.43 degree Celsius.

Table 4.7.1 Certified concentration and the uncertainty (k=2) of CRMs (μmol kg^{-1}).

Lot	Nitrate	Nitrite*	Silicate	Phosphate	Ammonia**
CQ	0.06 ± 0.03	0.075 ± 0.07	2.20 ± 0.07	0.030 ± 0.009	1.76 ± 0.07
CU	3.06 ± 0.05	0.04 ± 0.04	7.77 ± 0.09	0.262 ± 0.011	1.02 ± 0.04
CW	21.2 ± 0.2	0.24 ± 0.07	41.6 ± 0.5	1.45 ± 0.03	1.102
CT	40.1 ± 0.4	0.35 ± 0.07	85.3 ± 0.9	2.13 ± 0.03	0.785
CN	43.6 ± 0.4	0.02 ± 0.004	152.7 ± 0.8	2.94 ± 0.03	0.455
CX	39.4 ± 0.4	0.024 ± 0.019	121.4 ± 1.3	2.77 ± 04	0.599

* For Nitrite concentration, there is a trend that the value has been increased 0.004 ± 0.002 μmol kg^{-1} per year. The values of CQ and CN were determined by JAMSTEC in April 2025.

** Ammonia values are all reference value. The value of CQ and CU were reported by KANSO. The other values were determined by JAMSTEC.

(5) Standards

To obtain the calibration curves, we prepared in-house standard solutions because (1) nutrient concentrations in seawater samples may exceed CRM, (2) the ammonia concentrations in the CRMs are not certified values.

(5.1) Volumetric laboratory-ware of in-house standards

All volumetric glassware and polymethylpentene (PMP) volumetric flasks were gravimetrically calibrated. Plastic volumetric flasks were calibrated gravimetrically at their water temperature, within 0.4 K of approximately 19.5 degree Celsius. “Class A” volumetric flasks were used for their nominal tolerances of 0.05 % or less across the size ranges relevant to this work. Since Class A flasks are made of borosilicate glass, standard solutions were transferred to plastic bottles immediately after being made up to volume and thoroughly mixed to prevent excessive silicate dissolution from the glass. PMP volumetric flasks were also gravimetrically calibrated and used only within 2.6 K of their calibration temperature. Volume adjustments for the glass flasks at temperatures other than the calibration temperatures were calculated using the linear expansion coefficient for borosilicate crown glass. The cubical expansion coefficients for each glass and PMP volumetric flask were determined through measurements in 2025. The cubical expansion coefficient of the glass volumetric flask (SHIBATA HARIO) ranged from 0.000011 to 0.0000172 K^{-1}, and for the PMP volumetric flask (NALGEN PMP), from 0.00038 to 0.00042 K^{-1}. Calibration weights were corrected for the water density and air buoyancy. All glass pipettes, which have nominal calibration tolerances of 0.1 % or better, were gravimetrically calibrated to verify and, where possible, improve upon there nominal tolerances.

(5.2) Reagents

For nitrate standard, we used “potassium nitrate 99.995 suprapur®” provided by Merck, Batch B1983565, CAS No. 7757-79-1. For nitrite standard solution, nitrite ion standard solutions (NO_2^- 1000) from Wako Chemicals (Lots KSK1433 and ACH2582, Code. No. 146-06453) was used, with the certified standard solutions from Wako Chemicals. The calibration results of lots KSK1433 and ACH2582 were 1006 and 1002 mg L^{-1} at 20 degrees Celsius respectively, with an expanded uncertainty of 0.8 % (k=2). For the silicate standard solution, Si standard solutions Lot. AA produced by KANSO, was used. The silicon mass fraction in the Lot. AA solution was calibrated based on NMIJ CRM 3645-a Si standard solution. For the phosphate standard, “potassium dihydrogen phosphate anhydrous 99.995 suprapur®” provided by Merck (Batch B2076208, CAS No.: 7778-77-0), was used. For the ammonia standard, we used ammonium chloride (CRM 3011-a) from NMIJ, CAS No. 12125-02-9, with a reported purity of >99.9 % by the manufacturer. The expanded uncertainty of calibration (k=2) was 0.026 %.

(5.3) Low nutrients seawater (LNSW)

Surface water with low nutrient concentrations was taken and filtered using a 0.20 μm pore capsule cartridge filter near 13°N and 136°E during the MR21-03 cruise in June 2021. The filtered seawater was drained into multiple 20 L Cubitainer (flexible containers) and stored in cardboard boxes. This water has since been used as low-nutrients seawater (LNSW) for nutrients measurements. The concentrations in each LNSW container were measured in June 2022, yielding average values of 0.01, 0.003, 1.08, 0.075, and 0.01 μmol L^{-1} for nitrate, nitrite, silicate, phosphate, and ammonia, respectively. The concentrations

of nitrate and ammonia were below the detection limit.

(5.4) Standard solutions and calibration curves

Concentrations of nutrients for standard solutions A, B, C, and D are shown in Table 4.7.2. The KANSO Si standard solution was used for the A standard of silicate, which doesn't require neutralization with hydrochloric acid. The B standard was diluted from the A standard following the recipes shown in Table 4.7.3. To match the salinity and the density of the B standard solution to those of the LNSW, 15.00 g of sodium chloride powder was dissolved in the B standard solution, and then the final volume was adjusted to 500 mL. The C standard solution was prepared in the LNSW following the recipes shown in Table 4.7.4. The actual concentrations of nutrients in each standard solution were calculated based on the solution temperature and the calibrated factors of volumetric laboratory wares. Calibration curves for each run of nitrate, nitrite, silicate, and phosphate were obtained using six levels: C-2, C-3, C-4, C-6, C-7, C-8. For ammonia, calibration was achieved using three levels: C-1, C-5, C-8. C-1 was LNSW, C-2, C-3, C-4, C-6 and C-7 were the CRM of nutrients in seawater, and C-5 and C-8 were diluted using the B standard solution. The D standard solutions, used to calculate the reduction rate of the Cd coil, were diluted from the A standard solution with pure water (milli-Q). In-house standard solutions were remade according to the "renewal time" intervals listed in Table 4.7.5.

Table 4.7.2 Nominal concentrations of nutrients for A, D, B and C standards (μmol L^{-1}).

	A	B	D	C-1	C-2	C-3	C-4	C-5	C-6	C-7*	C-8
NO_3	45000	900	900	-	CQ	CU	CW	-	CT	CN	54
NO_2	21900	26	870	-	CQ	CU	CW	-	CT	CN	1.6
SiO_2	35500	2850		-	CQ	CU	CW	-	CT	CN	171
PO_4	6000	60		-	CQ	CU	CW	-	CT	CN	3.7
NH_4	4000	40		LNSW	-	-	-	1.2	-	-	2.4

*C-7 was excluded from the calibration curve for nitrate and nitrite at Stn.36.

Table 4.7.3 B standard recipes. Final volume was 500 mL.

	A Std.
NO_3	10 mL
NO_2*	15 mL
SiO_2	40 mL
PO_4	5 mL
NH_4	5 mL

*NO_2 was D standard solution which was diluted from A standard.

Table 4.7.4 Working calibration standard recipes. Final volume was 500 mL.

C Std.	B Std.
C-5	15 mL
C-8	30 mL

Table 4.7.5 Renewal times of in-house standards.

Standard	Renewal time
A-1 Std. (NO_3)	maximum a month
A-2 Std. (NO_2)	commercial prepared solution
A-3 Std. (SiO_2)	commercial prepared solution
A-4 Std. (PO_4)	maximum a month
A-5 Std. (NH_4)	maximum a month
D-1 Std.	maximum 8 days
D-2 Std.	maximum 8 days
B Std. (mixture of A-1, D-2, A-3, A-4 and A-5 Std.)	maximum 8 days
C Std.	every 24 hours
36 μM NO_3 (diluted D-1 Std. for reduction estimate)	when C Std. renewed
35 μM NO_2 (diluted D-2 Std. for reduction estimate)	when C Std. renewed

(6) Data quality

During this cruise, a total of 41 runs were conducted to measure samples collected by 47 casts at 40 stations. In total, 1531 seawater samples were collected. The samples were collected into two vial tubes and measured independently as basically replicate measurements.

(6.1) Precision

The highest-concentration standard solution (C-8) was repeatedly determined every 8 to 12 sample to assess the analytical precision of the nutrient analyses during this cruise. Each run, included 11 to 16 C-8 determinations, depending on the run. Analytical precision for each run was calculated from these C-8 results, and overall precision for this cruise were calculated from the combined precision across all runs (Table 4.7.6). The overall median precisions during this cruise were 0.10%, 0.19%, 0.10%, 0.11%, and 0.45% for nitrate, nitrite, silicate, phosphate, and ammonia, respectively.

Table 4.7.6 Overall precisions (k=1)

	Nitrate CV %	Nitrite CV %	Silicate CV %	Phosphate CV %	Ammonia CV %
Median	0.10	0.19	0.10	0.11	0.45
Mean	0.11	0.20	0.10	0.11	0.47
Maximum	0.19	0.36	0.19	0.20	0.70
Minimum	0.04	0.11	0.03	0.07	0.19
n	40	41	40	40	41

(6.2) Comparability

CRM lot CX was measured during each run to evaluate the comparability across the measurements during this cruise. All measured concentrations were within the uncertainty of certified values for nitrate, nitrite, silicate, and phosphate (Table 4.7.7).

Table 4.7.7 CRM lot CX measurements (μmol kg^{-1}).

	Nitrate	Nitrite	Silicate	Phosphate	Ammonia
Median	39.47	0.02	121.49	2.779	0.66
Mean	39.46	0.02	121.49	2.778	0.66
STDEV	0.06	0.002	0.15	0.007	0.01
n	19	20	19	19	20

(6.3) Carryover

We also summarized the magnitudes of carry over, which refers to sample-to-sample contamination during flow analysis. To evaluate carryover in each run, we measured the C-8 standard solution followed by two consecutive measurements of the LNSW solution. The difference from LNSW-1 to LNSW-2 was used to estimate the carryover (%) using the following equation (1) where [ ] denotes concentrations.

$$\text{Carryover (\%)} = ([\text{LNSW-1}] - [\text{LNSW-2}]) / ([\text{C-8}] - [\text{LNSW-2}]) * 100 \quad (1)$$

The carryover (%) are shown in Table 4.7.8. Overall, the results indicated low carryover percentages. These low percentages suggest that there was no significant issue during this cruise.

Table 4.7.8 Carryovers (%)

	Nitrate	Nitrite	Silicate	Phosphate	Ammonia
Median	0.20	0.15	0.19	0.21	0.79
Mean	0.20	0.16	0.20	0.20	0.85
Maximum	0.26	0.48	0.33	0.29	1.99
Minimum	0.15	0.00	0.14	0.09	0.00
n	40	41	40	40	41

(6.4) Uncertainty (Repeatability)

Empirical equations of (2), (3) and (4) were obtained based on 41 measurements of 23 sets of CRMs (Table 4.7.1) to estimate the uncertainty (repeatability) of measurements of nitrate, silicate, and phosphate, respectively (Figs. 4.7.6-8).

$$\text{Uncertainty of measurement of nitrate (\%)} = 0.13523 + 1.1342 * (1 / C_{NO3}) \quad (2)$$

$$\text{Uncertainty of measurement of silicate (\%)} = 0.1575 + 1.0121 * (1 / C_{SiO2}) + 5.1491 * (1 / C_{SiO2}) * (1 / C_{SiO2}) \quad (3)$$

$$\text{Uncertainty of measurement of phosphate (\%)} = 0.065399 + 0.38134 * (1 / C_{PO4}) \quad (4)$$

where C_{NO3}, C_{SiO2}, and C_{PO4} are nitrate, silicate, and phosphate concentrations of sample (μmol kg^{-1}), respectively.

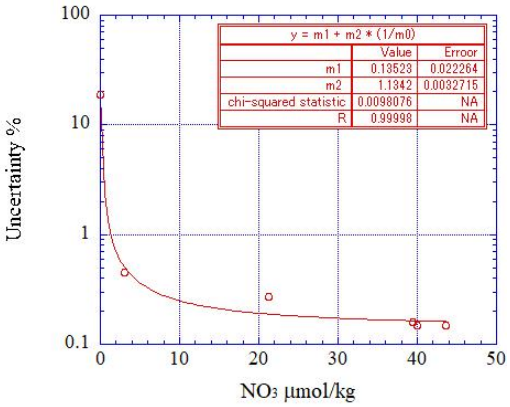

Figure 4.7.6 Uncertainty for NO_3

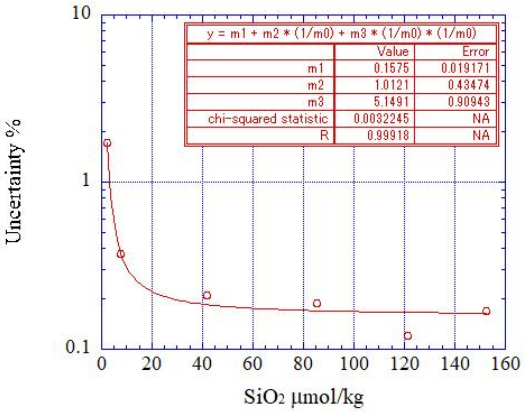

Figure 4.7.7 Uncertainty for SiO_2

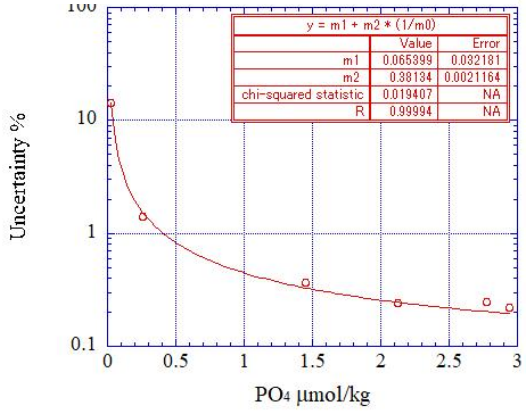

Figure 4.7.8 Uncertainty for PO_4

Empirical equations, eq. (5) and (6) were obtained based on duplicate measurements of the samples to estimate the uncertainty (repeatability) of measurements of nitrite and ammonia (Figs. 4.7.9-10).

Uncertainty of measurement of nitrite (%) =

$$- 0.036739 + 0.17072 * (1 / C_{NO2}) - 0.000012233 * (1 / C_{NO2}) * (1 / C_{NO2}) \quad (5)$$

Uncertainty of measurement of ammonia (%) = $4.3512 + 0.77811 * (1 / C_{NH4})$ (6)

where C_{NO2} and C_{NH4} are nitrite and ammonia concentrations of sample (µmol kg^{-1}), respectively.

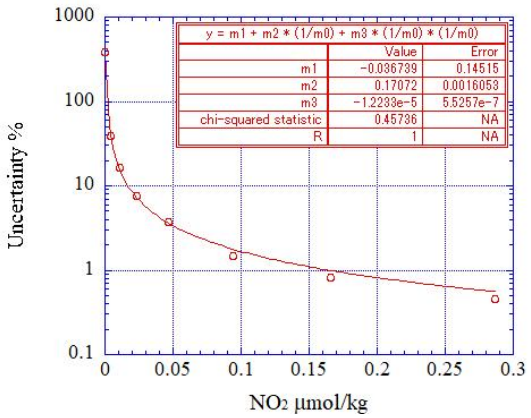

Figure 4.7.9 Uncertainty for NO_2

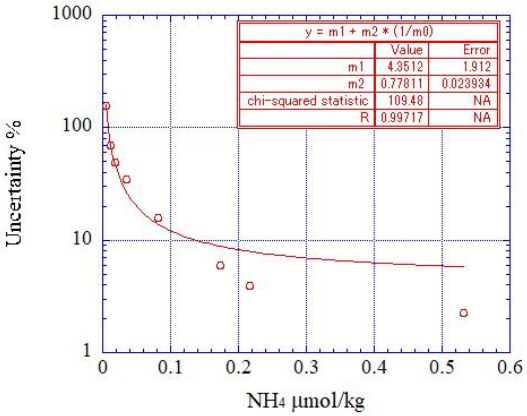

Figure 4.7.10 Uncertainty for NH_4

(6.5) Detection limit and quantitative determination

The LNSW was measured every 8 to 12 samples to estimate the detection limit of nutrient analyses during this cruise. In each run, the total number of the LNSW determination ranged from 10 to 15, depending on the specific run. The detection limit was calculated using the following equation:

Detection limit = 3 * standard deviation of repeated measurement of LNSW (7)

The estimated detection limits are shown in Table 4.7.9. The quantitative determination of nutrient analyses reflects concentrations with an uncertainty of 33 % as indicated in the empirical equations, eq. (2) to (6). The estimated quantitative determinations are also shown in Table 4.7.9.

Table 4.7.9 Detection limit.

	Nitrate µmol kg^{-1}	Nitrite µmol kg^{-1}	Silicate µmol kg^{-1}	Phosphate µmol kg^{-1}	Ammonia µmol kg^{-1}
Detection limit	0.02	0.003	0.07	0.005	0.02
Quantitative determination	0.03	0.01	0.41	0.012	0.03

Replicate samples were taken at most of the layers. The summary of average and standard deviation of the difference between each replicate pair of analysis was shown in Table 4.7.10.

Table 4.7.10 Average and standard deviation of the difference between each replicate pair of analysis.

	Nitrate µmol kg^{-1}	Nitrite µmol kg^{-1}	Silicate µmol kg^{-1}	Phosphate µmol kg^{-1}	Ammonia µmol kg^{-1}
Average	0.04	0.002	0.10	0.003	0.02
Standard deviation	0.04	0.002	0.11	0.003	0.01
n	1393	1390	1396	1396	1382

(6.6) Quality control flag assignment

The quality control (flag “2 (good)”, “3 (questionable)”, or “4 (bad)”) of the concentration in the seawater samples proceeded as follows.

1) We found outliers (flag “3” or “4”) on vertical profiles of the concentrations of nitrite, nitrate, phosphate, and silicate.

2) We found outliers from the ratios of nitrate/phosphate.

3) Considering the comparison of our results with those obtained using the OPA (o-phthalaldehyde)

method (Holmes et al., 1999) at some stations, all the ammonia concentrations were flagged “3” or “4”.

(7) Problems

There is no significant issue of this data set during this cruise.

(8) List of reagents

List of reagents used in this cruise is shown in Table 4.7.11.

(9) Data archives

These data obtained in this cruise will be submitted to the Data Management Group of JAMSTEC, and will be opened to the public via “Data Research System for Whole Cruise Information in JAMSTEC (DARWIN)” in JAMSTEC web site. <https://www.godac.jamstec.go.jp/darwin/en/index.html>

Table 4.7.11 List of reagents used in this cruise

IUPAC name	CAS Number	Formula	Compound Name	Manufacture	Grade
4-Aminobenzenesulfonamide	63-74-1	$C_6H_8N_2O_2S$	Sulfanilamide	FUJIFILM Wako Pure Chemical Corporation	JIS Special Grade
Ammonium chloride	12125-02-9	NH_4Cl	Ammonium Chloride	FUJIFILM Wako Pure Chemical Corporation	JIS Special Grade
Antimony potassium tartrate trihydrate	28300-74-5	$K_2(SbC_4H_2O_6)_2 \cdot 3H_2O$	Bis[(+)-tartrato]diantimonate(III) Dipotassium Trihydrate	FUJIFILM Wako Pure Chemical Corporation	JIS Special Grade
Boric acid	10043-35-3	H_3BO_3	Boric Acid	FUJIFILM Wako Pure Chemical Corporation	JIS Special Grade
Hydrogen chloride	7647-01-0	HCl	Hydrochloric Acid	FUJIFILM Wako Pure Chemical Corporation	JIS Special Grade
Imidazole	288-32-4	$C_3H_4N_2$	Imidazole	FUJIFILM Wako Pure Chemical Corporation	JIS Special Grade
L-Ascorbic acid	50-81-7	$C_6H_8O_6$	L-Ascorbic Acid	FUJIFILM Wako Pure Chemical Corporation	JIS Special Grade
N-(1-Naphthalenyl)-1,2-ethanediamine, dihydrochloride	1465-25-4	$C_{12}H_{16}Cl_2N_2$	N-1-Naphthylethylenediamine Dihydrochloride	FUJIFILM Wako Pure Chemical Corporation	for Nitrogen Oxides Analysis
Oxalic acid	144-62-7	$C_2H_2O_4$	Oxalic Acid	FUJIFILM Wako Pure Chemical Corporation	Wako Special Grade
Phenol	108-95-2	C_6H_6O	Phenol	FUJIFILM Wako Pure Chemical Corporation	JIS Special Grade
Potassium nitrate	7757-79-1	KNO_3	Potassium Nitrate	Merck KGaA	Suprapur®
Potassium dihydrogen phosphate	7778-77-0	KH_2PO_4	Potassium dihydrogen phosphate anhydrous	Merck KGaA	Suprapur®
Sodium chloride	7647-14-5	NaCl	Sodium Chloride	FUJIFILM Wako Pure Chemical Corporation	TraceSure®
Sodium citrate dihydrate	6132-04-3	$Na_3C_6H_5O_7 \cdot 2H_2O$	Trisodium Citrate Dihydrate	FUJIFILM Wako Pure Chemical Corporation	JIS Special Grade
Sodium dodecyl sulfate	151-21-3	$C_{12}H_{25}NaO_4S$	Sodium Dodecyl Sulfate	FUJIFILM Wako Pure Chemical Corporation	for Biochemistry
Sodium hydroxide	1310-73-2	NaOH	Sodium Hydroxide for Nitrogen Compounds Analysis	FUJIFILM Wako Pure Chemical Corporation	for Nitrogen Analysis
Sodium hypochlorite	7681-52-9	NaClO	Sodium Hypochlorite Solution	Kanto Chemical co., Inc.	Extra pure
Sodium molybdate dihydrate	10102-40-6	$Na_2MoO_4 \cdot 2H_2O$	Disodium Molybdate(VI) Dihydrate	FUJIFILM Wako Pure Chemical Corporation	JIS Special Grade
Sodium nitroferricyanide dihydrate	13755-38-9	$Na_2[Fe(CN)_5NO] \cdot 2H_2O$	Sodium Pentacyanonitrosylferrate(III) Dihydrate	FUJIFILM Wako Pure Chemical Corporation	JIS Special Grade
Sulfuric acid	7664-93-9	H_2SO_4	Sulfuric Acid	FUJIFILM Wako Pure Chemical Corporation	JIS Special Grade
tetrasodium;2-[2-[bis(carboxylatomethyl)amino]ethyl-(carboxylatomethyl)amino]acetate;tetrahydrate	13235-36-4	$C_{10}H_{12}N_2Na_4O_8 \cdot 4H_2O$	Ethylenediamine-N,N,N',N'-tetraacetic Acid Tetrasodium Salt Tetrahydrate (4NA)	Dojindo Molecular Technologies, Inc.	-
Synonyms: t-Octylphenoxypolyethoxyethanol 4-(1,1,3,3-Tetramethylbutyl)phenyl-polyethylene glycol Polyethylene glycol tert-octylphenyl ether	9002-93-1	$(C_2H_4O)_nC_{14}H_{22}O$	Triton®X-100	MP Biomedicals, Inc.	-

(10) References

Becker, S., Aoyama, M., Malcolm E., Woodward, S., Bakker, K., Coverly, S., Mahaffey, C., Tanhua, T., (2019) The precise and accurate determination of dissolved inorganic nutrients in seawater, using Continuous Flow Analysis methods, n: The GO-SHIP Repeat Hydrography Manual: A Collection of Expert Reports and Guidelines. Available online at: http://www.go-ship.org/HydroMan.html. DOI: http://dx.doi.org/10.25607/OBP-555

Grasshoff, K. (1976). Automated chemical analysis (Chapter 13) in Methods of Seawater Analysis. With contribution by Almgreen T., Dawson R., Ehrhardt M., Fonselius S. H., Josefsson B., Koroleff F., Kremling K. Weinheim, New York: Verlag Chemie.

Grasshoff, K., Kremling K., Ehrhardt, M. et al. (1999). Methods of Seawater Analysis. Third, Completely Revised and Extended Edition. WILEY-VCH Verlag GmbH, D-69469 Weinheim (Federal Republic of Germany).

Holmes, R. M., Aminot, A., Kérouel, R., Hooker, B. A., Peterson, B. J. (1999). A simple and precise method for measuring ammonium in marine and freshwater ecosystems. Canadian Journal of Fisheries and Aquatic Sciences 56, 1801-1808.

Hydes, D.J., Aoyama, M., Aminot, A., Bakker, K., Becker, S., Coverly, S., Daniel, A., Dickson, A.G., Grosso, O., Kerouel, R., Ooijen, J. van, Sato, K., Tanhua, T., Woodward, E.M.S., Zhang, J.Z., (2010). Determination of Dissolved Nutrients (N, P, Si) in Seawater with High Precision and Inter-Comparability Using Gas-Segmented Continuous Flow Analysers, In: GO-SHIP Repeat Hydrography Manual: A Collection of Expert Reports and Guidelines. IOCCP Report No. 14, ICPO Publication Series No 134.

Kimura (2000). Determination of ammonia in seawater using a vaporization membrane permeability method. 7th auto analyzer Study Group, 39-41.

Murphy, J., and Riley, J.P. (1962). Analytica Chimica Acta 27, 31-36.

4.8 Chlorofluorocarbons and Sulfur hexafluoride

November 17, 2025
Yuichiro Kumamoto
Japan Agency for Marine-Earth Science and Technology

(1) Personnel

Yuichiro Kumamoto (Principal Investigator), Yumi Takabayashi, and Yuto Ooishi

Japan Agency for Marine-Earth Science and Technology

Noriyuki Kisen

Marine Works Japan Co. Ltd

(2) Objectives

Chlorofluorocarbons (CFCs) and sulfur hexafluoride (SF_6) are anthropogenic stable gases. These atmospheric gases can slightly dissolve in sea surface water by air-sea gas exchange and then spread into the ocean interior. Thus, these gases could be used as chemical tracers for ocean circulation and ventilation. To discuss the ventilation rates and pathways of the North Pacific water, we collected seawater samples at every water sampling station, and measured concentrations of CFCs, namely CFC-11 (CCl_3F), CFC-12 (CCl_2F_2), CFC-113 ($C_2Cl_3F_3$), and SF_6 in the seawater samples on board.

(3) Instruments

Two sets (A and B) of the analyzing system, each of which consists of seawater stripping, gas traps, standard gas loops, and gas chromatograph, were used (Fig. 4.8.1). The system was driven by pure N_2 gas. We employed the first-grade N_2 gas (Purity > 99.99995%) supplied by Taiyo Nippon Sanso Corporation. The N_2 gas passed through the purifier column with Molecular Sieve 13X before it was introduced into the system (CFCs/SF_6-free N_2 gas). A volume of seawater sample (about 200 ml) was transported into a stripping chamber. Dissolved SF_6 and CFCs in the seawater were extracted by the CFCs/SF_6-free N_2 gas purging for 8 minutes at 220 ml min^{-1}. The gases were dried in the desiccant tube (magnesium perchlorate), and trapped in the main trap at -80 ℃. The main trap was a 30-cm length of 1/8-inch stainless steel tube with 80/100 mesh Porapak Q (5 cm) and 60/80 mesh Carboxen 1000 (5 cm). Stripping efficiency was estimated from repeat stripping (three times) of surface seawater for every station. More than 99 % of dissolved SF_6 and CFCs were extracted in the first stripping. The trapped gases in the main trap were released by heating at 180 ℃. After one minute of heating, the released gases were transferred into the focus trap, which is the same as the main trap but with 1/16-inch tube, at -80 ℃ for 30 seconds.

The gases trapped in the focus trap were released by heating at 180 ℃ and then the first carrier N_2 gas transferred the gases into the pre-column 1 (PC 1, ~6 m of Silica Plot capillary column with 0.53 mm i.d. and 6 μm film thickness) in the oven of the gas chromatograph (Shimadzu GC-2014) at 95 ℃. The injected gases were roughly separated in the PC 1, and the SF_6 and CFCs were eluted into the pre-column 2 (PC 2, ~5 m of Molsieve 5A Plot capillary column with 0.53 mm i.d. of and 15 μm film thickness). Then, the PC 1 was connected to a cleaning (back flush) line, and the remained gases in the PC 1, which have high boiling points, were flushed out by a counter flow of the back-flush N_2 gas. SF_6 and CFCs were eluted from the PC 2 into the main column 1 (MC 1, ~9 m of Pola Bond-Q capillary column with 0.53 mm i.d. and 6 μm film thickness, and ~18 m of Silica Plot capillary column) but N_2O was retained in the PC 2. The PC 2 was then connected to the second carrier N_2 gas and N_2O was transported into the main column 2 (MC 2, ~3 m of Molsieve 5A Plot connected to ~9 m of Pola Bond-Q capillary column). SF_6 and CFCs were further separated in the MC 1 and detected separately in the first Electron Capture Detector (ECD) at 300 ℃. N_2O eluted from the MC 2 was detected in the second ECD. Although the chromatogram of N_2O was obtained, the concentration of N_2O was not calculated in this cruise for some reasons. The mass flow rates of the carrier/back-flush and detector make-up N_2 gases are about 10 ml min^{-1} and 27 ml min^{-1}, respectively.

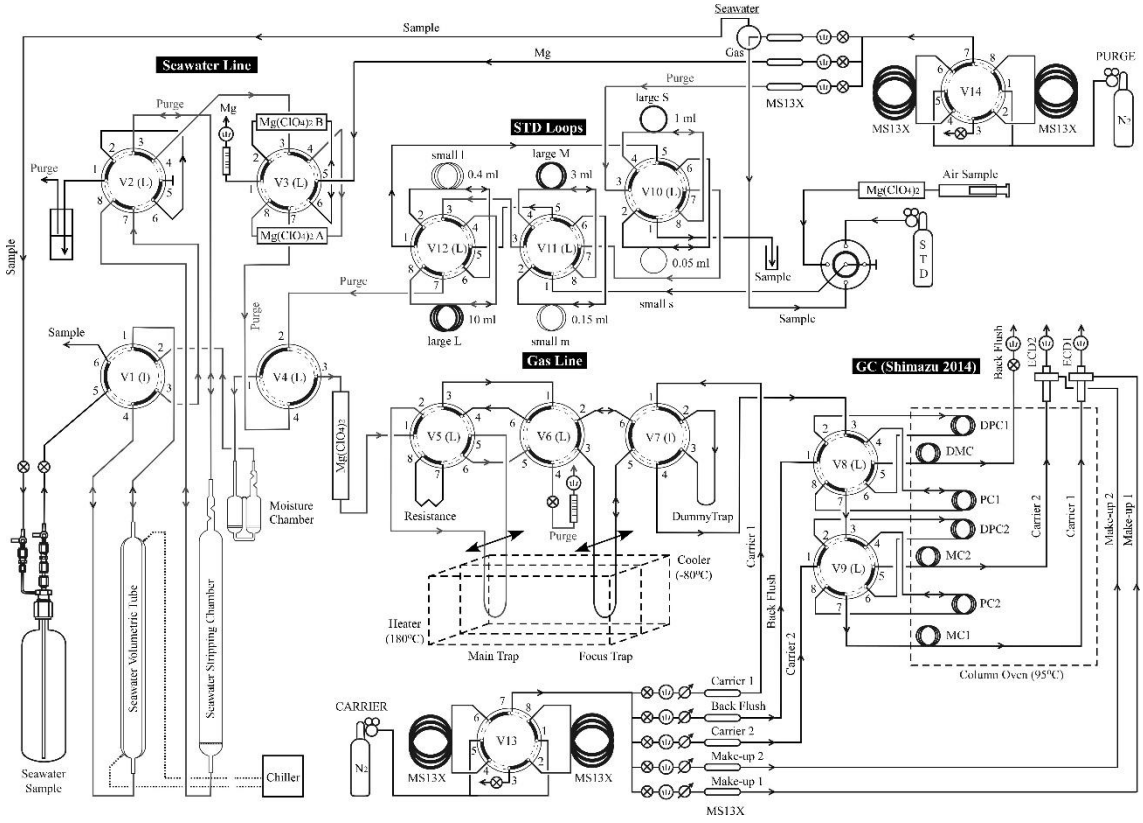

Figure 4.8.1 Outline of the analyzing system for measurements of CFC-11, CFC-12, CFC-113, SF_6, and N_2O.

(4) Standard gases

Two high-pressure gas cylinders of the standard gas for CFCs/SF_6 (Taiyo Nippon Sanso Corporation) were employed during this cruise (Table 4.8.1). We got the calibration curve (cubic curve) by combining of the standard gas loops (Table 4.8.2) after corrections for the temperature of the gas loops and atmospheric pressure. We also measured the standard gas every 10-15 sample measurements for the sensitivity correction.

Table 4.8.1 Concentration of the standard gases.

System	Cylinder Lot	SF_6 (ppt)	CFC-11 (ppt)	CFC-12 (ppt)	CFC-113 (ppt)	(N_2O) (ppm)
A	CPB-25811	9.74	927	502	78.7	14.7
B	CPB-29404	9.87	912	494	80.3	14.8

Table 4.8.2 Volumes of the standard gas loops (ml).

System	L (large)	l (small)	M (large)	m (small)	S (large)	s (small)
A	9.985	0.244	3.291	0.117	1.130	0.055
B	9.965	0.416	3.107	0.156	1.005	0.078

(5) Air sampling and measurement

During the cruise, we measured concentrations of CFCs/SF_6 in the atmosphere to confirm the concentrations of the standard gases and to check saturation levels in the sea surface water. The air

sample was continuously introduced into a laboratory using an air pump. The other end of 10 mm OD Dekaron tube was put on the head of the compass deck. The tube was relayed by a three-way stopcock. An air sample was collected from the flowing air into a 200 ml glass cylinder by attaching the cylinder to the cock. A volume of air sample (about 10 ml) was introduced into the system using the L(large)-loop (Table. 4.8.2). The results are shown in Table 4.8.3.

Table 4.8.3 Atmospheric concentrations.

System	Lat. (ºN)	Long. (ºE)	Sampling Date (UTC)	SF_6 (ppt)	CFC-11 (ppt)	CFC-12 (ppt)	CFC-113 (ppt)
A	9.50	145.79	2025/04/19 01:10	13.2 ± 0.1 (n = 4)	488 ± 2 (n = 4)	224 ± 1 (n = 4)	73.2 ± 4.0 (n = 4)
B	9.37	143.69	2025/04/18 05:32	12.6 ± 0.2 (n = 4)	494 ± 4 (n = 3)	217 ± 3 (n = 4)	74.5 ± 5.7 (n = 3)

(6) Seawater sampling and measurement

Discrete water samples from each station were collected using 12-liter niskin-type sampling bottles mounted on the CTD system. Each sample was collected into a glass bottle of 600 ml from a spigot of the sampling bottle through a Tygon tube (about 45 cm length) after water sampling for dissolved oxygen measurement. Before water sampling, the glass bottle was purged with the CFCs/SF_6-free N_2. The seawater was overflowed by twice the bottle volume. The samples were stored in a water bath at about 7°C immediately after the water sampling and then were measured within 12 hours after the sampling. Every 10-15 seawater sample measurements, we also measured the line blanks (the gas blank for air sample and water blank for seawater sample) and the standard gas for the blank correction and sensitivity corrections, respectively.

(7) Calculation of concentrations

The measured chromatograms (Fig. 4.8.2) were treated as follows. The original chromatogram was corrected for the baseline and then the smooth fitting, based on a method of Eilers (2003). The peak area of each gas on the processed chromatogram was integrated using exponential-Gaussian hybrid function (Lan and Jorgenson, 2001) to eliminate interference of adjacent peaks. Because this automatic integration did not work for the broader peak of CFC-113 (Fig. 4.8.2) in some samples, all the peak areas of CFC-113 were integrated manually. The gas and water blanks (peak areas) were subtracted from the peak area of each gas for the air and seawater samples, respectively. The moles were calculated using the peak areas and the calibration curve. Then the concentrations were calculated using the moles and the sample volumes. The concentrations were collected for the temporal change in the sensitivity of the detectors (the sensitivity correction). Finally, for the seawater sample, the corrections for the stripping efficiency and the contamination from the sampling tube were also applied.

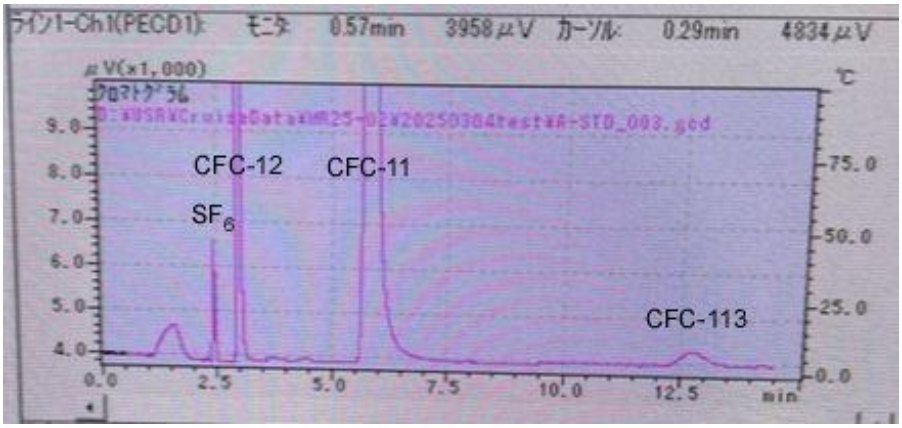

Figure 4.8.2 An example of chromatogram of the standard gas measurement.

(8) Repeatability and detection limit for seawater measurements

We collected seawater samples in two glass bottles from the same sampling bottle collected at about 250 and 900 dbar (replicate sampling). We estimated the analytical precision (repeatability) of the seawater measurement from the results of the replicate pair samples with the good quality (flag "2"). The approximate detection limits were estimated using the 3-sigma method. The results are shown in Table 4.8.4.

Table 4.8.4 The analytical precision (repeatability) and detection limit for seawater measurement.

	SF_6 (fmol kg^{-1})	CFC-11 (pmol kg^{-1})	CFC-12 (pmol kg^{-1})	CFC-113 (pmol kg^{-1})
Standard deviation	0.09	0.008	0.005	0.005
Rough estimate of C.V. (%) relative to the maximum concentration	5	0.5	0.5	3
n	32	78	78	34
Rough estimate of detection limit	0.01	<0.001	<0.001	<0.001

(9) Contamination from Tygon sampling tube

During the sampling and measurement, contamination of the water sample from CFCs/SF_6 in the atmosphere should be avoided as much as possible. In this cruise, we tested the contamination from the Tygon sampling tube (about 45 cm length) used in the seawater sampling. We collected seawater in the glass bottles from 4500 dbar at station 61 (9.5°N/161.7°E) in three ways; without the sampling tube, with the sampling tube (about 45 cm), and with double-length sampling tube (about 90 cm). The results are shown in Fig. 4.8.3. Measured concentrations of CFC-11 and CFC-12 show that a 45 cm length of the sampling Tygon tube causes about 0.009 pmol kg^{-1} of CFC-11 and 0.003 pmol kg^{-1} of CFC-12 contaminations. The intercepts of the linear regressions (0.009 pmol kg^{-1} of CFC-11 and 0.003 pmol kg^{-1} of CFC-12) were derived from the seawater samples because the line blank during analysis was corrected. In these test measurements, CFC-113 and SF_6 were not detected.

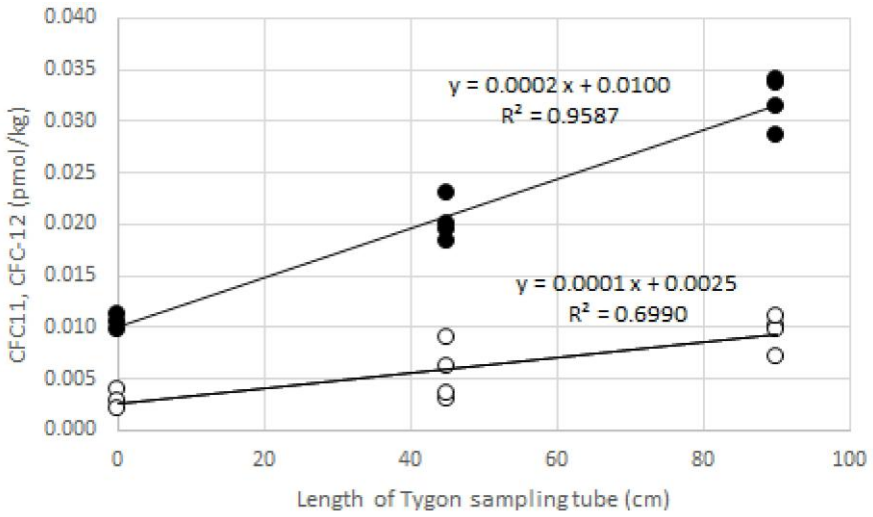

Fig. 4.8.3 Estimate of contamination of CFC-11 and CFC-12 from the Tygon sampling tube.

(10) Quality control flag assignment

The quality control (flag "2 (good), "3 (questionable)", or "4 (bad)") of the concentration in the seawater samples proceeded as follows.

1) We found outliers (flag "3" or "4") on vertical profiles of concentrations.
2) We found outliers from the ratios of CFC-11/CFC-12 and SF_6/CFC-113.
3) Considering variation in the tube contamination, CFC-11 and CFC-12 concentrations lower than 0.010 and 0.005 pmol kg^{-1}, respectively, were flagged "3".

4) SF_6 concentrations below 500 m depth were assumed to be zero.

5) CFC-113 concentrations (not zero) in a seawater sample, whose SF_6 concentration was zero or SF_6 concentration flag was “3” or “4”, were assigned to the flag “3”.

(11) Problems

1) The line blanks during analysis (“gas blank” and “water blank”) of both the systems A and B were higher than those in analyses during previous cruises.

2) During the measurements of seawater samples from station 39, 41, 43, and 46 using the system A, a large unknown peak appeared between the peaks of CFC-12 and CFC-11 on the chromatogram. The unknow peaks appeared in samples collected in deeper than about 200 m depth.

3) Valve #3 of the system B was stuck due to sea salt.

4) Some data of standard gas measurements for the calibration curve were lost because of wrong operation in the standard gas measurements.

(12) Data archives

The data obtained in this cruise will be submitted to the Data Management Group of JAMSTEC, and will be open to the public via “Data Research System for Whole Cruise Information in JAMSTEC (DARWIN)” in the JAMSTEC web site.

(13) References

Eilers, P.H.C (2003) A perfect smoother, Analytical Chemistry 75, 3631-3636.

Lan, K. and J.W. Jorgenson (2001) A hybrid of exponential and gaussian functions as a simple model of asymmetric chromatographic peaks. J. Chromatogr. 915, 1-13.

4.9 Dissolved inorganic carbon (C_T), total alkalinity (A_T) and pH

January 23, 2026

(1) Personnel

Masahito Shigemitsu (JAMSTEC)

Akihiko Murata (JAMSTEC)

Yumiko Tange (JAMSTEC)

Nagisa Fujiki (MWJ)

Yasuhiro Arii (MWJ)

Mikio Kitada (MWJ)

Yuta Oda a(MWJ)

Tomoki Nakamura (MWJ)

(2) Objectives

The concentration of CO_2 in the atmosphere is now anthropogenically increasing at a rate of about 5.1 PgC yr^{-1} owing to fossil fuel and net land-use change emissions (Friedlingstein et al., 2020). It is an urgent task to estimate as accurately as possible the absorption capacity of the ocean against the increased atmospheric CO_2, and to clarify the mechanism behind the CO_2 absorption, because the magnitude of projected global warming depends on the levels of CO_2 in the atmosphere, and because the ocean currently absorbs ~20% of the 11 Pg of carbon emitted into the atmosphere each year by human activities.

In this cruise, we try to gain some insights into how much anthropogenic CO_2 was absorbed in the ocean interior of the tropical North Pacific. To this end, we measured CO_2-system parameters such as dissolved inorganic carbon (C_T), total alkalinity (A_T) and pH.

(3) Apparatus

i. C_T

Measurement of C_T was made with automated TCO_2 analyzer (Nippon ANS, Inc., Japan). The system comprises of a seawater dispensing system, a CO_2 extraction system and a coulometer (Model 3000, Nippon ANS, Inc., Japan). Specifications of the system are as follows:

The seawater dispensing system has an auto-sampler (6 ports), which dispenses seawater from a 250 ml borosilicate glass bottle (DURAN® glass bottle, 250ml) into a pipette of about 15 ml volume by PC control. The pipette is kept at 20 °C by a water jacket, in which water from a water bath set at 20 °C is circulated. CO_2 dissolved in a seawater sample is extracted in a stripping chamber of the CO_2 extraction system by adding phosphoric acid (~ 10 % v/v) of about 2 ml. The stripping chamber is approx. 25 cm long and has a fine frit at the bottom. The acid is added to the stripping chamber from the bottom of the chamber by pressurizing an acid bottle for a given time to push out the right amount of acid. The pressurizing is made with nitrogen gas (99.9999 %). After the acid is transferred to the stripping chamber, a seawater sample kept in a pipette is introduced to the stripping chamber by the same method as in adding an acid. The seawater reacted with phosphoric acid is stripped of CO_2 by bubbling the nitrogen gas through a fine frit at the bottom of the stripping chamber. The CO_2 stripped in the chamber is carried by the nitrogen gas (flow rates is 140 ml min^{-1}) to the coulometer through a dehydrating module. The module consists of two electric dehumidifiers (kept at ~4 °C) and a chemical desiccant ($Mg(ClO_4)_2$).

The measurement sequence such as system blank (phosphoric acid blank), 1.5 % CO_2 gas (nitrogen-base) in a nitrogen base, sea water samples (6) is programmed to repeat. The measurement of 1.5 % CO_2 gas is made to monitor response of coulometer solutions purchased from UIC, Inc.

The repeatability calculated from replicate seawater samples was 1.1 ± 1.0 μmol kg^{-1} (n = 102).

ii. A_T

Measurement of A_T was made based on spectrophotometry with a single acid addition procedure using a custom-made system (Nippon ANS, Inc., Japan). The system comprises of a water dispensing unit, an auto-syringe (Hamilton) for hydrochloric acid, a spectrophotometer (TM-UV/VIS C10082CAH, Hamamatsu Photonics, Japan), and a light source (Mikropack, Germany), which are automatically controlled by a PC. The water dispensing unit has a water-jacketed pipette (~40 mL at

25°C) and a titration cell, which is also controlled at 25°C.

A seawater of approx. 40 ml is transferred from a sample bottle (DURAN® glass bottle, 100 ml) into the pipette by pressurizing the sample bottle (nitrogen gas), and is introduced into the titration cell. The seawater is used to rinse the titration cell. Then, Milli-Q water is introduced into the titration cell, also for rinse. A seawater of approx. 40 ml is measured again by the pipette, and is transferred into the titration cell. Then, for seawater blank, absorbances are measured at three wavelengths (730, 616 and 444 nm). After the measurement, an acid titrant, which is a mixture of approx. 0.05 M HCl at 25°C in 0.65 M NaCl and ~40 μM bromocresol green (BCG) is added into the titration cell. The volume of the acid titrant is changed between ~1.9 mL and ~2.1 mL according to estimated values of A_T. The seawater + acid titrant solution is stirred for over 9 minutes with bubbling by nitrogen gas in the titration cell. Then, absorbances at the three wavelengths are measured.

Calculation of A_T is made by the following equation:

$$A_T = (-[H^+]_T V_{SA} + M_A V_A) / V_S,$$

where MA is the molarity of the acid titrant added to the seawater sample, $[H^+]_T$ is the total excess hydrogen ion concentration in the seawater, and VS, VA and VSA are the initial seawater volume, the added acid titrant volume, and the combined seawater plus acid titrant volume, respectively. $[H^+]_T$ is calculated from the measured absorbances based on the following equation (Yao and Byrne, 1998):

$$pH_T = -\log[H^+]_T = 4.2699 + 0.002578(35 - S) + \log((R - 0.00131)/(2.3148 - 0.1299R)) - \log(1 - 0.001005S),$$

where S is the sample salinity, and R is the absorbance ratio calculated as:

$$R = (A_{616} - A_{730})/(A_{444} - A_{730}),$$

where A_i is the absorbance at wavelength i nm.

The repeatability calculated from replicate seawater samples was 1.3 ± 1.1 μmol kg^{-1} (n = 95).

iii. pH

Measurement of pH was made by a pH measuring system (Nippon ANS, Inc.). For the detection of pH, spectrophotometry is adopted. The system comprises of a water dispensing unit and a spectrophotometer (HPX-2000, Ocean Optics). For an indicator, m-cresol purple (2 mM), which is purified based on Patsavas et al. (2013), is used.

Seawater is transferred from borosilicate glass bottle (250 ml) to a sample cell in the spectrophotometer. The sample cell is kept at 25.00 ± 0.3°C in a thermostated compartment. First, absorbance of seawater only is measured at four wavelengths (730, 578, 488, and 434 nm). Then the indicator is injected and circulated for about 2 and a half minutes to mix the indicator and seawater sufficiently. After the pump is stopped, the absorbance of seawater + indicator is measured at the same wavelengths. The pH is calculated based on the following equation (Liu et al., 2011):

$$pH_T = -\log(\boldsymbol{K_2^T e_2}) + \log\left(\frac{\boldsymbol{R - e_1}}{\boldsymbol{1 - R(e_3/e_2)}}\right),$$

where $-\log(K_2^T e_2) = a + (b/T) + c\ln T - dT$; a = –246.64209 + 0.315971S + 2.86855×$10^{-4}S^2$; b = 7229.23864 – 7.098137S – 0.057034S^2; c = 44.493382 – 0.052711S; d = 0.007762; e_1 = –0.007762 + 4.5174×$10^{-5}T$; e_3/e_2 = –0.020813 + 2.60262×$10^{-4}T$ + 1.0436×10^{-4}(S – 35). The T and S indicate temperature in K and salinity, respectively. The K_2^T is the dissociation constant of HI-, which is a protonated species of sulfonephthalein indicators. The R is the ratio of sulfonephthalein absorbances (= $_{578}A/_{433}A$) at wavelengths of 578 nm and 434 nm.

The repeatability calculated from replicate seawater samples was 0.0018 (n = 76).

(4) Shipboard measurement

(4.1) Sampling

i. C_T

All seawater samples were collected from depth with 12 liter Niskin bottles basically at every other station. The seawater samples for C_T were taken with a plastic drawing tube (PFA tubing connected to silicone rubber tubing) into a 250 ml DURAN. glass bottle. The glass bottle was filled with seawater

smoothly from the bottom following a rinse with sample seawater of 2 full, bottle volumes. The glass bottle was closed by an inner cap loosely, which was fitted tightly to the bottle mouth after mercuric chloride was added.

At a chemical laboratory on ship, a volume of about 3mL seawater was removed with a plastic pipette from sampling bottles to have a headspace of approx. 1 % of the bottle volume. A saturated mercuric chloride of 100 µl was added to poison seawater samples. The seawater samples were kept at 5 ℃ in a refrigerator until analysis. A few hours just before analysis, the seawater samples were kept at 2 ℃ in a water bath.

ii. A_T

All seawater samples were collected from depth using 12 liter Niskin bottles at the same stations as for C_T. The seawater samples for A_T were taken with a plastic drawing tube (PFA tubing connected to silicone rubber tubing) into DURAN glass bottles of 100 ml. The glass bottle was filled with seawater smoothly from the bottom after rinsing it with sample seawater of 2 full, bottle volume.

The samples were stored at about 5 ℃ in a refrigerator. A few hours before analysis, the seawater samples were kept at 25 ℃ in a water bath.

iii. pH

All seawater samples were collected from depth with 12 liter Niskin bottles at the same stations as for C_T and A_T. The seawater samples for pH were taken with a plastic drawing tube (PFA tubing connected to silicone rubber tubing) into a 250 ml borosilicate glass bottle. The glass bottle was filled with seawater smoothly from the bottom following a rinse with sample seawater of 2 full, bottle volumes. The glass bottle was closed by a stopper, which was fitted to the bottle mouth gravimetrically without additional force.

A few hours just before analysis, the seawater samples were kept at 25 ℃ in a water bath.

(4.2) Analyses

i. C_T

First, we calibrated the measuring systems by blank and 5 kinds of Na_2CO_3 solutions (nominally 500, 1000 1500, 2000, 2500 µmol/L). As it was empirically known that coulometers do not show a stable signal (low repeatability) with fresh (low absorption of carbon) coulometer solutions. Therefore, we measured 1.865% CO_2 gas repeatedly until the measurements became stable. Then we started the calibration.

The measurement sequence such as system blank (phosphoric acid blank), 1.865% CO_2 gas in a nitrogen base, seawater samples (6) was programmed to repeat. The measurement of 1.865% CO_2 gas was made to monitor response of coulometer solutions (from UIC, Inc. or in-house made). For every renewal of coulometer solutions, certified reference materials (CRMs, batch 209, certified value = 2059.4 µmol kg^{-1}) provided by Prof. A. G. Dickson of Scripps Institution of Oceanography were analyzed. In addition, in-house reference materials (RM) (batch QRM Q44) were measured at the initial, intermediate and end times of a coulometer solution's lifetime.

The preliminary values were reported in a data sheet on the ship. Repeatability and vertical profiles of C_T based on raw data for each station helped us check performances of the measuring systems. In the cruise, we finished all the analyses for C_T on board the ship.

ii. A_T

We analyzed reference materials (RM), which were produced for C_T measurement by JAMSTEC, but were efficient also for the monitor of A_T measurement. In addition, certified reference materials (CRM, batch 209, certified value = 2264.2 µmol kg^{-1}; batch 217, certified value =2265.8 µmol kg^{-1}) were analyzed periodically to monitor systematic differences of measured A_T. The reported values of A_T were set to be comparable to the certified value of the batches 209 and 217.

The preliminary values were reported in a data sheet on ship. Repeatability calculated from replicate samples and vertical profiles of A_T based on raw data for each station helped us check performance of the measuring system.

In the cruise, we finished all the analyses for A_T on board the ship.

iii. pH

For an indicator solution, purified m-cresol purple (2 mM) was used. The indicator solution was

produced on land just before this cruise, and retained in a 1000 ml DURAN. laboratory bottle. The solution was set to pH of ~7.9 by adding acid or alkali solution appropriately. It is difficult to mix seawater with an indicator solution sufficiently under no headspace condition. However, by circulating the mixed solution with a peristaltic pump, a well-mixed condition came to be attained rather shortly, leading to a rapid stabilization of absorbance. We renewed a TYGON. tube of a peristaltic pump periodically, when a tube deteriorated. We measured absorbances at 25 ℃.

Absorbances of seawater only and seawater + indicator solutions were measured 5 times each after stable absorbances were attained, and the averaged values were used for the calculation of pH.

The preliminary values of pH were reported in a data sheet on the ship. Repeatability calculated from replicate samples and vertical profiles of pH based on raw data for each station helped us check performance of the measuring system.

We finished all the analyses for pH on board the ship.

References

Clayton T. D. and R. H. Byrne (1993) Spectrophotometric seawater pH measurements: total hydrogen ion concentration scale calibration of m-cresol purple and at-sea results. Deep-Sea Research 40, 2115-2129.

Dickson, A. G., C. L. Sabine and J. R. Christian eds. (2007) Guide to best practices for ocean CO_2 measurements, PICES Special Publication 3, 191 pp.

Friedlingstein et al. (2020) Global Carbon Budget 2020. Earth Syst. Sci. Data, 12, 3269–3340, https://doi.org/10.5194/essd-12-3269-2020.

Liu, X., M. C. Patsavas and R. H. Byrne (2011) Purification and characterization of meta-cresol purple for spectrophotometric seawater pH measurements. Environmental Science and Technology, 45, 4862-4868.

Patsavas, M. C., R. H. Byrne and X. Liu (2013) Purification of meta-cresol purple and cresol red by flash chromatography: Procedures for ensuring accurate spectrophotometric seawater pH measurements. Marine Chemistry, 150, 19-24.

Yao, W. and R. B. Byrne (1998) Simplified seawater alkalinity analysis: Use of linear array spectrometers. Deep-Sea Research 45, 1383-1392.

4.10 Chlorophyll *a*

(1) Personnel

Kosei Sasaoka (JAMSTEC)

Misato Kuwahara (MWJ)

Katsunori Sagishima (MWJ)

Masahiro Orui (MWJ)

(2) Objectives

Chlorophyll *a* is one of the most convenient indicators of phytoplankton biomass and has been used extensively for the estimation of phytoplankton abundance in various aquatic environments. In this study, we investigated equatorial distribution of phytoplankton biomass along the P04W section. The chlorophyll *a* data is also utilized for calibration of fluorometers, which were installed in the surface water monitoring and CTD profiler system.

(3) Instrument and Method

Seawater samples were collected in 500 mL brown Nalgene bottles without head-space, by using the Niskin bottles and a bucket at the surface. All samples were gently filtrated by low vacuum pressure (<0.02 MPa) through Whatman GF/F filter (diameter 25 mm) in the dark room. Whole volume of each sampling bottle was precisely measured in advance. After filtration, phytoplankton pigments were immediately extracted in 7 ml of N,N-dimethylformamide (DMF), and samples were stored at –20°C under the dark condition to extract chlorophyll *a* more than 24 hours. Chlorophyll *a* concentrations were measured by the Turner fluorometer (10-AU-005, TURNER DESIGNS), which was previously calibrated against a pure chlorophyll *a* (Sigma-Aldrich Co., LLC) (Figure 4.10.1). To estimate the chlorophyll *a* concentrations, we applied to the fluorometric "Non-acidification method" (Welschmeyer, 1994).

(4) Preliminary results

Vertical distributions of chlorophyll *a* concentration at each station (n=40) along P04W line were shown in Figure 4.10.2. Cross section of chlorophyll *a* concentration along the P04W line was shown in Figure 4.10.3. Chlorophyll *a* concentrations were relatively low (less than about 0.4 mg m^{-3}) in all sampling depths (surface to 250m) and at all stations along P04W section. Subsurface chlorophyll *a* maximum (about 0.2-0.44 mgm^{-3}) were clearly captured between 70-175m depth along the section. The depths of the subsurface chlorophyll *a* maximum gradually deepened from Stn.1 to 170E. On the other hand, it was seen that it became shallower from 170E towards St80.

To examine the measurement precision, 68-pairs of replicate samples were obtained from hydrographic casts at the chlorophyll *a* maximum and a bucket sampling. The absolute values of the difference between replicate samples were 0-0.02 mgm^{-3}, and the precision estimated from the standard deviation of them were approximately less than 0.01.

(5) Reference

Welschmeyer, N. A. (1994): Fluorometric analysis of chlorophyll a in the presence of chlorophyll b and pheopigments. Limnor. Oceanogr., 39, 1985-1992.

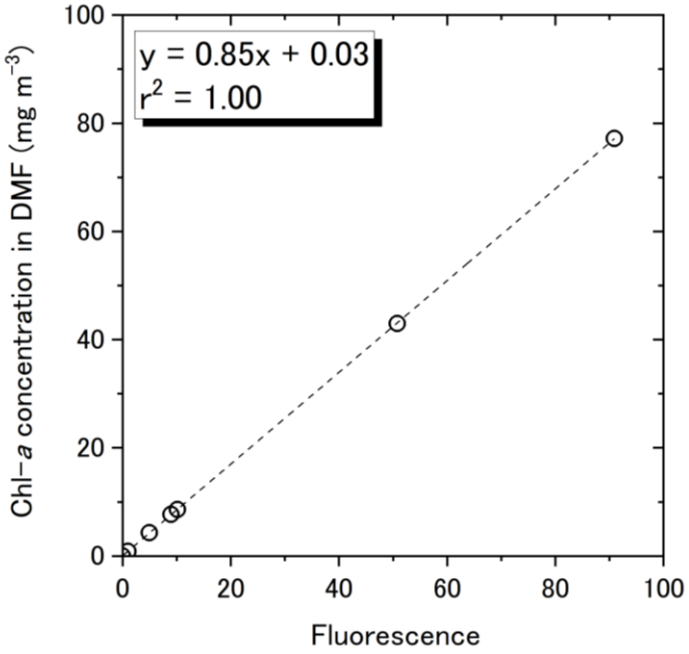

Figure 4.10.1 Relationships between pure chlorophyll *a* concentrations and fluorescence light intensity (n=7).

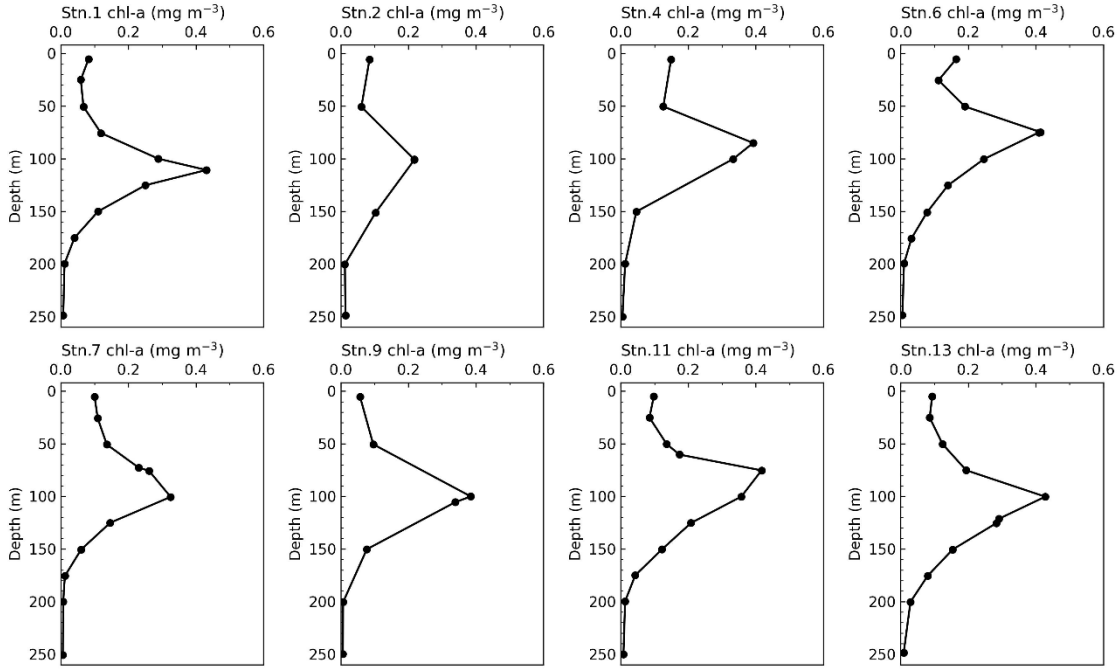

Figure 4.10.2 Vertical profiles of chlorophyll *a* concentration at each station (n=40) along the P04W section obtained from hydrographic casts.

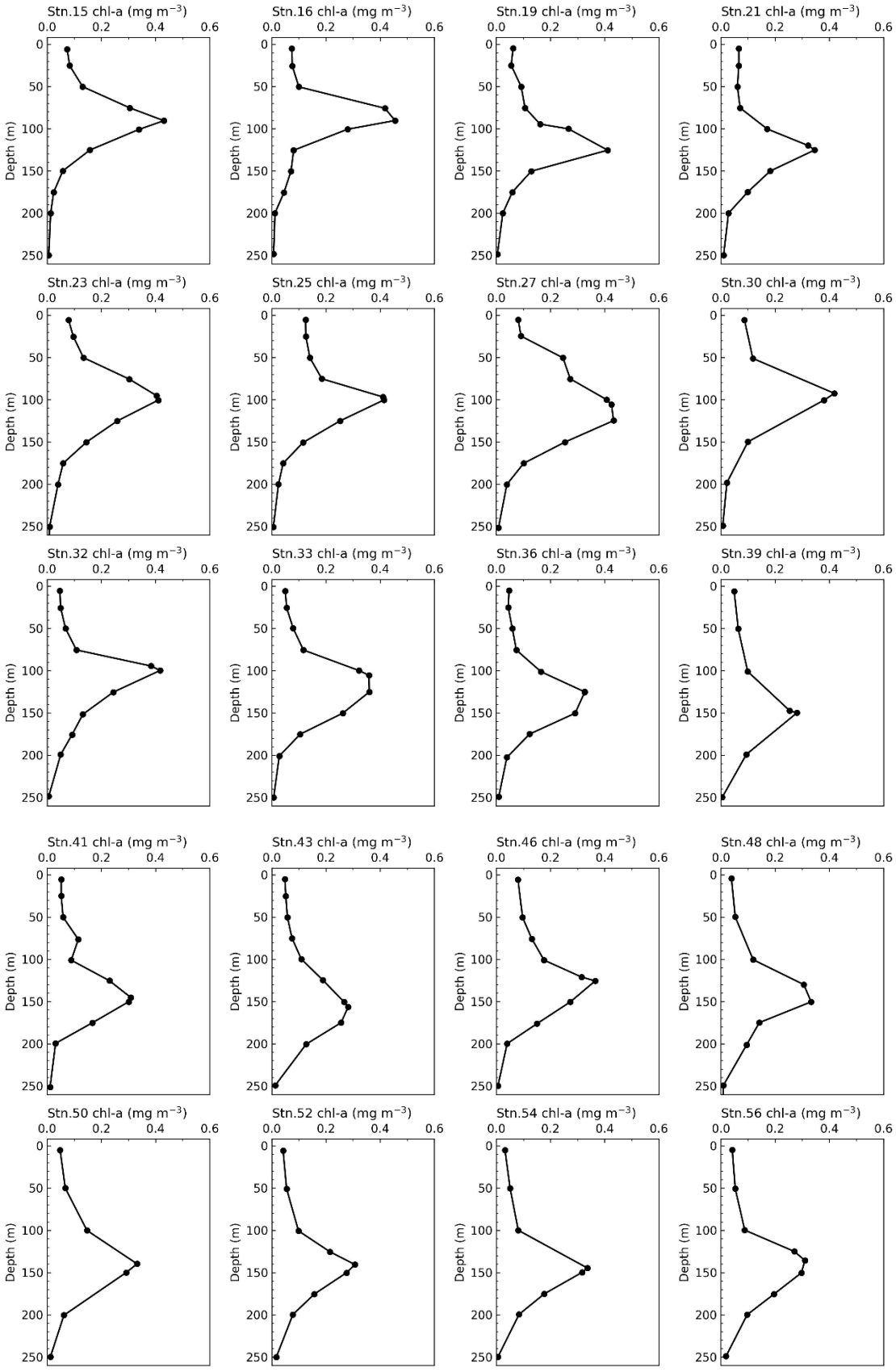

Figure 4.10.2 (Continued)

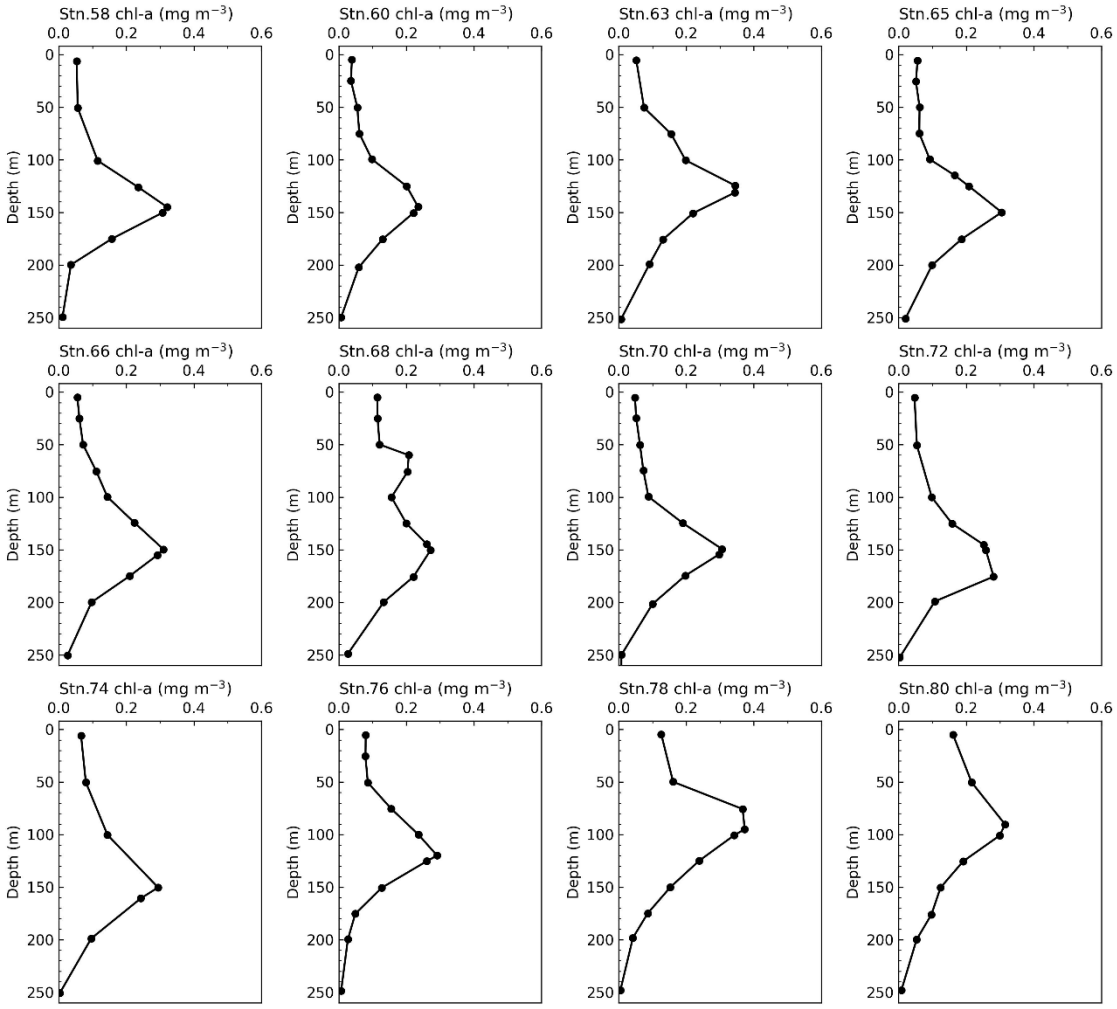

Figure 4.10.2 (Continued)

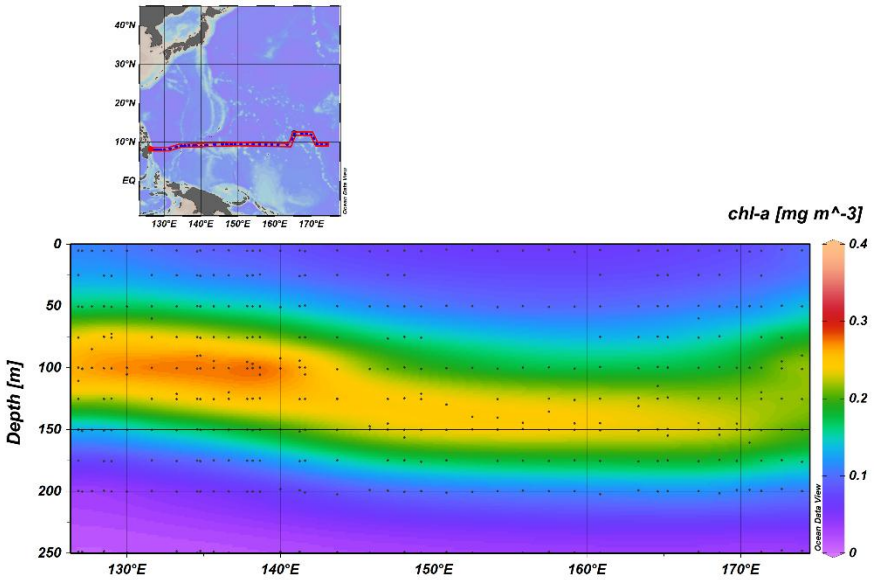

Figure 4.10.3 Cross section of chlorophyll *a* concentrations along the P04W section (upper map) obtained from hydrographic casts.

4.11 Carbon isotopes

May 12, 2025

Yuichiro Kumamoto

Japan Agency for Marine-Earth Science and Technology (JAMSTEC)

(1) Personnel

Yuichiro Kumamoto (Principal Investigator)

Japan Agency for Marine-Earth Science and Technology

(2) Objective

In order to investigate the water circulation and carbon cycle in the western equatorial North Pacific Ocean, seawaters for measurements of carbon-14 (radiocarbon) and carbon-13 (stable carbon) ratios of dissolved inorganic carbon were collected by the hydrocasts from surface to near bottom.

(3) Sample collection

The sampling stations and number of samples are summarized in Table 4.11.1. All samples for carbon isotope ratios (total 95 samples) were collected at 8 stations using the 12-liter bottles. The seawater sample was siphoned into a 250 cm^3 glass bottle with enough seawater to fill the glass bottle 2 times. Within a few hours after sampling, 10 cm^3 of seawater was removed from the bottle and poisoned by 0.1 cm^3 µl of saturated $HgCl_2$ solution. Then the bottle was sealed by a glass stopper with Apiezon grease M and stored in a dark space on board.

Table 4.11.1 Sampling stations and number of samples for carbon isotopic ratios.

Station	Lat. (N)	Long. (E)	Sampling Date (UTC)	Number of samples	Max. Pressure (dbar)
011	8.34	131.62	2025/04/12	24	4944.8
027	8.98	138.67	2025/04/16	23	4861.4
046	9.49	149.17	2025/04/20	24	5300.7
058	9.49	159.16	2025/04/25	24	5299.5
			Total	95	

(4) Sample preparation and measurements

In our laboratory, dissolved inorganic carbon in the seawater samples will be stripped as CO_2 gas cryogenically and split into three aliquots: radiocarbon measurement (about 200 µmol), carbon-13 measurement (about 100 µmol), and archive (about 200 µmol). The extracted CO_2 gas for radiocarbon will be then converted to graphite catalytically on iron powder with pure hydrogen gas. The carbon-13 ratio ($^{13}C/^{12}C$) of the extracted CO_2 gas will be measured using a mass spectrometer (Finnigan MAT253). The carbon-14 ratio ($^{14}C/^{12}C$) in the graphite sample will be measured by Accelerator Mass Spectrometry.

(5) Data archives

The data obtained in this cruise will be submitted to the Data Management Group of JAMSTEC and will be opened to the public via “Data Research System for Whole Cruise Information in JAMSTEC (DARWIN)” in the JAMSTEC web site.

4.12 Dissolved organic carbon (DOC), fluorescent dissolved organic matter (FDOM), and molecular size distribution of dissolved organic matter (DOM)

January 23, 2026

(1) Personnel

Masahito Shigemitsu, Kosei Sasaoka, Daichi Koshiishi, Yukino Hambara and Masahide Wakita (JAMSTEC)

(2) Introduction

Marine dissolved organic matter (DOM) is known to be the largest ocean reservoir of reduced carbon, and a large fraction of the carbon exists as refractory DOM (RDOM) (Hansell et al., 2009). RDOM is considered to be generated during microbial degradation of organic matter produced in the sunlit surface ocean, and is hypothesized to play an important role in the atmospheric CO_2 sequestration (Jiao et al., 2010). A fraction of the RDOM can be detected as fluorescent DOM (FDOM). In the intermediate waters of the North Pacific, allochthonous RDOM is introduced from the surrounding marginal seas and is mixed into the above-mentioned autochthonous RDOM (Yamashita et al., 2021).

In this cruise, we try to gain insights into the relative proportion of allochthonous and autochthonous RDOM in the intermediate waters of the North Pacific. To this end, we measured FDOM on board and will measure DOC and molecular size distribution of DOM.

(3) Instruments and methods

Bottle sampling

Discrete water samples for each station were collected using 12L Niskin bottles mounted on a CTD system. Each sample for FDOM and DOC taken in the upper 250 m was filtered using a pre-combusted glass fiber filter (GF/F, Whatman), while all the samples for molecular size distribution of DOM were filtered by an acid-cleaned 0.2 μm Acropac filters (Pall Co. Ltd).

Filtrates were collected for DOC, FDOM, and molecular size distribution of DOM measurements in acid-washed 60 mL High Density Polyethylene (HDPE) bottles, pre-combusted glass vials with acid-washed teflon-lined caps, and acid-washed 1L HDPE bottles after triple rinsing, respectively. Other samples taken below 250 m for DOC and FDOM were unfiltered. The samples for DOC, FDOM, and molecular size distribution of DOM were collected at the stations 1, 2, 4, 6, 7, 9, 11, 13, 15, 16, 19, 21, 23, 25, 27, 30, 32, 33, 36, 39, 41, 42, 43, 46, 48, 50, 52, 54, 56, 58, 60, 63, 65, 66, 68, 70, 72, 74, 76, 78, and 80.

DOC measurement

The samples for DOC were immediately stored frozen onboard until analysis on land. The samples will be thawed at room temperature and measured by a Shimadzu TOC-L system coupled with a Shimadzu Total N analyzer in JAMSTEC. The standardization will be achieved using glucose, and the analyses will be referenced against reference material provided by Hansell Laboratory, University of Miami.

FDOM measurement

Fluorescence excitation-emission matrices (EEMs) were measured onboard using the Horiba Scientific Aqualog after the samples were allowed to stand until reaching near room temperature. Emission scans from 248 to 829 nm taken at 2.33-nm intervals were obtained for the excitation wavelengths between 240 and 560 nm at 5-nm intervals. The fluorescence spectra were scanned with a 12-s integration time and acquired in the high CCD gain mode. The fluorescence intensities were converted to Raman Units (R.U.) (Lawaetz and Stedmon, 2009) using the water Raman peak of Milli-Q water (excitation = 350 nm) analyzed daily.

Molecular size distribution of DOM

The samples obtained were first acidified to pH 2 with HCl. Then, the samples were passed through the styrene divinyl benzene polymer cartridges (PPL) which were rinsed with 2 cartridge volumes of methanol immediately before use. After that, the samples were rinsed by using 2 cartridge volumes of 0.01 M HCl to remove salt from the samples. Finally, the cartridges were wrapped with pre-combusted aluminum foil and stored frozen onboard until analysis on land. The samples will be

thawed at room temperature and DOM for each cartridge will be eluted with 1 cartridge volume of methanol after the sorbent is dried with N_2. The elutes will be dried and redissolved in ultra-pure water followed by the measurements by size exclusion chromatography system at JAMSTEC.

(4) References

Coble, P.G. (2007). Marine optical biogeochemistry: the chemistry of ocean color. Chem. Rev. 107, 402–418.

Hansell, D.A., C.A. Carlson, D.J. Repeta, and R. Schlitzer (2009). Dissolved organic matter in the ocean: New insights stimulated by a controversy. Oceanography 22, 52-61.

Jiao, N., G. Herndl, D.A. Hansell, R. Benner, G. Kattner, S. Wilhelm, et al. (2010). Microbial production of recalcitrant dissolved organic matter: long-term carbon storage in the global ocean. Nat. Rev. Microbiol. 8, 593–599. doi:10.1038/nrmicro2386

Lawaetz, A.J., and C.A. Stedmon (2009). Fluorescence intensity calibration using the Raman scatter peak of water. Appl. Spectrosc. 63(8), 936-940.

Yamashita, Y., T. Tosaka, R. Bamba, R. Kamezaki, S. Goto, J. Nishioka, et al. (2021). Widespread distribution of allochthonous fluorescent dissolved organic matter in the intermediate water of the North Pacific. Prog. Oceanogr. 191, 102510.

4.13 Absorption coefficients of Colored Dissolved Organic Matter (CDOM)

(1) Personnel

Kosei Sasaoka (JAMSTEC)

Masahito Shigemitsu (JAMSTEC)

Daichi Koshiishi (JAMSTEC)

Yukino Hambara (JAMSTEC)

(2) Objectives

Oceanic dissolved organic matter (DOM) is the largest pool of reduced carbon, and its inventory in the ocean is approximately 660 Pg C (Hansell et al., 2009). Thus, investigating the behavior of oceanic DOM is important to exactly evaluate the carbon cycle in the ocean. As the part of the DOM, Colored (or Chromophoric) Dissolved Organic Matter (CDOM) play an important role in determining the optical properties of seawater, and the global CDOM distribution appears regulated by a coupling of biological, photochemical, and physical oceanographic processes all acting on a local scale, and greater than 50% of blue light absorption is controlled by CDOM (Siegel et al., 2002). Additionally, some investigators have reported that CDOM emerges as useful tracers for diagnosing changes in the overturning circulation and evaluating DOC quality, similar to dissolved oxygen (e.g., Nelson et al., 2010; Catala et al., 2015). The objectives of this study are to clarify the equatorial distributions of light absorption by CDOM along P04W section in the North Pacific.

(3) Methods

Seawater samples for determination of the absorption coefficient of CDOM ($a_{cdom}(\lambda)$) were taken from a spigot of Niskin bottles directly at 300m - bottom depths (non-filtration), and through silicone tube to an inline plastic filter holder with a pre-combusted 47mm Whatman GF/F filter (450℃ for 4 hours) at the shallow depths above 200m (filtration). According to the method of Catala et al. (2015) and Shigemitsu et al. (2021), CDOM samples were not filtered to remove particles in the seawater except for 6-samples of shallow depth, using the same way as DOC and FDOM. All samples were collected in 60 ml pre-combusted glass vials with acid-washed Teflon-lined caps after triple rinsing. We stored the samples in the dark in refrigerator until analysis. After the samples were acclimated to laboratory temperature in the dark, optical absorbance of CDOM (Abs(λ)) in seawaters between 190 and 750 nm were measured at 0.5 nm intervals by an UV-VIS recording spectrophotometer (UV-2600, Shimadzu Co.) onboard, using 10-cm pathlength quartz cells. We measured Milli-Q water as a blank every 5-7 samples to correct linearly any instruments drift. To correct baseline offsets in the measurements, we subtracted average values ranging from 590 to 600 nm from the entire absorbance spectrum of each sample (Yamashita and Tanoue, 2009). The absorption coefficient of CDOM ($a_{cdom}(\lambda)$ (m^{-1})) was calculated from the absorbance at wavelength (Abs(λ)) as follows (Green and Blough, 1994):

$$a_{cdom}(\lambda) = 2.303 \times [\ Abs(\lambda) - Abs_{590\text{-}600}] / l$$

where $Abs_{590\text{-}600}$ is the average absorbance between 590 and 600 nm, l is the path length of quartz cell (0.1 m), and 2.303 is the factor that converts from decadic to natural logarithms.

(4) Preliminary results

Vertical profiles of $a_{cdom}(\lambda=325)$ (as absorption coefficient at 325nm, unit = m^{-1}) at each station (n=40) were shown in Fig. 4.14.1. Cross sections of $a_{cdom}(\lambda=325)$ along P04W section was shown in Fig. 4.13.2. CDOM ($a_{cdom}(\lambda=325)$) was extremely low in the surface layer (0 to 150 m) at all stations along P04W section, which is suggested to be caused by photodecomposition due to strong ultraviolet light. Furthermore, $a_{cdom}(\lambda=325)$ increased from the surface, reached a maximum value at about 300m, and then gradually decreased toward deeper layers.

We measured PRE21 standard seawater (Multiparametric Standard Seawater: MSSW, lot PRE21, KANSO TECHNOS Co., Ltd.) once a day during the cruise as reference. The mean ± S.D of $a_{cdom}(\lambda=325)$ of all PRE21 bottles (n=25) was 0.243 ± 0.005 (Fig.4.13.3). 151-pairs of replicate CDOM samples were obtained from hydrographic casts. The absolute values of the difference between replicate samples of a_{cdom} (λ=325nm) were 0-0.05 m^{-1}, and the precision estimated from SD of them were approximately 0.008. This variability (=0.008) was not significantly different from that

of the PRE21 (=0.005).

(5) References

Catala, T. S., et al., 2015, Turnover time of fluorescent dissolved organic matter in the dark global ocean, *Nat. Com., 6*, 1-8, doi:10.1038/ncomms6986.

Green, S. A. and N. V. Blough, 1994, Optical absorption and fluorescence properties of chromophoric dissolved organic matter in natural waters. *Limnol. Oceanogr. 39*, 1903–1916.

Hansell, D. A., C. A. Carlson, D. J. Repeta, and R. Shlitzer, 2009, Dissolved organic matter in the ocean: A controversy stimulates new insight, *Oceangr., 22*, 202-211

Nelson, N. B., D. A. Siegel, C. A. Carlson, and C. M. Swan, 2010, Tracing global biogeochemical cycles and meridional overturning circulation using chromophoric dissolved organic matter, *Geophys. Res. Lett., 37*, L03610, doi:10.1029/2009GL042325.

Shigemitsu, M., T. Yokokawa, H. Uchida, S. Kawagucci, and A. Murata. 2021. Sedimentary supply of humic-like fluorescent dissolved organic matter and its implication for chemoautotrophic microbial activity in the Izu-Ogasawara trench. *Sci. Rep. 11*: 19006, doi:10.1038/s41598-021-97774-7

Siegel, D.A., Maritorena, S., Nelson, N.B., Hansell, D.A., Lorenzi-Kayser, M., 2002, Global distribution and dynamics of colored dissolved and detrital organic materials. *J. Geophys. Res., 107*, C12, 3228, doi:10.1029/2001JC000965.

Yamashita, Y. and E. Tanoue, 2009, Basin scale distribution of chromophoric dissolved organic matter in the Pacific Ocean, *Limnol. Oceanogr., 54*, 598–609.

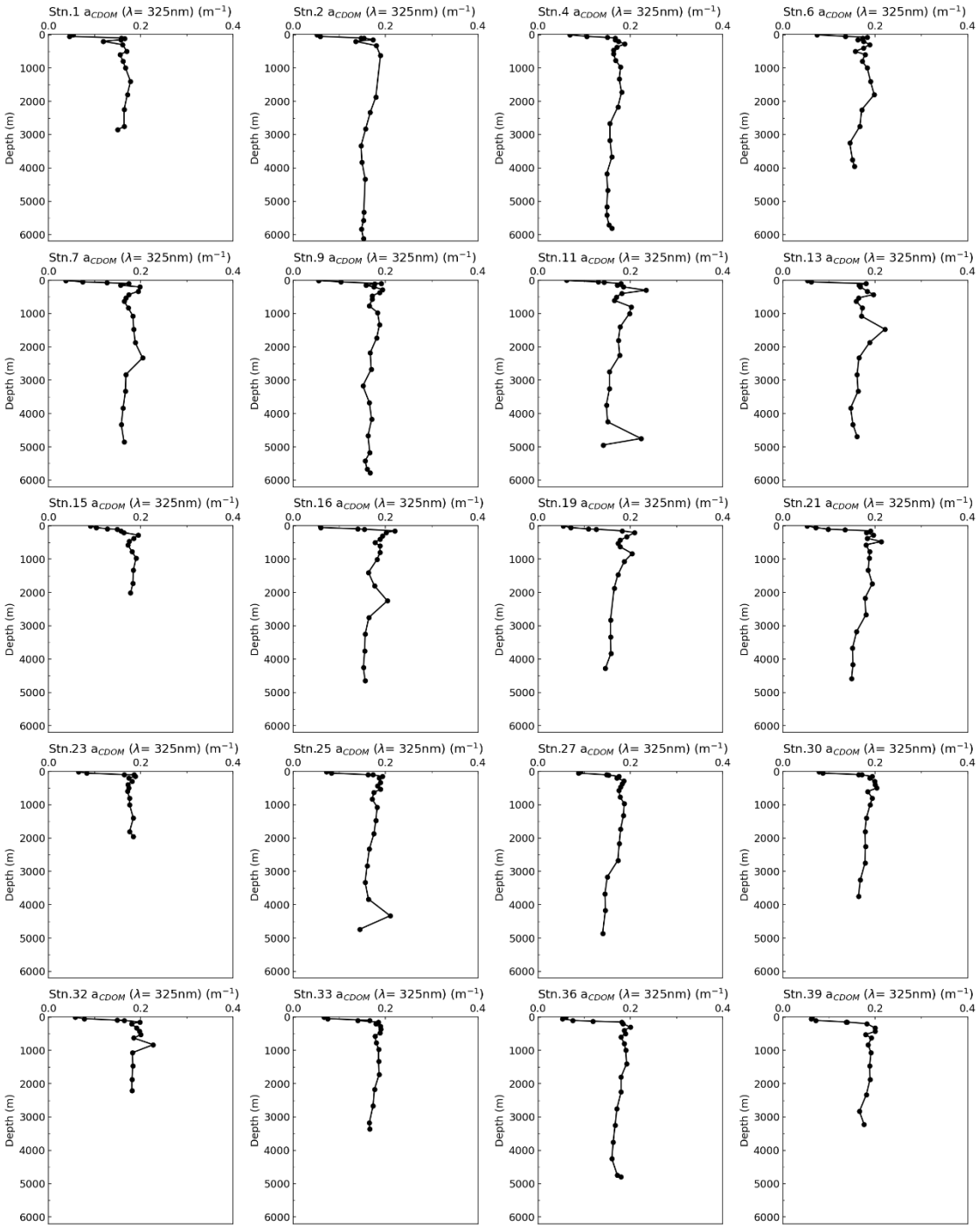

Fig.4.13.1 Vertical profiles of CDOM (as absorption coefficient at 325 nm, unit = m^{-1}) at all sampling stations.

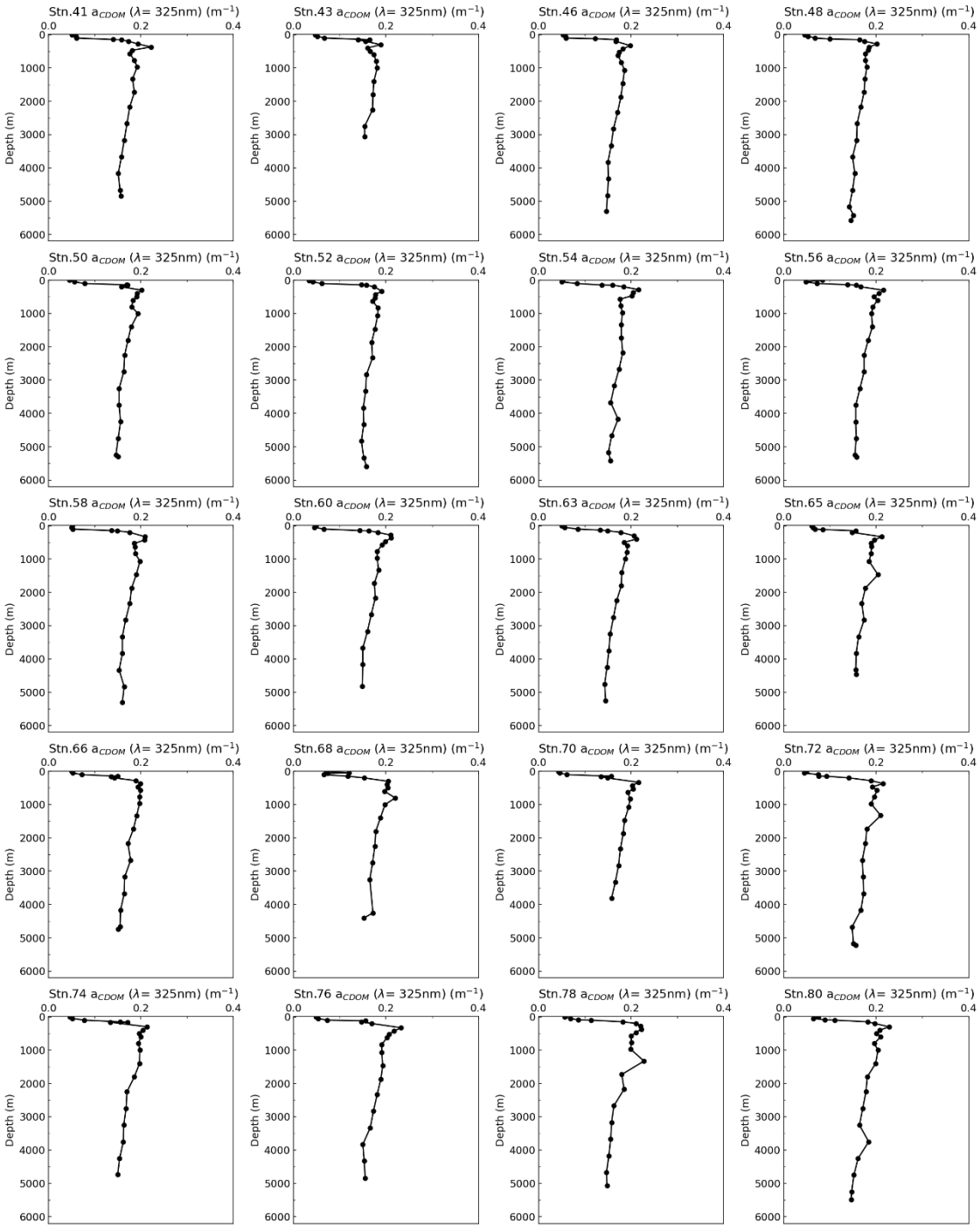

Fig.4.13.1 (Continued).

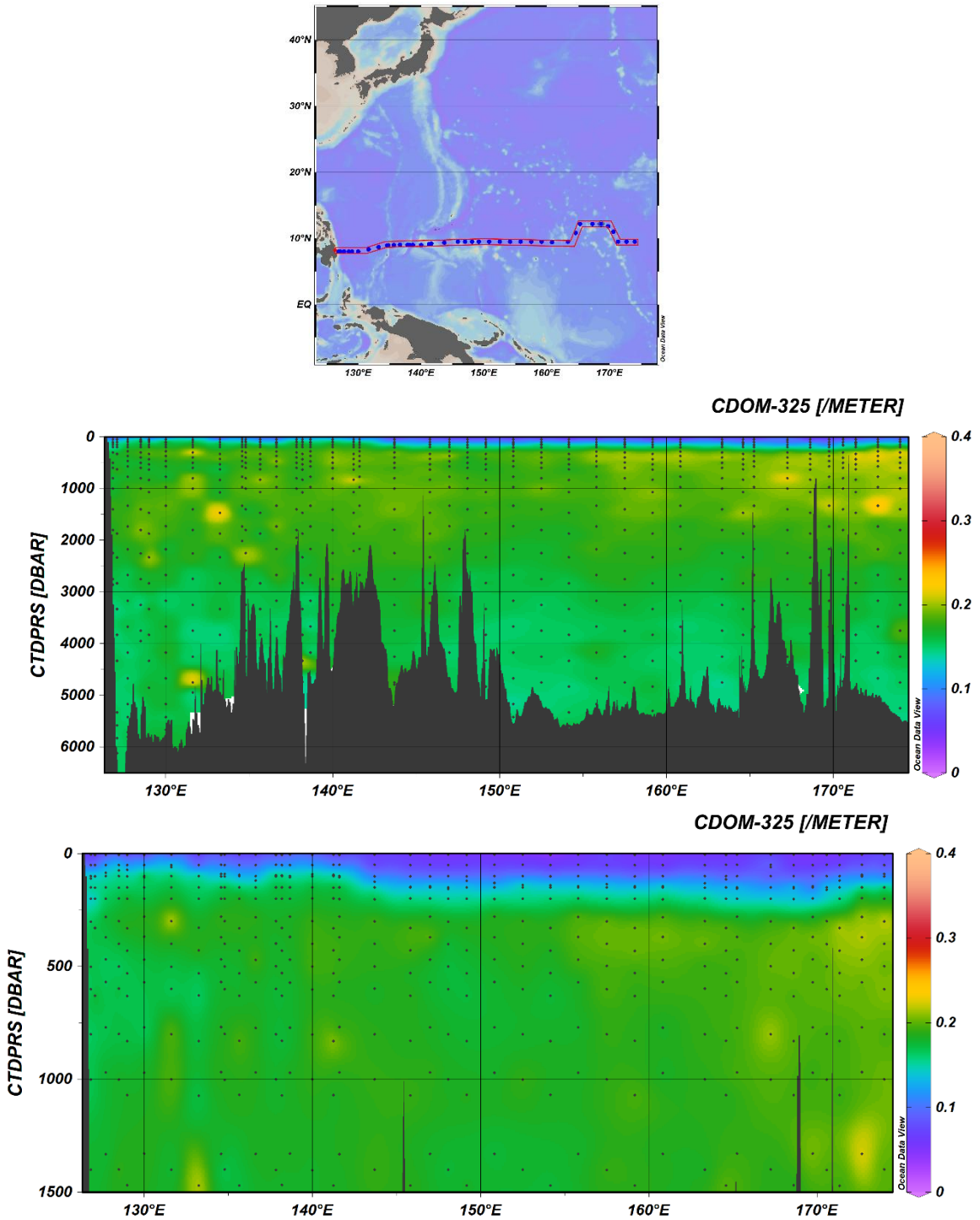

Fig.4.13.2 Sections of CDOM (as absorption coefficient at 325 nm, unit = m^{-1}) along P04W section obtained from hydrographic casts. The top section covers surface to the bottom and the lower section covers the upper 1,500 m.

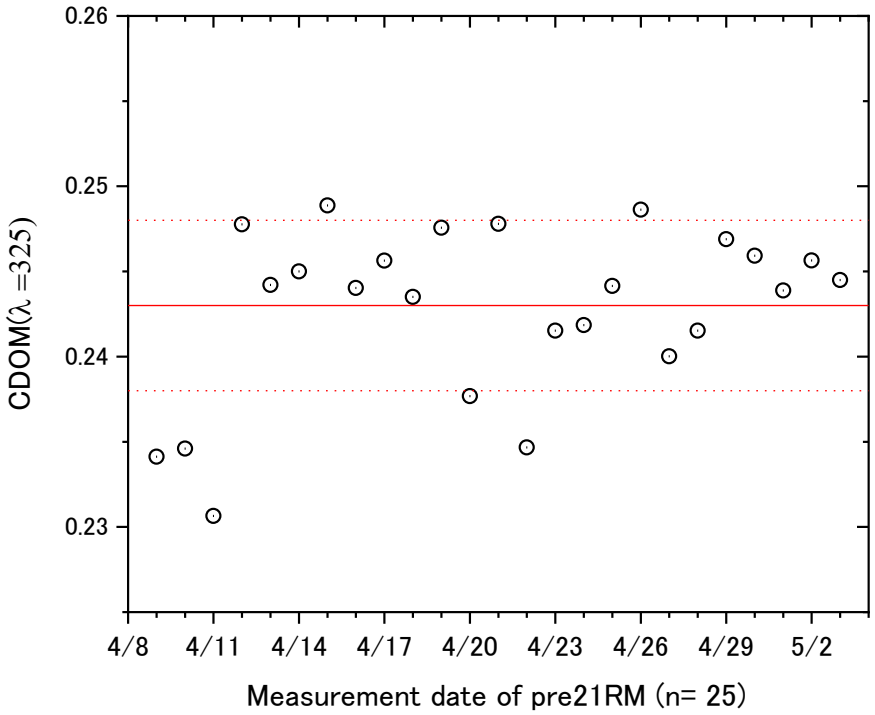

Fig.4.13.3 $a_{cdom}(\lambda=325)$ values of PRE21 bottles (n=25, x-axis indicates measurement date during cruise). The mean ± SD of all PRE20 bottles was 0.243 (red solid-line) ± 0.005 (red dotted-lines).

4.14 Organic Alkalinity

Personal

Yuko Tange (JAMSTEC)

Objective

In recent years, it has been suggested that unspecified dissolved substances in open ocean seawater samples, which have been ignored by conventional total alkalinity measurement methods, may have an influence on total alkalinity. Since these unidentified dissolved substances are considered to be mainly organic acids and organic acid salts, we refer to them here as "organic alkalinity".

Organic alkalinity can be obtained by calculation (TA measured by spectrophotometry - TA calculated from DIC and pH) and measurement (potentiometric titration), but most of the reports are based on calculated organic alkalinity. Therefore, we will collect samples of organic alkalinity on this cruise and attempt to measure organic alkalinity in a laboratory on land.

Sample Collection and Storage.

Organic alkalinity samples were collected from Niskin bottles or buckets into a 250 ml borosilicate glass bottles using a silicone tube. After overflow of at least twice the sample volume, the sample tube was pinched and pulled out. Before the lid and inner cover were put on, 3 ml (about 1 %) of sample was removed from each sample and 100 µl of saturated mercuric chloride was added. After disembarkation, the samples were measured in a laboratory on land. Samples were stored in a cool and dark place until measurement.

Sampling Point

Organic alkalinity samples were collected at Stns. 1C, 2C, 4C, 6C, and 7C by surface bucket only, and at Stns. 2C, 23C, 41C, 68C and 80C by CTD + Niskin water sampler. Spectrophotometric TA, DIC, and pH samples were also collected at the latter sites.

4.15 Nitrogen Cycles

(1) Personnel

Akiko Makabe (JAMSTEC)

Chisato Yoshikawa (JAMSTEC)

(2) Objectives

The marine nitrogen cycle in surface waters is known to control biological activity in the ocean because inorganic forms of nitrogen, such as ammonium and nitrate, are essential nutrients for phytoplankton. Following the primary production, organic nitrogen compounds are metabolized to ammonium and low molecular organic nitrogen compounds that are substrates for nitrification and/or nitrogen sources for microbes. Ammonium is oxidized to nitrate via nitrite by nitrification. In nutrient-poor regions, nitrogen fixation is an important source of nitrogen. Nitrous oxide (N_2O), a significant anthropogenic greenhouse gas and a stratospheric ozone depleter, is known to be produced by microbial activities such as nitrification.

To understand the transformation of nitrogen compounds by (microbial) organisms and the production processes of greenhouse gasses (N_2O and CH_4), both natural abundance and tracer stable isotope techniques are useful. We collected water samples and analyzed low concentrations of ammonium, nitrite, and nitrate on board. We also collected water samples to analyze natural abundance stable isotope ratios of dominant nitrogen species such as nitrate, nitrite, ammonium, organic nitrogen, and nitrous oxide that would have records of biological processes. Furthermore, we conducted on-board incubation experiments with tracer compounds to analyze nitrification activities.

(3) Methods

i. Nitrate and nitrite concentration

Samples for low concentration of nitrate and nitrite analysis were collected directly from Niskin samplers into 15 mL HDPE bottles. The samples were stored at 0°C until analysis. Nitrite concentration was measured using modified the Griess reaction (Grasshoff et al. 1983) by García-Robledo et al. (2014). Nitrate concentration was measured as nitrite after conversion to nitrite by VCl_3 (García-Robledo et al. 2014). Sample and reagents were mixed in 2 mL tubes and incubated at room temperature for more than 1 hour and at 60°C for 30 minutes for nitrite and nitrate, respectively. The mixed solution was flowed at 1.0 mL/min into a 100 cm path length capillary cell using a pelistar pump. The absorbance of the solution at 540 nm was measured using a spectrophotometer (Flame, Ocean Optics).

Samples for nitrate and nitrite concentration were collected at Station#: 1, 9, 21, 30, 39, 48, 54, 60, 65, and 74.

ii. Ammonium concentration

Samples for low concentration of ammonium analysis were collected directly from Niskin samplers into 30 mL 4 HDPE bottles. Two bottles were used to measure the raw ammonium concentration and the other two bottles were spiked with ammonium solution and then used to correct for the matrix effect between Milli-Q water and seawater. Ammonium concentration was measured by the OPA method (Holmes et al. 1999) using a fluorescence spectrophotometer (FP-8350, JASCO Co.).

Samples for ammonium concentration were collected at Station#: 1, 9, 21, 30, 39, 48, 54, 60, 65, and 74.

iii. Nitrate isotope ratio

For interlaboratory comparisons between JAMSTEC and Princeton University, seawater samples were collected for nitrate isotope measurements at JAMSTEC and Princeton University, respectively.

For JAMSTEC, full depth samples for nitrate stable isotope analysis were collected in 30 mL or 50 mL plastic syringes with caps and then filtered into 50 mL of PE bottles or 15 mL of PP tubes through MCE filters (pore size: 0.45 μm) immediately after sampling at the routine cast. Surface water samples (~200 m) were also collected directly from Niskin samplers into 50 mL PE bottles through 0.2 μm filters at the biocast. The filtrates were frozen until analysis at JAMSTEC. We will measure both nitrogen and oxygen stable isotope ratios of nitrate by a GC-IRMS after conversion to N_2O using the bacterial method. Samples for nitrate stable isotope ratio were collected at Station#: 1, 9, 21, 30, 39, 48, 54, 60, 65, and 74.

For Princeton University, samples shallower than 400 m were collected in 60 mL syringes equipped with a disposable membrane filter unit (0.45 μm pore size) and filtered immediately after collection. Of

these samples, those shallower than 100 m, where low nitrate concentrations were expected, were collected in duplicate. Samples deeper than 400 m were collected in 60 mL Nalgene bottles. Theses samples were stored at −20 °C until isotope analysis. Nitrogen and oxygen isotope ratios of nitrate for samples will be determined by a PT-GC-IRMS in Princeton University after conversion to N_2O using the bacterial method. Water was sampled in all layers at approximately 2 degree intervals (Stations. 1, 6, 9, 11, 13, 16, 21, 27, 30, 33, 36, 39, 43, 46, 48, 50, 52, 54, 56, 58, 60, 63, 65, 68, 70, 74, 78, and 80).

iv. Nitrite isotope ratio

Samples for nitrite stable isotope analysis were collected directly from Niskin samplers into 100 mL PE bottles through 0.2 μm filters. The filtrates were frozen until analysis at JAMSTEC. We will measure both nitrogen and oxygen stable isotope ratios of nitrite by a GC-IRMS after conversion to N_2O using the azide method.

Samples for nitrite stable isotope ratio were collected at Station#: 1, 9, 21, 30, 39, 48, 54, 60, 65, and 74.

v. Ammonium isotope ratio

Samples for ammonium stable isotope analysis were collected directly from Niskin samplers into 50 mL PE bottles through 0.2 μm filters. A glass fiber filter (GF/D) with sulfuric acid solution and MgO were added to subsamples of 50 ml of filtrate. The glass fiber filters, which trapped ammonia after shaking for 5 days at 25°C, were transferred from the subsamples to glass bottles with silica gel desiccant for analysis at JAMSTEC. We will measure the nitrogen stable isotope ratio of ammonium by a GC-IRMS after conversion to N_2O using wet oxidation and the bacterial method.

Samples for ammonium stable isotope ratio were collected at Station#: 1, 9, 21, 30, 39, 48, 54, 60, 65, and 74.

vi. Particulate organic nitrogen (PON) isotope ratio

Samples for nitrogen stable analysis of PON were collected in 500 mL PC bottles. The seawater samples were filtered through 0.3 μm glass fiber filters (GF-75) on board. The GF-75 was wrapped in aluminum foil and frozen until analysis at JAMSTEC. We will measure nitrogen stable isotope ratio of PON by a GC-IRMS after conversion to N_2O using wet oxidation and the bacterial method.

Samples for PON stable isotope ratio were collected at Station#: 1, 9, 21, 30, 39, 48, 54, 60, 65, and 74.

vii. Dissolved organic nitrogen (DON) isotope ratio

Samples for nitrogen stable analysis of DON were collected directly from Niskin samplers into 25 mL PP bottle through 0.2μm filters. The filtrates were frozen until analysis at JAMSTEC. We will measure nitrogen stable isotope ratio of DON by a GC-IRMS after conversion to N_2O using wet oxidation and the bacterial method.

Samples for DON stable isotope ratio were collected at Station#: 1, 9, 21, 30, 39, 48, 54, 60, 65, and 74.

viii. Nitrous oxide (N_2O) and Methane (CH_4) isotope ratio

Samples for N_2O and CH_4 stable isotope analysis were collected into 100 mL glass vials through a tube after water as two volumes of the vial were overflowed. The vials were added with 100 μL of saturated $HgCl_2$ solution and sealed with butyl rubber and aluminum caps immediately after sampling. Nitrogen and oxygen stable isotope ratio of N_2O and carbon stable isotope ratio of CH_4 will be measured by GC-IRMS at JAMSTEC.

Samples for nitrous oxide and methane stable isotope ratio were collected at Station#: 1, 9, 21, 30, 39, 48, 54, 60, 65, and 74.

ix. Nitrification activity

Samples for nitrification activity measurement were collected in 100 mL amber glass vials and 100 mL PE bottles without head space. Substrates for nitrification, ammonium or urea (^{15}N 99 atom %), were added to the bottles and incubated in the dark at near in situ temperature on board. At the end of the incubation period, water samples were filtered through MCE filters (pore size: 0.45 μm) and frozen until analysis at JAMSTEC. The rate of transfer from substrates to nitrite and nitrate is determined by ^{15}N enrichment in nitrite and nitrate.

Samples for nitrification activities were collected at Station#: 1, 21, 48, and 60.

4.16 Spatial patterns of prokaryotic abundance and community composition

(1) Personnel

Taichi Yokokawa	JAMSTEC/WPI-AIMEC
Eiji Tasumi	JAMSTEC

(2) Introduction

Prokaryotes (bacteria and archaea) play a crucial role in regulating marine biogeochemical fluxes, driving transformations of both organic and inorganic matter. While microbial functional diversity and biogeochemical processes have been central topics in marine microbial ecology, the links between prokaryotic community properties and biogeochemical dynamics in the mesopelagic and bathypelagic zones remain poorly resolved. Recent studies have increasingly highlighted the significance of microbial processes in deep ocean ecosystems; however, systematic investigations of the vertical structure and biogeographical patterns of prokaryotic communities—from the surface to the deep ocean—are still limited. In particular, how microbial community composition and diversity vary across oceanic depth and longitude, and how these patterns are shaped by water mass properties and large-scale circulation, remain open questions. Understanding these spatial structures is essential for elucidating the mechanisms that control microbial distribution and function in the pelagic ocean. To address these gaps, this study examined full-depth water column profiles in the central Pacific Ocean, from the surface to 10 meters above the seafloor, along a longitudinal transect. The specific objectives were: (1) to quantify microbial abundance; (2) to characterize the taxonomic composition of prokaryotic communities; and (3) to evaluate microbial diversity and biogeographical patterns across depth and longitude.

(3) Methods

i) Microbial abundance

Samples for quantifying microbial abundances (prokaryotes, eukaryotes and viruses) were collected in Station 1, 9, 13, 21, 25, 30, 36, 39, 43, 48, 50, 54, 56, 60, 63, 65, 68, 74 and 80. The samples were fixed with glutaraldehyde (final concentration 0.5%) or glycerol-TE (final concentration 1%), and frozen at -80°C. Microbial and viral abundance and relative size will be determined at JAMSTEC by flow cytometry following nucleic acid staining with SYBR-Green I.

ii) Microbial diversity

Microbial cells in water samples were filtrated on cellulose acetate filter (0.2μm) and stored at -80˚C. Environmental DNA or RNA will be extracted from the filtrated cells and used for 16S rRNA gene tag sequencing, quantitative PCR for genes for 16S rRNA, shotgun sequencing and metatranscriptomics. Samples for microbial diversity were taken at stations 1, 9, 21, 30, 39. 48, 54, 60, 65 and 74.

iii) Microbial isolation and cultivation

Samples intended for microbial isolation and cultivation were collected at stations 60 and 65 and stored at 4°C until processing in a land-based laboratory. There, selected physicochemical parameters were adjusted to promote microbial growth and facilitate isolation and cultivation.

4.17 Urea (University of Galway)

(1) Personnel

Delon Earle (University of Galway) Shipboard participant onboard during the expedition

Peter Croot (University of Galway): Principal investigator

(2) Objective

The key objective of this work was to obtain data on urea ($CO(NH_2)_2$), for which there are little or no data from the Western Pacific Ocean nor any basin scale overview for any of the ocean basins currently available. The rationale for measuring urea on a GO-SHIP basin scale expedition, comes from recent discoveries as to the significant role of urea in the nitrogen cycle, particularly in the mesopelagic ocean. The dataset generated here will also provide baselines for ongoing ocean and atmospheric modelling efforts into the nitrogen cycles. Importantly, urea can now be measured at sea relatively quickly and cheaply, using a spectrophotometric technique, which could be easily replicated by other countries in their GO-SHIP related activities so that in the future urea becomes a routine measurement during GO-SHIP.

Urea is a small nitrogen containing organic molecule, which plays an important role in the marine nitrogen cycle, as it is rapidly turned over in the environment and acts as a nitrogen shuttle within the microbial loop. Urea is mostly produced in the ocean via excretion from heterotrophic organisms of all size classes from bacteria upwards, this urea provides a source of bioavailable nitrogen for heterotrophic bacteria, cyanobacteria and eukaryotic phytoplankton (Solomon et al., 2010). Recently studies (Arandia-Gorostidi et al., 2024; Wan et al., 2024) have shown that the direct oxidation of urea also contributes significantly to nitrite production by ammonia oxidizers in the North Pacific ocean, this represents a recent change in paradigm, as previously it was thought that urea was first converted to ammonia via the action of urease before oxidation to nitrite.

In the Tropical Western Pacific (Wan et al., 2024) urea concentrations were reported to vary from 50 -200 nmol N L^{-1} throughout the upper water column and that urea concentrations were higher than that of ammonia, 0-120 nmol N L^{-1}. As the turnover time for urea in the upper ocean is believed to be on the order of days to months (Alonso-Sáez et al., 2012; Herbland, 1976; Mitamura and Saijo, 1975), urea might be considered a transient species in some regards, though the recent discovery of its role in nitrification and in cycling nitrogen in mesopelagic waters, suggests that we still don't have a good account of the sources and sinks for urea in the ocean. The MR25-02 transect is adjacent to the North Pacific Subtropical Gyre, which is also believed to be expanding under climate change (Dai et al., 2023; Polovina et al., 2011), however anthropogenic nitrogen supply to this region ocean may be increasing (Jiang et al., 2021; Seok et al., 2021). The recent detection of gas phase urea in the atmosphere (Matthews et al., 2023) and suggestion that the ocean can be a source to the atmosphere, also indicates that the air/sea exchange of urea is still poorly studied and understood. Thus, the MR25-02 GO-SHIP expedition provides an excellent opportunity to obtain basic scale data on urea and its role in nitrogen dynamics from the western tropical Pacific.

(3) Apparatus

Seawater samples were collected, filtered (0.2 µm syringe filter, Sarstedt) and analyzed from water collected in the upper 1700 m of the water column from 16 stations during MR25-02 (Table 4.17-1) .

(i) Urea

During MR25-02 we used an adaptation of an existing methods using a single reagent (COLDER) (Alam et al., 2017) for dissolved urea with a low level approach using LWCC (Chen et al., 2015), applying it to small volume samples (2 mL or less) and removing the need for a 70° or 85° water bath by utilizing a thermostated dry bath (Fisher Scientific) instead. This same approach had been used previously during MR19-04 in the Indian Ocean (Standard Operating Procedure is available from https://doi.org/10.5281/zenodo.15544777). During MR25-02 we employed a World Precision Instruments LWCC-3050 (pathlength 49.3 cm) connected to an Ocean Optics USB2000+ spectrophotometer and an Ocean Optics DH-mini light source. The use of a dry bath and small volume samples significantly reduces the risks in this analysis but does not completely eliminate them as sulfuric acid is still required in this procedure. Care was taken at all times to minimize contamination in the laboratory, particularly during filtration of the samples.

(4) Preliminary Results

All samples were analyzed onboard the ship during MR25-02, however all data should be considered preliminary as there are still post-processing corrections to be applied before the data sets are finalized. Currently there is no Certified Reference Material (CRM) for urea in seawater that we are aware of and so carried out quality assurance and quality control (QA/QC) checks via comparison of the analytical sensitivity of daily standard additions to ultrapure water.

It is also noted that the monoxime reaction employed here will react with urea preferably but can also form a coloured complex with other molecules containing the ureido functional group, $R_1NH(CO)NHR_2$, this includes Citrulline, Allantoate and Allantoin (Reay et al., 2019). Previous studies have shown that in the coastal ocean (Aminot and Kerouel, 1982), other ureido containing molecules are not likely to be present in significant amounts but this has not been verified for low urea containing open ocean waters.

(i) Urea

Examples of upper water column profiles for Urea during MR25-02 are shown in Figure 4.17.1. Overall, concentrations ranged from 40-660 nmol N L^{-1} throughout the water column and along the transect. There were frequently elevated urea concentrations in the near surface and at some mid-depths, these are from locally local sources of urea, sourced from zooplankton or other diel vertical migrating species. The background concentrations of 100-200 nmol N L^{-1} encountered here, across the transect may represent the presence of a less bioavailable ureido species than urea, or that urea is very slowly turned over in these waters. The future development of a more specific urea analysis would aid in reconciling these two scenarios.

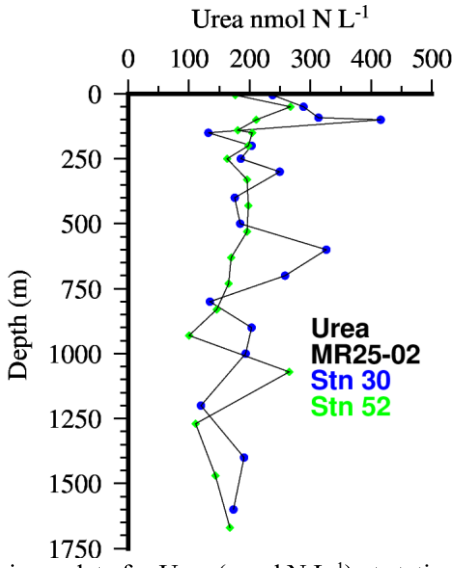

Figure 4.17.1: Preliminary data for Urea (nmol N L^{-1}) at stations 30 and 52 during MR25-02.

Post-cruise the data will be finalized and made freely available.

(5) Acknowledgments

We are extremely grateful to JAMSTEC and the Scientists and Crew of the RV Mirai who helped support our work at sea during the MR25-02 GO-SHIP expedition. Funding for participation in the MR25-02 GO-SHIP expedition was provided by the Marine Institute of Ireland through the Changing Ocean Ireland: Forecasting Biodiversity and Ecosystem Response. (CÓIR) project (SPDOC/CC/20/001).

References

Alam, M.S., Casareto, B.E., Suzuki, Y., Sultana, R. and Suzuki, T., 2017. Optimization of dissolved urea measurements in coastal waters with the combination of a single reagent and high temperature. Journal of Oceanography, 73(2): 249-258.

Alonso-Sáez, L. et al., 2012. Role for urea in nitrification by polar marine Archaea. Proceedings of the

National Academy of Sciences.
Aminot, A. and Kerouel, R., 1982. Dosage automatique de l'urée dans l'eau de mer : une méthode très sensible à la diacétylmonoxime. Canadian journal of fisheries and aquatic sciences, 39: 174-183.
Arandia-Gorostidi, N. et al., 2024. Urea assimilation and oxidation support activity of phylogenetically diverse microbial communities of the dark ocean. The ISME Journal, 18(1).
Chen, L., Ma, J., Huang, Y., Dai, M. and Li, X., 2015. Optimization of a colorimetric method to determine trace urea in seawater. Limnology and Oceanography: Methods, 13(6): 303-311.
Dai, M. et al., 2023. Upper Ocean Biogeochemistry of the Oligotrophic North Pacific Subtropical Gyre: From Nutrient Sources to Carbon Export. Reviews of Geophysics, 61(3): e2022RG000800.
Herbland, A., 1976. In situ utilization of urea in the euphotic zone of the tropical atlantic. Journal of Experimental Marine Biology and Ecology, 21(3): 269-277.
Jiang, S. et al., 2021. Nitrogen in Atmospheric Wet Depositions Over the East Indian Ocean and West Pacific Ocean: Spatial Variability, Source Identification, and Potential Influences. Frontiers in Marine Science, Volume 7 - 2020.
Matthews, E. et al., 2023. Airborne observations over the North Atlantic Ocean reveal the importance of gas-phase urea in the atmosphere. Proceedings of the National Academy of Sciences, 120(25): e2218127120.
Mitamura, O. and Saijo, Y., 1975. Decomposition of urea associated with photosynthesis of phytoplankton in coastal waters. Marine Biology, 30(1): 67-72.
Polovina, J.J., Dunne, J.P., Woodworth, P.A. and Howell, E.A., 2011. Projected expansion of the subtropical biome and contraction of the temperate and equatorial upwelling biomes in the North Pacific under global warming. ICES Journal of Marine Science, 68(6): 986-995.
Reay, M.K. et al., 2019. High resolution HPLC-MS confirms overestimation of urea in soil by the diacetyl monoxime (DAM) colorimetric method. Soil Biology and Biochemistry, 135: 127-133.
Seok, M.-W. et al., 2021. Atmospheric deposition of inorganic nutrients to the Western North Pacific Ocean. Science of The Total Environment, 793: 148401.
Solomon, C.M., Collier, J.L., Berg, G.M. and Glibert, P.M., 2010. Role of urea in microbial metabolism in aquatic systems: a biochemical and molecular review. Aquatic Microbial Ecology, 59(1): 67-88.
Wan, X.S. et al., 2024. Significance of Urea in Sustaining Nitrite Production by Ammonia Oxidizers in the Oligotrophic Ocean. Global Biogeochemical Cycles, 38(10): e2023GB007996.

Table 4.17-1 Samples analyzed during MR25-02

Station	Urea
1	18
2	18
7	18
11	18
16	18
21	18
30	18
36	18
46	18
48	18
52	18
58	18
63	18
68	18
74	18
80	18
Σ 16	**Σ 288**

4.18 Shipboard pH measurement – University of Galway

(1) Personnel

Delon Earle (University of Galway) Shipboard participant onboard during the expedition

Peter Croot (University of Galway): Principal investigator

(2) Objective

Ocean pH is a key parameter that forms part of the Inorganic Carbon essential ocean variable (EOV) (https://goosocean.org/document/17475) and is critical to addressing the impacts of Ocean Acidification and climate change on the marine environment. The importance of pH to ocean health is recognized by it's inclusion in the UN Sustainable Development Goal 14 (Life Under Water), and Target 14.3 calls to minimize and address the impacts of ocean acidification through enhanced cooperation at all levels. The International Oceanographic Commission (IOC) developed the SDG Indicator 14.3.1 methodology which calls for the measurement of pH throughout the global ocean.

Spectrophotometric measurements of the pH of seawater using sulfonephthalein indicators (Clayton and Byrne, 1993) now are routine on research vessels, through the development of manual and automated systems for use on a wide range of sampling platforms (Bellerby et al., 2002; Nehir et al., 2022). The Global Ocean Observing System (GOOS) have set a current goal of ± 0.005 for pH in the Inorganic Carbon EOV. While the Global Ocean Acidification Observing Network (GOA-ON) has set "weather" and "climate" goals for pH measurements, requiring uncertainties of ± 0.02 and ± 0.003, respectively (Alexis et al., 2025). However at present, achieving these goals is still challenging, as a number of inter-laboratory pH intercomparison have shown (Bockmon and Dickson, 2015; Takeshita et al., 2020; Takeshita et al., 2021). The present study represented an opportunity to perform a shipboard intercalibration between two analytical systems for measuring seawater pH spectrophotometrically onboard during the MR25-02 GO-SHIP expedition along the P04W line.

(3) Apparatus

Seawater samples were collected directly into gas tight Labco Exetainers from the Niskin bottles on the CTD via a plastic tube, allowed to overflow the Exetainer and then the cap screwed on. Exetainers were visibly checked to see that no bubbles were present. The samples were then analyzed spectrophotometrically for pH as described below. Samples were taken from the upper 1700 m of the water column from 16 stations in (Table 4.20-1) during MR25-02.

(i) pH_T^{25}

In this work pH_T^{25} was measured spectrophotometrically with the acid base indicator dye m-cresol purple (mCP) (Figure 4.18.1) using a Q-POD (Quantum Northwest) thermostated cuvette set to 25.00° C (±0.02° C), a 1 cm cuvette (Hellma QS-101), an Ocean Optics USB2000+ spectrophotometer and Ocean Optics DH-Mini light source were connected to the Q-POD via 600 μm diameter solar resistant fibre optic cables. The sample was stirred with a Teflon stirrer bar to ensure it was well mixed.

Purified methyl cresol purple (mCP) in solution (concentration 3.78 x 10^{-4} mol/kg) was kindly provided to us by Prof. Mike DeGrandpre and Cory Beatty at the University of Montana, U.S.A in an aluminum lined Tedlar bag. The mCP had been purified using an existing protocol (DeGrandpre et al., 2014) by Sunburst Sensors LLC (Missoula, Montana, U.S.A) and was left over material from earlier expeditions by the University of Montana. More details on the use of mCP as a pH indicator in seawater can be found in these works (Clayton and Byrne, 1993; DeGrandpre et al., 2014; Li et al., 2020; Liu et al., 2011; Takeshita et al., 2020; Takeshita et al., 2021).

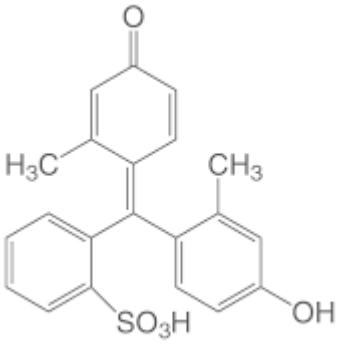

Figure 4.18.1 Chemical structure of m-cresol purple (mCP)

(4) Preliminary Results

All samples were analyzed within a few hours of collection onboard the ship during MR25-02, however all data should be considered preliminary as there are still post-processing corrections to be applied before the data sets are finalized.

(i) pH measurements during MR25-02

During MR25-02 we measured using the 1cm cuvette system, 288 samples for pH_T^{25} using the purified mCP from the USA and also ran 18 samples with the JAMSTEC purified mCP in a further intercalibration exercise (Table 4.18-1). Data was converted from absorbance to pH_T^{25} using the absorbance maximums of 434 and 578 nm (isobestic point 487 nm) for the HL^- and L^{2-} species of mCP and the algorithm developed for purified mCP by Liu et al. (2011). Sample salinity was obtained from the onboard measurements made by JAMSTEC.

Results from the intercomparison on the University of Galway system using two different batches of purified mCP that were onboard is shown in Figure 4.18.2. The preliminary data, which does not include the contribution to the pH from the dye addition, indicates a mean difference in pH_T^{25} of 0.053 ± 0.017.

A full analysis of this dataset is underway and this will include, corrections for dye addition (Li et al., 2020) and for possible impurities in the mCP (Douglas and Byrne, 2017), as while purified mCP (Woosley, 2021) has been shown to be stable for several years in the laboratory, there have been only a few studies on this to date. Once this dataset is finalized it will allow a full comparison to the larger JAMSTEC dataset and provide a better assessment of the two approaches.

(5) Acknowledgments

We are extremely grateful to JAMSTEC and the Scientists and Crew of the RV Mirai who helped support our work at sea during the MR25-02 GO-SHIP expedition. Thanks also to Prof. Mike DeGrandpre and Cory Beatty at the University of Montana, U.S.A for the purified mCP solutions. Funding for participation in the MR25-02 GO-SHIP expedition was provided by the Marine Institute of Ireland through the Changing Ocean Ireland: Forecasting Biodiversity and Ecosystem Response. (CÓIR) project (SPDOC/CC/20/001).

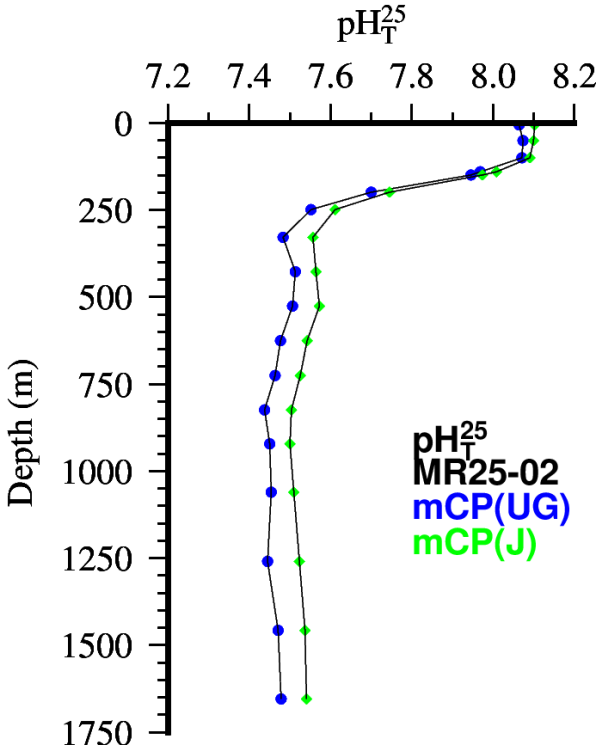

Figure 4.18.2: Vertical profiles of pH_T^{25} (preliminary data) at station 52 during MR25-02 using the University of Galway analytical system (1 cm pathlength). The blue circles were with the purified mCP supplied by the University of Galway, the green triangles are with the purified mCP supplied by JAMSTEC. No corrections have been applied yet for the dye addition.

References

Alexis, V.-O. et al., 2025. Perspectives from Developers and Users of the GOA-ON in a Box Kit: A Model for Capacity Sharing in Ocean Sciences. Oceanography, 38.

Bellerby, R., Olsen, A., Johannessen, T. and Croot, P., 2002. The Automated Marine pH sensor (AMpS); a high precision continuous spectrophotometric method for seawater pH measurements. Talanta, 56: 61-69.

Bockmon, E.E. and Dickson, A.G., 2015. An inter-laboratory comparison assessing the quality of seawater carbon dioxide measurements. Marine Chemistry, 171: 36-43.

Clayton, T.D. and Byrne, R.H., 1993. Spectrophotmetric seawater pH measurements: total hydrogen ion concentration scale calibration of m-cresol purple and at-sea results. Deep-Sea Research, 40: 2115-2129.

DeGrandpre, M.D. et al., 2014. Considerations for the measurement of spectrophotometric pH for ocean acidification and other studies. Limnology and Oceanography: Methods, 12(12): 830-839.

Douglas, N.K. and Byrne, R.H., 2017. Achieving accurate spectrophotometric pH measurements using unpurified meta-cresol purple. Marine Chemistry, 190: 66-72.

Li, X. et al., 2020. Purified meta-Cresol Purple dye perturbation: How it influences spectrophotometric pH measurements. Marine Chemistry, 225: 103849.

Liu, X., Patsavas, M.C. and Byrne, R.H., 2011. Purification and Characterization of meta-Cresol Purple for Spectrophotometric Seawater pH Measurements. Environmental Science & Technology, 45(11): 4862-4868.

Nehir, M., Esposito, M., Loucaides, S. and Achterberg, E.P., 2022. Field Application of Automated Spectrophotometric Analyzer for High-Resolution In Situ Monitoring of pH in Dynamic Estuarine and Coastal Waters. Frontiers in Marine Science, 9.

Takeshita, Y. et al., 2020. Assessment of pH dependent errors in spectrophotometric pH measurements of seawater. Marine Chemistry, 223: 103801.

Takeshita, Y. et al., 2021. Consistency and stability of purified meta-cresol purple for spectrophotometric pH measurements in seawater. Marine Chemistry, 236: 104018.
Woosley, R.J., 2021. Long-term stability and storage of meta-cresol purple solutions for seawater pH measurements. Limnology and Oceanography: Methods, 19(12): 810-817.

Table 4.18-1 Samples analyzed for pH during MR25-02

Station	pH (UG)	pH (JAMSTEC)
1	18	-
2	18	-
7	18	-
11	18	-
16	18	-
21	18	-
30	18	-
36	18	-
46	18	-
48	18	-
52	18	18
58	18	-
63	18	-
68	18	-
74	18	-
80	18	-
Σ 16	**Σ 288**	**Σ 18**

Note: At station 52 samples were run using the purified mCP employed in the pH analysis by the University of Galway (supplied by University of Montana) and an independent batch of purified mCP used by JAMSTEC.

4.19 Radiocesium and uranium isotopes

May 6, 2025

(1) Personnel

Tzu-Hao Wang (Technical University of Denmark) – Investigator (onboard)

Jixin Qiao (Technical University of Denmark) – Principal Investigator

(2) Objective

To investigate the patterns of long-lived anthropogenic radionuclides, i.e., ^{135}Cs – ^{137}Cs, ^{233}U – ^{236}U, in the seawater profiles obtained from the western equatorial Pacific Ocean for oceanic tracer studies.

(3) Sample collection

The sampling stations, locations and dates are summarized in Table 4.19.1. Seawater samples at 6 different depths (5 m, 25 m ,100 m, 200 m, 500 m and 1000 m) were collected using 12-L Niskin bottles mounted on the CTD sampling system onboard. The CTD sampling system consists of 36 Niskin bottles, every 6 bottles were designated to one depth of interest. 50 L and 10 L of seawater samples were collected for Cs isotope analysis and U isotope analysis, respectively. Each water container (20 L) was rinsed once with deionized water and twice with seawater at the depth of interest at every sampling station. Samples were drained from Niskin bottles through connected Acropak 500 capsule filters (Pall corporation) and stored in room temperature until further processing.

Table 4.19.1 Sampling stations, locations and dates

Station	Latitude (N)	Longitude (E)	Sampling date (UTC)
8	7.9972	129.5004	11/04/2025
17	9.002	134.9984	13/04/2025
26	8.9949	138.3842	16/04/2025
37	9.4484	144.5019	18/04/2025
45	9.4967	148.7554	20/04/2025
53	9.4913	155.0584	23/04/2025
64	9.4878	164.165	27/04/2025
75	10.5838	170.9992	01/05/2025

(4) Sample preparation and measurements

For Cs isotopes –

Prior to seawater sample collection, 10 g of AMP-PAN resins were packed onto each 45-mL cartridge, equivalent to 4 cm tall including two frits on the top and at the bottom of the resin, conditioned and stored in 0.5M HNO_3 before use. For each depth, 50 L of seawater samples were acidified to pH $\leq$ 2 with concentrated (60 wt%) HNO_3. The acidified 50-L seawater samples were pumped through the cartridges packed with AMP-PAN resins at a controlled flow rate (~120 mL/min) using peristaltic pump (Longer four-channel peristaltic pump BT100-1L-A with pump head YZII15). 50 mL of seawater samples were collected separately both before and after the cartridge preconcentration step, to monitor the recovery of AMP-PAN resins, then parafilmed and stored in plastic bags at room temperature. Once the sample introduction finished, the cartridges were capped, parafilmed and stored in plastic bags at room temperature until further analysis on land.

The activity of ^{137}Cs in the cartridges packed with AMP-PAN resins will be measured by a HPGe gamma detector in the Department of Environmental and Resource Engineering at the Technical University of Denmark (DTU). The HPGe gamma detector will be calibrated with a reference cartridge spiked with known ^{137}Cs prior to the measurements. The Cs in the resins will be eluted with 1.5M $HN_3{\cdot}H_2O$, evaporated to dryness and re-dissolved in 0.3M HNO_3 for isotope analysis (Zhu et al., 2020). The isotope ratio of ^{135}Cs/^{137}Cs in the collected seawater samples will be determined using triple-quadrupole inductively-

coupled plasma mass spectrometer (ICP-QQQ, Agilent 8800) at DTU (Zhu et al., 2021), with ratio-reported reference materials IAEA-375 and IAEA-447. With ^{137}Cs standard, the concentration/activity of ^{137}Cs will also be determined and compared to the results obtained from the gamma analysis. The concentration/activity of ^{135}Cs in collected seawater samples will then be calculated from known $^{135}Cs/^{137}Cs$ ratio and ^{137}Cs concentration/activity.

For U isotopes –

Prior to seawater sample collection, weighed $FeCl_3 \cdot 6H_2O$ powders were dissolved in 3M HNO_3 and passed through 2-mL UTEVA columns to remove potential U background. The columns were washed with the same volume of 3M HNO_3 again, to prepare the 0.05 g/mL Fe solution for later precipitation experiment. Collected and filtered 10-L seawater samples were acidified to pH ≤ 2 with concentrated (60 wt%) HNO_3, added with 20 mL 0.05 g/mL Fe solution and bubbled with N_2 gas for 10 minutes (Qiao et al., 2015). The seawater samples were adjusted to pH ≥ 9 with 28% $HN_3 \cdot H_2O$, bubbled with N_2 gas for 1 minute and let the precipitate settle down for 30 minutes. The supernatant was then pumped out with peristaltic pump (Masterflex) and poured out to collect the precipitates ultimately in a 500-mL bottle for each seawater sample. The bottle with precipitates was then parafilmed and stored at room temperature until further processing on land.

The precipitates will be centrifuged, re-dissolved in 3M HNO_3 for chemistry, passed through a 2-mL UTEVA column again. Part of the eluate will be subsampled for ^{238}U measurement on ICP-MS (Agilent 8800) at DTU. The rest of the eluate will be co-precipitated as $Fe(OH)_3$, centrifuged, evaporated to dryness and combusted (Lin et al., 2021), to prepare for the $^{236}U/^{238}U$ and $^{233}U/^{238}U$ isotope ratio measurement using the accelerator mass spectrometry (AMS) in the Vienna Environmental Research Accelerator (VERA) facility in the University of Vienna.

(5) Data archives

The data obtained in this cruise will be submitted to the Data Management Group of JAMSTEC and will be opened to the public via “Data Research System for Whole Cruise Information in JAMSTEC (DARWIN)” in the JAMSTEC website.

(6) References

Lin, M., Qiao, J., Hou, X., Golser, R., Hain, K., Steier, P., 2021. On the Quality Control for the Determination of Ultratrace-Level 236U and 233U in Environmental Samples by Accelerator Mass Spectrometry. Anal. Chem. 93, 3362–3369. https://doi.org/10.1021/acs.analchem.0c03623

Qiao, J., Hou, X., Steier, P., Nielsen, S., Golser, R., 2015. Method for 236U Determination in Seawater Using Flow Injection Extraction Chromatography and Accelerator Mass Spectrometry. Anal. Chem. 87, 7411–7417. https://doi.org/10.1021/acs.analchem.5b01608

Zhu, L., Hou, X., Qiao, J., 2021. Determination of low-level 135Cs and 135Cs/137Cs atomic ratios in large volume of seawater by chemical separation coupled with triple-quadrupole inductively coupled plasma mass spectrometry measurement for its oceanographic applications. Talanta 226, 122121. https://doi.org/10.1016/j.talanta.2021.122121

Zhu, L., Hou, X., Qiao, J., 2020. Determination of Ultralow Level 135Cs and 135Cs/137Cs Ratio in Environmental Samples by Chemical Separation and Triple Quadrupole ICP-MS. Anal. Chem. 92, 7884–7892. https://doi.org/10.1021/acs.analchem.0c01153

4.20 Radio-iodine, -uranium, -thorium

May 11, 2025

(1) Personnel

Hiroyuki Matsuzaki (The University of Tokyo)

Yuanzhi Qi (The University of Tokyo)

Qiuyu Yang (The University of Tokyo)

(2) Objective

The objective of this study is to investigate the cycling processes of radioiodine (^{129}I), radiouranium (^{238}U and ^{236}U), and radiothorium (^{228}Th and ^{230}Th) in the Pacific Ocean environment. Additionally, these radioactive isotopes will be used to trace Pacific Ocean currents and to study iodine cycling processes, including sea-air exchange and redox reactions.

(3) Sample collection

The sampling stations are summarized in Table 4.20-1. Surface seawater samples were collected using the sampling pump system installed on the research vessel, while seawater samples from other depths were obtained using 12 L Niskin bottles mounted on a CTD/Carousel Water Sampling System (CTD system).

Immediately after collection, seawater samples for iodine analysis were filtered through 0.45 μm mixed cellulose ester membrane filters (ADVANTEC). The filtered seawater was then stored in 1 L polypropylene (PP) bottles at room temperature until further processing. Seawater samples for thorium analysis and surface suspended particulate matter (SPM) were filtered through 0.5 μm glass fiber membranes (ADVANTEC). The glass fiber membranes containing SPM were stored at –18 °C after filtration. The filtered seawater for thorium analysis was acidified with concentrated nitric acid (60%) at a volume ratio of 1:1000 (acid to seawater) and stored in 20 L plastic containers at room temperature for further analysis. The filtered seawater for surface SPM analysis was discarded. Uranium samples were directly collected into 5 L plastic containers and stored at room temperature until further analysis.

In addition to seawater samples, atmospheric aerosol samples were collected using an aerosol sampler equipped with cellulose filter membranes (particle retention size: 20–25 μm). Sampling was conducted throughout the cruise (April 3 to May 12, 2025) with a sampling period of 48 hours and an air flow rate of 1000 L/min, for subsequent iodine analysis.

(4) Instruments and method

The bulk concentrations of ^{127}I and ^{238}U will be measured by Inductively Coupled Plasma Mass Spectrometry (ICP-MS) after ten-fold dilution with 0.5% tetramethylammonium hydroxide (TMAH) and 1 M HNO_3, respectively. The iodide ($^{127}I^-$) concentration in seawater will be measured directly by Ion Chromatography (IC). Since the concentration of dissolved organic iodine is very low in the open ocean, the iodate ($^{127}IO_3^-$) concentration will be calculated by subtracting the measured $^{127}I^-$ concentration from the bulk ^{127}I concentration.

Different ^{129}I species, including bulk ^{129}I, $^{129}I^-$, and $^{129}IO_3^-$, will be separated using a coprecipitation method and measured by the ^{129}I-AMS system at MALT (Micro Analysis Laboratory, Tandem Accelerator, The University of Tokyo). Uranium in seawater will be adsorbed onto hydrated titanium oxide (HTO), then dissolved in 3 M HNO_3. The uranium in the resulting acidic solution will be coprecipitated with $Fe(OH)_3$, and ^{236}U in the obtained precipitate will be analyzed by the ^{236}U -AMS system at MALT.

Both aerosol and SPM samples will be separated from the filters by combustion, and the released molecular iodine will be trapped in a solution containing 0.5 mol L^{-1} NaOH and 0.02 mol L^{-1} $NaHSO_3$. A small aliquot of the trapping solution will be used to measure stable iodine using ICP-MS, while iodine in the remaining solution will be separated and prepared as an AgI–AgCl precipitate for ^{129}I analysis by AMS.

After spiking with Th-229, the dissolved Th isotopes in seawater samples will be extracted by $Fe(OH)_3$ co-precipitation, purified by anion exchange chromograph, and extracted again by a second $Fe(OH)_3$ co-precipitation. The $Fe(OH)_3$ pellet will be combusted to Fe_2O_3, mixed will metal powder, and pressed into cathodes for the measurement of ^{230}Th and ^{228}Th by AMS.

(5) Data archive

The data obtained in this cruise will be submitted to the Data Management Group of JAMSTEC and will be opened to the public via “Data Research System for Whole Cruise Information in JAMSTEC (DARWIN)” in the JAMSTEC web site.

Table 4.20-1 Sampling stations of seawater for iodine

Station	Sampling Date (UTC)	Position		Depth (m)	Soluble radio isotopes			Iodine in surface SPM
		Latitude	Longitude		I	U	Th	
03	2025/04/09	07-59.29N	127-17.91E	9259	✓	✓	✓	
12	2025/04/12	08-30.10N	132-26.29E	4539	✓	✓		✓
22	2025/04/15	09-00.14N	137-14.83E	3619	✓	✓		✓
31	2025/04/17	09-05.12N	140-24.17E	3112	✓	✓		✓
40	2025/04/19	09-29.74N	146-19.71E	4222	✓	✓	✓	
49	2025/04/22	09-29.21N	151-40.29E	5097	✓	✓		✓
59	2025/04/26	09-29.30N	159-59.80E	5278	✓	✓		✓
69	2025/04/29	12-10.11N	167-56.95E	5000	✓	✓	✓	

Acronym: SPM, Suspended Particulate Matter

4.21 Total inorganic and organic iodine-129

May 12, 2025
Yuichiro Kumamoto
Japan Agency for Marine-Earth Science and Technology (JAMSTEC)

(1) Personnel

Tetusya Matsunaka (Principal Investigator)
Kanazawa University (not on board)

Hikaru Miura
Central Research Institute of Electric Power Industry (not on board)

Yuichiro Kumamoto
Japan Agency for Marine-Earth Science and Technology (on board)

(2) Objectives

Determination of activity concentrations of inorganic and organic iodine-129 (^{129}I) in the North Pacific Ocean.

(3) Sample collection

The sampling stations and number of samples are summarized in Table 4.21.1. All samples for total inorganic and organic iodine-129 were collected at 10 and 5 stations, respectively, using the 12-liter Niskin-type bottles. The seawater samples were collected into a 500 mL plastic bottle for total inorganic and organic ^{129}I, respectively, and stored in a freezing store room.

Table 4.21.1 Sampling stations and number of samples for ^{129}I.

Station	Lat. (N)	Long. (E)	Sampling Date (UTC)	Number of samples		Max. Pressure(dbar)
				Inorganic ^{129}I	Organic ^{129}I	
006	8.01	128.51	2025/04/10	8	0	799.2
016	8.97	134.79	2025/04/13	8	0	798.6
025	9.00	138.19	2025/04/15	8	0	828.9
033	9.20	141.62	2025/04/17	8	0	769.1
043	9.50	148.08	2025/04/20	8	8	800.4
052	9.50	154.16	2025/04/23	8	8	830.5
056	9.48	157.49	2025/04/25	15	15	5309.6
063	9.49	163.33	2025/04/27	15	15	5256.5
072	11.83	169.75	2025/04/30	15	15	5219.1
078	9.49	172.66	2025/05/02	11	0	1920.0
			Total	104	61	

(4) Sample preparation and measurements

The filtered seawater (400 ml) for analyzing organic ^{129}I is placed in a sealed quartz reactor and exposed to ultraviolet light using a low-pressure Hg grid lamp for 24 h to convert organic iodine to inorganic iodine. ^{129}I is pretreated and measured using the following methods for seawater exposed to ultraviolet radiation (organic plus total inorganic iodine) and seawater not exposed to ultraviolet radiation (total inorganic iodine). The difference between the two was used to calculate the organic ^{129}I.

After adding 1 mg of iodine carrier (Deep water old iodine) with an ^{129}I/^{127}I ratio of 1.5×10^{-14} to the 400 ml seawater sample, iodine is isolated by solvent extraction with CCl_4. The purified iodide is precipitated as AgI by the addition of $AgNO_3$. The AgI precipitate is then washed with NH_4OH and ultrapure water, dried, and loaded into an Al holder with Nb powder.

The ^{129}I/^{127}I ratio of the AgI targets is measured using an accelerator mass spectrometry (AMS) system at the University of Tsukuba. A terminal voltage of 5 MV and charge state of 5^+ are chosen for

acceleration and detection. The measurement ratios are normalized against the Purdue-1 reference material, which has an $^{129}I/^{127}I$ ratio of 8.37×10^{-12} and is obtained from Purdue University, USA. ^{127}I in the water sample is measured using inductively coupled plasma-mass spectrometry (ICP–MS). The original $^{129}I/^{127}I$ ratios and ^{129}I concentrations in seawater are calculated using the ^{127}I concentration from ICP-MS and the $^{129}I/^{127}I$ ratio from AMS.

(5) Data archives

The data obtained in this cruise will be submitted to the Data Management Group of JAMSTEC and will be opened to the public via "Data Research System for Whole Cruise Information in JAMSTEC (DARWIN)" in the JAMSTEC web site.

4.22 Radiocesium, radiostrontium, and radium isotopes

May 12, 2025
Yuichiro Kumamoto
Japan Agency for Marine-Earth Science and Technology (JAMSTEC)

(1) Personnel

Mutsuo Inoue (Principal Investigator)
Kanazawa University (not on board)

Hirofumi Tazoe (Principal Investigator)
Hirosaki University (not on board)

Yuichiro Kumamoto
Japan Agency for Marine-Earth Science and Technology (on board)

(2) Objectives

In order to investigate the water circulation process in the western equatorial North Pacific Ocean, seawater samples were collected for measurements of radiocesium (^{137}Cs) and radiostrontium (^{90}Sr), and radium isotopes (^{226}Ra and ^{228}Ra).

(3) Sample collection

We collected seawater at 5 stations using the 12-liter Niskin-type bottles at 6 depths between surface to 800 m depth (Table 4.22.1). Seawater samples for radiocesium and radium isotopes measurements were also collected at 11 stations from surface water that pumped up from about 4 m depth from the sea surface (Table 4.22.2). The volume of seawater samples for radiocesium/radium isotopes and radiostrontium were 20 L and 40 L, respectively. The seawater samples were not filtered and collected in a 20-L plastic container after two time washing.

(4) Sample preparation and measurements

The seawater sample was not filtered and acidified by adding nitric acid. ^{137}Cs in the seawater sample is concentrated using ammonium phosphomolybdate (AMP) that forms an insoluble compound with cesium. ^{137}Cs in the compound is measured using Ge detectors. Ra-free barium carrier and SO_4^{2-} are added to the supernatant seawater for ^{137}Cs to coprecipitate ^{226}Ra and ^{228}Ra with $BaSO_4$. After evaporating to dryness, the $BaSO_4$ fractions are compressed to disc as a mixture of $Fe(OH)_3$ and NaCl for gamma-spectrometry.

For ^{90}Sr analysis, we add 300 g of $(NH_4)_2C_2O_4$ H_2O to 40 L of seawater and shook the solution vigorously. Sr is precipitated with Ca oxalate. Oxalate precipitate is decomposed to carbonate at 550 ^{o}C in a muffle oven. Then, the precipitate is dissolved in HCl and diluted to about 200 mL with Milli-Q water. A small portion of sample solution is used for determination of stable Sr yield by ICP-OES. After secular equilibrium between ^{90}Sr and ^{90}Y (>2 weeks), ^{90}Y with stable Y carrier (0.1 mg) is “milked” from the ^{90}Sr by precipitating the Fe hydroxide and purified by solid phase extraction using DGA Resin (DN1ML-R50-S) purchased from Eichrom Technologies. Beta particles are counted by a low background gas flow proportional counter during 120 min intervals for more than 20 hours

(5) Data archives

The data obtained in this cruise will be submitted to the Data Management Group of JAMSTEC and will be opened to the public via “Data Research System for Whole Cruise Information in JAMSTEC (DARWIN)” in the JAMSTEC web site.

Table 4.22.1 Sampling stations of deep seawaters.

Station	Lat.	Long.	Sampling Date (UTC)	Number of samples		Max. Pressure (dbar)
				^{137}Cs, ^{226}Ra, and ^{228}Ra	^{90}Sr	
05	08-00.01N	128-09.79E	2025/04/10	6	6	800
18	08-59.81N	135-19.58E	2025/04/14	6	6	800
35	09-17.23N	142-50.05E	2025/04/17	6	6	800
51	09-29.81N	153-19.63E	2025/04/23	6	6	800
62	09-29.68N	162-29.77E	2025/04/27	6	6	800

Table 4.22.2 Sampling stations of surface seawaters for ^{137}Cs, ^{226}Ra, and ^{228}Ra

Station	Latitude End time	Longitude End time	Sampling Date (UTC)	Sampling Time (UTC)
10	08-10.51N	130-50.03E	2025/04/12	23:56-00:05
28	08-59.62N	139-09.92E	2025/04/16	10:00-10:21
46	09-29.51N	149-10.00E	2025/04/20	17:35-17:46
58	09-29.28N	159-09.93E	2025/04/25	19:35-19:40
66	12-10.27N	165-15.08E	2025/04/29	00:05-00:12
78	09-29.65N	172-39.86E	2025/05/02	03:46-03:57
-	13-55.88N	168-07.44E	2025/05/04	04:16-04:22
-	17-17.50N	163-19.34E	2025/05/05	08:09-08:15
-	20-03.17N	159-33.18E	2025/05/06	05:44-05:50
-	23-04.22N	155-21.79E	2025/05/07	05:16-05:22
-	25-51.14N	151-36.23E	2025/05/08	02:04-02:13

4.23 Tritium

May 12, 2025
Yuichiro Kumamoto
Japan Agency for Marine-Earth Science and Technology (JAMSTEC)

(1) Personnel

Hyoe Takata (Principal Investigator)

Fukushima University (not on board)

Yuichiro Kumamoto

Japan Agency for Marine-Earth Science and Technology (on board)

(2) Objectives

For the better understanding of the fate of tritium released from Fukushima Dai-ichi Nuclear Power Plant, it is required to measure this nuclide level in the surface layers of the North Pacific.

(3) Sample collection

We collected surface water that pumped up from about 4 m depth from the sea surface at 11 stations (Table 4.23.1). We also collected seawater at 3 stations using the 12-liter Niskin-type bottles at 8 depths between surface to bottom depth (Table 4.23.2). The volume of seawater samples was 1 L. The seawater samples were not filtered and collected in a 2-L plastic container after two time washing.

Table 4.23.1 Sampling stations of surface seawaters

Station	Latitude End time	Longitude End time	Sampling Date (UTC)	Sampling Time (UTC)
10	08-10.51N	130-50.03E	2025/04/12	23:56-00:05
28	08-59.62N	139-09.92E	2025/04/16	10:00-10:21
46	09-29.51N	149-10.00E	2025/04/20	17:35-17:46
58	09-29.28N	159-09.93E	2025/04/25	19:35-19:40
66	12-10.27N	165-15.08E	2025/04/29	00:05-00:12
78	09-29.65N	172-39.86E	2025/05/02	03:46-03:57
-	13-55.88N	168-07.44E	2025/05/04	04:16-04:22
-	17-17.50N	163-19.34E	2025/05/05	08:09-08:15
-	20-03.17N	159-33.18E	2025/05/06	05:44-05:50
-	23-04.22N	155-21.79E	2025/05/07	05:16-05:22
-	25-51.14N	151-36.23E	2025/05/08	02:04-02:13

Table 4.23.2 Sampling stations of deep seawaters.

Station	Lat.	Long.	Sampling Date (UTC)	Number of samples	Max. Pressure (dbar)
19	08-59.98N	135-39.50E	2025/04/14	8	4214.6
36	09-22.12N	143-41.59E	2025/04/18	8	4711.2
50	09-29.74N	152-30.10E	2025/04/22	8	5198.2

(4) Sample preparation and measurements

Collected water samples that had been stored in the dark area with room temperature will be distilled, and enriched by an electric enrich system, then measured by liquid scintillation counter.

(5) Data archives

The data obtained in this cruise will be submitted to the Data Management Group of JAMSTEC and

will be opened to the public via “Data Research System for Whole Cruise Information in JAMSTEC (DARWIN)” in the JAMSTEC web site.

4.24 XCTD

November 26, 2025

(1) Personnel

Hiroshi UCHIDA (JAMSTEC RIGC)
Shinya KOUKETSU (JAMSTEC RIGC)
Fumine OKADA (NME)
Satomi OGAWA (NME)
Haruna YAMANAKA (NME)
Masanori MURAKAMI (NME, Mirai crew)

(2) Objective

The objective of this study is to evaluate XCTD (eXpendable Conductivity, Temperature and Depth profiler) data by side-by-side comparisons with the shipboard CTD measurements, and to obtain temperature and salinity profiles as an alternative to CTD measurements.

(3) Instruments and method

The XCTD used were XCTD-4A (up to 2000 m) and test its probes (Tsurumi-Seiki Co., Ltd., Yokohama, Kanagawa, Japan) (Table 4.24-1) with an MK-150N deck unit and a data acquisition software AL12 version 1.8.0 (Tsurumi-Seiki). The XCTD probes were deployed during the down cast of the shipboard CTD measurements by using a 12-loading automatic launcher or a hand launcher (Tables 4.24-2 and 4.24-3). The test probes were prepared as modified versions of the normal probe to investigate the cause of the thermal bias (see Uchida et al. 2011).

(4) Results

For the side-by-side comparisons with the shipboard CTD, two XCTD probes were deployed at each CTD cast by using a hand launcher except for the first deployment by using an automatic launcher (Table 4.26-2). After the first deployment, the canister of the first probe got stuck in the automatic launcher and the second probe couldn't be launched. It took time to remove the second probe from the automatic launcher, and the deployment of the second probe was delayed.

For the underway measurements, six XCTD probes (XCTD-4A) were deployed between the CTD stations 64 and 76 (Fig. 4.24-1). Low-salinity biases (about −0.07) were observed in the XCTD salinity data (Fig. 4.24-2). These salinity biases likely due to the thermal bias (Uchida et al. 2011), and the XCTD data will be calibrated by using the results of the side-by-side comparisons.

Table 4.24-1. List of XCTD probes used in this cruise. The test probes were modified versions of XCTD-4A to investigate cause of the thermal bias. Coefficients of the fall rate equation are 3.68081 (terminal velocity [m/s]) and −0.00047 (acceleration [m/s^2]) for all probes.

Probe type	Board version	Resolution of A/D converter Temperature (°C)	Conductivity (mS/cm)	Depth interval (m)	Note
XCTD-4A	XCTP R1.2	0.001 (16 bit)	0.001 (16 bit)	0.27	
XCTD-4A[1]	XCTP R1.2	0.001 (16 bit)	0.001 (16 bit)	0.27	Test probe 1
XCTD-4A[2]	XCTP R1.2	0.001 (16 bit)	0.001 (16 bit)	0.27	Test probe 2
XCTD-4A[3]	XCTP R1.2	0.001 (16 bit)	0.001 (16 bit)	0.27	Test probe 3
XCTD-4A[4]	XCTP R1.2	0.001 (16 bit)	0.001 (16 bit)	0.27	Test probe 4
XCTD-4A[5]	XCTD R2.0	0.001 (16 bit)	0.001 (16 bit)	0.27	Test probe 5

Table 4.24-2. List of the side-by-side comparisons with the shipboard CTD measurements.

Probe type	Serial no.	CTD pressure	Note
Station 014_1, 8° 50.00'N, 134° 05.08'E, 4288 m, SST 29.937 °C, SSS 33.793			
XCTD-4A	25010003	5–490 dbar	Automatic launcher
XCTD-4A[1]	24113002	1819–2530 dbar	Deployment delayed
Station 018_1, 8° 59.73'N, 135° 19.67'E, 4047 m, SST 29.453 °C, SSS 33.944			
XCTD-4A[2]	24106002	10–492 dbar	
XCTD-4A	25010006	582–1239 dbar	
Station 019_1, 8° 59.99'N, 135° 39.65'E, 4246 m, SST 29.599 °C, SSS 33.977			
XCTD-4A[4]	24101201	6–457 dbar	
XCTD-4A	25010009	577–1197 dbar	
Station 021_2, 9° 02.01'N, 136° 38.52'E, 4537 m, SST 29.437 °C, SSS 33.922			
XCTD-4A[5]	24114002	10–494 dbar	
XCTD-4A	25010002	641–1290 dbar	
Station 022_1, 9° 00.10'N, 137° 14.86'E, 3618 m, SST 29.937 °C, SSS 33.818			
XCTD-4A[3]	24109002	4–481 dbar	
XCTD-4A	25010010	561–1181 dbar	
Station 027_1, 8° 58.79'N, 138° 40.43'E, 4802 m, SST 29.755 °C, SSS 33.777			
XCTD-4A[1]	24113001	5–505 dbar	
XCTD-4A	25010001	597–1267 dbar	
Station 036_1, 9° 22.08'N, 143° 41.63'E, 4730 m, SST 29.458 °C, SSS 34.063			
XCTD-4A[2]	24016001	9–31 dbar	Failed at 137 m
XCTD-4A	25010007	384–995 dbar	
Station 039_1, 9° 29.90'N, 145° 49.98'E, 3193 m, SST 29.321 °C, SSS 34.089			
XCTD-4A[3]	24109001	5–471 dbar	
XCTD-4A	25010004	577–1223 dbar	
Station 040_1, 9° 29.70'N, 146° 19.66'E, 4225 m, SST 29.371 °C, SSS 34.190			
XCTD-4A[5]	24114001	12–514 dbar	
XCTD-4A	25010008	651–1298 dbar	
Station 044_1, 9° 30.07'N, 148° 25.37'E, 4012 m, SST 29.437 °C, SSS 34.130			
XCTD-4A[4]	24101202	11–530 dbar	
XCTD-4A	25010005	623–1273 dbar	

Table 4.24-3. List of the underway XCTD (XCTD-4) measurements. The automatic launcher was used to deploy the XCTD, except for the station 903 where the hand launcher was used to avoid having the measurement terminated midway due to wind. No data was transmitted for depths from 1855 m to 1879 m for the station 902, and from 1794 m to 1805 m for the station 073. The measurement was terminated at 1916 m for the station 067, at 1641 m for the station 071, and at 1826 m for the station 073.

Station	Serial no.	Date, Time (UTC)	Latitude	Longitude	Depth	SST	SSS
901	24018899	April 28, 03:25	10° 09.59'N	164° 22.49'E	4651 m	28.631 °C	34.533
902	24018898	April 28, 18:33	11° 29.98'N	164° 49.99'E	4584 m	28.392 °C	34.537
067	24018888	April 29, 08:10	12° 09.99'N	166° 25.00'E	3771 m	28.175 °C	34.744
071	24018886	April 30, 08:43	12° 00.00'N	169° 16.79'E	4168 m	27.923 °C	34.599
073	24018891	April 30, 18:27	11° 19.99'N	170° 14.99'E	4995 m	27.891 °C	34.620
903	24018887	May 1, 09:25	10° 02.18'N	171° 12.00'E	4798 m	28.007 °C	34.510

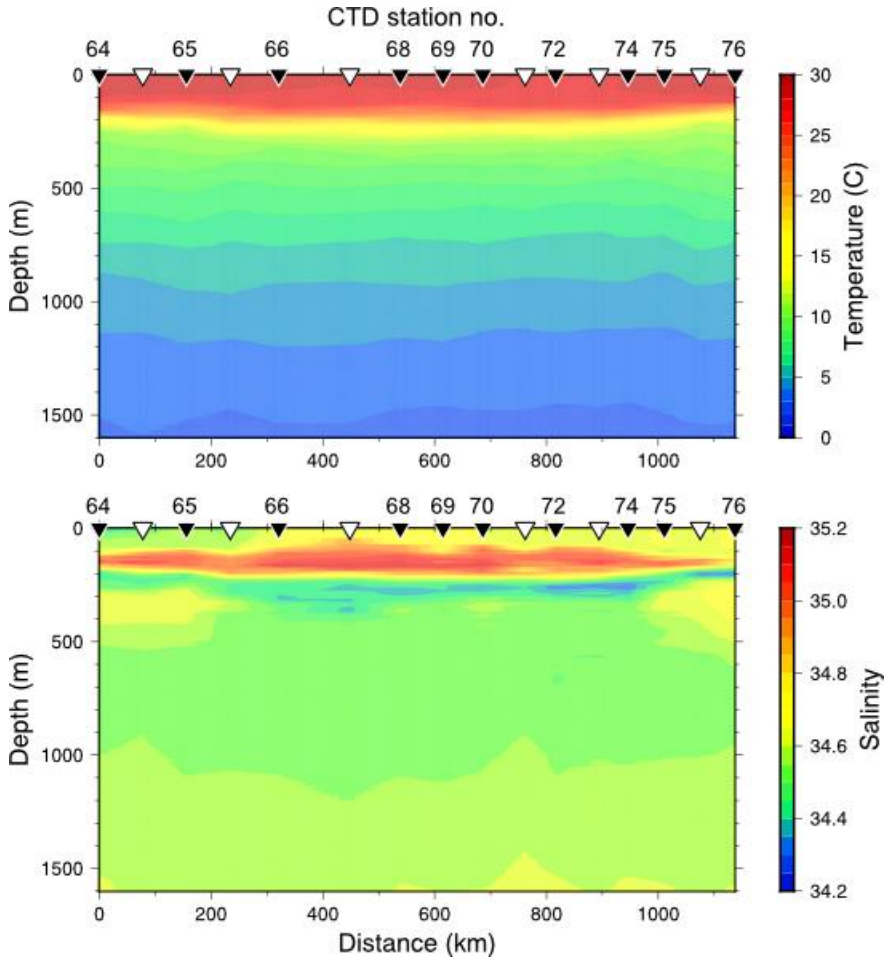

Figure 4.24-1. Vertical sections of temperature (upper) and salinity (lower) obtained by the CTD and XCTD measurements between the stations 64 and 76. The open inverted triangles indicate the locations of the XCTD deployment. A simple bias correction (−0.07) was applied to the XCTD salinity data for this plot.

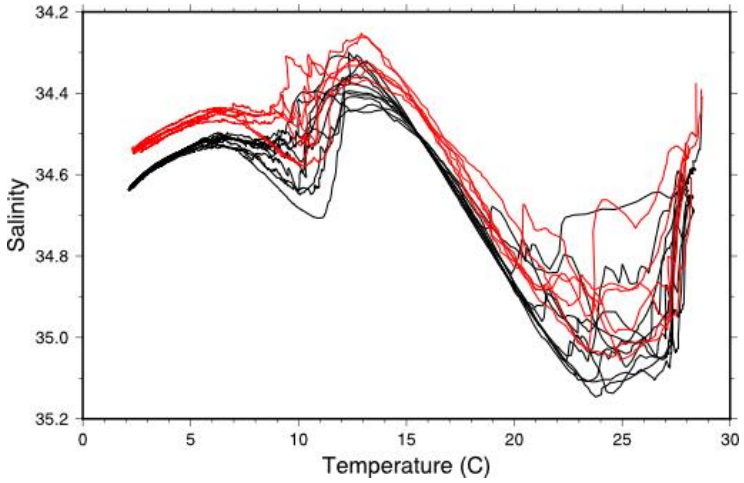

Figure 4.24-2. Temperature–salinity relationships for the CTD (black lines) and the XCTD (red lines) obtained between the stations 64 and 76. The data for depths shallower than 2000 m were plotted.

(5) Post-cruise data processing and quality control

The XCTD data were processed and quality controlled by using the XCTD data averaged over 1 m by the manufacturer's software. The mismatch of the recording timing of the temperature and conductivity data (Uchida et al. 2011) has been fixed starting with serial number 23045111, and all probes used on this cruise are the corrected versions. The results of the side-by-side comparisons of XCTD-4A with the shipboard CTD were used to determine coefficients of the fall rate equation for XCTD-4A and magnitude of the thermal bias and conductivity bias following the method of Uchida et al. (2011).

Differences between XCTD and CTD depths were shown in Fig. 2.24-3. The terminal velocity error was estimated to be −0.01405 for the XCTD-4A. The XCTD data were corrected for the depth error by using the estimated terminal velocities. Differences of temperature on pressure surfaces were examined by using side-by-side XCTD and CTD data (Fig. 2.24-4). Average thermal bias below 900 dbar was 0.0245±0.0026 °C. Differences of conductivity on pressure surfaces were examined by using side-by-side XCTD and CTD data (Fig. 2.24-5). Average conductivity bias below 900 dbar was −0.0002±0.0033 mS/cm. The XCTD data were corrected for the depth error, thermal bias, and conductivity bias.

For the six XCTD-4A probes used in the underway measurements, salinity bias still existed. The cause appears to be the different probe lots used in the side-by-side comparisons and the underway measurements, but the nature of the bias remains unclear. Hear, the average conductivity at a temperature of 3 °C was calculated for both the CTD and XCTD at station from 64 to 76. The difference between these values (−0.0337 mS/cm) was then corrected as the additional conductivity bias for the XCTD-4A.

Temperature-salinity plot using the quality-controlled XCTD-4A data is shown in Fig. 2.24-6.

(6) Reference

Uchida, H., K. Shimada, and T. Kawano (2011): A method for data processing to obtain high-quality XCTD data. *J. Atmos. Oceanic Technol.*, **28**, 816–826.

(7) Data archive

These obtained data will be submitted to JAMSTEC Data Management Group (DMG)

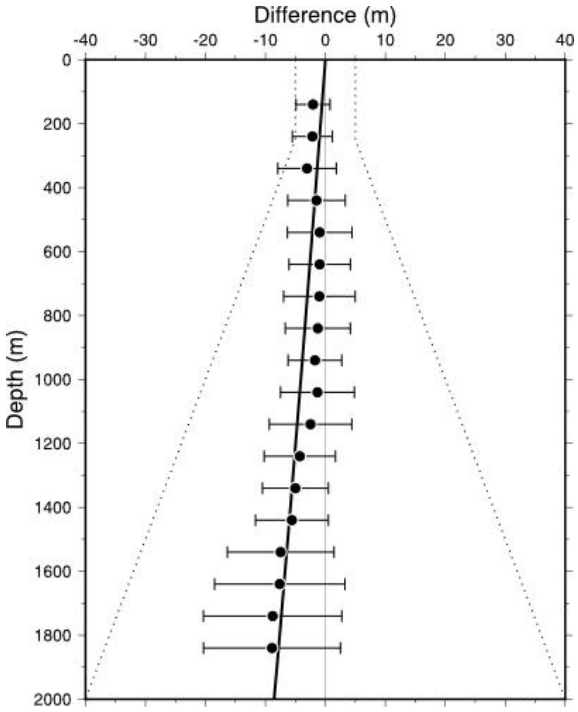

Figure 4.24-3. Differences between XCTD and CTD depths for XCTD-4. Differences were estimated with the same method as Uchida et al. (2011). Standard deviation of the estimates (horizontal bars) and the manufacturer's specification for XCTD depth error (dotted lines) are shown. The regression (solid line) for the data is also shown.

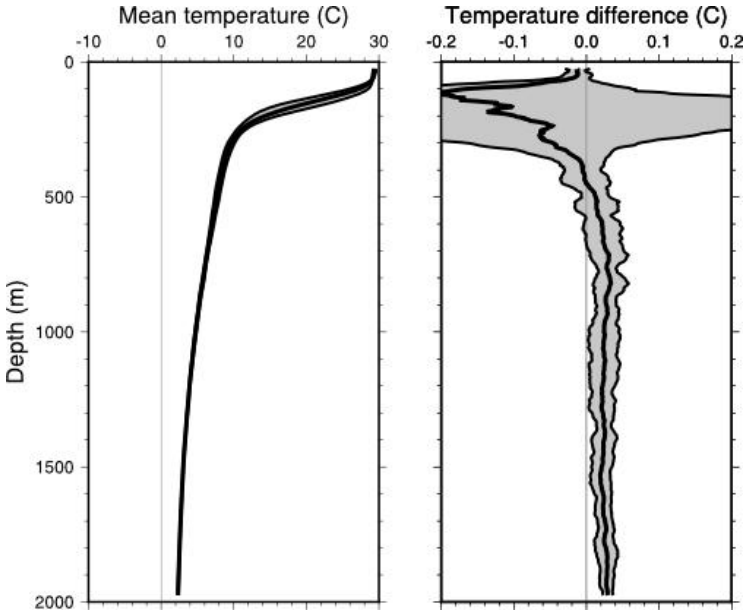

Figure 4.24-4. Comparison between XCTD and CTD temperature profiles. (a) Mean temperature of CTD profiles with standard deviation (shade) and (b) mean temperature difference with standard deviation (shade) between the XCTD and CTD. Mean profiles were low-pass filtered by a running mean with a window of 51 dbar.

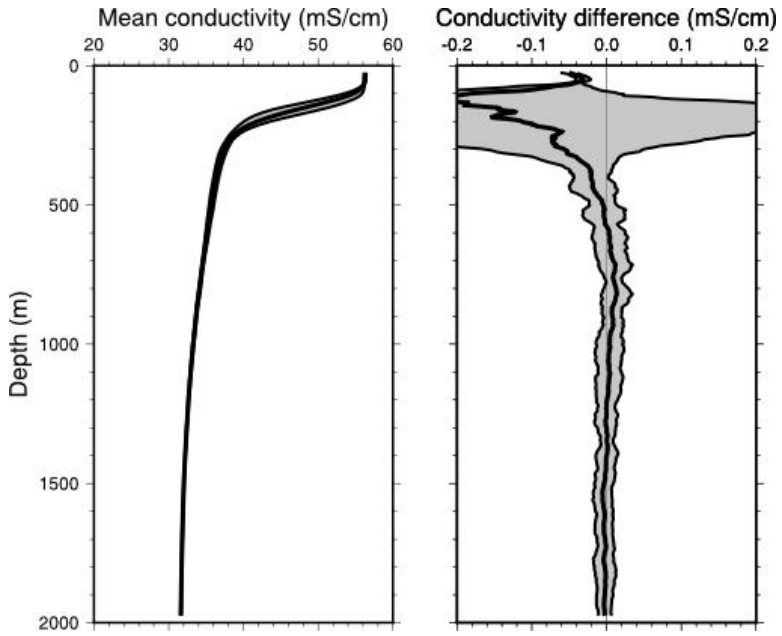

Figure 4.24-5. Comparison between XCTD and CTD conductivity profiles. (a) Mean conductivity of CTD profiles with standard deviation (shade) and (b) mean conductivity difference with standard deviation (shade) between the XCTD and CTD. Mean profiles were low-pass filtered by a running mean with a window of 51 dbar.

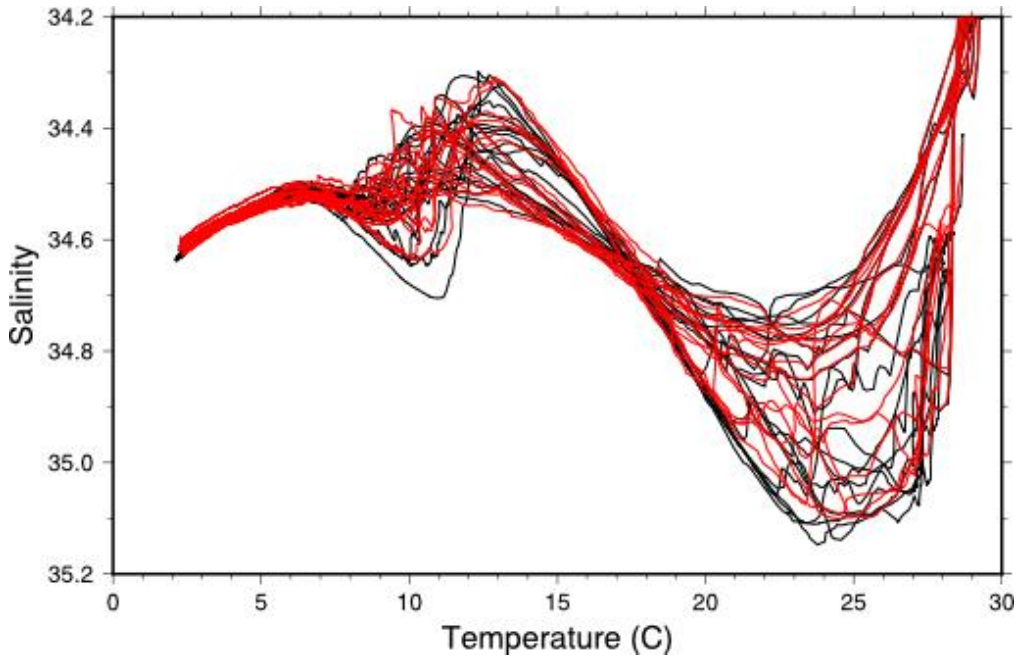

Figure 4.24-6. Temperature–salinity relationships for the CTD (black lines) and the XCTD (red lines) obtained at stations 14, 18, 19, 21, 22, 27, 36, 39, 40, 44 and between the stations 64 and 76. The data for depths shallower than 2000 m were plotted.

5. Float Deployments

5.1 Argo Floats

(1) Personnel

Shigeki Hosoda (JAMSTEC): Principal investigator
Kanako Sato (JAMSTEC)
Mizue Hirano (JAMSTEC)
Kou Arihara (MWJ) Technical Staff
Tun Htet Aung (MWJ) Technical Staff

(2) Objective

The research objectives are to monitor the global ocean and to clarify the mechanisms of climate and oceanic environment variability for better understanding changes in earth system, within the framework of the Argo programme. To achieve the objectives, 2 core Argo floats and 5 bio-geochemical (BGC) Argo floats were deployed in the North Pacific Ocean where the spatial density of the Core and BGC Argo floats is not enough due to a lack of float deployment opportunities. The BGC Argo floats equipped with RINKO ARO-FT dissolved oxygen sensor which is manufactured by JFE Advantec, Japanese company. One of the objectives of this BGC Argo float deployment is to evaluate performance of the ARO-FT whether it is to be a formal Argo dissolved oxygen sensor. Data accumulated from Argo floats also contribute to improve long-term forecasts of climate changes through data assimilation systems.

(3) Parameters

・Core Argo float :Water temperature, salinity and pressure.

・BGC Argo float :Water temperature, salinity, pressure and dissolved oxygen.

(4) Method

We launched APEX floats manufactured by Teledyne Web Research. Those floats are equipped with SBE41 CTD sensor manufactured by Sea-Bird Electronics Inc. The float drifts at a depth of 1000dbar (called the parking depth) between profiles, then goes upward from a depth of 2000dbar to the sea surface every 1-10 days. During the ascent, physical and bio-geochemical values are measured. During surfacing for approximately half an hour, the float sends all measured data to the land via the Iridium RUDICS telecommunication system. The lifetime of floats is expected to be about four-eight years. The status of float and its launching information is shown in Table 5.1. 1.

(5) Data archive

The Argo float data will be provided from Japan DAC, conducting the real-time quality control within 24 hours following the procedure decided by Argo data management team. Within 6 months ~ 1 years, the delayed mode quality control will be conducted, to satisfy their data accuracy for climate research use. Those quality-controlled data are freely available via internet and utilized for not only research but also weather forecasts and any other variable use through internet. Global Data Assembly Center (GDAC: https://usgodae.org/argo/argo.html, https://www.coriolis.eu.org/Observing-the-Ocean/ARGO, https://dataselection.euro-argo.eu/), Global Telecommunication System (GTS).

Table 5.1. 1 Specifications of floats and their launching positions

Float Type	Core BGC	APEX float manufactured by Teledyne Webb Research.
CTD sensor	Core BGC	SBE41 manufactured by Sea-Bird Electronics Inc.
Dissolved oxygen sensor	BGC	ARO-FT manufactured by JFE Advantech Co., Ltd..
Cycle	Core	every 10 day (approximately 30minutes at the sea surface)
	BGC	every 1-10 day (approximately 30minutes at the sea surface)
Iridium transmit type	Core BGC	Router-Based Unrestricted Digital Internetworking Connectivity Solutions (RUDICS)
Target Parking Pressure	Core BGC	1000 dbar
Sampling layers	Core BGC	2dbar interval from 2000 dbar to surface (approximately 1000 levels) Biogeochemical parameter(dissolved oxygen) interval 10dbar from 2000dbar to 1400 dbar interval 5dbar from 1400dbar to 500 dbar interval 2dbar from 500 dbar to 2 dbar and surface

Table 5.1.2 Floats launching positions

Float S/N	WMO ID	Date and Time of Launch (UTC)	Location of Launch		Station
10776	3902452	2025/04/20 18:33:00	9°29’30.480"N	149°09’51.480"E	046M001
10777	5906601	2025/04/24 14:24:00	9°30’19.080"N	155°48’33.120"E	054M002
10778	5906602	2025/04/25 21:18:00	9°29’18.600"N	159°10’19.200"E	058M001
10779	5906603	2025/04/28 15:02:00	10°50’03.120"N	164°35’01.320"E	065M002
10781	5906604	2025/05/01 00:43:00	11°00’05.400"N	170°35’15.720"E	071M001
10800	3902453	2025/05/04 21:55:00	15°59’58.200"N	165°04’27.480"E	N/A
10801	3902455	2025/05/07 07:25:00	23°21’49.320"N	155°00’46.080"E	N/A

Table 5.1.3 Floats configrations.

Float S/N	Type of type	Name of product	CTD sensor	Oxygen sensor
10776	BGC	APEX	SBE41	ARO-FT
10777	BGC	APEX	SBE41	ARO-FT
10778	BGC	APEX	SBE41	ARO-FT
10779	BGC	APEX	SBE41	ARO-FT
10781	BGC	APEX	SBE41	ARO-FT
10800	Core	APEX	SBE41	N/A
10801	Core	APEX	SBE41	N/A

(a)S/N10776

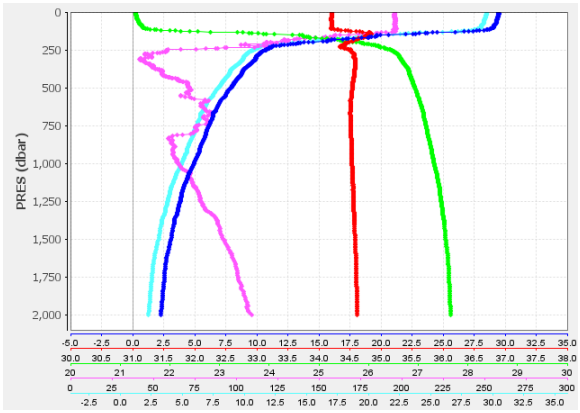

(b) S/N 10777

No show

(c) S/N 10778

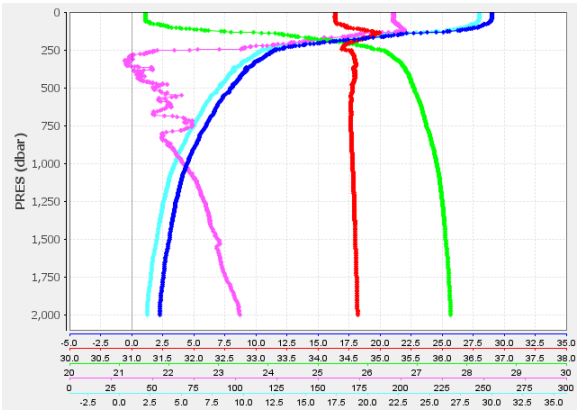

(d)S/N 10779

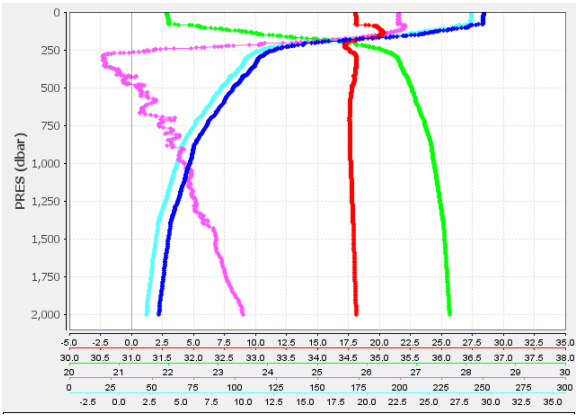

(e)S/N 10781

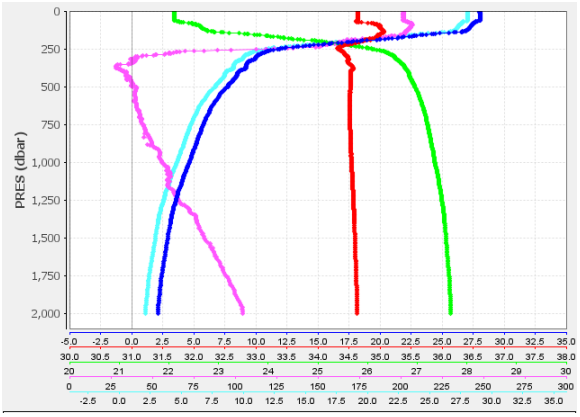

Fig. 5.1.1 (a, b, c, d and e). Vertical temperature, salinity and density profiles of their first measurements for four BGC Argo floats (SN10776, SN10777, SN10778, and SN10781). Blue and red lines show temperature and salinity profiles. And light green and pink lines show density and dissolved oxygen profiles. Float S/N10779 are not shown because it does not yet data from the float.

(f) 10800

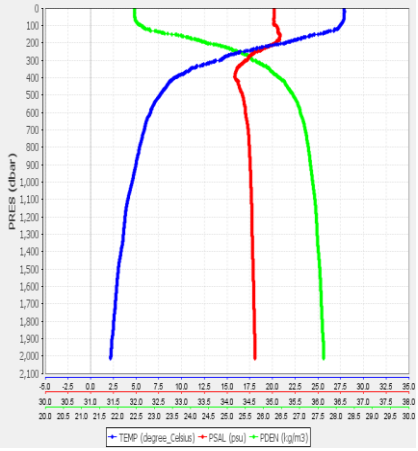

(g) 10801

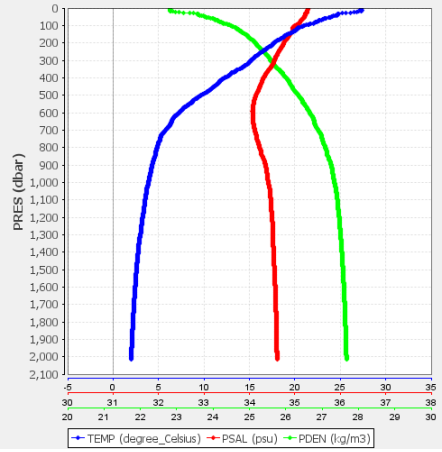

Fig. 5.1.2 (f and g). Vertical temperature, salinity and density profiles of their first measurements for two Core Argo floats (SN10800 and SN 10801). Blue, red and light green lines show temperature, salinity and density profiles.

5.2 Argo float observation of surface and mixed layers

(1) Personnel

Satoru Yokoi	(JAMSTEC)	Principal Investigator
Ayako Seiki	(JAMSTEC)	
Mizue Hirano	(JAMSTEC)	
Kou Arihara	(MWJ)	Technical staff
Tun Htet Aung	(MWJ)	Technical staff

(2) Objective

The objective of the observation is to measure vertical profiles of sea-water temperature and salinity for investigating variability in structure of surface and mixed layers regarding air-sea interaction and diurnal cycle.

(3) Method

An APEX profiling float manufactured by Teledyne Webb Research was deployed on the way from Shimizu to the tropical western Pacific. Information on the deployment is summarized in Table 5.2-1. It has been measuring vertical profile of sea-water temperature and salinity from 250 dbar to near the sea surface at about 01, 07, 13, and 19 UTC (10, 16, 22, and 04 Japan Standard Time (JST)) every day. Note that the float is equipped with RBRargo CTD sensor, which can collect data as close to the sea surface as possible.

(4) Preliminary results

Figure 5.2-1 shows the time-depth cross section of temperature and salinity observed from May 6 to 10, as an example of the collected data. The diurnal cycle of temperature is clearly visible above a depth of 5 meters.

(5) Data archive

The Argo float data will be provided from Japan DAC, conducting the real-time quality control within 24 hours following the procedure decided by Argo data management team. Within 6 months ~ 1 year, the delayed mode quality control will be conducted, to satisfy their data accuracy for climate research use. Those quality-controlled data are freely available through Global Data Assembly Center (GDAC: https://usgodae.org/argo/argo.html, https://www.coriolis.eu.org/Observing-the-Ocean/ARGO, https://dataselection.euro-argo.eu/).

Table 5.2-1: Information on the deployment of the float.

Float S/N	WMO ID	Data and time (UTC)	Latitude	Longitude
10463	3902451	2025/04/07 16:10:00	14-30.12N	129-29.31E

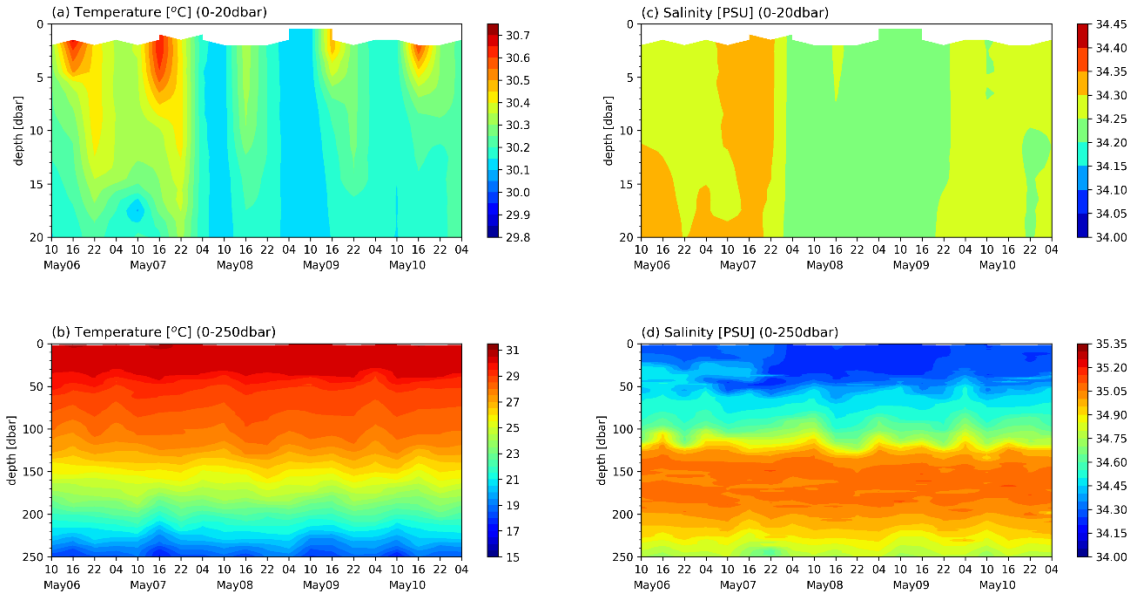

Figure 5.2-1: Time-depth cross section of (a, b) temperature (unit: °C) and (c, d) salinity (unit: PSU) observed by the float from 01 UTC on May 6 to 19 UTC on May 10 (from 10 JST on May 6 to 04 JST on May 11), shown as an example. The horizontal axis represents time in JST.

5.3 BGC Argo float observation

(1) Personnel

Sayaka Yasunaka	Tohoku University, JAMSTEC: Principal Investigator; not on board
Kanako Sato	JAMSTEC; not on board
Mizue Hirano	JAMSTEC; not on board
Shinya Kouketsu	JAMSTEC

(2) Purpose

To understand the formation mechanism of subsurface chlorophyll maximum at the northern edge of the warm pool in the tropical Pacific.

(3) Methods

We deployed APEX floats manufactured by Teledyne Webb Research at 8.5996N, 135.3958E, 8:24 GMT, April 14, 2025. The float is equipped with Sea-Bird Scientific SBE 41, Scattering Fluorescence Sensor (ECO FLBBCD), and Multispectral Radiometers (OCR504). The float drifts at a depth of 1000dbar (called the parking depth) during waiting measurement, then goes upward from a depth of 1000dbar to the sea surface two times a day (at 12AM and 12PM GMT). During the ascent, physical and biogeochemical values are measured. During surfacing for approximately half an hour, the float sends all measured data to the land via the Iridium RUDICS telecommunication system. The lifetime of floats is expected to be about six months.

(4) Data archive

The CTD data is provided conducting the real-time quality control within 24 hours following the procedure decided by Argo data management team. Then the delayed mode quality control will be conducted within 6 months ~ 1 years, to satisfy their data accuracy for climate research use. Those quality-controlled CTD data and other non-quality-controlled biogeochemical data will be freely available via internet and utilized for not only research but also weather forecasts and any other variable use through internet. Global Data Assembly Center (GDAC: http://www.usgodae.org/argo/argo.html, http://www.coriolis.eu.org/), Global Telecommunication System (GTS).

(4) Remarks

Data from Multispectral Radiometers (OCR504) are extremely low even in day-time profiles. Therefore, day-time observation was suspended since April 25, and OCR measurements since April 30.

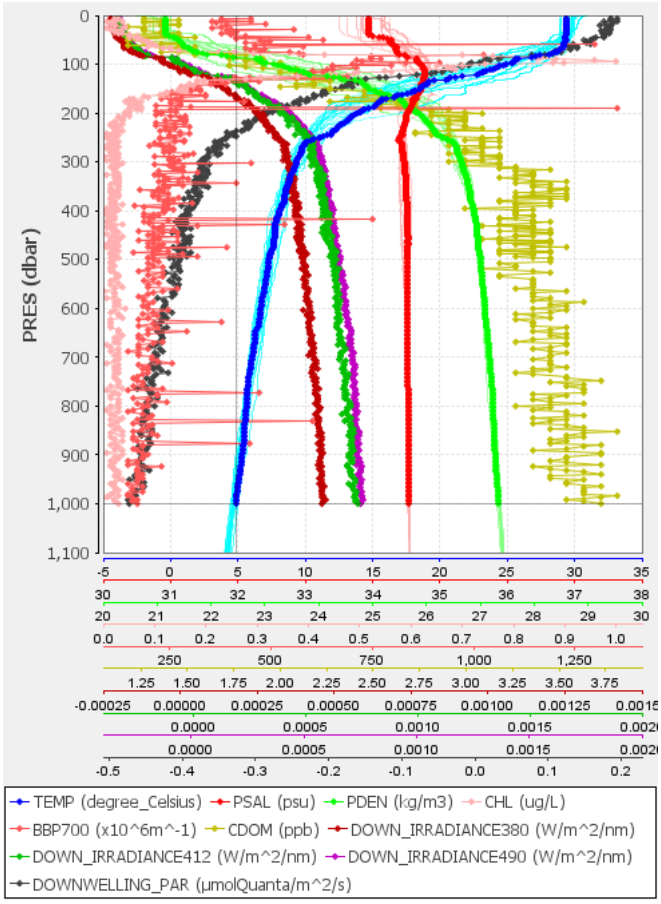

Figure 5.3.1. Vertical profiles of the first measurements.

6. Notice on Using

This cruise report is a preliminary documentation as of the end of cruise.

This report is not necessarily corrected even if there is any inaccurate description (i.e. taxonomic classifications). This report is subject to be revised without notice. Some data on this report may be raw or unprocessed. If you are going to use or refer the data on this report, it is recommended to ask the Chief Scientist for latest status.

Users of information on this report are requested to submit Publication Report to JAMSTEC.

https://www.godac.jamstec.go.jp/darwin/en/note.html#report

E-mail: submit-rv-cruise@jamstec.go.jp